



TITLE:

# ICR ANNUAL REPORT 1994(Volume 1)

AUTHOR(S):

---

CITATION:

ICR ANNUAL REPORT 1994(Volume 1). ICR Annual Report 1995, 1

ISSUE DATE:

1995-03

URL:

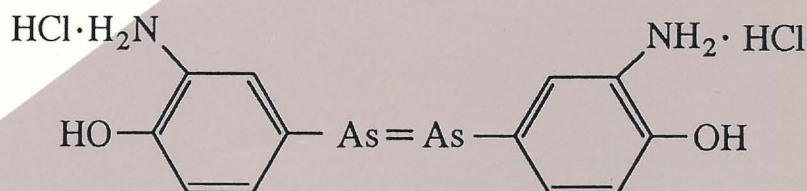
<http://hdl.handle.net/2433/65683>

RIGHT:

**ICR**

# ANNUAL REPORT

**1994**



**Kyoto University  
Institute for Chemical Research**



**Volume 1**



**Front cover:** *Historical remarks to the Institute for Chemical Research (ICR)*

The chemical structure is arsphenamine, i.e., 4, 4'-arsenobis(2-aminophenol)dihydrochloride, called Salvarsan commercially, first prepared by Paul Ehrlich and Sahachiro Hata in 1909 for medical use as an antisyphilitic drug. The Institute for Chemical Research originates from the Special Institute for Chemistry, founded in 1915 as a satellite facility of the College of Science, Kyoto Imperial University (the ancestor of the Faculty of Science, Kyoto University) with the intension of both exploring and manufacturing medical drugs such as Salvarsan; they had been in short supply because of World War I. The Institute for Chemical Research was established in 1926 as a general institution of chemical research closely connected to the related laboratories in the Faculties of Science, Medicine, Engineering and Agriculture. This Institute aimed to pursue fundamental principles in chemistry and their applications, an intension which has been continued until the present day.

**ICR ANNUAL REPORT 1994 (Volume 1)**

For the calendar years 1 January 1993 to 31 December 1994

**Editors:**

Professor Keisuke KAJI

Professor Akira NODA

Professor Atsuhiro OKA

Professor Kunihiro UEDA

**Managing editor:**

Misae HIRAMOTO

**Published and distributed by:**

Institute for Chemical Research (ICR),

Kyoto University, Uji, Kyoto-fu 611,

Japan

TEL : +81-(0)774-32-3111 (Ext. 2008)

FAX : +81-(0)774-32-1247

Note : ICR Annual Report available from the ICR Library

**Printed by:**

Yamashiro Printing Co. Ltd.

TEL : +81-(0)75-441-8177

FAX : +81-(0)75-441-8179

31 March 1995

# CONTENTS

## Inside front cover:

*Historical remarks to the Institute for Chemical Research (ICR)*

## Preface

## TOPICS AND INTRODUCTORY COLUMNS OF LABORATORIES ..... 1

### Investigation of the L-Series Lines of Tungsten with a New X-ray Spectrometer

K. Akita, Y. Ito, K. Ohno, M. Yasumoto, K. Tanno, K. Kondo, Y. Isozumi and  
T. Mukoyama

(STATES AND STRUCTURE—Atomic and Molecular Physics) ..... 4

### Application of an Imaging Plate to Electron Crystallography at Atomic Resolution

T. Ogawa, S. Moriguchi, S. Isoda and T. Kobayashi

(STATES AND STRUCTURE—Crystal Information Analysis) ..... 6

### Structural Changes during Uniaxial-Drawing and/or Heating of Poly(ethylene naphthalene-2, 6-dicarboxylate) Films

S. Murakami, M. Tsuji and S. Kohjiya

(STATES AND STRUCTURE—Polymer Condensed States Analysis) ..... 8

### Jump in the Rotational Mobility of Benzene Induced by the Clathrate Hydrate Formation

M. Nakahara, C. Wakai and N. Matubayasi

(INTERFACE SCIENCE—Solutions and Interfaces) ..... 10

### Characteristic Electronic Structures of Organic Solids Classified in Terms of Molecular Electronic

Relaxation

N. Sato

### The Scanning Dielectric Microscope

Koji Asami

(INTERFACE SCIENCE—Molecular Aggregates) ..... 12

### New Mode of Ion Size Discrimination for Group 2 Metals Using Poly(pyrazolyl)borate Ligands.

Control of Stability and Structure of Chelate Complexes by Intra- and InterLigand  
Contact and Shielding Effect

Y. Sohrin, M. Matsui and H. Kokusen

(INTERFACE SCIENCE—Separation Chemistry) ..... 14

### <sup>119</sup>Sn Mössbauer Study of Cu/Co and Au/Co Multilayers

T. Shinjo, T. Emoto, Y. Kawawake, K. Mibu and N. Hosoi

(SOLID STATE CHEMISTRY—Artificial Lattice Alloys) ..... 16

### Effect of Lattice Strain on Ferroelectric Properties of Epitaxially Grown BaTiO<sub>3</sub> Thin Films by

Reactive Evaporation

Y. Bando, T. Terashima and Y. Yano

(SOLID STATE CHEMISTRY—Artificial Lattice Compounds) ..... 18

### Application of High Pressure to Complex Copper Oxide Systems as a Way to Find New

Superconductors

M. Takano and Z. Hiroi

(SOLID STATE CHEMISTRY—Multicomponent Materials) ..... 20

### Inorganic Photonic Materials—Preparation and Third Order Non-Linear Optical Properties

T. Yoko, H. Kozuka and T. Hashimoto

(SOLID STATE CHEMISTRY—Amorphous Materials) ..... 22



Dynamic Birefringence of Amorphous Polymers K. Osaki, H. Watanabe, T. Inoue and H. Okamoto (FUNDAMENTAL MATERIAL PROPERTIES—Molecular Rheology) .....	24
Crystal Nucleation in Polymer Glasses M. Imai, K. Kaji and T. Kanaya (FUNDAMENTAL MATERIAL PROPERTIES—Polymer Materials Science).....	26
Selective Excitation Switching Angle Sample Spinning $^{13}\text{C}$ NMR Study of the Local Motion of Glassy Polymers F. Horii, T. Beppu, N. Takaesu and M. Ishida (FUNDAMENTAL MATERIAL PROPERTIES—Molecular Motion Analysis) .....	28
Mechanisms of Segmental Orientation in Deformed Polymer Melts T. Fukuda, K. Kawabata, K. Fujimoto, Y. Tsujii and T. Miyamoto (ORGANIC MATERIALS CHEMISTRY—Polymeric Materials) .....	30
Chemical Transformation of Fullerene $\text{C}_{60}$ K. Komatsu, Y. Murata, A. Kagayama, N. Takimoto, S. Mori and N. Sugita (ORGANIC MATERIALS CHEMISTRY—High-Pressure Organic Chemistry) .....	32
Retention of Configuration in the Ritter-type Substitution Reaction of Chiral $\beta$ -Arylthio Alcohols through the Anchimeric Assistance of the Arylthio Group A. Toshimitsu, C. Hirosawa and K. Tamao Oligosiloles: First Synthesis Based on a Novel <i>Endo-Endo</i> Mode Intramolecular Reductive Cyclization of Diethynylsilanes K. Tamao and S. Yamaguchi (SYNTHETIC ORGANIC CHEMISTRY—Synthetic Design) .....	34
Desymmetrization of <i>meso</i> -Dicarbonyl Compounds by the Horner-Wadsworth-Emmons Reaction K. Fuji, K. Tanaka, Y. Ohta and T. Watanabe (SYNTHETIC ORGANIC CHEMISTRY—Fine Organic Synthesis) .....	36
Electronically Controlled Stereochemistry in the Reaction of Chiral $\text{NAD(P)}^+/\text{NAD(P)H}$ Analogues A. Ohno, A. Tsutsumi, Y. Kawai and N. Yamazaki (BIOORGANIC CHEMISTRY—Bioorganic Reaction Theory).....	38
A Novel Zinc Finger-Based DNA Cutter: Biosynthetic Design and Highly Selective DNA Cleavage M. Nagaoka, M. Hagihara, J. Kuwahara and Y. Sugiura (BIOORGANIC CHEMISTRY—Bioactive Chemistry) .....	40
Molecular Etiology of Alzheimer's Disease: Aberrant Splicing of APP Gene Transcript and Linkage to Apolipoprotein e4 Allele S. Tanaka and K. Ueda (BIOORGANIC CHEMISTRY—Molecular Clinical Chemistry) .....	42
Mechanism-Based Inactivation of Glutathione Synthetase by Phosphinic Acid Transition-State Analogue J. Hiratake, H. Kato and J. Oda (MOLECULAR BIOFUNCTION—Functional Molecular Conversion) .....	44
Evolutional Origin of Bacterial Glutamate Racemase K. Soda, N. Esaki and T. Yoshimura (MOLECULAR BIOFUNCTION—Molecular Microbial Science) .....	46

Peptide Induce Membrane Fusion: Peptide Structure Required for the Fusion S. Takahashi, R. Ishiguro and T. Matsumoto (MOLECULAR BIOLOGY AND INFORMATION—Biopolymer Structure) .....	48
Transcriptional Control of the <i>Agrobacterium</i> Virulence Genes by Two Proteins VirA and VirG A. Oka, T. Aoyama and H. Endoh (MOLECULAR BIOLOGY AND INFORMATION—Molecular Biology) .....	50
BRITE: Biomolecular Reactions for Information Transmission and Expression S. Goto, K. Suzuki, Y. Akiyama and M. Kanehisa (MOLECULAR BIOLOGY AND INFORMATION—Biological Information Science) .....	52
Improvements of the Beam Characteristics of the 7 MeV Proton Linear Accelerator A. Noda, H. Dewa, H. Fujita, M. Kando, M. Ikegami, Y. Iwashita, S. Kakigi and M. Inoue (NUCLEAR SCIENCE RESEARCH FACILITY—Particle and Photon Beams) .....	54
Search for Dark Matter Axions with Rydberg Atoms in a Resonant Cavity I. Ogawa, S. Nakamura, T. Takimoto, M. Tada and S. Matsuki (NUCLEAR SCIENCE RESEARCH FACILITY—Beams and Fundamental Reaction) .....	56
The 5' Terminal Region of the Apocytochrome b Transcript in <i>Crithidia fasciculata</i> is Successively Edited by Two Guide RNAs in the 3' to 5' Direction H. Sugisaki (NUCLEIC ACID RESEARCH FACILITY) .....	58
<b>LABORATORIES OF VISITING PROFESSORS</b> .....	60
SOLID STATE CHEMISTRY DIVISION—Structure Analysis	
FUNDAMENTAL MATERIAL PROPERTIES DIVISION—Composite Material Properties	
SYNTHETIC ORGANIC CHEMISTRY DIVISION—Synthetic Theory	
<b>PUBLICATIONS</b> .....	62
<b>SEMINARS</b> .....	83
<b>MEETINGS AND SYMPOSIUMS</b> .....	86
<b>THESES</b> .....	88
<b>ORGANIZATION AND STAFF</b> .....	91
<b>NAME INDEX</b> .....	95
<b>KEYWORD INDEX</b> .....	97







## Preface

It is a pleasure to introduce here the first Annual Report of the Institute for Chemical Research (ICR), Kyoto University. Henceforth, this Report will be presented annually to distribute widely the current activities of the Institute. Included will be Abstracts of selected papers, the range of research activities, details of publications, and other relevant information. Exceptionally, this first issue covers the work of two calendar years, from January 1993–December 1994, with publications from July 1993 documented.

The Institute was formally established in 1926, to undertake fundamental studies and their application to particular fields of chemistry. The Institute was reorganized in 1992, and now comprises 9 divisions and 2 satellite facilities. Each division, on average, is made up of 3 laboratories. In all there are 31 laboratories, including 3 laboratories for guest members of staff (visiting professors). The on-going research embraces a broad range of chemistry; *nuclear chemistry and physics; physical chemistry; surface chemistry; solid state chemistry; analytical chemistry; organic and inorganic chemistry; polymer chemistry; bio-organic chemistry; protein and enzyme chemistry; molecular biology and human genome science.*

Since 1929, the Institute has published the Bulletin of the Institute for Chemical Research, which has been valuable in disseminating the activities of the Institute. Currently, there are, in residence, more than 300 researchers, which include 170 graduate students and approximately 40 foreign researchers. These are distributed over the various research fields already mentioned. More than 400 papers are published annually from the Institute in leading Journals and Conference Proceedings. Consequently, it has been necessary to reconsider the function of the Bulletin. Within its present format it is proving increasingly difficult to accurately portray the expanded ICR activities. Thus we have taken the opportunity which the reorganization offers to present this new Report. An English Edition will describe concisely the essential activities of ICR. We hope also that it will be a vehicle to exchange mutual information with outside Societies.

We, therefore, enthusiastically initiate this new Annual Report at this time. We hope that not only domestic, but also international collaborations will be catalyzed via this Annual Report. We also recognized our responsibility to make the *ICR* a Center of Excellence in these key areas of chemistry, as soon as possible. Consequently, we would appreciate receiving advice and comments about this Report from outside Societies and individuals. Our desire is to achieve the highest possible standards.

Finally, I wish to thank members of the Publication Committee for their wholehearted efforts, and all researchers for their valuable contributions.

*T. Miyamoto*

Takeaki Miyamoto

DIRECTOR

March 15, 1995



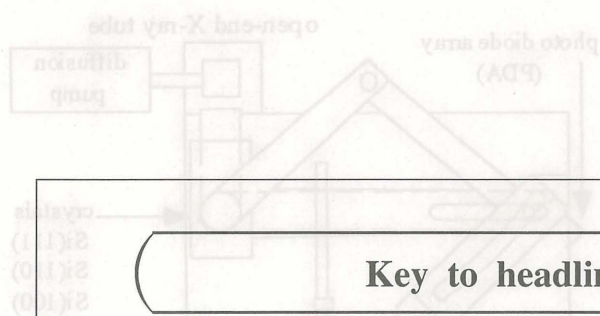
**TOPICS AND INTRODUCTORY COLUMNS  
OF LABORATORIES**



# Investigation of the L-Series Lines of Tungsten with a New X-ray Spectrometer

Katsushi Akita, Yoshiaki Ito, Kichizo Ohno, Mitsuo Yasumoto,  
Kiyomitsu Tanno, Kazumasa Kondo\*, Yasuhito Isozumi and Takeshi Mukoyama

Keywords: Photo diode array; Coster-Kronig transition; Wenzel-Dryvestein theory



## Key to headline in the cloumns

### RESEARCH DIVISION—Laboratory (Subdivision)\*

\* See also "Organization and Staff" on page 91.

## Abbreviations used in the columns

Prof	Professor	GS	Graduate Student
Vis Prof	Visiting Professor	DC	Doctor's Course (Program)
Assoc Prof	Associate Professor	MC	Master's Course (Program)
Lect	Lecturer	UG	Undergraduate Student
Lect (pt)	Lecturer (part-time)	RFR	Research Fellow
Instr	Instructor	RS	Research Student
Assoc Instr	Associate Instructor		
Techn	Technician	D Sc	Doctor of Science
Guest Scholar	Guest Scholar	D Eng	Doctor of Engineering
Guest Res Assoc	Guest Research Associate	D Agr	Doctor of Agricultural Science
Univ	University	D Pharm Sc	Doctor of Pharmaceutical Sciences
		D Med Sc	Doctor of Medical Science



## Investigation of the L-Series Lines of Tungsten with a New X-ray Spectrometer

Katsushi Akita, Yoshiaki Ito, Kichizo Ohno, Mitsuo Yasumoto,  
Kiyomitsu Tanno, Katsumi Kondo\*, Yasuhito Isozumi and Takeshi Mukoyama

We have developed a new type of a high resolution X-ray spectrometer. This is a Johann-type crystal spectrometer whose radius of Rowland circle is 750 mm. Moreover, in order to get characteristic X-ray generated by electron excitation, we have made an open-end X-ray tube. With this instrument we observed the L-series lines of tungsten, and measured natural widths. Satellites observed on high energy side of the diagram lines are also examined.

**Keywords:** Photo diode array/ Coster-Kronig transition/ Wentzel-Druyvesteyn theory

To investigate electron transitions between inner-shells and to have information about atomic configurations, it is very effective to measure X-ray fluorescence spectra. We have developed a new type of a high resolution X-ray spectrometer with which we can observe a X-ray spectrum instantly. The spectrometer is shown in Fig. 1. The radius of Rowland circle is 750 mm. It has three Johann-type crystals, which are Si(111), Si(110), and Si(100).  $2\theta$  ( $\theta$ : Bragg angle) can be changed from about 65 to 95 degrees. The detector is a linear image sensor, a photo diode array (Hamamatsu Photonics S3904-1024Q). Because the path of X-ray is longer than 170 cm, X-ray generated by photo excitation does not have enough intensity to observe a spectrum instantly. Therefore we adopted X-ray by electron excitation as the light source and have made an open-end X-ray tube to get characteristic X-rays of various elements. It is a X-ray

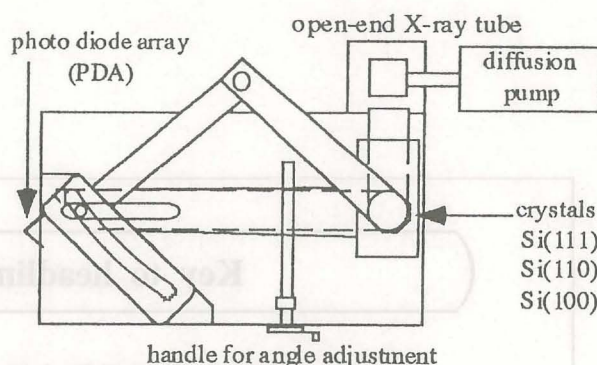


Figure 1. Schematic illustration of a spectrometer.

tube with a pipe for evacuation. It can be disjointed and a target element in it is remountable. After it is evacuated in the tube about  $1 \times 10^{-6}$  torr, high voltage is applied on the filament. Voltage and current can be applied on the filament up to 50 kV and 50 mA, respectively. The horizontal width of the light source

\* Plasma Physics Laboratory, Gokasho, Uji Kyoto 611.

### STATES AND STRUCTURE —Atomic and Molecular Physics—

#### Scope of research

*In order to obtain fundamental information on the property and the structure of materials, the electronic states of atoms and molecules are investigated in detail using X-ray, SR, ion beam from accelerator and nuclear radiation from radioisotopes. Theoretical analysis of the electronic states and development of new radiation detectors are also performed.*



Professor  
MUKOYAMA, Takeshi  
(D Eng)



Associate Professor  
ISOZUMI, Yasuhito  
(D Eng)



Instructor  
ITO, Yoshiaki  
(D Sc)



Instructor  
NAKAMATSU, Hirohide

#### Instructor

ITO, Yoshiaki (D Sc)  
NAKAMATSU, Hirohide  
**Associate Instructor:**  
KATANO, Rintarou  
(D Eng)

#### Students:

YAMAGUCHI, Kouichirou  
(DC)  
AKITA, Katsushi (MC)  
OHSAWA, Daisuke (MC)  
TOCHIO, Tatsunori (MC)  
SONG, Bin (RS)



enabled to have a spectrum because this spectral system is a focusing system. X-ray emitted from different point of the light source enters into a crystal with different angle and focuses on a different channel of PDA. The intensity of X-ray from each point is considered to be equal since the filament length corresponding to energy width of a spectrum is very short. The energy region measured by each crystal is shown in Table 1.

**Table 1.** Energy region corresponding to each crystal.

Reflection plane	2d (Å)	Energy region (keV)
(111)	6.267	2.7– 3.7
(220)	3.838	4.4– 6.6
(400)	2.714	6.2– 8.5
(333)	2.089	8.0–11.0
(440)	1.919	8.7–12.0

One of applications of this instrument is to study natural widths of characteristic X-rays of various elements. Natural widths of characteristic X-rays or atomic levels have long been investigated experimentally and theoretically. Although there are many reports about K-series lines, there are only a few about L-series lines. Theoretically the energy distribution of the radiation emitted in the electron transition has the lorentzian form of following expression.

$$J(\nu)d\nu = \frac{\Gamma}{2\pi} \frac{d\nu}{(\nu - \nu_0)^2 + \left(\frac{\Gamma}{2}\right)^2}$$

where  $\nu$  is frequency,  $\nu_0$  is frequency of the peak, and  $\Gamma$  is the full width at half maximum of the peak. A spectrum observed actually is a convolution of this lorentzian and an instrumental broadening. But an instrumental broadening of this spectrometer is considered to be very small and neglected since each peak can be fitted by only one lorentzian sufficiently. An example of measured spectrum is shown in Fig. 2.

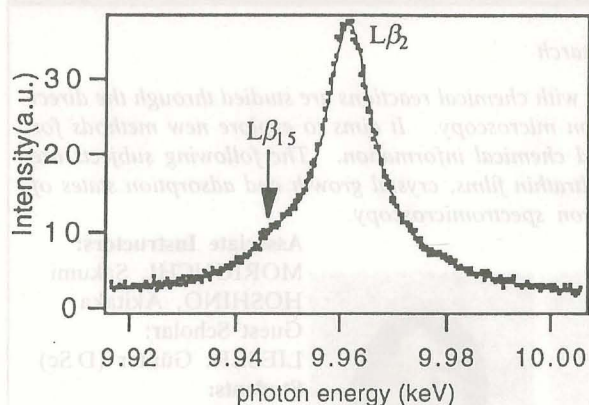


**Figure 2.** Spectrum of  $L\beta_2$  and  $L\beta_{15}$  line. Tube voltage is 30 kV, tube current is 15 mA. Crystal is Si(333) and  $2\theta$  is 73.13 degrees. Dots are measured value and solid line is fitted by lorentzians.

We show a comparison of the natural widths of L-series lines of tungsten measured in this work and in previous work in Table 2.

**Table 2.** Natural widths of L-series line of tungsten.

Line	This Work	Ref. 1	Ref. 2	Theory
$L\alpha_1$	7.45	7.16	6.50	5.63
$L\alpha_2$	7.69		7.20	7.90
$L\beta_1$	8.15	7.11	6.90	9.16
$L\beta_2$	10.75	10.1	9.06	12.37
$L\beta_3$	14.32		13.10	16.61
$L\beta_4$	16.85		14.60	17.81
$L\beta_{15}$	11.66			12.54

Theoretical value is derived from calculation of level widths in ref. 3, 4, where we used the fact that the width of characteristic X-ray irradiated by electron transition between two levels is the sum of the widths of each level. There is no drastic difference compared with other measurements, but discrepancy among each value means that more accurate investigations are necessary to be performed on the natural widths of characteristic X-rays.

Observing the spectra, we found some of them have shoulders on high energy side of the diagram lines. These can be explained by Wentzel-Dryvesteyn theory. According to this theory, these are the satellites caused by LX (X=M or N) double holes configuration. For tungsten, such double holes states are created mainly by Coster-Kronig  $L_1-L_{2,3}X$  or  $L_2-L_{2,3}X$  transitions. So far, we couldn't assign the satellites which correspond to X=N, because the energy shifts of the satellites due to LN double holes are very small. But satellites were observed in the region of energy which correspond to X=M in  $L\alpha_1$  and  $L\beta_1$  spectra. This fact suggests the existence of Coster-Kronig transition  $L_1-L_3M$  as suggested by Salgueiro *et al* [5] in the  $L\beta_2$  line, although theoretical calculation of Chen *et al* predicted [6] Coster-Kronig transition  $L_1-L_3M$  is energetically forbidden.

The greatest advantage of this instrument is that we can observe phenomena which change time-dependently like chemical reactions. In the future, we will try to observe such phenomena.

#### References

1. Williams JH, *Phys. Rev.*, **45**, 71 (1934).
2. Salem SI and Lee PL, *At Data and Nuclear Data Tables*, **18**, 233 (1976).
3. McGuire EJ, *Phys. Rev.*, **A5**, 1043 (1972).
4. Crasemann B, *et al*, *Phys. Rev.*, **A4**, 2161 (1971).
5. Salgueiro L, *et al*, *J. de Phys.*, **C9**, 609 (1987).
6. Chen MH, *et al*, *At Data and Nuclear Data Tables*, **19**, 97 (1977).



## Application of an Imaging Plate to Electron Crystallography at Atomic Resolution

Tetsuya Ogawa, Sakumi Moriguchi, Seiji Isoda and Takashi Kobayashi

An imaging plate was used to measure quantitatively the electron diffraction intensities of graphite and polyethylene single crystals. It is shown that the high sensitivity, the wide dynamic range, the good linear response and the digital output data of the imaging plate are useful for structure analysis by using electron diffraction. For polyethylene, hydrogen atoms were resolved, in addition to carbon atoms, owing to the higher scattering power of hydrogen for electron beam than X-ray.

**Keywords:** Structure Analysis/ Electron Diffraction/ Potential Map

Imaging plate (IP) was developed at first as a high sensitive two-dimensional detector in X-ray radiography in place of conventional X-ray films and soon applied to the field of X-ray crystallography. Recently, from the reason for its suitability in electron detection, it was also applied to the field of electron microscopy [1]. IP has more than three orders higher sensitivity in these accelerating voltages than that of conventional electron microscopic films. It exhibits also wide dynamic range of about four orders and very good linear response of the output signals for the logarithm of incident electron dosage in this range. In diffraction observation, the wide dynamic range of four orders may be appropriate to cover over from strong to weak scattering, and the good linear response and the digital data make it easy to collect the intensity data as the output signals of IP.

In the determination of structures of very small crystallites or thin layer (for example, polymer single crystals or pseudomorphic epitaxial layers), electron diffraction might be a better technique to analyze their

structures rather than X-ray or neutron diffraction. Although it has been commonly thought that the electron diffraction is unfavorable in quantitative data collection so far, Dorset has shown that electron diffraction technique is useful for crystal structure analysis using the so-called direct phasing procedure [2] as employed in X-ray crystallography. Accordingly, quantitative data collection with a good recording medium may expected to realize reliable structure determination by electron diffraction.

We prepared thin flaky graphite as a specimen having a simple and well known structure and single crystals of polyethylene as an example of irradiation sensitive polymer crystal, which was grown from dilute xylene solution. Electron diffraction patterns were recorded on IP using transmission electron microscopes. After the data were transformed to electron beam intensities using the calibration line, integral intensities were measured for each diffraction spot. Then absolute intensities and a mean temperature factor were determined using Wilson

### STATES AND STRUCTURES —Electron Microscopy and Crystal Chemistry—

#### Scope of research

*Structures of materials and their structural transition associated with chemical reactions are studied through the direct observation of atomic or molecular imaging by high resolution microscopy. It aims to explore new methods for imaging with high resolution and for obtaining more detailed chemical information. The following subjects are studied: direct structure analysis of ultrafine crystallites and ultrathin films, crystal growth and adsorption states of organic materials, and development in high resolution electron spectromicroscopy.*



Professor  
KOBAYASHI, Takashi  
(D Sc)



Associate Professor  
ISODA, Seiji  
(D Sc)



Instructor  
KURATA, Hiroki  
(D Sc)



Instructor  
OGAWA, Tetsuya  
(D Sc)

#### Associate Instructors:

MORIGUCHI, Sakumi  
HOSHINO, Akitaka

#### Guest Scholar:

LIESER, Günter (D Sc)

#### Students:

HASHIMOTO, Syugo (DC)  
TSUKIMOTO, Seiji (MC)  
ITOH, Toshihiko (MC)  
IRIE, Satoshi (MC)  
KUWAMOTO, Kiyoshi (MC)  
KOSHINO, Masanori (MC)  
NAGAI, Kazuhiro (RF)  
KAWASE, Noboru (RF)



plot, and the signs of structure factors were assigned so that the electrostatic potential map was synthesized.

Electron diffraction pattern of graphite was recorded on IP (hk0-reflections). The integral intensities of 130 diffraction spots were measured over the intensity range of about four orders with only one sheet of IP. Finally, 19 symmetrically independent diffraction intensities were obtained. The signs of structure factors are assigned plus for all reflections due to the crystal structure of graphite. Then the electrostatic potential map was synthesized from the structure factors, where potential peaks corresponding to the carbon atom positions in the unit cell are clearly seen. The peak at (0, 0) is about two times higher than those at (1/3, 2/3) (2/3, 1/3), which means two carbon atoms exist at (0, 0) in the unit cell, and one atom locates at (1/3, 2/3) and (2/3, 1/3) as expected. Applying a least squares fit, the R-factor of 0.228 was obtained. This result demonstrates the good applicability of IP for quantitative detection of electron beam intensity of diffraction.

The single crystal of PE is lamellar crystal, whose normal is almost parallel to the c-axis. Therefore, electron diffraction shows the c-axis incident pattern. Integral intensities of 164 spots (48 symmetrically independent spots) with the intensity magnitude over more than four orders could be measured. Since the two dimensional space group of polyethylene crystal projected onto the ab-plane is pgg, the structure factor is a real number. The direct phasing method was used to assign the signs of the observed structure factors [3]. In this space group, signs of two reflections with the indices of (hk)≠(gg), where g is an even integer, could be assigned arbitrarily in order to define the origin of the unit cell. From these signs, the signs of the other reflections were determined using the  $\Sigma 2$ -relationship,  $S(h)S(h')S(h+h')=1$  ( $S(h)$  was the sign of reflection h), for the sets of these reflections h, h' and h+h' with large values of the multiples of their normalized structure factors.

Using these signs and observed structure factors, potential map is synthesized as in Figure 1. In addition to four clear peaks corresponding to carbon atoms, weak peaks corresponding to hydrogen atoms, which is not easy to be detected by X-ray experiment, can be seen due to the higher ratio of the scattering amplitude of a hydrogen atom to a carbon atom for electron beam compared to X-ray. This point is one of the merits of analyzing

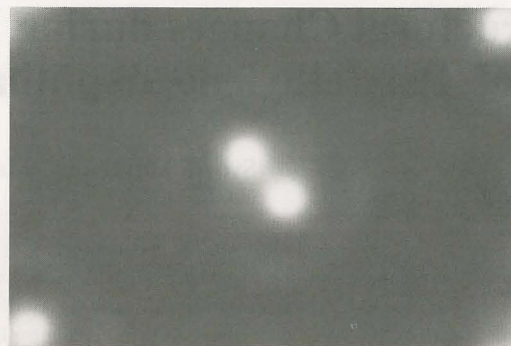


**Figure 1.** Electrostatic potential map for polyethylene calculated from observed structure factor magnitudes and signs assigned by direct method. There can be seen clearly four peaks corresponding to carbon atoms and weak peaks corresponding to hydrogen atoms.

structures of organic crystals by electron diffraction. Refinement of atomic positions by a least squares fit was carried out using the different temperature factors for carbon and hydrogen atoms. The result showed that the setting angle, i.e. the angle between the plane of zig-zag chain and the b-axis was  $46^\circ$ . It coincides with the results of X-ray experiments of  $44\text{--}48^\circ$ . R-factor was 0.198 with the temperature factors of  $0.063\text{ nm}^2$  for C and  $0.093\text{ nm}^2$  for H.

In the present cases, the potential maps show the good availability of IP to the structure analysis of crystals by electron diffraction [4]. In comparison with conventional electron microscopic films, we can record a large number of diffraction peaks on a sheet of IP. Because of the high sensitivity, it has great advantage, in particular, for the experiment of organic crystals which are damaged easily by electron irradiation.

#### References

1. Ichihara S, Hayakawa S, Saga S, Hoshino M, Sakuma S, Ikeda M, Yamaguchi H, Hanaichi T and Kamiya Y, *J. Electron Microsc.*, **33**, 255 (1984).
2. Dorset D L and Hauptman H A, *Ultramicroscopy*, **1**, 195 (1976).
3. Hauptman H A, 'Crystal Structure Determination, The Role of the Cosine Seminvariants', Plenum, New York (1972).
4. Ogawa T, Moriguchi S, Isoda S and Kobayashi T, *Polymer*, **35**, 1132 (1994).





# Structural Changes during Uniaxial-Drawing and/or Heating of Poly(ethylene naphthalene-2, 6-dicarboxylate) Films

Syozo Murakami, Masaki Tsuji and Shinzo Kohjiya

The structural changes in the uniaxial-drawing process of an unoriented amorphous film of poly(ethylene naphthalene-2, 6-dicarboxylate) [PEN] and in the heating process of an oriented amorphous film of PEN were studied respectively using the heating/drawing device and the high-temperature furnace designed for the X-ray diffraction apparatus equipped with imaging plates.

**Keywords:** Poly(ethylene-2, 6-naphthalate)/ Oriented crystallization/ X-ray diffraction/ Imaging plate/ Stress-strain curve/ Birefringence/ Density

Poly(ethylene naphthalene-2, 6-dicarboxylate) [PEN] possesses naphthalene rings in its main chain in place of all the benzene rings of poly(ethylene terephthalate) [PET]. Accordingly, PEN has a higher modulus and a higher melting temperature than PET, and thus has started to be utilized, e.g., for electric appliances such as videotapes. Except for a few structural studies, however, the solid-state structure of PEN has not been studied extensively. Here, some experimental results [1] will be shown, which were obtained in the studies on the structural formation/changes in an unoriented amorphous PEN film in the uniaxial-drawing process at various temperatures and on the oriented crystallization of the pre-deformed amorphous PEN film in the heating process using the X-ray diffraction system equipped with imaging plates [IP]: with this system, we can record a time-resolved series of two-dimensional X-ray diffraction/scattering patterns and afterwards analyse their intensity profiles [2].

For time-resolved wide-angle X-ray diffraction

[WAXD] measurements using the IP system in the uniaxial-drawing and/or heating process of polymer solids, a high-temperature furnace and a heating/drawing device were newly designed and constructed [3]. The working temperature range of the furnace is from room temperature to 500°C. The precision of temperature regulation is within  $\pm 0.5^\circ\text{C}$  for a given temperature between room temperature and 200°C, and within  $\pm 1^\circ\text{C}$  for 200°C through 500°C. For heat treatment, say at 180°C, it needs only 30 sec to reach 97% of the expected equilibrium temperature after introducing the specimen holder into the furnace which is thermostated beforehand at 180°C. The new heating/drawing device was also constructed. In this device, the specimen is to be stretched in the horizontal direction. The specimen temperature is controlled by blowing thermostated hot air vertically into the specimen chamber in order to attain uniform temperature distribution over the whole specimen and to raise the specimen temperature as quickly as possible up to a given temperature below

## STATES AND STRUCTURES —Polymer Condensed States—

### Scope of research

*Attempts have been made to elucidate the molecular arrangement and the mechanism of structural formation/change in crystalline polymer solids, polymer gels and elastomers, polymer liquid crystals and polymer composites, mainly by electron microscopy and X-ray diffraction/scattering. The major subjects are: synthesis and structural analysis of polymer composite materials, preparation and characterization of elastomeric materials, structural analysis of crystalline polymer solids by direct observation at molecular level resolution and in situ studies on structural formation/change in crystalline polymer solids.*



Professor  
KOHJIYA, Shinzo  
(D Eng)



Associate Professor  
TSUJI, Masaki  
(D Eng)



Instructor  
URAYAMA, Kenji

### Associate Instructor:

MURAKAMI, Syozo

### Students:

YAMAKAWA, Masahiro (MC)

HIRATA, Yoshitaka (MC)

HAMADA, Noritaka (MC)

TSUJIMOTO, Jun-ichi (UG)

MIURA, Hirofumi (UG)



160°C. The precision of temperature regulation is within  $\pm 1^\circ\text{C}$  at a specimen temperature between room temperature and 160°C.

When an unoriented amorphous PEN film was stretched below  $T_g$  ( $=117^\circ\text{C}$ ), it could be elongated up to a draw ratio [DR] of 4–5 via neck formation and this stretching resulted in an oriented amorphous film of PEN. The WAXD pattern of the film drawn using the heating/drawing device at  $65^\circ\text{C}$  up to  $\text{DR}=3.7$  showed a broad, asymmetrical halo maximum on the equator: the higher-scattering-angle side of the maximum is steeper than its lower-angle side. This asymmetrical profile indicates that the polymer chains are not randomly oriented but ordered to some extent.

When the oriented amorphous film of PEN, which had been made by drawing an unoriented amorphous film of PEN up to  $\text{DR}=3.6$  at  $65^\circ\text{C}$ , was heat-treated using the high-temperature furnace at a temperature below  $T_g$ , for example at  $115^\circ\text{C}$ , then practically no crystalline reflections were observed in the WAXD patterns. When it was heat-treated at  $118^\circ\text{C}$ , however, the crystalline reflections appeared gradually with time: all the crystalline reflections in this report were well attributed to the  $\alpha$  modification [4]. Concludingly, highly oriented amorphous films of PEN are able to crystallize above  $T_g$ , which was also confirmed by the DSC measurement.

The oriented amorphous film ( $\text{DR}=3.6$ ,  $65^\circ\text{C}$ ) of PEN was heated using the furnace at a heating rate of  $3^\circ\text{C}/\text{min}$ . At  $120^\circ\text{C}$ , crystalline reflections of (010), (100) and ( $-110$ ) were clearly observable. These equatorial reflections became sharper and increased in their intensities with increasing temperature up to around the melting temperature ( $270^\circ\text{C}$ ). This result suggests the increase in crystallite size with an increase in temperature. On the off-equatorial layer lines, however, streak-like scatterings were observed up to  $160^\circ\text{C}$ . These streaks demonstrate the existence of paracrystalline nature, which is caused by the axial shift of polymer chains with respect to one another in the direction of the chain axis. All the streaks became stronger in intensity with increasing temperature, and finally they turned to spot-like reflections above  $180^\circ\text{C}$ . The whole pattern of the final film ( $255^\circ\text{C}$ ) showed fairly high crystallinity and the so-called fiber orientation of crystallites.

When an unoriented amorphous film of PEN was drawn using the heating/drawing device at  $150^\circ\text{C}$ , the broad amorphous halo moved to and became concentrated on the equator in the WAXD pattern with increasing DR for  $\text{DR}<1.5$ . At  $\text{DR}=\text{ca. } 1.5$ , the crystalline reflections started to appear on the equator, and thereafter increased in their intensities with increasing DR. The reflections were accompanied by streaks on the off-equatorial layer lines, as mentioned above: the intensities of the streaks were greater than those observed in the heating process of the oriented amorphous film. The WAXD photographs were taken from the films, which had been drawn at various temperatures up to a

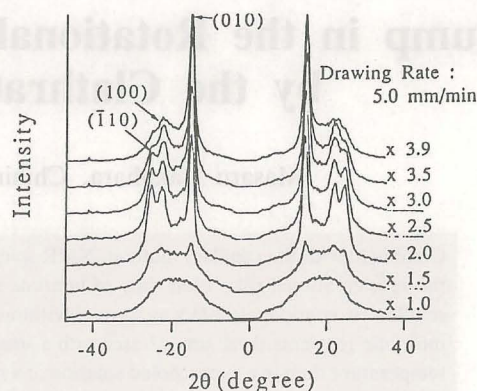


Figure 1. Equatorial intensity profiles of a time-resolved series of WAXD patterns obtained from an unoriented amorphous PEN film during uniaxial drawing at  $150^\circ\text{C}$ .

given DR and then been quenched, in order to elucidate the relationship between structural information and some properties such as stress-strain curves, birefringence and density [5]. In the case of uniaxial drawing above  $130^\circ\text{C}$ , the crystalline reflections appeared to be superposed on the oriented amorphous halo in the WAXD photograph taken from the film quenched at a DR just before the onset of necking. Beyond this point, the necking took place. The birefringence and density increased via neck formation.

Figure 1 shows the equatorial intensity profiles of a time-resolved series of WAXD patterns which were obtained in the uniaxial-drawing process of an unoriented amorphous film of PEN at  $150^\circ\text{C}$ . At  $\text{DR}=\text{ca. } 2$  (beyond the yield point), the (010), (100) and ( $-110$ ) reflections became still stronger. These reflections are clearly separated from one another during neck formation, and then the (010) reflection became strong and sharp with increasing DR. The ( $-110$ ) reflection, however, decreases in its intensity with increasing DR for  $\text{DR}>3.0$ , and finally the reflection has almost disappeared at  $\text{DR}=3.9$ . It is, therefore, concluded that in the drawing process of an unoriented amorphous film of PEN at a high temperature, the film has fiber structure accompanied by lattice distortion due to the axial shift of polymer chains relative to one another along the chain axis, and frequently the film finally shows uniplanar axial texture with the ( $-110$ ) lattice planes parallel to the film surface: in the  $\alpha$  modification, the unit cell contains one monomer unit of PEN and its naphthalene ring is set nearly parallel to the ( $-110$ ) plane [4].

#### References

1. Murakami S, Nishikawa Y, Tsuji M, Kawaguchi A, Kohjiya S and Cakmak M, *Polymer*, **36**, 291–297 (1995).
2. Tsuji M and Murakami S, *SEN-I GAKKAISHI*, **50**, P-607–P-613 (1994).
3. Murakami S, Tanno K, Tsuji M and Kohjiya S, *Bull. Inst. Chem. Res., Kyoto Univ.*, **72**, 418–428 (1995).
4. Mencik Z, *Chem. Prum.*, **17**, 78–80 (1976).
5. Murakami S, Yamakawa M, Tsuji M, Kawaguchi A and Kohjiya S, *Sen-i Gakkai Prepr.*, 'G-104 (1994); *idem*, *Proc. ISF '94, Yokohama*, p.40 (1994).



## Jump in the Rotational Mobility of Benzene Induced by the Clathrate Hydrate Formation

Masaru Nakahara, Chihiro Wakai, and Nobuyuki Matubayasi

Combined with the capillary method, NMR spin-lattice relaxation time measurements were performed to obtain the reorientational relaxation time of benzene in water between  $-50$  and  $120^{\circ}\text{C}$ . A clathrate hydrate of the smallest aromatic molecule was formed without high pressure or help gas. It is found that the guest benzene molecule reorients three times faster with a smaller friction in a clathrate hydrate (probably, type II) at a lower temperature than in a supercooled solution at a higher temperature. Correspondingly, the activation energy for the reorientation of the guest benzene molecule is found to be smaller in the clathrate hydrate.

**Keywords:** Water structure/ Binary aqueous solution/ Hydrophobic hydration/ Hydration cage/ NMR

Hydrophobic hydration, which is a very important phenomenon in biology, reflects the unique geometrical nature of water, which develops more at lower temperatures, in particular in a supercooled regime. The study of supercooled water is important for understanding the anomalous dynamic and static properties of ambient water [1]. Recently we have examined the rotational motions in hydrophobic hydration of benzene below the water freezing point in order to investigate the dynamical aspects of supercooled aqueous solutions and clathrate hydrates. Here we report this work [2].

Under some pressures and at relatively low temperatures (recall  $\text{CO}_2$ ), clathrate hydrates may be prepared in laboratory, found in nature, and proposed to exist as the "snows" on planets. Thermodynamic, structural, and dynamical studies on clathrate hydrates have been accelerated by technical interest in the natural

gas pipeline blockage and potential fuel resources in perpetually frozen lands and deep-sea sedimentary deposits. The aliphatic hydrocarbons from methane to butane are included as guests in the cages of hydrogen-bonded polyhedral frameworks formed by host water molecules.

The clathrate hydrate structures are classified into types I, II, etc. In the type II structure, the smaller and the larger cages are formed by 12 pentagonal faces ( $5^12$ ) and 12 pentagonal and 4 hexagonal faces ( $5^{12}6^4$ ), respectively. The latter and the former are occupied by larger guests and smaller help gas molecules like  $\text{H}_2\text{S}$ , respectively. The upper limit of the larger cage radius is  $3.3 \text{ \AA}$ , which is slightly smaller than the effective radius of a benzene molecule ( $3.6 \text{ \AA}$ ).

The experimental difficulties such as low solubility of the hydrophobic solute, low measurement sensitivity, and solute disturbance of supercooling can be overcome by

### INTERFACE SCIENCE —Solutions and Interfaces—

#### Scope of research

Structure and dynamics of a variety of ionic and nonionic solutions of physical, chemical, and biochemical interests are systematically studied by NMR under extreme conditions. Simple and complex solution systems are supercooled, overheated, and compressed to high pressures to shed light on microscopic factors which control rotational and translational motions of ions and molecules. Vibrational spectroscopic studies are carried out to elucidate structure and orientations of organic and water molecules in ultra-thin films. Crystallization of protein monolayers, advanced dispersion systems at liquid-liquid interfaces, and biomembranes are also investigated.



Professor  
NAKAHARA, Masaru  
(D Sc)



Associate Professor  
UMEMURA, Junzo  
(D Sc)



Instructor  
MATSUMOTO, Mutsuo  
(D Sc)

#### Technicians:

KIMURA, Noriyuki  
OKAMURA, Emiko

#### Students:

TANO, Takanori (DC)  
WAKAI, Chihiro (DC)  
SAKAI, Hiroshi (DC)  
MAEDA, Hideyuki (MC)  
YOSHIMOTO, Yoshitaka (MC)



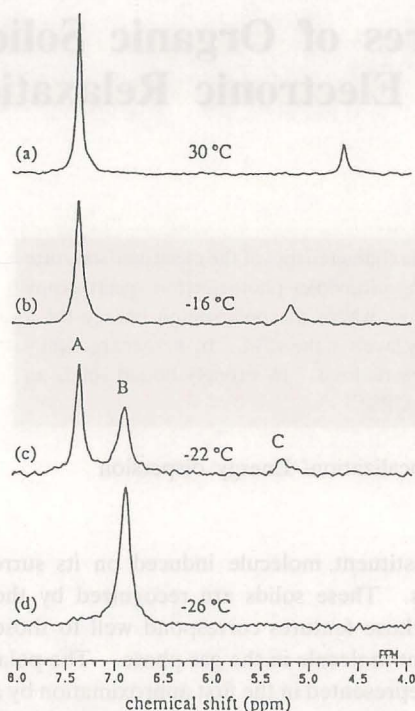


**Figure 1.** Temperature dependence of  $^2\text{H}$  spectra of  $\text{C}_6\text{D}_6$  (23 mM) in  $\text{H}_2\text{O}$  (HOD, 0.032%).

using bundled capillaries in a large sample tube for the high-resolution  $^2\text{H}$ -NMR spin-lattice relaxation time measurement. By using the integrated capillary method, we could not only supercool the aqueous solution but also prepare a clathrate hydrate [2]. Figure 1 shows the  $^2\text{H}$  spectra for solute benzene- $\text{d}_6$  and solvent water over a temperature range of  $-50$  to  $120^\circ\text{C}$ . The dilute benzene solution can be supercooled down to about  $-20^\circ\text{C}$ , as indicated by the presence of the sharp signal assigned to water (HOD, signal C in spectrum c); cf., spectra a, b, and c. The sharp water signal, which reflects the very rapid rotational dynamics of the solvent, shifts to a lower field. The temperature dependence of the water chemical shift is steeper at lower temperatures as already noticed. The down-field shift, indicative of stronger hydrogen bonds, continues in the supercooled regime. At about  $-20^\circ\text{C}$ , however, the sharp water signal disappears as a result of the solvent freezing. At the same time, the solute benzene signal at 7.5 ppm begins to be taken over by a sharp new signal at a higher field; see signals A and B in spectrum c. The up-field shift would be due to the complete loss of weak hydrogen bonding interactions [3] between benzene and water molecules induced by the phase transition.

These spectral changes observed both on the host and guest sides indicate that a clathrate hydrate of benzene is formed at about  $-20^\circ\text{C}$ , and that the benzene molecule encaged reorients very rapidly in the cavities, probably in the type II structure; this is expected from the fact that formation of a cyclohexane clathrate hydrate of type II with a help gas is reported [4]. The effective radius of a benzene molecule is estimated as  $3.6 \text{ \AA}$ , which is slightly larger than the upper-limit cage radius ( $3.3 \text{ \AA}$ ) in the type II structure. The clathrate formation can be regarded as

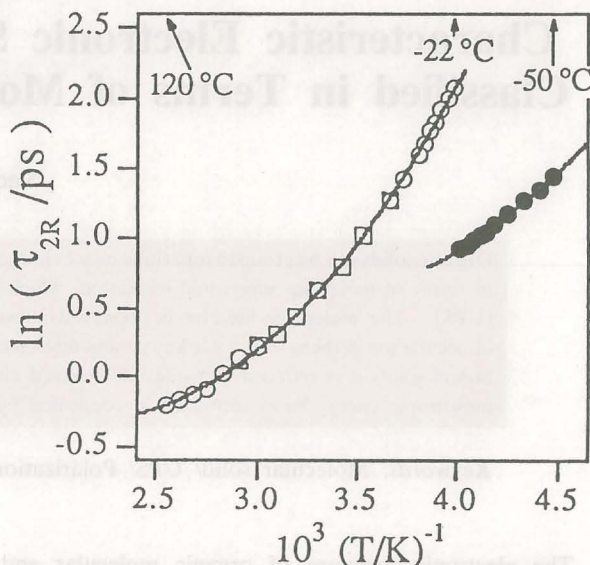


**Figure 2.** Arrhenius plots of the rotational correlation times  $\tau_R$  for  $\text{C}_6\text{D}_6$  in water. Open squares and circles are results obtained from a usual NMR tube of  $\sim 4 \text{ mm}$  i.d. and capillaries of  $0.2\text{--}0.3 \text{ mm}$  i.d., respectively; the agreement of the results between the large tube and capillaries shows that our capillary data at lower temperatures are not affected by capillary interfaces. The solid circles indicate  $\tau_R$  for  $\text{C}_6\text{D}_6$  in clathrate hydrates.

an indication of the hydrophobicity of the benzene molecule, though it is not so strong as lower aliphatic hydrocarbons which more easily yield a clathrate hydrate.

The experimental results are transformed into the rotational correlation times  $\tau_R$  by the usual method [5, 6]. Figure 2 shows the logarithm of the rotational correlation time as a function of the inverse temperature ( $1/T$ ). Noticeably, the rotational correlation time jumps within the transition temperature range, where the local environment of the solute changes from a vigorously fluctuating solution cage into a somewhat rigid clathrate cage. At  $-22^\circ\text{C}$ , the  $\tau_R$  value is  $7.96 \text{ ps}$  in the supercooled aqueous solution cage and  $2.45 \text{ ps}$  in the clathrate hydrate cage. Unexpectedly, the reorientational correlation decays  $3.2$  times faster in the clathrate cage than in the solution cage. Corresponding to the rotational mobility jump, the activation energy for the molecular rotation at  $-22^\circ\text{C}$  drops from  $22 \text{ kJ mol}^{-1}$  in the solution to  $7.6 \text{ kJ mol}^{-1}$  in the clathrate hydrate.

#### References

1. Angell CA in "Water. A Comprehensive Treatise", Franks, F, Ed.; Plenum: New York, Vol. 7, pp. 1–81.
2. Nakahara M, Wakai C and Matubayashi N, *J. Phys. Chem.*, **99**, 1377 (1995).
3. Nakahara M and Wakai C, *J. Chem. Phys.*, **97**, 4413–4420 (1992).
4. Ripmeester JA, Tes JS, Ratcliffe CI and Powell BM, *Nature*, **325**, 135–136 (1987).
5. Matsubayashi N and Nakahara M, *J. Chem. Phys.*, **94**, 653–661 (1991).
6. Wakai C and Nakahara M, *J. Chem. Phys.*, **100**, 8347–8358 (1994).



# Characteristic Electronic Structures of Organic Solids Classified in Terms of Molecular Electronic Relaxation

Naoki Sato

Organic solids can be grouped into three classes in accordance with their characteristics of the electronic structure in terms of molecular electronic relaxation, which is examined using ultraviolet photoelectron spectroscopy (UPS). The molecular identity is preserved in weakly bound solids, where the polarization energy for a molecular ion in them works as a key parameter determining the energy levels in the solid. In mesoenergetically bound solids it is reduced and quasi-delocalized electronic states are realized. In strongly bound solids an anisotropic energy band formation is confirmed by angle-resolved UPS.

**Keywords:** Molecular solid/ UPS/ Polarization energy/ Delocalization/ Energy dispersion

The electronic structure of organic molecular and polymeric solids are characterized by the fact that their constituent has structural and/or electronic 'molecular identity' more or less. In other words, those solids consist of molecular units. Here we do not restrict the meaning of the word a 'molecular unit' only to a practical molecule, but extend it even to an undefined entity such as a repeating unit in a polymeric chain. On the basis of such an idea of the molecular unit, organic solids can be grouped into three classes in terms of the molecular electronic relaxation in them, which is examined by ultraviolet photoelectron spectroscopy (UPS) [1].

The first group of materials are typical molecular solids, in which molecular units identical to constituent molecules are bound by a weak intermolecular interaction or the van der Waals force. The molecular identity is preserved most obviously in these solids, the energy levels of which are settled by the polarization energy evaluating the degree of electrostatic stabilization for an extra charge

on a constituent molecule induced on its surrounding molecules. These solids are recognized by their UPS spectra whose features correspond well to those of the constituent molecule in the gas phase. The polarization energy, represented in the first approximation by a simple relation comprising a mean molecular polarizability and a molecular packing density in the solid, can disclose the energy structure with relation to the intermolecular interaction when it is examined more carefully. Thus the polarization energy works as the key parameter in the weakly bound organic solids.

The second group of materials are mesoenergetically bound systems, in which some inter-unit or inter-molecular interactions extra to the van der Waals force work efficiently in the solid or the molecular identity is reduced to some extent to form quasi-delocalized electronic states over the molecular unit. These systems show a poor correspondence of UPS spectral features between the gaseous and solid states and are

## INTERFACE SCIENCE —Molecular Aggregates—

### Scope of research

*The research at this subdivision is devoted to correlation studies on structures and properties of both natural and artificial molecular aggregates from two main standpoints: photoelectric and dielectric behaviors. The electronic structure of molecular and/or polymeric thin films is studied in connection with the former, and its results are applied to create novel molecular systems with characteristic functions. The latter is concerned with heterogeneous structures in microcapsules, biopolymers, biological membranes and biological cells, and the nonlinearity in their dielectric properties is also studied in relation to molecular motions.*



Professor  
SATO, Naoki  
(D Sc)



Associate Professor  
ASAMI, Koji  
(D Sc)



Instructor  
KITA, Yasuo  
(D Sc)



Instructor  
SEKINE, Katsuhisa  
(D Sc)

### Students:

KAWAMOTO, Ikuko (MC)  
KOIDE, Norihiro (MC)  
HASEGAWA, Masahiro (MC)  
MATSUBARA, Akira (MC)  
ODA, Masao (MC)



characterized by an only apparently large polarization energy. The polarization energy, however, has no longer original physical meaning, and should be regarded as the solid-state relaxation energy including the contribution from additional interactions which are not observed in the weakly bound systems. Such additional inter-unit interactions are caused by 1) a multipole interaction, 2) a charge-transfer interaction, 3) a valence electron mixing, and so on. Now that these interactions are found to work efficiently, those systems have high potentialities to exhibit novel and/or eminent physical properties. As an example of so-called molecular design in expectation of an additional interaction working in the crystal, polythienoacenes are synthesized and examined [2,3].

As the last group of organic systems classified here, strongly bound ones will be referred. Strong inter-unit interactions with a high anisotropy are characteristic of these systems, which consist predominantly of organic polymeric solids and include a few organic molecular solids confirmed so far [4]. Such systems often show the energy dispersion along the strongly coupled direction, e.g., one-dimensional energy band formation along the chain axis of long-chain alkanes, as could be examined by

the angle-resolved ultraviolet photoelectron spectroscopy (ARUPS). Further, electronic relaxation energies in these systems are evaluated to be no less than those of mesoenergetically bound systems [5].

Thus, the magnitude and the dimensionality of inter-unit interactions will determine the nature of a particular system concerned. Information on the electronic structure of organic solids is therefore useful in developing new organic-based molecular systems with a view to realizing molecular electronic devices.

### References

1. Sato N, *Synth. Metals*, **64**, 133 (1994).
2. Sato N, Mazaki Y, Kobayashi K and Kobayashi T, *J. Chem. Soc. Perkin Trans. II*, 765 (1992).
3. Mazaki Y and Kobayashi K, *J. Chem. Soc. Perkin Trans. II*, 761 (1992).
4. Hasegawa S, Mori T, Imaeda K, Tanaka S, Yamashita Y, Inokuchi H, Fujimoto H, Seki K and Ueno N, *J. Chem. Phys.*, **100**, 6969 (1994).
5. Sato N, Lödlund M, Lazzaroni R, Salaneck WR, Brédas J-L, Bradley D D C, Friend R H and Ziemelis K E, *Chem. Phys.*, **160**, 299 (1992).

## The Scanning Dielectric Microscope

Koji Asami

A new instrument has been developed to image the local capacitance (or permittivity) and conductance (or conductivity) of colloidal particles and membranes in an aqueous environment.

**Keywords:** Dielectric image/ Dielectric relaxation/ Capacitance/ Conductance/ Colloidal particle/ Membrane

Electrical properties of colloidal particles including biological cells have been extensively studied by the dielectric technique referred to as suspension method. The method provides average electrical properties of colloidal particles which are extracted from the dielectric data of their suspension using an appropriate dielectric mixture equation. This method, however, is difficult to characterize individual particles. Hence, a new dielectric technique, termed scanning dielectric microscopy, has been developed. Capacitance and conductance are measured by the three-terminal method with a coaxial probe electrode, which is laterally scanned over samples on a plate electrode. The images of the local capacitance and conductance are obtained at frequencies between 1 kHz and 10 MHz, which enables the study of dielectric relaxation of individual particles and local areas of membranes.

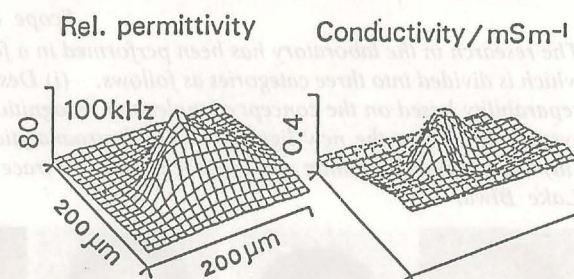


**Figure 1.** Dielectric images of a cultured MDCK cell in 0.3 M mannitol obtained at 0.1 MHz. The image area is 200 mm by 200 mm.



## New Mode of Ion Size Discrimination for Group 2 Metals Using Poly(pyrazolyl)borate Ligands. Control of Stability and Structure of Chelate Complexes by Intra- and InterLigand Contact and Shielding Effect

Yoshiki Sohrin, Masakazu Matsui and Hisao Kokusen\*

Selectivity of  $[\text{HB}(\text{pz})_3]^-$ ,  $[\text{B}(\text{pz})_4]^-$  and  $[\text{HB}(3,5\text{-Me}_2\text{pz})_3]^-$  ( $\text{A}^-$ ;  $\text{pz}$  = 1-pyrazolyl) for group 2 metal ions has been studied by liquid-liquid extraction. Although all the extracted species of  $\text{Mg}^{2+}$ ,  $\text{Ca}^{2+}$ ,  $\text{Sr}^{2+}$  and  $\text{Ba}^{2+}$  were distorted octahedral  $\text{A}_2\text{M}$ , the selectivity was highly dependent on the ligand. The steric properties of the ligands and complexes have been elucidated by X-ray diffraction, NMR and molecular mechanics calculations. Poly(pyrazolyl)borates are unusual chelating ligands due to the steric effects.

**Keywords:** Metal ion recognition/ Ligand design/ Liquid-liquid extraction/ X-ray crystallography/ Molecular mechanics

Discrimination of the ion size is an essential factor in ligand design for selective complexation of metal ions. The size distinction with conventional organic ligands is roughly divided into two types [1]. The first is based on the chelate ring size. The chelate ring size is principally determined by the kind and number of atoms, and the order of bonds contained in the ring. For hard metal ions, such as group 2 and lanthanide, the stability constants of conventional chelating complexes decreases gradually with the increase in the ion size. The other type of ion size discrimination is due to the cavity size of macrocyclic ligands. It is especially visible in rigid and

preorganized macrocycles that the most stable complex is formed when the cation diameter matches the cavity size. The type of distinction of ion size more or less restricts the variety of selectivity pattern for ions. The creation of a new mode of ion size discrimination is desirable to produce a novel pattern of ion selectivity and expand the possibility of metal ion recognition.

The coordination chemistry of poly(pyrazolyl)borate ( $\text{A}^-$ ) is being extensively studied [2]. Many unusual features of the ligands are largely derived from their unique structure. All poly(pyrazolyl)borate complexes contain the six membered ring  $\text{RR}'\text{B}(\mu\text{-pz})_2\text{M}$  structure (1), where R and R' can be pz, H, alkyl, aryl, and so forth ( $\text{pz}$  = 1-pyrazolyl). The chelate ring has a boat configu-

\* Tokyo Gakugei University.

### INTERFACE SCIENCE —Separation Chemistry—

#### Scope of research

The research in the laboratory has been performed in a few years on the design of novel molecular recognition system which is divided into three categories as follows. (i) Design and synthesis of novel ligands with improved stability and separability based on the concept of molecular recognition, and the separation chemistry in the selective metal chelate system employing the new ligands. (ii) Electroanalytical chemistry at liquid-liquid or liquid-membrane interface. (iii) Separation, circulation and biogeochemistry of trace elements in the hydrosphere such as the Pacific Ocean and the Lake Biwa.



Professor  
MATSUI,  
Masakazu  
(D Sc)



Associate Prof.  
KIHARA,  
Sorin  
(D Sc)



Instructor  
SASAKI,  
Yoshihiro  
(D Sc)



Instructor  
UMETANI,  
Shigeo  
(D Sc)



Instructor  
SOHRIN,  
Yoshiki  
(D Sc)

#### Lecturer (part-time):

FUJINO, Osamu  
(Assoc Prof of Kinki Univ.)

#### Technician:

SUZUKI, Mitsuko

#### Students:

SHIRAI, Osamu (DC)  
OBATA, Hajime (DC)  
SASAKI, Takayuki (DC)  
YOSHIDA, Yumi (DC)  
LE, TH Quyen (DC)  
KAWASE, Yusuke (DC)  
TOMITA, Takeshi (MC)  
IWAMOTO, Shunichi (MC)  
TATEISHI, Takuya (MC)



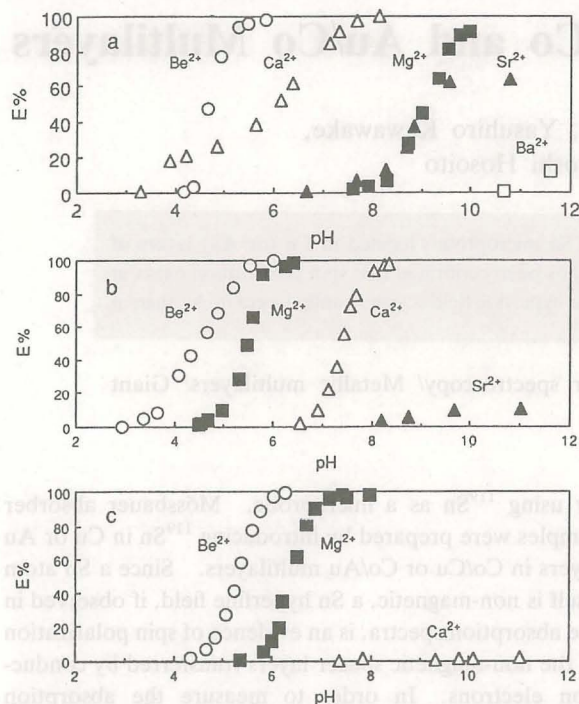
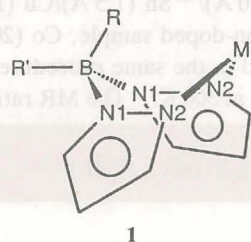


**Figure 1.** Effect of pH on the extraction of group 2 metal ions. Aqueous phase:  $1 \times 10^{-2}$  M KA,  $1 \times 10^{-2}$  M buffer,  $1 \times 10^{-4}$  M  $M^{2+}$  (10 mL). Organic phase: chloroform (10 mL). (a)  $K[HB(3,5-Me_2pz)_3]$ , (b)  $K[HB(pz)_3]$ , (c)  $K[B(pz)_4]$ .

ration, which enables the R group to approach the metal and bond to it. Trofimenko has termed the ligands "scorpionate," since the  $(\mu-pz)_2$  moiety looks like claws and the pseudoaxial R group looks like the stinger of the curving tail.



It is fundamentally important in poly(pyrazolyl)borate chemistry to determine how the scorpionate discriminates its prey (metal ion). However, few studies have been reported on the selectivity of the ligands for metal ions and on the stability of their complexes. We have been studying the liquid-liquid extraction of group 2 metal ions with poly(pyrazolyl)borates, and found selectivity trends that are different from conventional chelating ligands [3]. These selectivity trends are derived from the different mode of ion size discrimination.

Figure 1 shows the relationship between extracted percentage of a metal ion (E%) and pH of the aqueous phase. The selectivity pattern is very different depending on the substituents on the ligand molecule. All ligands are tripodal-tridentate and form octahedral  $A_2M$  complexes. The stability of the complexes is

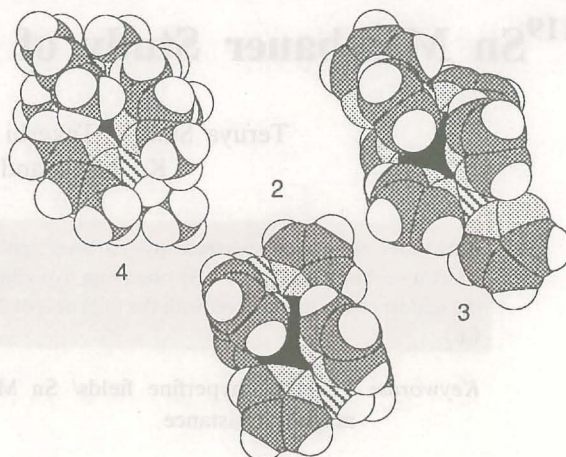


**Figure 2.** Space-filling views of X-ray structure of  $[HB(pz)_3]_2Mg$  (2),  $[B(pz)_4]_2Mg$  (3) and  $[HB(3,5-Me_2pz)_3]_2Mg$  (4). The central metals are shown by black balls.

principally responsible for the selectivity. The stability is controlled by the steric effects of the substituents. Because  $[HB(pz)_3]^-$  has no specific steric effect on formation of the  $A_2M$  complex, its stability decreases in the order  $Mg^{2+} > Ca^{2+} > Sr^{2+}$  which is the usual pattern for chelating ligands. The stability for  $[B(pz)_4]^-$  remarkably drops between  $Mg^{2+}$  and  $Ca^{2+}$ . The complex formation with a large metal ion is prohibited by the intraligand contact due to steric crowding around the boron atom (Figure 2). For  $[HB(3,5-Me_2pz)_3]^-$ , methyl groups on the 3-position of the pyrazolyl ring hinder the  $A_2M$  complex formation for small metal ions through the interligand contact, while they stabilize the complex of large metal ions through the shielding effect. As a result, the order of stability is  $Ca^{2+} > Mg^{2+} > Sr^{2+} > Ba^{2+}$ . These steric factors make  $[B(pz)_4]^-$  and  $[HB(3,5-Me_2pz)_3]^-$  unique ligands in selectivity for the metal ions. It has also been proved that these steric factors produce distinct compositions and structures for  $Be^{2+}$  complexes.

The results of this work demonstrate a new mode of ion size discrimination by chelating ligands. In this mode, selectivity of ligands for metal ions can be readily changed by introduction of substituents on the ligand. Furthermore, such high selectivity of  $[B(pz)_4]^-$  for  $Mg^{2+}$  over  $Ca^{2+}$  has not been attained by conventional chelating ligands.

#### References

- (a) Hancock RD and Martell AE, *Chem. Rev.*, **89**, 1875–1914 (1989). (b) Hancock RD, *Prog. Inorg. Chem.*, **37**, 187–291 (1989).
- Trofimenko S, *Chem. Rev.* **93**, 943–980 (1993).
- (a) Sohrin Y, Kokusen H, Kihara S, Matsui M, Kushi Y and Shiro M, *J. Am. Chem. Soc.*, **115**, 4128–4136 (1993). (b) Sohrin Y, Matsui M, Hata Y, Hasegawa H and Kokusen H, *Inorg. Chem.*, **33**, 4376–4383 (1994).



# <sup>119</sup>Sn Mössbauer Study of Cu/Co and Au/Co Multilayers

Teruya Shinjo, Takeshi Emoto, Yasuhiro Kawawake,  
Ko Mibu and Nobuyoshi Hosoi

Mössbauer absorption spectroscopy has been applied for <sup>119</sup>Sn microprobes located in Cu (or Au) layers of Co/(Cu or Au) multilayers. By observing hyperfine field, it has been confirmed that spin polarization exists in the middle of the spacer layer with the thickness of 20 Å. The hyperfine field is significantly larger in Au than in Cu.

**Keywords:** Magnetic hyperfine fields/ Sn Mössbauer spectroscopy/ Metallic multilayers/ Giant magnetoresistance

Since the discovery of antiferromagnetic interlayer coupling in Fe/Cr/Fe sandwiches [1] and the corresponding giant magnetoresistance (GMR) effect in Fe/Cr multilayers [2], the role of non-magnetic spacer metal layers inserted between magnetic layers has been a subject of intensive studies. The oscillation of interlayer coupling strength is attributed to the Fermi surface nesting of the spacer metal but the mechanism still remains an open question. There have been various measurements to study the properties of magnetic layers. However, the tools to observe directly the magnetic behaviors of spacer layers are very limited and therefore the nature of spacer layers is often speculated from the results on magnetic layers. Studies on spacer layers so far reported are NMR [3] and X-ray dichroism experiments [4], both of which have insisted on the existence of magnetic excitation in Cu layers of Co/Cu multilayers.

In the present study, the Mössbauer spectroscopy has been applied to observe spin polarization in non-magnetic spacer layers sandwiched in between ferromagnetic layers

by using <sup>119</sup>Sn as a microprobe. Mössbauer absorber samples were prepared by introducing <sup>119</sup>Sn in Cu or Au layers in Co/Cu or Co/Au multilayers. Since a Sn atom itself is non-magnetic, a Sn hyperfine field, if observed in the absorption spectra, is an evidence of spin polarization in the non-magnetic spacer layers transferred by conduction electrons. In order to measure the absorption spectra, the samples are required to include a certain amount of the Mössbauer isotope. In the present experiment, the nominal thickness of <sup>119</sup>Sn probing layers is 1.5 Å.

Several Co/Cu and Co/Au multilayer samples including 1.5 Å <sup>119</sup>Sn probing layers were prepared by vacuum deposition method. Samples prepared on polyimide substrates and those on glass ones are used respectively for Mössbauer and X-ray diffraction measurements. The structure of the prepared sample, for example, is; [Co (20 Å)/Cu (10 Å)/<sup>119</sup>Sn (1.5 Å)/Cu (10 Å)]×8. For comparison, a non-doped sample, Co (20 Å)/Cu (20 Å), was also prepared in the same procedure, which showed MR ratio of 17% at 300 K. The MR ratio of the sample

## SOLID STATE CHEMISTRY —Artificial Lattice Alloys—

### Scope of research

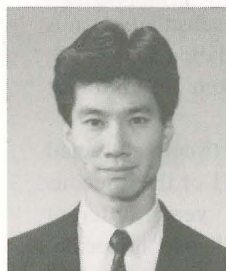
By using vacuum deposition method, artificial multilayers have been prepared by combining various metallic elements. The recent major subject is the giant magnetoresistance (MR) in magnetic/non-magnetic multilayers. Non-coupled type MR multilayers including two magnetic components are found to have high sensitivities in low fields. Fundamental magnetic properties of large MR multilayers have been studied by applying Mössbauer spectroscopy, using Fe-57, Sn-119, Eu-151 and Au-197 as microprobes and by neutron diffraction. Multilayers are also prepared on microstructured substrates and their novel magnetic and MR properties are being investigated.



Professor  
SHINJO, Teruya  
(D Sc)



Associate Professor  
HOSOITO, Nobuyoshi  
(D Sc)



Instructor  
MIBU, Ko  
(D Sc)

### Technician:

KUSUDA, Toshiyuki

### Students:

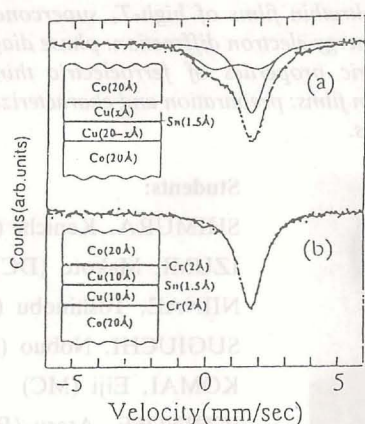
ONO, Teruo (DC)  
EMOTO, Takeshi (DC)  
HIRANO, Koichi (MC)  
SUGITA, Yasunari (MC)  
NAGAHAMA, Taro (MC)  
HAMADA, Sunao (MC)



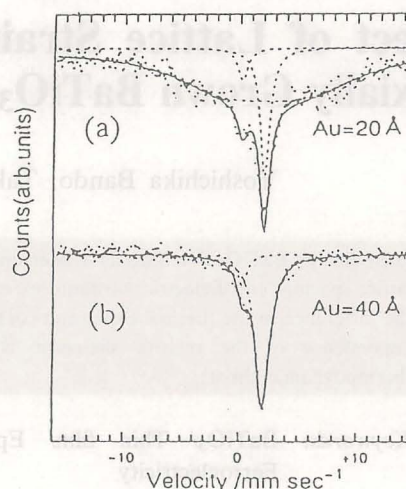
with 1.5 Å Sn layer, 3% is considerably smaller than the standard value. However, the profile of MR curve of the doped sample is very similar to that of non-doped one and therefore the antiferromagnetic interlayer coupling is believed to exist in the doped sample.

Figure 1a shows the  $^{119}\text{Sn}$  absorption spectrum at 300 K for the sample with the illustrated structure. The  $^{119}\text{Sn}$  probing layer has been located in the middle of 20 Å Cu layer sandwiched in between Co layers. The line profile of the spectrum is very broad but can be interpreted as a superposition of two parts; a non-magnetic fraction and another one with a hyperfine broadening. The broadening corresponds to a magnetic field of 16 kOe. The fraction with the broadening is enhanced in the spectra of samples whose Sn probing layer is located closer to the Cu/Co interface. Therefore the origin of the broadening is suggested to be a magnetic hyperfine splitting.

Figure 1b shows the spectrum for a sample whose interface is doped with 2 Å Cr layers (The structure is illustrated in the figure). Although the thickness of Cu layer is the same, 20 Å, the interface-doped sample does not show any MR effect. Therefore, it is suggested that an antiferromagnetic interlayer coupling is cut by inserting a Cr layer in between Co and Cu layers. Consistently, the  $^{119}\text{Sn}$  Mössbauer spectrum is a sharp single line, indicating that no spin polarization exists in the middle of 20 Å Cu layer. From these results, the existence of spin polarization in the Cu layer, at the distance of 10 Å from the interface with Co, is confirmed. The non-magnetic fraction coexisting in Fig. 1a is interpreted as Sn microclusters. If several Sn atoms are coagulated, the spin polarization in Cu layer would not be transferred at the Sn sites. Another interpretation is as follows: The spin polarization is spatially oscillating and the hyperfine field should be zero at the site where the spin polarization is zero. If it is the case, the relative amount of non-magnetic fraction may depend on the magnetic structure, being parallel or anti-parallel. We have measured the spectra for parallel magnetization with applying an external field but the non-magnetic fraction does not show any change. Therefore, it is not probable



**Figure 1.**  $^{119}\text{Sn}$  Mössbauer absorption spectra at 300 K of (a)  $[\text{Co} (20 \text{ Å})/\text{Cu} (10 \text{ Å})/^{119}\text{Sn} (1.5 \text{ Å})/\text{Cu} (10 \text{ Å})] \times 8$ . (b)  $[\text{Co} (20 \text{ Å})/\text{Cr} (2 \text{ Å})/\text{Cu} (10 \text{ Å})/^{119}\text{Sn} (1.5 \text{ Å})/\text{Cu} (10 \text{ Å})/\text{Cr} (2 \text{ Å})] \times 8$ .



**Figure 2.**  $^{119}\text{Sn}$  Mössbauer absorption spectra at 300 K of (a)  $[\text{Co} (20 \text{ Å})/\text{Au} (10 \text{ Å})/^{119}\text{Sn} (1.5 \text{ Å})/\text{Au} (10 \text{ Å})] \times 16$ . (b)  $[\text{Co} (20 \text{ Å})/\text{Au} (20 \text{ Å})/^{119}\text{Sn} (1.5 \text{ Å})/\text{Au} (20 \text{ Å})] \times 16$ .

that the non-magnetic absorption is originated from an intrinsic properties of the spacer layers.

Similar experiments have been carried out for Co/Au multilayers in order to elucidate the difference of spin polarization in Cu and Au layers. The probing layers, 1.5 Å  $^{119}\text{Sn}$ , are located in the middle of 20 Å Au and 40 Å Au layers sandwiched between in Co layers. As shown in Fig. 2a, the spectrum for the 20 Å has a magnetic hyperfine structure, while the 40 Å sample shows only a single line pattern without a magnetic hyperfine broadening. These results suggest that the spin polarization originated from an adjacent ferromagnetic Co layer extends in a Au layer for more than 10 Å but less than 20 Å. Similarly to the case of 20 Å Cu, a non-magnetic fraction coexists in the spectrum for 20 Å Au. A remarkable contrast between the results on Sn impurities in Cu and Au layers is the magnitude of hyperfine field, which suggests a difference between an induced hyperfine field at Sn nuclei by 4s electron spin polarization in Cu and that by 6s electron spin polarization in Au. The spectrum for  $^{119}\text{Sn}$  in the middle of 20 Å Au layer sandwiched between Co layers exhibits a very large broadening, which corresponds to about 70 kOe. This value is much larger than the hyperfine field of Sn impurity in bulk Co at 0 K (25 kOe) [5]. It is therefore suggested that a core electron spin polarization at Sn atom is induced via 6s electron of Au layer.

In summary, using  $^{119}\text{Sn}$  Mössbauer probe, the spin polarization in a non-magnetic metal layer is able to be detected. However, the resolution is not enough to study the oscillatory behaviors of spin polarization.

## References

1. Grünberg P, *et al*, *Phys. Rev. Lett.*, **57**, 2442 (1986).
2. Baibich MN, *et al*, *Phys. Rev. Lett.*, **61**, 2472 (1988).
3. Goto A, *et al*, *J. Phys. Soc. Jpn.*, **62**, 2129 (1993).
4. Bobo JF, *et al*, *J. Magn. & Magn. Mater.*, **126**, 251 (1993).
5. Cranshaw TE, *J. Appl. Phys.*, **40**, 1481 (1969).



# Effect of Lattice Strain on Ferroelectric Properties of Epitaxially Grown BaTiO<sub>3</sub> Thin Films by Reactive Evaporation

Yoshichika Bando, Takahito Terashima, and Yoshihiko Yano\*

Ferroelectric BaTiO<sub>3</sub> thin films have been epitaxially grown by reactive evaporation. The thickness variation of lattice spacings and dielectric constants are caused by the two-dimensional stress due to the lattice mismatch and the difference in the thermal expansion coefficients between an epitaxial layer and a substrate. The thickness dependence of the relative dielectric constant  $\epsilon_r$  can be explained by Landau-Ginsburg-Devonshire thermodynamic theory.

**Keywords:** BaTiO<sub>3</sub>/ Thin film/ Epitaxial growth/ Reactive evaporation/ Lattice strain/ Ferroelectricity

Recently, thin films of ferroelectric oxides are widely studied for the applications in nonvolatile memories, infrared sensors, and electro-optic devices. BaTiO<sub>3</sub> is known as a typical ferroelectric oxide having relatively large dielectric constants. We report structural and dielectric properties of epitaxially grown BaTiO<sub>3</sub> thin films.

BaTiO<sub>3</sub> films are grown by a reactive evaporation method [1]. Essentially, this method is a co-evaporation of metal elements under an oxygen atmosphere [2]. The local oxygen pressure near the substrate is  $10^0$ – $10^1$  Pa. The deposition rate is about 0.2 nm/s. The substrate temperature is 700°C. The (100) SrTiO<sub>3</sub> and the (100) oriented Pt single crystal thin film (100 nm) grown on MgO (100) are used as substrates.

Atomic force microscope (AFM) observation has

\* Permanent Address: R & D Center, TDK Corporation, Ichikawa-shi, Chiba 272, Japan.

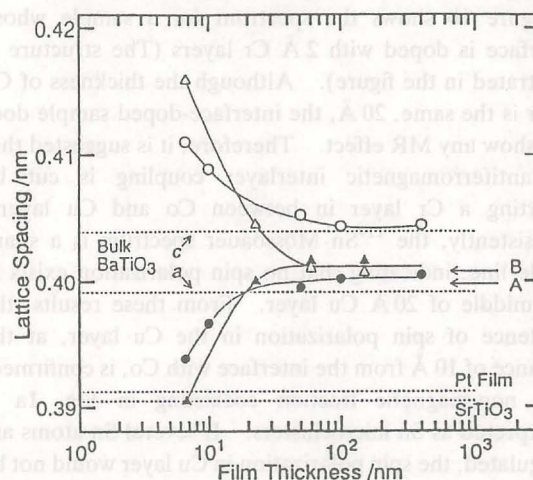


**Figure 1.** Lattice spacings as a function of film thickness. The lattice spacings of bulk BaTiO<sub>3</sub> and SrTiO<sub>3</sub> and *a* of Pt film on MgO are given by the dashed lines. ○, ●: lattice spacings *c* and *a* on Pt/MgO; △, ▲: *c* and *a* on SrTiO<sub>3</sub>.

## SOLID STATE CHEMISTRY —Artificial Lattice Compounds—

### Scope of research

*Syntheses of oxide thin films by reactive evaporation and ceramics by solid state reaction and their characterizations are studied. The main subjects are: preparation and characterization of ultrathin films of high-*T<sub>c</sub>* superconductors: investigation of growth mechanism of thin films by in situ reflection high-energy electron diffraction: phase diagram of Bi<sub>2</sub>O<sub>3</sub>-SrO-CaO-CuO system: preparation and observation of dielectric properties of ferroelectric thin films: preparation and characterization of metallic and ferromagnetic SrRuO<sub>3</sub> thin films: preparation and characterization of artificial superlattices comprising of oxides, metals, and semiconductors.*



Professor  
BANDO, Yoshichika  
(D Sc)



Instructor  
IKEDA, Yasunori  
(1993)



Instructor  
TERASHIMA, Takahito  
(D Sc)

### Students:

SHIMURA, Kenichi (DC)  
IZUMI, Makoto (DC)  
NIINAE, Toshinobu (DC)  
SUGIUCHI, Nobuo (MC)  
KOMAI, Eiji (MC)  
ICHINOSE, Ataru (RS)



shown that a two-dimensional growth occurs from the initial stage on SrTiO<sub>3</sub> substrate and an island growth occurs on Pt substrate. The island structure changes into a continuous layer when the thickness is over 1.2 nm. *In situ* reflection high-energy electron diffraction (RHEED) observation has revealed that the initial nuclei on Pt have perovskite structure.

In Fig. 1, the lattice spacings  $a$  and  $c$  of BaTiO<sub>3</sub> films determined from X-ray diffraction are given as a function of film thickness [3]. The lattice spacing  $a$  decreases and  $c$  increases with decreasing film thickness. The ultrathin films with the thickness below 10 nm show a large contraction along the  $a$ -direction by accommodating elastically the lattice mismatch between BaTiO<sub>3</sub> and Pt or SrTiO<sub>3</sub>. A large elongation along the  $c$ -direction originates from the large contraction of the  $a$ -axis.

For the films with the thickness over 50 nm, the lattice spacings get close to the bulk values due to the introduction of misfit dislocations. The lattice spacings, however, are not in agreement with the bulk values even at a thickness of 400 nm. Figure 2(a) shows thermal expansion curves for BaTiO<sub>3</sub>, MgO, and SrTiO<sub>3</sub>. While the BaTiO<sub>3</sub> film is cooled from the growth temperature of 700°C to room temperature, the lattice of the BaTiO<sub>3</sub> film may not be contracted according to its thermal expansion curve due to the strong effect from the substrate. If the lattice spacing of the BaTiO<sub>3</sub> film grown on the both substrates with the thickness larger than 50 nm is the same to the bulk value at the growth temperature of 700°C and is contracted according to the thermal expansion curve for the substrate, the lattice spacing  $a$  would be varied with temperature as shown in Fig. 2(b). The lattice spacing  $a$ 's of 0.4007 nm (B) for SrTiO<sub>3</sub> and 0.3999 nm (A) for Pt/MgO at the room temperature derived from the curves of Fig. 2(b) are in good agreement with those from X-ray measurement.

Figure 3 shows the thickness dependence of the observed relative dielectric constant  $\epsilon_r$  for the BaTiO<sub>3</sub> films grown on Pt/MgO substrate.  $\epsilon_r$  increases with increasing film thickness and is saturated to  $\epsilon_r \sim 700$  which is larger than bulk value along the  $c$ -axis. We have calculated the thickness dependence of  $\epsilon_r$  by the Landau-Ginsburg-Devonshire thermodynamic theory [4]. For BaTiO<sub>3</sub> in tetragonal state ( $P4mm$ ), the spontaneous polarization,  $P_s$ , is determined to be  $P_s^2 = \{-\alpha_{11} + [\alpha_{11}^2 - 3\alpha_{111}(\alpha_{11} - 2Q_{12}H)]^{1/2}\} / 3\alpha_{111}$  (i), where  $H$  is a two-dimensional stress;  $\alpha_1$ ,  $\alpha_{11}$ , and  $\alpha_{111}$  are dielectric stiffness and higher-order stiffness coefficients at constant stress; and  $Q_{12}$  is a cubic electrostrictive constant. We can relate  $H$  to a lattice strain  $x_1$  ( $= (a_o - a_c)/a_c$ ) as  $x_1 = Q_{12}P_s^2 + (s_{11} + s_{12})H$  (ii), where  $a_o$  is a lattice spacing determined from X-ray diffraction and  $a_c$  is a calculated lattice spacing of strained structure extrapolated to room temperature (point A in Fig. 2(b)); and  $s_{11}$  and  $s_{12}$  are elastic compliance coefficients. Thus,  $\epsilon_r$  is given by  $\epsilon_r = 1 + \eta_{33} = 1 + [2\epsilon_0(\alpha_1 - 2Q_{12}H + 6\alpha_{11}P_s^2 + 15\alpha_{111}P_s^4)]^{-1}$  (iii). The dotted line in Fig. 3 is a calculated curve for the thickness dependence of  $\epsilon_r$  using Eqs. (i)–(iii), bulk values of dielectric parameters [5, 6] and X-ray data in

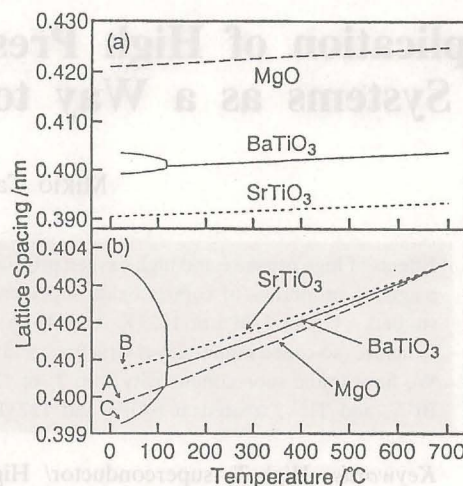


Figure 2. (a) Thermal expansion curves of BaTiO<sub>3</sub>, MgO and SrTiO<sub>3</sub>. (b) The calculated thermal expansion curves for the BaTiO<sub>3</sub> films grown on Pt/MgO and SrTiO<sub>3</sub>, where the thermal expansion of the film is dominated by the substrate.

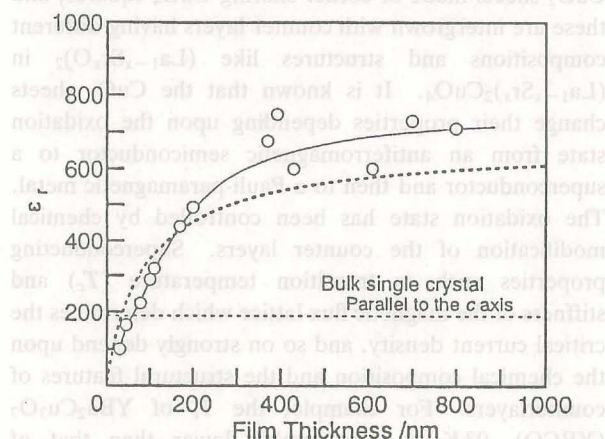


Figure 3. Relative dielectric constant  $\epsilon_r$  as a function of film thickness at room temperature. Calculated curve of  $\epsilon_r$  is given by dashed line.

Fig. 1. The agreement between the experimental results and the theoretical curve is fairly good, indicating that the thickness dependence of  $\epsilon_r$  originates from the two-dimensional stress in BaTiO<sub>3</sub> films due to the lattice mismatch and/or the difference in the thermal expansion coefficient.

#### References

1. Iijima K, Terashima T, Yamamoto K, Hirata K and Bando Y, *Appl. Phys. Lett.*, **56**, 527–529 (1990).
2. Terashima T, Iijima K, Yamamoto K, Bando Y and Mazaki H, *Jpn. J. Appl. Phys.*, **27**, L91–L93 (1988).
3. Terauchi H, Watanabe Y, Kasatani H, Kamigaki K, Yano Y, Terashima T and Bando Y, *J. Phys. Soc. Jpn.*, **61**, 2194–2197 (1992).
4. Devonshire A F, *Philos. Mag.*, **40**, 1040–1063 (1949).
5. Buessem WR, Cross LE and Goswami AK, *J. Am. Ceram. Soc.*, **49**, 33–36 (1966).
6. Goswami AK, *J. Phys. Soc. Jpn.* **21** 1037–1040 (1966).



# Application of High Pressure to Complex Copper Oxide Systems as a Way to Find New Superconductors

Mikio Takano and Zenji Hiroi

Effects of high pressure and high oxygen pressure on the formation, structure, oxygen content, and electrical and magnetic properties of copper oxide superconductors crystallizing in perovskite-related structures have been studied. Under 6 GPa at 1223 K  $\text{ACuO}_2$  (A:  $\text{Ba}_{1/3}\text{Sr}_{2/3}$ – $\text{Sr}_{1/3}\text{Ca}_{2/3}$ ) is stabilized in the  $\text{Ca}_{0.84}\text{Sr}_{0.16}\text{CuO}_2$  type structure (so-called infinite-layer structure) and  $\text{R}_2\text{CuO}_4$  (R: Y, Dy, Ho, Er, Tm) in the  $\text{Nd}_2\text{CuO}_4$ -type structure. We have found superconductivity with  $T_c$  of 110 K in the  $\text{Sr}_{1-x}\text{Ca}_x\text{CuO}_2$  system, free from any rare earth ion,  $\text{Bi}^{3+}$ , and  $\text{Ti}^{3+}$ , treated at 6 GPa and 1273 K.

**Keywords:** High- $T_c$  superconductor/ High pressure synthesis/ Infinite-layer structure/  $\text{ACuO}_2$ /  
 $\text{R}_2\text{CuO}_4$

All the known cupric oxide superconductors contain  $\text{CuO}_2$  sheets made of corner sharing  $\text{CuO}_4$  squares, and these are intergrown with counter layers having different compositions and structures like  $(\text{La}_{1-x}\text{Sr}_x\text{O})_2$  in  $(\text{La}_{1-x}\text{Sr}_x)_2\text{CuO}_4$ . It is known that the  $\text{CuO}_2$  sheets change their properties depending upon the oxidation state from an antiferromagnetic semiconductor to a superconductor and then to a Pauli-paramagnetic metal. The oxidation state has been controlled by chemical modification of the counter layers. Superconducting properties such as transition temperature ( $T_c$ ) and stiffness of the magnetic flux lattice which determines the critical current density, and so on strongly depend upon the chemical composition and the structural features of counterlayers. For example, the  $T_c$  of  $\text{YBa}_2\text{Cu}_3\text{O}_7$  (YBCO), 93 K, is considerably lower than that of  $\text{HgBa}_2\text{CaCu}_2\text{O}_{6+\delta}$ , 125 K, while the stiffness of the magnetic flux lattice, a very important parameter from

the viewpoint of practical application, is considerably larger for YBCO. YBCO consists of a superconducting  $[\text{CuO}_2/\text{Y}/\text{CuO}_2]$  unit and a counter unit of  $[\text{BaO}/\text{CuO}/\text{BaO}]$ , while the Hg-based phase contains corresponding units of  $[\text{CuO}_2/\text{Ca}/\text{CuO}_2]$  and  $[\text{BaO}/\text{HgO}_8/\text{BaO}]$ . Optimization of superconducting properties thus requires a further search for new counterlayers.

Since the discovery of the high- $T_c$  superconductor by Bednorz and Müller [1] the search for new superconducting compounds has been pursued mainly by exploring a range of chemical compositions (counter cations and oxygen content) and reaction temperatures. To such a trend, we have added one more degree of freedom, pressure, and found some new complex cupric oxides including three superconductors [2–4]. Since the Cu-O bond and the counter cation-O bond should have different compressibilities, it is quite reasonable to assume that use of high pressure leads us to finding new

## SOLID STATE CHEMISTRY —Multicomponent Materials—

### Scope of Research

*Inorganic materials that have new and useful functions such as superconductivity and ferromagnetism are synthesized by novel methods. Particularly the search for new high- $T_c$  superconductors is intensively conducted using a high pressure synthesis technique at a pressure range of 3–8 GPa, where materials of high density unavailable under ambient pressure can form.*



Professor  
TAKANO, Mikio  
(D Sc)



Instructor  
HIROI, Zenji  
(D Sc)

### Students:

AZUMA, Masaki (DC)  
CHONG, Iksu (DC)  
KOBAYASHI, Naoya (DC)  
YAMAURA, Kazunari (DC)  
IZAKI, Yoshihito (MC)  
KAWASAKI, Shuji (MC)  
POULSEN, Jakob (RS)  
WADA, Masayoshi (RF)



phases and new compositions.

The simplest composition and structure containing the above type of  $\text{CuO}_2$  sheets can be seen in  $\text{ACuO}_2$  having the so-called infinite-layer structure. This structure was reported for the first time by Siegrist *et al.* for  $\text{Ca}_{0.84}\text{Sr}_{0.16}\text{CuO}_2$  [5]. Along the tetragonal  $c$  axis regular  $\text{CuO}_2$  sheets alternate with A layers without oxygen as shown in Fig. 1. Although a monophasic sample can be obtained only for a narrow composition range of  $A \sim \text{Ca}_{0.9}\text{Sr}_{0.1}$  at ambient pressure, we found that application of high pressure stabilizes this structure for a wide composition range of  $A = \text{Ba}_{1/3}\text{Sr}_{2/3} - \text{Sr}_{1/3}\text{Ca}_{2/3}$  at least [6]. It is noticed from a comparison of specific density that application of high pressure induces a crystalline transition to a high density form. In the case of  $A = \text{Sr}$ , the ambient pressure phase contains double Cu-O chains bundled by edge-sharing, which are sandwiched by a pair of SrO layers of the rock-salt type. In comparison with this the high pressure form is more compact, higher in specific density by more than 7%.

Goodenough and Manthiram pointed out the relation between the sign of carriers to be injected into  $\text{CuO}_2$  sheets and the mechanical stress imposed upon the  $\text{CuO}_2$  sheets. Bond-length mismatch across the interface between the  $\text{CuO}_2$  sheets and the counter layers creates a tensile stress within one layer and a compressive stress in the other.  $\text{CuO}_2$  sheets under compression as in  $\text{La}_2\text{CuO}_4$  are readily doped p-type, but those under tension as in  $\text{Nd}_2\text{CuO}_4$  are doped n-type, because the mismatch can be eased by contraction and expansion of the  $\text{CuO}_2$  sheets on oxidation (p-type) and reduction (n-type), respectively.

The  $\text{CuO}_2$  sheets in  $\text{ACuO}_2$  may be subject to a considerably strong tensile stress for a composition range around  $A = \text{Sr}$ . This structural instability may be relaxed in the following ways. One is to make the Cu-O bond longer by injecting excess electrons into the  $\text{CuO}_2$  sheets. The other is to introduce vacancies to the A cation sites and, thereby, make the average A ion size smaller. We reported the presence of superconducting phases in the Sr(Ba)-Cu-O system with  $T_c = 60\text{--}100\text{ K}$  [7], while Smith *et al.* found superconductivity with a  $T_c \sim 40\text{ K}$  in the Sr-Nd-Cu-O system more recently [8]. In the latter system the superconducting phase seems to be of the infinite-layer structure formulated as  $\text{Sr}_{1-x}\text{Nd}_x\text{CuO}_2$ . As  $x$  increases, the  $a$  axis is elongated but the  $c$  axis is shortened as expected above.


Another remarkable result of our high pressure synthesis under 6 GPa at 1223 K–1273 K is the stabilization of  $\text{R}_2\text{CuO}_4$  with  $R = \text{Y, Dy, Ho, Er, and Tm}$  in the  $\text{Nd}_2\text{CuO}_4$ -type structure [9]. Under ambient pressure this structure is stabilized only for R ions larger than  $\text{Gd}^{3+}$ . These results are consistent with a general tendency that high pressure increases the coordination number of a small cation.

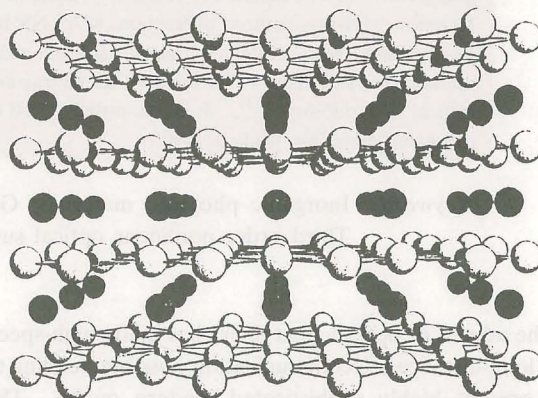


**Figure 1.** Infinite-layer structure, the parent structure of all the known cupric oxide superconductors. The  $\text{CuO}_2$  planes and the alkaline-earth atom planes stack alternately along the  $c$  axis. Large dark and bright spheres represent A and oxygen atoms, respectively, and small dark spheres copper atoms.

#### References

1. Bednorz J G and Müller K A, *Z. Phys. B*, **64**, 189–193 (1986).
2. Azuma M, Hiroi Z, Takano M, Bando Y and Takeda Y, *Nature*, **356**, 775–776 (1992).
3. Hiroi Z, Takano M, Azuma M and Takeda Y, *Nature*, **364**, 315–317 (1993).
4. Hiroi Z, Kobayashi N and Takano M, *Nature*, **371**, 139–141 (1994).
5. Siegrist T, Schneemeyer LF, Sunshine SA and Waszczak J V, *Mat. Res. Bull.*, **23**, 1429–1438 (1988).
6. Takano M, Takeda Y, Okada H, Miyamoto M and Kusaka K, *Physica C*, **159**, 375–378 (1989).
7. Takano M, Azuma M, Hiroi Z, Bando Y and Takeda Y, *Physica C*, **176**, 441–444 (1991).
8. Smith M G, Manthiram A, Zhou J, Goodenough J B and Market J T, *Nature*, **351**, 549–551 (1991).
9. Okada H, Takano M and Takeda Y, *Physica C*, **166**, 111–114 (1990).

 N. Kuroki (D Eng)	 K. Kozuka (D Eng)	 Y. Yoko (D Eng)
---	--	---



## Inorganic Photonic Materials — Preparation and Third Order Non-Linear Optical Properties

Toshinobu Yoko, Hiromitsu Kozuka and Tadanori Hashimoto

Third order nonlinear optical properties of various non-conventional glasses such as  $\text{TeO}_2$ -,  $\text{Ga}_2\text{O}_3$ -,  $\text{Sb}_2\text{O}_3$ -based glasses have been examined in relation to glass structure which was studied by using a number of experimental techniques (X-ray, neutron diffraction, MAS-NMR, IR, Raman Spectroscopy etc.). In addition, coating films of transition metal oxides and metal oxides containing metal fine particles have been prepared by the sol-gel method and subjected to various optical characterizations by focusing especially on the third order nonlinear optical susceptibility,  $\chi^{(3)}$ . It is found that  $\alpha\text{-Fe}_2\text{O}_3$  exhibits the highest  $\chi^{(3)}$  value of  $5.8 \times 10^{-11}$  esu among the inorganic materials studied so far.

**Keywords:** Inorganic photonic materials/ Glasses/ Thin films/ Sol-gel method/ Glass Structure/ Third order nonlinear optical susceptibility  $\chi^{(3)}$

The advent of optical glass fibers has made high-speed and long-distance telecommunication possible, leading to the present highly sophisticated modern media. The present optical telecommunication system is, however, limited by the processing speed of electronics currently used. Nonlinear optical (NLO) devices will overcome this problem because they can switch and process signal in a time scale of  $10^{-15}$  s inaccessible to electronics ( $10^{-12}$  s) without converting it into electronic form. Moreover, it is anticipated that the ultrahigh-speed "optical computer," in which optical switching devices are utilized, will replace the conventional, semiconductor-driven computer in the near future. Therefore, it is urgently necessary to develop nonlinear optical materials which can be used as NLO devices. In our laboratory, two types of inorganic NLO materials are studied: (1) non-conventional glasses by melting method, (2) coating

films formed on a glass substrate by the sol-gel method. We will present several representative results currently obtained in the following.

A thin plate of  $\text{TeO}_2$  glass of  $5.0 \times 4.0 \times 0.25 \text{ mm}^3$  in size, which was large enough for various optical measurements, was obtained by a rapid quenching method. The linear refractive index was measured as a function of wavelength from 486.1 to 1000 nm. The refractive index at 486.1 nm was as high as 2.239. The optical energy band gap was estimated as 3.37 eV from the optical absorption spectrum. The third-order nonlinear optical susceptibility,  $\chi^{(3)}$ , was determined by the third-harmonic generation (THG) method. The  $\chi^{(3)}$  value was as high as  $1.4 \times 10^{-12}$  esu, about 50 times as large as that of  $\text{SiO}_2$  glass. The results are discussed based on Lines' model in which an influence of cationic empty  $d$ -orbital on the nonlinear properties is taken into

### SOLID STATE CHEMISTRY —Amorphous Materials—

#### Scope of research

Two main subjects have been studied in this laboratory. The first is to develop a new family of glasses which do not contain so-called glass formers such as  $\text{SiO}_2$ ,  $\text{P}_2\text{O}_5$ ,  $\text{B}_2\text{O}_3$  and so on. Relationships between glass formation and structure, and then relationships between structure and properties, especially nonlinear optical properties, are tried to be established. The second is to synthesize new functional inorganic thin films by the sol-gel method which is known as one of the most advantageous low temperature synthesis processes. Our attention is focused especially on the nonlinear optical properties of these films.



Professor  
YOKO, Toshinobu  
(D Eng)



Associate Professor  
KOZUKA, Hiromitsu  
(D Eng)



Instructor  
HASHIMOTO, Tadanori  
(D Eng)

#### Guest Research

##### Associates:

INNOCENZI, Plinio  
JIN, Jisun  
KIM, Sae-Hoon  
KITAOKA, Kenji  
ZHAO, Gaoling

##### Students:

FUJIHARA, Shinobu (DC)  
TERASHIMA, Kentaro (DC)  
ISHIBASHI, Keiji (MC)  
OKUNO, Masahiro (MC)  
UTSUMI, Shigeru (MC)  
SAKAI, Hideo (MC)  
SAKIDA, Shinichi (MC)  
YAMADA, Tetsuya (MC)  
HATTORI, Takeshi (UG)  
NAKATA, Kunihiko (UG)



account.

Rutile and anatase thin films have been prepared by sol-gel method using  $\text{Ti}(\text{OC}_3\text{H}_7)_4$ . Third-order nonlinear optical properties of both  $\text{TiO}_2$  thin films have been investigated by the third-harmonic generation (THG) method and the effect of the polymorph of  $\text{TiO}_2$  on the third-order nonlinear optical susceptibility,  $\chi^{(3)}$ , has been examined. The measured  $\chi^{(3)}$  values of rutile and anatase thin films were  $1.4 \times 10^{-12}$  and  $9.7 \times 10^{-13}$  esu, respectively. The  $\chi^{(3)}$  values corrected for the porosity of the film were  $4.0 \times 10^{-12}$  (rutile) and  $2.4 \times 10^{-12}$  esu (anatase), which are about 100 times as high as that of  $\text{SiO}_2$  glass used as standard sample ( $2.8 \times 10^{-14}$  esu). The measured and corrected  $\chi^{(3)}$  values were discussed in comparison with those calculated on the basis of several models.

The third-order nonlinear optical properties of sol-gel derived transition metal oxide,  $\text{V}_2\text{O}_5$ ,  $\text{Nb}_2\text{O}_5$  and  $\text{Ta}_2\text{O}_5$ , thin films have been investigated by the third-harmonic generation method and the effect of the metal-oxygen bond length on the third-order nonlinear optical susceptibility,  $\chi^{(3)}$ , has been examined. The  $\chi^{(3)}$  values of  $\text{V}_2\text{O}_5$ ,  $\text{Nb}_2\text{O}_5$  and  $\text{Ta}_2\text{O}_5$  thin films were  $1.1 \times 10^{-11}$ ,  $1.3 \times 10^{-12}$  and  $6.1 \times 10^{-13}$  esu, respectively, which corresponds to an increase of the average bond length,  $l_b$ , in the order of V-O ( $l_b = 0.183$  nm), Nb-O ( $l_b = 0.200$  nm) and Ta-O ( $l_b = 0.204$  nm). The present and previous results indicate that  $\chi^{(3)}$  of these transition metal oxides with the empty d orbitals is dominated mainly by the metal-oxygen bond length rather than the valence of metal cation. It is predicted on the basis of Lines' model that transition metal oxides with the shortest  $l_b$  exhibit the highest  $\chi^{(3)}$  while non-transition metal oxides with the longest  $l_b$  do the highest  $\chi^{(3)}$ .

The third-order nonlinear optical properties of sol-gel  $\alpha\text{-Fe}_2\text{O}_3$ ,  $\gamma\text{-Fe}_2\text{O}_3$  and  $\text{Fe}_3\text{O}_4$  thin films have been investigated by the third-harmonic generation (THG) method. Especially, the effects of the valence and coordination number of Fe ions on the third-order nonlinear optical susceptibility,  $\chi^{(3)}$ , have been examined. The  $\chi^{(3)}$  values of  $\alpha\text{-Fe}_2\text{O}_3$ ,  $\gamma\text{-Fe}_2\text{O}_3$  and  $\text{Fe}_3\text{O}_4$  thin films were  $5.8 \times 10^{-11}$ ,  $2.1 \times 10^{-11}$  and  $4.0 \times 10^{-10}$  esu, respectively, which are the highest values among inorganic oxides reported so far. It was considered that  $\chi^{(3)}$  of  $\alpha\text{-Fe}_2\text{O}_3$  and  $\gamma\text{-Fe}_2\text{O}_3$  was enhanced by the pair excitation process involving the simulation of magnetically coupled two neighboring  $\text{Fe}^{3+}$  ions while  $\chi^{(3)}$  of  $\text{Fe}_3\text{O}_4$  by both one- and three-photon resonances. The higher second-hyperpolarizability,  $\gamma(\text{Fe}_{x/y}\text{O})$ , was obtained when the valence of Fe ions is 3+ rather than 2+ and octahedrally rather than tetrahedrally coordinated by oxygens.

Third-order nonlinear optical properties of sol-gel derived  $\text{FeTiO}_3$  thin films have been investigated by the

third-harmonic generation (THG) method, and the effect of valence of Fe ions on the third-order nonlinear optical susceptibility,  $\chi^{(3)}$ , has been examined. The  $\chi^{(3)}$  value of  $\text{FeTiO}_3$  thin film was  $3.3 \times 10^{-12}$  esu, which is comparable to those of  $\text{TiO}_2$  polymorphs (rutile and anatase) but one order of magnitude lower than of  $\alpha\text{-Fe}_2\text{O}_3$ . Second-hyperpolarizability per  $\text{Fe}^{2+}\text{O}$  formula unit,  $\gamma(\text{Fe}^{2+}\text{O})$ , was one fourth to one third of  $\gamma(\text{Fe}_{2/3}^{3+}\text{O})$  and about four times as large as  $\gamma(\text{Ti}_{1/2}^{4+}\text{O})$ , indicating that the  $\chi^{(3)}$  value of  $\text{FeTiO}_3$  may be dominated by the  $\gamma(\text{Fe}^{2+}\text{O})$  rather than  $\gamma(\text{Ti}_{1/2}^{4+}\text{O})$ .

The preparation process of single phase  $\text{Pb}(\text{Fe}_{1/2}\text{Nb}_{1/2})\text{O}_3$  (PFN) perovskite films on glass substrates by sol-gel method has been investigated and several optical properties of the resultant transparent PFN films have been examined. The refractive index at 633 nm of PFN perovskite films is as large as 2.409, which is larger than  $\text{Pb}_3\text{Nb}_4\text{O}_{13}$  pyrochlore films by 0.14–0.16 at any wavelength. The  $\chi^{(3)}$  of PFN films is estimated as  $7.5 \times 10^{-12}$  esu, which is the second highest value among oxides so far obtained. The  $\chi^{(3)}$  of pyrochlore films is estimated as  $2.8 \times 10^{-12}$  esu, which is one-third as small as that of PFN films.

Silica coating films of 0.5–0.7 mm thickness doped by gold metal particles were prepared by heating gel coating films obtained from solutions of acid-catalyzed methyltriethoxysilane (MTES) and tetraethoxysilane (TEOS) mixture containing chlorauric acid tetrahydrate. Transparent coating films with deep blue, red, and purple colors were obtained. Changes in size and shape of the gold particles with the MTES content were observed. Lower MTES contents gave bigger and non-spherical particles, while higher MTES contents produced smaller and more spherical particles with a more uniform size distribution. The effect of heat-treatment temperature on the shape, size, and size distribution of the metallic gold particles was also studied.

## References

1. Yoko T, Hashimoto T and Ishibashi K, *NEW GLASS*, **9**, 16–22 (1994) [in Japanese].
2. Hashimoto T, Yoko T and Sakka S, *Bull. Inst. Chem. Res., Kyoto Univ.*, **71**, 420–429 (1994).
3. Hashimoto T, Yoko T and Sakka S, *Bull. Chem. Soc. Jpn.*, **67**, 653–660 (1994).
4. Kim SH, Yoko T and Sakka S, *J. Am. Ceram. Soc.*, **76**, 2486–90 (1993).
5. Hashimoto T, Yoko T and Sakka S, *J. Ceram. Soc. Jpn.*, **101**, 52–56 (1993).
6. Hashimoto T and Yoko T, *Applied Optics*, in press.
7. Hashimoto T, Yamada T and Yoko T, submitted to *Phys. Rev. B*.
8. Innocenzi P, Kozuka H and Sakka S, *J. Sol-Gel Sci. Techn.*, **1**, 305–318 (1994).



# Dynamic Birefringence of Amorphous Polymers

Kunihiro Osaki, Hiroshi Watanabe, Tadashi Inoue, Hirotaka Okamoto

The birefringence in oscillatory deformation is related to the viscoelasticity through the stress-optical rule (SOR) in the rubbery and the terminal flow zones. The deviation from the SOR in the glassy and the glass-to-rubber transition zones can be described with a modified SOR, based on the assumption that the stress is a sum of two components associated with respective stress-optical coefficients.

**Keywords:** Dynamic birefringence/ Glass-to-rubber transition/ Stress-optical rule/ Polymer rheology

When a strain is applied to a polymeric material, the refractive index becomes anisotropic, i.e., the material becomes birefringent. The birefringence is deeply related with the stress and can be used in the studies of relaxation process of polymeric materials. Although its strong relation to the stress may mean that it does not give much additional information, the relation reveals specific features which cannot be studied by other methods such as the dielectric relaxation.

In the rubbery plateau zone or in the terminal flow zone of polymers, the deviatoric component of the refractive index tensor is proportional to that of the stress tensor. This relation, called the stress-optical rule (SOR), has extensively been employed in rheological studies of polymeric liquids in steady flow as well as in non-steady flow. The ratio of the birefringence to the stress is called the stress-optical coefficient. This is essentially determined by the polymer structure and is rather insensitive to the temperature, the solvent species, or the polymer concentration. The stress-optical rule is interpreted in terms of the deformation of Gauss segments for flexible polymers.

For polymers in the glassy zone or for crystalline polymers, the birefringence is proportional to the applied stress when the stress is varied. This relation is known as the photoelasticity (PE). The photoelastic coefficient is usually different from the stress-optical coefficient defined in the rubbery and terminal flow zones. It follows that the birefringence is not proportional to the stress in the process of the stress relaxation over the glassy and glass-to-rubber transition zones. Thus, the relaxation of birefringence at low temperatures or at the short times can be an interesting subject similar to the stress relaxation or the linear viscoelasticity.

In order to study the relaxation of the birefringence around the glass transition zone, an apparatus was built to measure the birefringence under oscillatory deformation as a function of frequency of deformation and temperature [1]. This apparatus can measure the dynamic viscoelasticity simultaneously.

The dynamic birefringence, frequency dependence of the birefringence, and the viscoelasticity around the glass transition zone have been measured for a number of polymers by our group [1-8]. These results show that

## FUNDAMENTAL MATERIAL PROPERTIES —Molecular Rheology—

### Scope of research

*The molecular origin of various rheological properties of materials is studied. Depending on time or temperature, polymeric materials exhibit typical features of glass, rubber or viscous liquid, which give rise to wide applicability and good processability of polymers. For a basic understanding of such features, the motion and the structural change of polymer molecules in deformed materials are studied. Measurements are performed of rheological properties with various rheometers, of molecular orientation with flow birefringence.*



Professor  
OSAKI, Kunihiro  
(D Eng)



Associate Professor  
WATANABE, Hiroshi  
(D Sc)



Instructor  
INOUE, Tadashi  
(D Eng)

### Technician:

OKADA, Shinichi

### Students:

OKAMOTO, Hirotaka (DC)

KOIKE, Akihiro (DC)

WATANABE, Yuichiro (MC)

MIZUKAMI, Yoshihiro (MC)

SATO, Tomohiro (UG)

MATSUI, Hiroto (UG)



the behavior of birefringence and stress of amorphous polymers can be separated into three groups [9].

Type I: Polystyrene [1], bisphenol A polycarbonate [2], some engineering plastics [3], amorphous polyolefin [5] and polyisoprene [7] form a group (Type I). In this group, a modified stress-optical rule (MSOR) holds well between birefringence and stress: The relaxation spectra of the two quantities can be decomposed into two component functions (R and G). The SOR holds well for each component individually. The two components can be determined by a simultaneous measurement of stress and birefringence. In the rubbery plateau and terminal flow zones, the G component has relaxed, and therefore the stress is supported by the R component. Molecular origin of the R component can be interpreted as the orientation of the statistical segments of the chain. In the glassy zone, the stress is mainly originated by the G component. The G components of various polymers have many similarities with each other and with other glass-forming materials like *o*-terphenyl and dibutyl phthalate.

Type II and III: It is expected that the MSOR fails for polymers that exhibit  $\beta$ -relaxation of viscoelasticity due to the side chain motion in the frequency range close to the main chain dispersion. This is the case with polymethacrylates. The birefringence as well as viscoelasticity is complicated in the glassy zone. On the other hand, the MSOR was found to fail for a few polymers for which no extra viscoelastic relaxation has been reported in the range close to the main chain dispersion. Examples are poly(2-vinyl naphthalene) (PVN) [6] and polyisobutylene (PIB) [8]. For the case of PVN (we call type II polymer), the behavior is markedly different from that of type I polymers only in the glassy zone; in the transition zone the behavior is similar to that of type I. For PIB which we call type III the difference is not limited to the glassy zone. A power law dependence of the loss modulus was observed over about three decades of frequency range just below the maximum of the loss modulus. A tendency similar to that of PIB, the failure of MSOR and a power law dependence of modulus in the transition zone, was observed for an ethylene-propylene rubber.

The obtained experimental results can be interpreted by using a simple molecular model [8, 9]. The polymer is supposed to be composed of identical units that do not change the shape over the time scale to be investigated. The polymer can change its shape by rotating the unit about the connecting bonds with fixed angle (freely

rotating chain). The birefringence due to the deformation can be written as a sum of two contributions, which can be derived from respective orientation functions describing the orientation of the unit along and about the connecting bond. The stress also can be described in the form similar to the birefringence by using the above two orientation functions and the time-averaged local stress tensor for each unit. However, in the expression for the stress, one additional term exists. This term is due to the fluctuation of local stress tensor which disappears in short time region. For such a case the MSOR holds well because both the stress and birefringence can be written as a linear combination of the two orientation functions. The failure of MSOR found in type II polymers can be attributed to the larger fluctuation term in the stress expression probably due to the large side chains. Anomalous frequency dependence found in type III polymer suggests the stronger intra-chain correlation in the rotation of the unit about the main chain [8].

Around the glass transition temperature, amorphous polymers show remarkable nonlinear viscoelasticity. The MSOR was applied for this subject and it is shown that these nonlinear viscoelasticity can be attributed to the nonlinearity of the G component [10]. Other interesting features of the glassy polymers like physical ageing are under progress.

#### References

1. Inoue T, Okamoto H and Osaki K, *Macromolecules*, **24**, 5670–5675, (1991).
2. Inoue T, Hwang E J and Osaki K, *J. Rheol.*, **36**, 1737–1755, (1992).
3. Hwang E J, Inoue T and Osaki K, *Polym. Eng. Sci.*, **34**, 135–140, (1994).
4. Hwang E J, Inoue T and Osaki K, *Polymer*, **34**, 1661–1666, (1993).
5. Inoue T, Takiguchi O and Osaki K, *Polym. J.*, **26**, 133–139, (1994).
6. Hwang E J, Inoue T, Osaki K and Takano A, *Nihon Reoroji Gakkaishi*, **22**, 129–134, (1994).
7. Okamoto H, Inoue T and Osaki K, *J. Polym. Sci. Polym. Phys. Ed.*, **33**, 417 (1995).
8. Okamoto H, Inoue T and Osaki K, *J. Polym. Sci. Polym. Phys. Ed.*, in press.
9. Osaki K, Okamoto H, Inoue T and Hwang E J, *Macromolecules*, in press.
10. Okamoto H, Inoue T and Osaki K, *Macromolecules*, **25**, 3413–3415, (1992).

(Prof. of Kyoto Univ.)  
KAWAGUCHI, Tatsuya (DC)  
TAKESHITA, Hiroaki (MC)  
MATSUNAGA, Shuji (MC)  
SHIBANO, Tomokazu (MC)  
SHICHIBE, Shozo (MC)  
BABA, Takehiro (UG)  
MIYAKAWA, Masafumi (UG)  
NAGAI, Masaru (RS)

Instructor  
NISHIDA, Koji

Associate Professor  
KANAYA, Toshiji  
(D Eng)

Professor  
KAI, Ken-ichi  
(D Eng)



# Crystal Nucleation in Polymer Glasses

Masayuki Imai, Keisuke Kaji and Toshiji Kanaya

A new finding is reported that the structure formation in the induction period of polymer crystallization involves a spinodal decomposition type of phase separation. This has been revealed for poly(ethylene terephthalate) using a small angle X-ray scattering technique when it was crystallized just above the glass transition temperature  $T_g$  from a melt-quenched glass. Further, the depolarized light scattering experiments have clarified that the cause for such phase separation is the local ordering due to parallel orientation of polymer segments before crystallization.

**Keywords:** Polymer crystallization/ Induction period/ Spinodal decomposition/ Small-angle X-ray scattering/ Depolarized light scattering

A great number of studies have been reported concerning the polymer crystallization, but the mechanism of crystal nucleation, which is one of the most important unsolved problems, has hardly been investigated probably because of the difficulty in finding a clue to solve it. In recent years we have been studying what happens during the induction period before the start of crystallization using a small-angle X-ray scattering (SAXS) and a depolarized light scattering (DPLS) techniques [1-4]. We first found that during the induction period a new SAXS peak appears at a very early stage and grows with time when poly(ethylene terephthalate) (PET) was crystallized from the glassy state just above the glass transition temperature  $T_g$ . In this report we will show the importance of this new peak as a clue to understand the nucleation in polymer crystallization.

When a melt-quenched amorphous PET sample was crystallized at 80°C, 5°C above  $T_g=75^\circ\text{C}$ , the induction period was about 120 min. During this induction period the macroscopic density of the sample did not change and no exotherm was observed, while after the start of

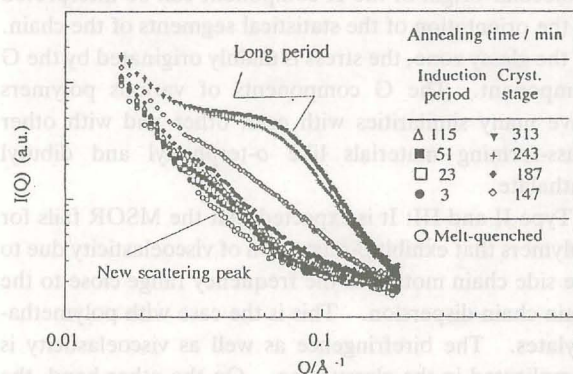


Figure 1. SAXS profiles of PET annealed at 80°C.

crystallization both the density and the isotherm increase rapidly. It was actually confirmed from wide-angle X-ray scattering experiments that these abrupt changes correspond to crystallization. Figure 1 shows the time-resolved SAXS profiles as a function of the length of scattering vector  $Q$  in the logarithmic expression. The scattering curve for the melt-quenched sample decreases monotonously with  $Q$ . Once the sample is annealed, a

## FUNDAMENTAL MATERIAL PROPERTIES —Polymer Materials Science—

### Scope of Research

The structure and molecular motion of polymer substances are studied mainly using scattering methods such as neutron, X-ray and light with the intention of solving fundamentally important problems in polymer science. The main projects are: the dynamics in disordered polymer materials including low-energy excitation or excess heat capacity at low temperatures, glass transition and local segmental motions; the mechanism of structural development in crystalline polymers from the glassy or molten state to spherulites; formation processes and structure of polymer gels; the structure and molecular motion of polyelectrolyte solutions; the structure of polymer liquid crystals.



Professor  
KAJI, Keisuke  
(D Eng)



Associate Professor  
KANAYA, Toshiji  
(D Eng)



Instructor  
NISHIDA, Koji

### Part Time Lecturer:

NAKAMAE, Katsuhiko  
(Prof of Kobe Univ.)

### Students:

KAWAGUCHI, Tatsuya (DC)  
TAKESHITA, Hiroki (MC)  
MATSUNAGA, Shuji (MC)  
SHIBANO, Tomokazu (MC)  
SHICHIBE, Syozo (MC)  
BABA, Takeichiro (UG)  
MIYAKAWA, Masafumi (UG)  
NAGAI, Masaru (RS)



maximum begins to appear at around  $Q=0.04 \text{ \AA}^{-1}$  and increases in intensity with time. After crystallization this new peak is covered with a well-known long period peak at around  $Q=0.07 \text{ \AA}^{-1}$ , which is due to the alternation of crystalline and amorphous regions. The scattering intensities of the annealed samples from which that of the quenched sample was subtracted are shown in the linear scale in Figure 2. When the scattering intensity at

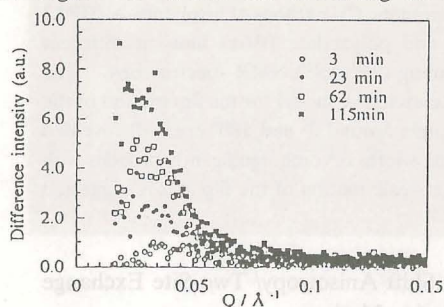


Figure 2. Difference SAXS profiles for the induction period after subtraction of that of the melt-quenched sample.

various  $Q$ s was plotted against the annealing time  $t$ , two stages were distinguished for each  $Q$ . In the early stage until about 20 min the intensity increased exponentially with the time, while in the late stage from 20 to 120 min the increasing rate of intensity considerably slowed down. These two stages are also observed in the time dependence of the peak position  $Q_m$  and the peak intensity  $I_m$  as shown in Figure 3. In the early stage  $Q_m$

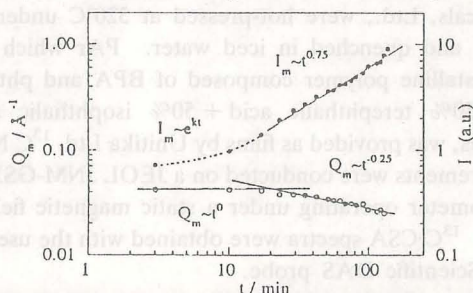


Figure 3. Annealing time dependence of  $Q_m$  and  $I_m$ .

does not change with the time while  $I_m$  increases exponentially. In the late stage the following experimental relations are obtained.

$$Q_m(t) \sim t^{-0.25}, \quad I_m(t) \sim t^{0.75} \quad (1)$$

These features agree well with the scattering behavior in the spinodal decomposition type of phase separation. Thus, the early and late stages can be described in terms of Cahn's linearized theory and Furukawa's scaling theory, respectively. According to the Cahn's theory, the density fluctuations with a constant wavelength increase in intensity with time, resulting that the scattering intensity  $I(Q)$  increases exponentially with time and its peak position does not change. These predictions agree with the above-described experimental results. Furukawa's theory describes that for the late stage the amplitude of density fluctuations reaches the equilibrium value and the characteristic size  $R(t)$  of a system grows through the diffusion and reactions of the clusters in the system, keeping a self-similarity. For the three-dimensional system ( $d=3$ ) the time evolution of the intensity function in the late stage then becomes

$$I(Q, t) \sim R^3(t)S(x) \sim Q_m^{-3}(t)S(x) \quad (2)$$

where  $x=Q/Q_m(t)$  and  $S(x)$  is a universal scaling function which is given by

$$S(x) = x^2/(2+x^6). \quad (3)$$

This theory assumes that the characteristic size changes following a power law  $R(t) \sim t^d$ . Then,  $Q_m$  and  $I_m$  are scaled as

$$Q_m(t) \sim t^{-a}, \quad I_m(t) \sim t^b \quad (4)$$

where  $b=3a$  and so  $b/a=d=3$ . The relations of eq. (4) are fairly in agreement with the experimental results of eq. (1) where  $a=0.25$  and  $b=0.75$ , supporting the above assumption of the power law. In addition the universal scaling function of eq. (3) is plotted in Figure 4 where the

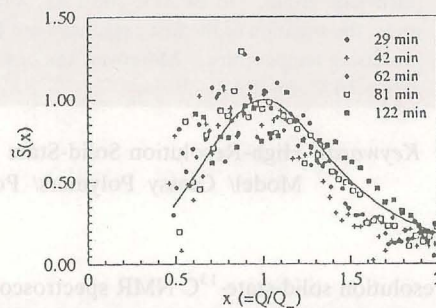


Figure 4. Observed universal scaling function  $S(x)$ .

function is normalized as  $S(1)=1$ . Independent of annealing time all the data in the late stage appear to be described by eq. (3). It can therefore be concluded that a kind of spinodal decomposition takes place during the induction period of crystallization. However, as the system investigated here consists of a single component, this conclusion further raises a new problem: what is the cause for such phase separation?

Doi *et al.* presented a kinetic theory of two order parameters, concentration and orientation, for the formation of the liquid crystalline phase of stiff polymers, predicting that the parallel orientation of stiff segments involves spinodal decomposition. In order to confirm this probability depolarized light scattering measurements were carried out. The total integrated intensity (invariant)  $I_{\text{orient}}$  due to orientation fluctuations increased exponentially in the early stage and then leveled off in the late stage. This shows that the parallel orientation of the segments actually occurs during the induction period.

The above experimental facts support the Flory's two-step crystallization model of cooperative ordering of the chains in a given region into a parallel alignment without changing intermolecular interactions and subsequent longitudinal adjustment to the more efficient packing of the chain in the parallel state. Our data also show that crystal nuclei do not appear until such local parallel ordering domains grow to a critical size, 85  $\text{\AA}$  in this case, which is considerably larger than the size of critical nuclei, 14  $\text{\AA}$ .

#### References

1. Imai M, Mori K, Mizukami T, Kaji K and Kanaya T, *Polymer*, **33**, 4451–4456 (1992).
2. Imai M, Mori K, Mizukami T, Kaji K and Kanaya T, *Polymer*, **33**, 4457–4462 (1992).
3. Imai M, Kaji K and Kanaya T, *Phys. Rev. Lett.*, **71**, 4162–4165 (1993).
4. Imai M, Kaji K and Kanaya T, *Macromolecules*, **27**, 7103–7108 (1994).



# Selective Excitation Switching Angle Sample Spinning <sup>13</sup>C NMR Study of the Local Motion of Glassy Polymers

Fumitaka Horii, Takayuki Beppu, Noboru Takaesu and Masato Ishida

Natural abundant <sup>13</sup>C chemical shift anisotropy (CSA) spectra of the aromatic CH carbons of bisphenol-A (BPA) residues have been measured for BPA polycarbonate (BPAPC) and polyarylate (PAr) films at different temperatures by the selective excitation switching angle sample spinning (SESASS) NMR spectroscopy. The CSA spectra thus obtained have been analyzed in terms of the two-site exchange model for the flip motion of the phenylene group. In BPAPC and PAr, wide distributions in flip angle around 0° and 180° are well revealed under the situation of the first exchange limit for the flip motion and the widths become significantly broader with increasing temperature. Moreover, the onset of the additional larger-scale motion of the flip axis is suggested above 60°C for PAr.

**Keywords:** High-Resolution Solid-State <sup>13</sup>C NMR/ Chemical Shift Anisotropy/ Two-Site Exchange Model/ Glassy Polymers/ Polycarbonates/ Molecular Motion

High-resolution solid-state <sup>13</sup>C NMR spectroscopy is a very powerful tool for characterizing molecular dynamics of glassy polymers. In particular, since the natural abundant <sup>13</sup>C nuclei are used in this method, the molecular motions of the respective carbons constituting polymer chains are well analyzed without using any labelling technique. As for the mid-kHz motion, lineshape analyses of <sup>13</sup>C chemical shift anisotropy (CSA) spectra seem to be one of the most suitable ways for glassy polymers. Although many sophisticated methods have been proposed for the measurements of CSA spectra, selective excitation switching angle sample spinning (SESASS) is a very convenient and timesaving method to measure CSA spectra because this is one-dimensional spectroscopy involving the cross polarization (CP), DANTE pulse sequence and SASS.

This report deals with measurements of the CSA spectra of the phenylene carbons of bisphenol-A residues for polycarbonate (BPAPC) or polyarylate (PAr) films at different temperatures by SESASS and analyses of those spectra in terms of the two-site exchange model considering the flip motion of the phenylene group.

BPAPC pellets, which were provided by Teijin Chemicals, Ltd., were hot-pressed at 320°C under 150 kg/cm<sup>2</sup> and quenched in iced water. PAr which is a noncrystalline polymer composed of BPA and phthalic acid (50% terephthalic acid + 50% isophthalic acid) residues, was provided as films by Unitika Ltd. <sup>13</sup>C NMR measurements were conducted on a JEOL JNM-GSX200 spectrometer operating under a static magnetic field of 4.7 T. <sup>13</sup>C CSA spectra were obtained with the use of a Doty Scientific DAS probe.

## FUNDAMENTAL MATERIAL PROPERTIES —Molecular Motion Analysis—

### Scope of research

The research activities in this subdivision cover structural studies and molecular motion analyses of polymers and related low molecular weight compounds in the crystalline, glassy, liquid crystalline, and solution states by high-resolution solid-state NMR, dynamic light scattering, electron microscopy, and so on, in order to obtain basic theories for the development of high-performance polymer materials. The processes of biosynthesis, crystallization, and higher-ordered structure formation are also studied for bacterial cellulose.



Professor  
HORII, Fumitaka  
(D Eng)



Associate Professor  
TSUNASHIMA Yoshisuke  
(D Eng)



Instructor  
KAJI, Hironori  
(D Eng)

### Associate Instructor:

HIRAI, Asako (D Eng)

### Technician:

OHMINE, Kyoko

### Guest Scholar:

HU, Shaohua (Assoc Prof, D Eng)

### Students:

SUZUKI, Shinji (MC)

ISHIDA, Hiroyuki (MC)

KAWANISHI, Hiroyuki (UG)

KUWABARA, Kazuhiro (UG)

ISHIDA, Masato (RF)



Figure 1(a) shows 50 MHz CP/MAS  $^{13}\text{C}$  NMR spectrum of BPAPC measured at  $25^\circ\text{C}$ . Almost no spinning side band appears for the C5 carbon as well as other aromatic and carbonyl carbons at the spinning with 7 kHz. First we have examined the selective observation of the C5 carbon by using the DANTE pulse sequence under the MAS condition. The result is shown in Figure 1(b). Since only the C5 resonance line can be observed, the selective excitation seems to be satisfactorily carried out for the C5 line by DANTE.

Figure 1(c) shows the CSA spectrum of the C5 carbon which was measured by the exact SESASS pulse sequence. The spinning angle  $\theta_s = 45^\circ$  seems to be suitable for the detection of the CSA with the enough precision. The CSA spectrum thus obtained is scaled along the frequency axis by setting the isotropic resonance center as an origin. In such a case the scaling factor  $f_s$  is expressed as  $(3\cos^2\theta_s - 1)/2$ . Considering this factor, the descaled spectrum (Figure 1(d)) has been obtained simply by using the scaling factor  $f_s = 0.25$ . The CSA line shape thus obtained seems to be almost axially symmetric, suggesting the enhanced flip motion of the phenylene group even at room temperature.

The descaled CSA spectra obtained at different temperatures for the C5 carbon were compared with computer-simulated spectra which were obtained by using the two-site exchange model for the phenylene motion. In this case the phenylene group is assumed to undergo the flip motion with a flip angle  $\delta$  between two sites.

Any simple flip motion including the  $180^\circ$  flip motion is not successful to reproduce the experimental CSA spectra. Therefore, we have introduced wide distributions of the flip angle  $\delta$  around  $0^\circ$  and  $180^\circ$  assuming Gaussian distribution curves. Here, two distributions in  $\delta$  indicate two types of flip motions which are allowed between  $0^\circ$  and an angle less than  $90^\circ$  and between  $0^\circ$  and another  $\delta$  that is described by  $90^\circ < \delta < 180^\circ$ . The simulated spectra are in good accord with the observed spectra at the respective temperatures except for the upfield small deviation at higher temperatures. According to this analysis, the flip frequency  $\kappa$  is found to be in the fast exchange limit ( $\kappa > 10^5$  Hz), which must be favorable for the detection of the distribution in flip angle. Moreover, the distribution width is increased with increasing temperature and the occurrence of the flip around  $180^\circ$  is also enhanced compared to the case around  $0^\circ$ . The upfield disagreement between the observed and simulated spectra at higher temperatures may suggest the onset of the thermal fluctuation of the flip axis of the phenylene ring.

To estimate the order of the flip frequency of the phenylene motion, the temperature dependency of  $^{13}\text{C}$

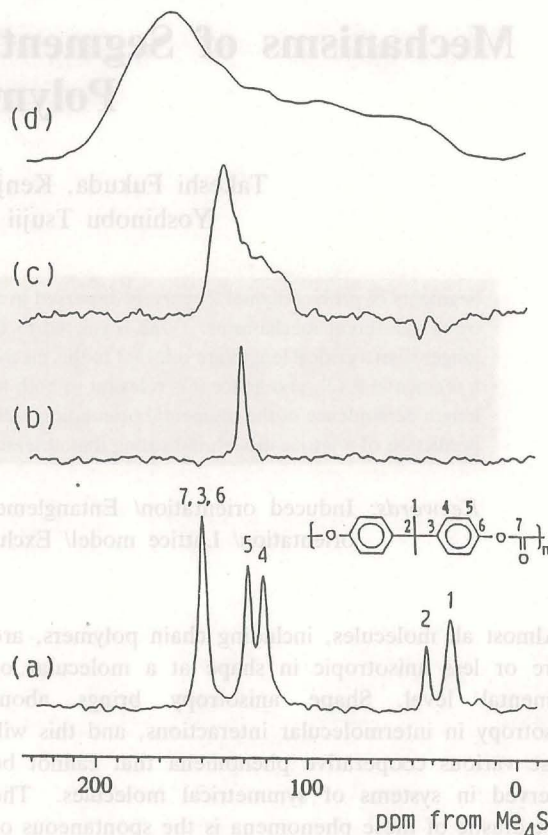


Figure 1. Solid  $^{13}\text{C}$  NMR spectra of BPAPC. As for the explanation of each figure, see text.

spin-lattice relaxation times for the C5 carbon of BPAPC has been analyzed by the model-free treatment previously proposed. The simulated results considering two kinds of random motions with different correlation times are in good accord with the observed data. It is, therefore, concluded that the slower motion should be assigned to the flip motion around  $180^\circ$  for the phenylene group, which has the correlation time of about  $10^8$  Hz at room temperature. On the other hand, the correlation time for the faster motion assigned to the rapid fluctuation around the potential minimum is found to be of the order of  $10^{12}$  Hz.

Similar SESASS measurements have been applied for the aromatic CH carbon of PAr at  $-30$ – $100^\circ\text{C}$ . The CSA spectra obtained at lower temperatures can be also well analyzed in terms of the two-site exchange model as the case of BPAPC and wider distributions in flip angles are found to exist in PAr compared to the case of BPAPC. Moreover, the phenylene flip axis may undergo additional larger-scale fluctuation above  $60^\circ\text{C}$  in this polymer. Further investigations are in progress to characterize the detailed motions even at temperatures near the glass transition temperatures.



# Mechanisms of Segmental Orientation in Deformed Polymer Melts

Takeshi Fukuda, Kenji Kawabata, Koji Fujimoto,  
Yoshinobu Tsujii and Takeaki Miyamoto

Segments of probe polymer 2 sparsely dispersed in a stretched network of polymer 1 were shown to be oriented by two different mechanisms. One is related to the entanglement interaction, and accordingly probe chains longer than a critical length are relevant to this mechanism. The other mechanism is related to the interaction at a segmental level, and hence it is relevant to both long and short probe molecules. The magnitude and chain-length dependence of the segmental orientation induced by the latter mechanism well agree with the theoretical prediction of a lattice model, indicating that at least an important part of that orientation is driven entropically.

**Keywords:** Induced orientation/ Entanglement interaction/ Segmental interaction/ Equilibrium orientation/ Lattice model/ Excluded volume interaction

Almost all molecules, including chain polymers, are more or less anisotropic in shape at a molecular or segmental level. Shape anisotropy brings about anisotropy in intermolecular interactions, and this will cause various cooperative phenomena that cannot be observed in systems of symmetrical molecules. The most drastic of these phenomena is the spontaneous or liquid crystalline ordering exhibited by stiff or semiflexible polymers as well as low-mass mesogenic molecules [1]. The effects of anisotropic or orientation-dependent interactions are not usually explicit in flexible polymers and non-mesogenic compounds. However, once the system is made anisotropic by an external force field, for example, the effects are expected to appear explicitly, affecting whatever properties in which orientation matters. In fact, there has been a large body of experimental evidence indicating the existence of

orientational correlations in various polymer systems [2].

Theoretically, this problem was first considered by Tanaka and Allen [3] using a lattice model, hence from an entropic point of view, and by Jarry and Monnerie from an enthalpic point of view [4]. We recently extended the Di Marzio lattice model to a multi-component polymer system, and combined it with the modified freely jointed chain (F-chain) to obtain volume-induced orientations in a miscible blends of two polymers of arbitrary chain length and flexibility [5]. This F-chain is equivalent to the wormlike chain with respect to mean dimensions of the chain but somewhat different from that with respect to orientational entropy. For example, the segments of polymer 2 sparsely dispersed in a weakly stretched network of polymer 1 are predicted to be oriented at equilibrium by an amount

$$\eta_2/\eta_1 = (1/5)x_2(1-n_2^{-1})/(1+x_2n_2^{-1}) \quad (1)$$

## ORGANIC MATERIALS CHEMISTRY —Polymeric Materials—

### Scope of research

Basic studies have been conducted for better understandings of the structure/property or structure/function relations of polymeric materials and for development of novel functional polymers. Among those have been the studies on (1) the synthesis and properties of cellulose- and oligosaccharide-based functional polymers, e.g., bio-degradable polymers, liquid crystals and polymers of well-defined structure having pendant oligosaccharides, (2) the structure and mechanism of polymer gels and gelation, and (3) various phenomena originating in orientation-dependent interactions in polymer systems.



Professor  
MIYAMOTO, Takeaki  
(D Eng)



Associate Professor  
FUKUDA, Takeshi  
(D Eng)



Instructor  
TSUJII, Yoshinobu  
(D Eng)



Instructor  
MINODA, Masahiko  
(D Eng)

### Associate Instructor:

DONKAI, Nobuo (D Eng)

### Guest Scholar:

GLATZ, Frank P. (D Sc)

### Guest Research Associate:

MURAKAMI, Mauro M.

LANG, Ming-fang

BEDEKAR, Beena A.

### Students:

SUGIURA, Makoto (DC)

FUJIMOTO, Koji (DC)

ITO, Hidehiro (MC)

IDE, Nobuhiro (MC)

TAKARAGI, Akira (MC)

OKAMURA, Haruyuki (MC)

TERAUCHI, Tomoya (MC)

YAMADA, Kenji (MC)

KUWAHARA, Shigenao (UG)

YAMAMOTO, Shinpei (UG)



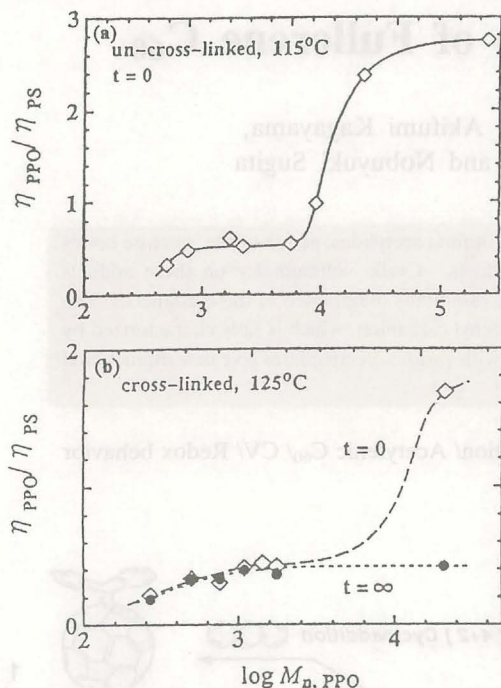


**Figure 1.** Plot of order parameter ratio  $\eta_2/\eta_1$  vs. PPO molecular weight  $M_n$  in (a) un-cross-linked PS ( $M_n = 2.4 \times 10^5$ ) and (b) cross-linked PS matrices.

where  $\eta = (3/2) \langle \cos^2 \theta \rangle - (1/2)$  is the order parameter,  $\eta_2 = L/D$  and  $x_2 = q/D$  with  $L$ ,  $D$ , and  $q$  being the contour length, diameter, and persistence length of polymer 2.

Experimentally, we have studied cross-linked and un-cross-linked polystyrene (PS) containing a small amount (3 wt-%) of well fractionated poly(2,6-dimethyl-1,4-phenylene oxide) (PPO) of various chain lengths [2]. By infrared dichroism (IRD), independent determination of  $\eta_1$  (PS) and  $\eta_2$  (PPO) of these miscible polymers is possible, enabling us to make a direct test of Eq. 1. Cross-linked samples were prepared by radical polymerization of styrene by use of divinyl benzene as a cross-linker. The blend film, about 50  $\mu\text{m}$  thick, was uniaxially stretched in a temperature-controlled stretching device to a desired extension ratio  $\lambda$ , and studied by IRD as a function of time  $t$ .

At  $t=0$ , i.e., immediately after the stretching was completed, both PS and PPO segments showed finite orientations  $\eta_1$  and  $\eta_2$ , and the ratio  $\eta_2/\eta_1$  vs.  $M_2$  curves for the un-cross-linked and cross-linked systems were very similar to each other (Fig. 1): as  $M_2$  increased,  $\eta_2/\eta_1$  increased at first, approaching a plateau for  $10^3 \leq M_2 \leq 10^4$ , where  $\eta_2/\eta_1 \approx 0.5$ , and then steeply increased, approaching another plateau, where  $\eta_2/\eta_1 \gg 1$ . This enormous increase in  $\eta_2/\eta_1$  is ascribed to the *entanglement interaction* of PPO chains with the PS matrix.

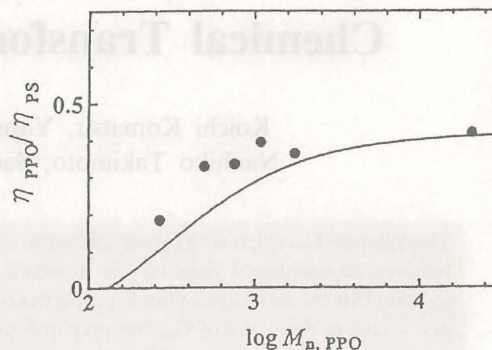


**Figure 2.** Comparison of the theory (full curve) and the experiment at  $t=\infty$ . The theoretical curve was obtained from Eq. 1 with the  $x_2$  value of 2.1 estimated from literature data.

Examination of the cross-linked systems, where the PS orientation did not relax owing to the cross-links, has revealed that PPO segments exhibit a finite, unrelaxing orientation even after a long time, giving a constant  $\eta_2/\eta_1$  ratio of about 0.4 for  $M_2 \geq 10^3$  (Fig. 1b). This unrelaxing orientation observed after a long time ( $t=\infty$ ) is ascribed to the *segmental orientation* between PPO and PS, and can be well interpreted by Eq. 1 with respect to both the magnitude of  $\eta_2/\eta_1$  and its chain length dependence (Fig. 2). This indicates that at least an important part of the equilibrium (unrelaxing) orientation of PPO in the oriented PS matrix is driven entropically.

Similar results have been obtained also for cross-linked and un-cross-linked PS containing poly(vinyl methyl ether) (PVME) as a minor component [6]. This system is particularly interesting, because it is a partially miscible one exhibiting an LCST behavior. A preliminary result indicates that the miscibility of PVME in a PS network becomes lowered as the matrix segments are oriented, in line with the theoretical prediction of the same model on which Eq. 1 is based.

#### References

1. Fukuda T, Takada A and Miyamoto T, *Cellulosic polymers, Blends and Composites*, Gilbert RD Ed., Hanser Publishers, Munich, 1994; Chap. 3(pp. 47–70).
2. Kawabata K, Fukuda T, Tsujii Y and Miyamoto T, *Macromolecules*, **26**, 3980–3985 (1993).
3. Tanaka T and Allen G, *Macromolecules*, **10**, 426–430 (1977).
4. Jarry JP and Monnerie L, *Macromolecules*, **12**, 316–320 (1979).
5. Fukuda T, Kawabata K, Tsujii Y and Miyamoto T, *Macromolecules*, **25**, 2196–2199 (1992).
6. Fujimoto K, Murakami MM, Tsujii Y, Fukuda T and Miyamoto T, *Proceedings of ISF '94 (Yokohama)*, 297 (1994).



## Chemical Transformation of Fullerene C<sub>60</sub>

Koichi Komatsu, Yasujiro Murata, Akifumi Kagayama,  
Naohiko Takimoto, Sadayuki Mori and Nobuyuki Sugita

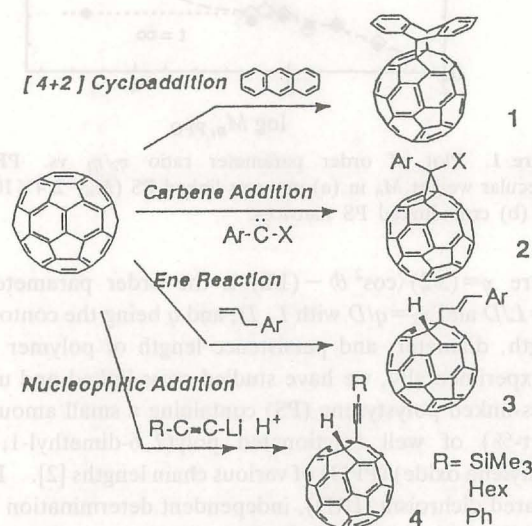
The fullerene C<sub>60</sub> reacts with dienes, carbenes, allylbenzenes, and lithium acetylides, at one of the juncture bonds between six-membered rings on the  $\pi$ -surface to give 1:1 adducts. Cyclic voltammetry on these adducts indicate that the intrinsic electronic properties of original C<sub>60</sub> are essentially maintained in these adducts. The first acetylene derivative of C<sub>60</sub> thus prepared gives a stable fullerenyl carbanion, which is fully characterized by <sup>1</sup>H and <sup>13</sup>C NMR as well as by CV. Reactions of this carbanion with various electrophiles give new difunctional derivatives.

**Keywords:** Carbon cluster/ [4+2] addition/ Carbene addition/ Acetylenic C<sub>60</sub>/ CV/ Redox behavior

Since the successful preparation of fullerene C<sub>60</sub> in macroscopic amount by Krätschmer and Huffman in 1990, the chemistry on C<sub>60</sub> has met with explosive development. The chemical transformation of C<sub>60</sub> is not only intriguing from a purely academic viewpoint but requisite for exploiting the applicability of this totally new carbon allotrope as a functional material.

We have investigated transformation of C<sub>60</sub> as summarized in Scheme 1, in order to examine the possible intramolecular electronic interaction of an electro-negative core of C<sub>60</sub> with rigidly held  $\pi$ -systems (compound 1) [1], to introduce a supposedly reactive benzylic C-X bond (compound 2) [2] and olefinic functionalization (compound 3) [3] to C<sub>60</sub>, and to attach a triple bond to the C<sub>60</sub>  $\pi$ -surface (compound 4) [4]. All the reactions have been found to take place specifically at one of the thirty  $\pi$ -bonds at the juncture between six-membered rings of C<sub>60</sub> as judged from the results of the <sup>13</sup>C NMR spectral analysis.

The redox behaviors of all the newly synthesized C<sub>60</sub>



Scheme 1

### ORGANIC MATERIALS CHEMISTRY —High-Pressure Organic Chemistry—

#### Scope of research

Fundamental studies are being made for utilization of high pressure in organic synthesis and for creation of new functional materials with novel structures and properties. The major subjects are: utilization of carbon monoxide and dioxide for organic synthesis; studies on the transition-metal catalyzed photochemical carbonylation; synthetic and structural studies on novel cyclic  $\pi$ -systems; chemical transformation of fullerene C<sub>60</sub>.



Professor  
SUGITA, Nobuyuki  
(D Eng)



Associate Professor  
KOMATSU, Koichi  
(D Eng)



Instructor  
MORI, Sadayuki  
(D Eng)



Instructor  
KUDO, Kiyoshi  
(D Eng)

#### Associate Instructor:

OHGA, Yasushi

#### Technician:

YASUMOTO, Mitsuo

#### Students:

NISHINAGA, Tohru (DC)

IKOMA, Futoshi (MC)

IZUMI, Yoshio (MC)

KAGAYAMA, Akifumi (MC)

KARITA, Tetsuya (MC)

MURATA, Yasujiro (MC)

OIDA, Hiromichi (MC)

MOTOYAMA, Kiyoto (MC)

TAKIMOTO, Naohiko (MC)

KAWAMURA, Tetsu (UG)

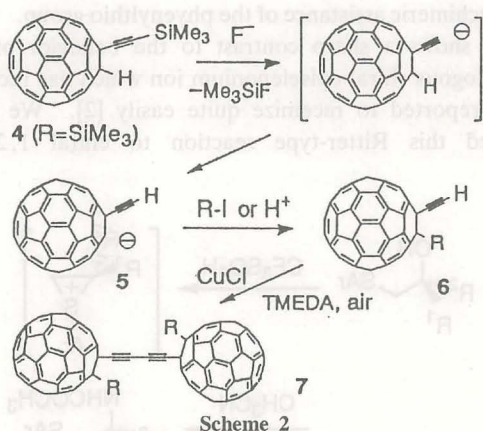
NETSU, Fuminori (UG)

NISHIOKA, Kentaro (UG)



derivatives were examined by cyclic voltammetry (CV). As shown by the typical voltammogram of **2** (Ar=Ph; X=Cl) in Fig. 1, reversible reduction waves are observed at  $-1.00$ ,  $-1.44$ , and  $-1.97$  V vs Ag/Ag<sup>+</sup> together with an irreversible oxidation peak at  $+1.39$  V, which are essentially similar to those of C<sub>60</sub> itself. These observations clearly indicate that the original electronic properties of C<sub>60</sub> are retained in these derivatives in spite of partial loss of full  $\pi$ -conjugation on the spherical surface of the fullerene molecule.

Compound **4** is the first C<sub>60</sub> derivative having a directly attached acetylene functionality. Desilylation of the trimethylsilyl group of **4** (R=Si(CH<sub>3</sub>)<sub>3</sub>) by fluoride ion was found to be immediately followed by proton migration to afford the fullerenyl carbanion **5**, which can be quenched by proton acid or alkyl iodides to give the corresponding difunctional derivatives **6** (Scheme 2). The oxidative coupling of the ethynyl group of **6** gives a new dimer of acetylenic C<sub>60</sub>, **7**.



Reflecting the high acidity due to the prominent electronegativity of the C<sub>60</sub> core, the fullerenyl proton of **4** (R=Hex) is readily abstracted by *t*-butoxide in THF to give a dark green solution of the stable fullerenyl carbanion **8**, which has a near IR absorption at  $\lambda_{\text{max}}$  990 nm and is fully characterized by <sup>1</sup>H and <sup>13</sup>C NMR (28 signals between  $\delta$  158.42 and 135.01, together with signals at  $\delta$  175.24, 120.99, 86.47, 83.40, 54.61, 32.51, 30.22, 29.85, 23.50, 20.50, and 14.44). The CV on this carbanion in THF demonstrates that the oxidation to the corresponding radical occurs at  $-0.39$  V but this process is not reversible due to rapid dimerization of the radical. The reduction peak of this fullerenyl dimer, which is associated with dissociation to the monomeric anion, is observed at  $-1.20$  V.

The carbanion **8** reacts with various alkyl and acyl halides to afford the 1,2-bisadducts **9** as shown in Scheme 3

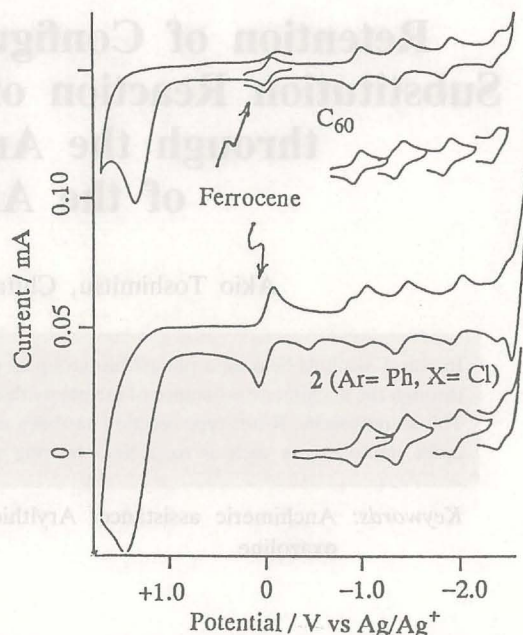
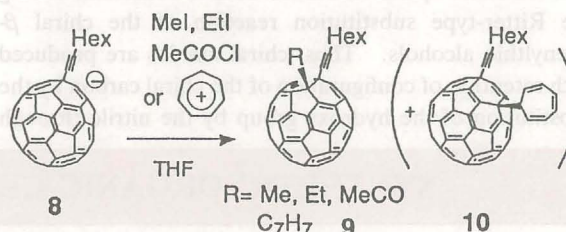


Figure 1. Cyclic voltammograms of C<sub>60</sub> and of **2** (Ar=Ph, X=Cl) in benzonitrile; scan rate  $0.1 \text{ V} \cdot \text{s}^{-1}$ .

**3.** In contrast, the reaction with the more sterically demanding electrophile such as tropylium ion gives a 1:1 mixture of the 1,2- (**9**) and 1,4-bisadducts (**10**). These results can be successfully interpreted by theoretical calculations using semi-empirical MO methods. A work is now underway to prepare a polymer-bound C<sub>60</sub> derivative in collaboration with Professor Miyamoto's group in this institute.



#### References

1. Komatsu K, Murata Y, Sugita N, Takeuchi K and Wan T S M, *Tetrahedron Lett.*, **34**, 8473 (1993).
2. Komatsu K, Kagayama A, Murata Y, Sugita N, Kobayashi K, Nagase S and Wan T S M, *Chem. Lett.*, 2163 (1993).
3. Komatsu K, Murata Y, Sugita N, Wan T S M, *Chem. Lett.*, 635 (1994).
4. Komatsu K, Murata Y, Takimoto N, Mori S, Sugita N and Wan T S M, *J. Org. Chem.*, **59**, 6101 (1994).



## Retention of Configuration in the Ritter-type Substitution Reaction of Chiral $\beta$ -Arylthio Alcohols through the Anchimeric Assistance of the Arylthio Group

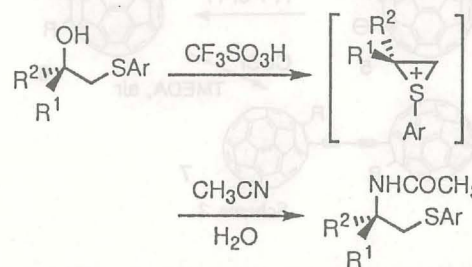
Akio Toshimitsu, Chitaru Hirosawa and Kohei Tamao

In chiral alcohols bearing a phenylthio group at the  $\beta$  carbon atom, the hydroxy group is replaced by nitriles through the anchimeric assistance of the phenylthio group to afford chiral amides with retention of configuration. This stereospecific Ritter-type reaction has been utilized in the conversion of chiral glycidol derivatives to chiral cyclic imino ethers such as oxazolines bearing an arylthio group.

**Keywords:** Anchimeric assistance/ Arylthio group/ Ritter-type reaction/ Chiral amide/ Chiral oxazoline

Anchimeric assistance of the arylthio group has been widely observed in the substitution reactions at the carbon atom  $\beta$  to the arylthio group, the three-membered cyclic intermediate being known as an episulfonium ion. Diastereoselectivity, namely the erythro-threo selectivity has been established in the substitution reactions via the episulfonium ion. Enantioselectivity, i.e., the stereochemistry of the substitution reaction at the chiral carbon through the anchimeric assistance of the arylthio group (the stereochemical behavior of a chiral episulfonium ion), however, has not been studied so far [1]. We find that the chiral episulfonium ion does not racemize during the Ritter-type substitution reaction of the chiral  $\beta$ -phenylthio alcohols. Thus, chiral amides are produced with retention of configuration of the chiral carbon by the substitution of the hydroxy group by the nitrile through

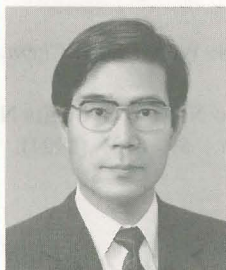
the anchimeric assistance of the phenylthio group. This result shows a sharp contrast to the behavior of the homologous chiral episelenonium ion which has recently been reported to racemize quite easily [2]. We have applied this Ritter-type reaction to chiral 1,2-diol



### SYNTHETIC ORGANIC CHEMISTRY —Synthetic Design—

#### Scope of research

(1) *Synthesis, structural studies, and synthetic applications of organosilicon compounds, such as pentacoordinated silicon compounds, functionalized silyl anions, and functionalized oligosilanes.* (2) *Design and synthesis of novel  $\pi$ -conjugated polymers containing silacyclopentadiene (silole) rings, based on new cyclization reactions and carbon-carbon bond formations mediated by the main group and transition metals.* (3) *Chiral transformations and asymmetric synthesis via organosulfur and selenium compounds, especially via chiral episulfonium and episelenonium ions.*



Professor  
TAMAO, Kohei  
(D Eng)



Associate Professor  
TOSHIMITSU, Akio  
(D Eng)



Instructor  
KAWACHI, Atsushi



Instructor  
YAMAGUCHI,  
Shigehiro

#### Associate Instructor:

INOUE, Yoshihiko

#### Guest Scholar:

SUN, Guangri

#### Students:

ASAHARA, Masahiro (DC)

KOZAWA, Masami (MC)

NAKAMURA, Kazunori (MC)

MUKAI, Takao (MC)

OHNO, Shigeki (UG)

DOI, Noriyuki (UG)



derivatives bearing the arylthio group to find that the intermediate iminium ion is trapped by the remaining hydroxy group to afford chiral cyclic imino ethers such as oxazolines.

The reaction described herein may be used as a new chiral pool method from readily accessible chiral oxiranes to chiral amine derivatives with retention of configuration of the chiral carbon [3].

## References

1. Williams D R and Philips J G, *Tetrahedron*, **42**, 3013 (1986). Wilson LJ and Liotta D, *Tetrahedron Lett.*, **31**, 1815 (1990).
2. Toshimitsu A, Ito M and Uemura S, *J. Chem. Soc., Chem. Commun.*, 530 (1989).
3. Toshimitsu A, Hirose C and Tamao K, *Tetrahedron*, **50**, 8997 (1994).

# Oligosiloles: First Synthesis Based on a Novel *Endo-Endo* Mode Intramolecular Reductive Cyclization of Diethynylsilanes

Kohei Tamao and Shigehiro Yamaguchi

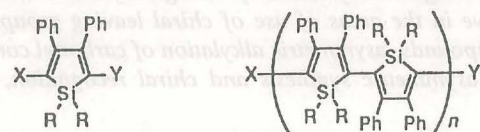
A general and versatile synthesis of 2,5-difunctionalized siloles is developed based on an *endo-endo* mode intramolecular reductive cyclization of diethynylsilanes upon treatment with lithium naphthalenide. With certain functionalized siloles in hand, oligosiloles, from bisiloles to quatersilole, are synthesized by oxidative coupling reaction via higher order cyanocuprates. Structural analysis and electronic properties of the oligosiloles have been investigated by means of X-ray crystallography, NMR studies, and UV-vis spectroscopy.

**Keywords:** 2, 5-Difunctionalized silole/ Intramolecular reductive cyclization/ Oligosiloles/ Oxidative coupling reaction

Silole (silacyclopentadiene) containing  $\pi$ -conjugated polymers have recently been highlighted as a promising candidate for novel  $\pi$ -electronic materials, because of their anticipated properties such as conductivity, thermochromism, and nonlinear optical properties [1]. Polysiloles, silole-2, 5-linked polymers, may be a center of target. Toward the polysilole synthesis, we succeeded in the first general and versatile synthesis of 2,5-difunctionalized siloles via a conceptually new intramolecular reductive cyclization of diethynylsilanes and the first synthesis of oligosiloles as models of the polysiloles by use of functionalized siloles in hand [2].

Bis(phenylethynyl)silane,  $(\text{PhC}\equiv\text{C})_2\text{SiR}_2$  ( $\text{R} = \text{Me}$ ,  $\text{Et}$ ,  $i\text{-Pr}$ , and  $\text{hexyl}$ ), underwent intramolecular reductive cyclization in an *endo-endo* mode upon treatment with lithium naphthalenide to form 2, 5-dilithiosiloles **1**. This is the first example of intramolecular reductive cyclization of diynes proceeding in an *endo-endo* mode. The compounds **1** were converted into various 2,5-difunctionalized siloles, including 2,5-dibromosilole **2**, 5,5'-Dibromo-2,2'-bisilole **4** and 5,5'''-dibromo-2,2':5',2'':5'',2'''-quatersilole **6**, were prepared by oxidative coupling via higher order cyanocuprate of 2-bromo-5-lithiosilole **3** and 5-bromo-5'-lithio-2,2'-bisilole **5**, respectively. X-ray crystal structures of the bisiloles show highly twisted arrangements between two silole

rings with torsion angle  $62\text{--}63^\circ$ .  $^1\text{H}$  NMR studies on bisiloles show a rapid equilibration between noncoplanar conformers in solution. Despite the noncoplanar arrangement, all of the oligosiloles have unusually long absorption maxima in UV-vis spectra:  $\lambda_{\text{max}}$  (nm) in  $\text{CHCl}_3$ ; bisilole **4**, 416; quatersilole **6**, 443. This remarkable electronic properties may be ascribed to an inherent unique electronic structures of silole ring. The present investigation on oligosiloles as models of polysiloles have enhanced our interests in the still veiled fascinating polysiloles.



- |  |  |
|--|--|
| <b>1</b> ( $\text{X}=\text{Y}=\text{Li}$ )               | <b>4</b> ( $\text{X}=\text{Y}=\text{Br}$ , $n=1$ )               |
| <b>2</b> ( $\text{X}=\text{Y}=\text{Br}$ )               | <b>5</b> ( $\text{X}=\text{Br}$ , $\text{Y}=\text{Li}$ , $n=1$ ) |
| <b>3</b> ( $\text{X}=\text{Br}$ , $\text{Y}=\text{Li}$ ) | <b>6</b> ( $\text{X}=\text{Y}=\text{Br}$ , $n=2$ )               |

## References

1. Tamao K, Yamaguchi S, Shiozaki M, Nakagawa Y and Ito Y, *J. Am. Chem. Soc.*, **114**, 5867 (1992).
2. Tamao K, Yamaguchi S and Shiro M, *J. Am. Chem. Soc.*, **116**, 11715 (1994).



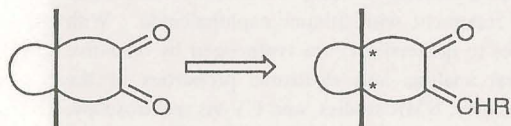
## Desymmetrization of meso-Dicarbonyl Compounds by the Horner-Wadsworth-Emmons Reaction

Kaoru Fuji, Kiyoshi Tanaka, Yoshihisa Ohta and Toshiyuki Watanabe

A chiral phosphonoacetate **1** differentiates the enantiotopic carbonyl groups in  $\alpha$ -diketones to afford the *Z*- or *E*-olefin as a major product. Enantiomeric excess (ee) was generally high in *Z*-olefins.

**Keywords:** Asymmetric synthesis/ Horner-Wadsworth reaction/  $\alpha$ -Diketone/ Wittig reaction/ Binaphthol

The olefination of a carbonyl group is an unsuitable reaction for asymmetric synthesis, since it does not create a new  $sp^3$ -carbon center. An attractive entry to optically active olefins would be opened, if one of the carbonyl groups of *meso*-diketone is transformed into the carbon-carbon double bond (Scheme I). Here we describe the



Scheme I

realization of this concept by the Horner-Wadsworth-Emmons (HWE) reaction utilizing a chiral phosphonoacetate **1**. Precedents for enantioselective desymmetrization of *meso*-dicarbonyl compounds include the reduction of cyclic diketones with baker's yeast [1] and intramolecular aldol condensations in the presence of an amino acid [2].

The reaction of  $\alpha$ -diketone **2** with the anion of **1** gave the *Z*-isomer **4** with 98% ee in 95% yield along with a

small amount (2%) of the corresponding *E*-isomer (~30% ee). The absolute stereochemistry of **4** was unambiguously determined by an X-ray analysis of the amide **5** derived from **4**. Noteworthy features of this reaction include, i) exclusive formation of the *Z*-isomer, which is unusual for the ordinary HWE reaction, and ii) attainment of nearly 100% transfer of chirality from the phosphinate **1** to the *Z*-isomer **4**. Although we have no precise and definite rationale for the extremely high ee of the product **4** at the moment, it is clear that both the geometry of the double bond and the absolute stereochemistry are determined by a combination of the initial *exo*-attack of the reagent to one of the carbonyl groups of **2**. The high *Z*-selectivity in the HWE reaction could be attributed to an increase in the rate of elimination relative to that of equilibrium between the adduct and the starting material [3].

In Order to extend the scope of this reaction and to shed light on the mechanism, enantioselective olefinations of bicyclic  $\alpha$ -diketones **3** and **6-9** were investigated. Preliminary results indicated that the *Z*-isomer was the major product in the 4, 5-substituted ketones **1**, **2**, and **6**

### SYNTHETIC ORGANIC CHEMISTRY —Fine Organic Synthesis—

#### Scope of research

The research interests of the laboratory include the development of new synthetic methodology, molecular recognition, and design and synthesis of biologically active compounds including functionalized DNA oligomers. Programs are active in the areas of use of chiral leaving groups for an asymmetric induction, desymmetrization of symmetrical compounds, asymmetric alkylation of carbonyl compounds based on "memory of chirality", use of binaphthalenes in the asymmetric synthesis and chiral recognition, and antitumor diterpenoids.



Professor  
FUJI, Kaoru  
(D Pharm Sc)



Associate Professor  
TANAKA, Kiyoshi  
(D Pharm Sc)



Instructor  
KAWABATA, Takeo  
(D Pharm Sc)

#### Technician:

TERADA Tomoko

#### Lecturer (part-time):

NODE, Manabu

(D Pharm Sc)

#### Guest Res Assoc:

ASHUTOSH, V Bedekar

(PhD)

PETER, Mátyus (PhD)

THOMAS, Wirth (PhD)

LI, Bo

YANG, Xiao-Sheng

HE, Zhen-Dan

#### Students:

YAHIRO, Kiyoshi (DC)

OHMORI, Toshiumi (DC)

OKA, Takahiro (DC)

MIZUCHI, Maki (DC)

ANN, Miza (DC)

OHTA, Yoshihisa (DC)

NAGATO, Minoru (DC)

TAKAHASHI, Thoru (DC)

YOSHIUCHI, Tatsuya

(MC)

IKEDA, Atsutoshi (MC)

KOITO, Seita (MC)

SUZUKI, Hideo (MC)

TAKASU, Kiyosei (MC)

THOKAI, Naoji (MC)

YOSHIKAWA, Seiji (MC)

WATANABE, Toshiyuki

(MC)

NAKATA, Eizo (UG)

KURODA, Akio (RS)

IKEDA, Hisafumi (RS)

OHTSUBO, Kenji (RS)

SAKURAI, Minoru (RS)



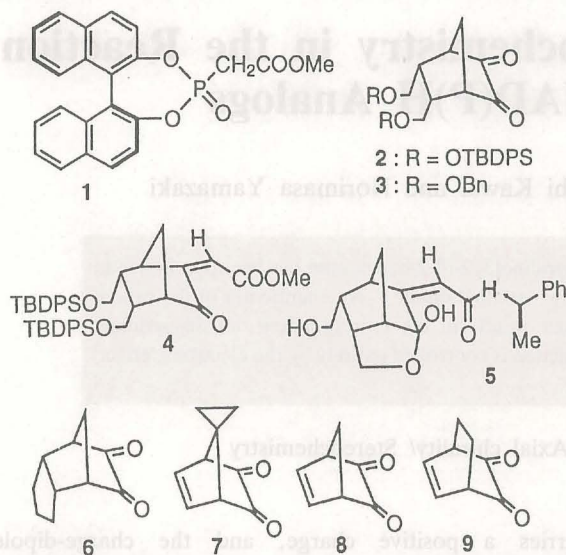


**Table.** *E/Z*-Ratio and Enantiomeric Excess of the Products

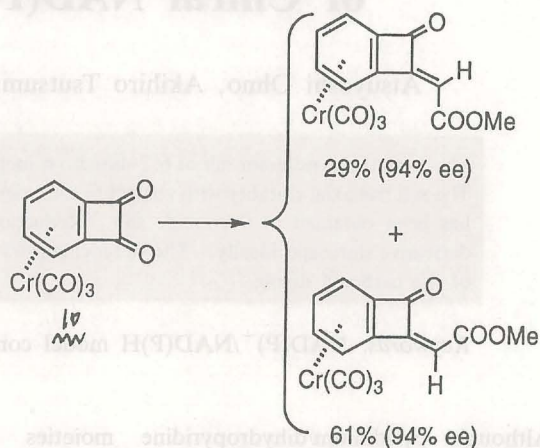
Diketone	<i>E</i> -isomer		<i>Z</i> -isomer	
	yield (%)	ee (%)	yield (%)	ee (%)
2	2	30	95	98
3	7	35	31	83
6	15	0	57	93
7	62	45	35	92
8	58	79	25	97
9	60	75	38	89

while the *E*-isomer was the major in  $\Delta^{4,5}$ -series 7–9. The ee was generally high for *Z*-isomer (83–98% ee).

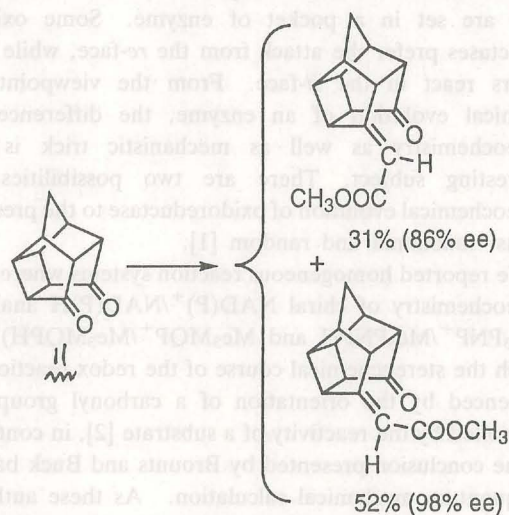
Interestingly, the phosphonate reagent 1 could discriminate the carbonyl group of a chromium complex 10 and  $\gamma$ -diketone 11 to afford *Z*- and *E*-isomers with high ee (Schemes II and III). The *Z*-isomer was the major product in both cases.

In conclusion, enantioselective desymmetrization of  $\alpha$ -dicarbonyl compounds by the HWE reaction was realized for the first time. The present approach offers a simple and versatile method for the enantioselective construction of the  $\alpha, \beta$ -unsaturated  $\gamma$ -ketoesters, which can serve as a starting material for the synthesis of

optically active natural and unnatural compounds because of a highly reactive double bond.



**Scheme II**



**Scheme III**

#### References

1. For a review, see: Csuk R and Glanzner B, *Chem. Rev.*, **91**, 49–97 (1991).
2. For a review, see: Fuji K, *Chem. Rev.*, **93**, 2037–2066 (1993).
3. Maryanoff BE and Reitz AB, *Chem. Rev.*, **89**, 863–927 (1989).

HIRANO, Toshiko  
Students:  
KAWASAKI, Masashi (RP)  
KONDO, Shin-ichi (DC)  
TSUTSUMI, Akihiro (DC)  
KINOSHITA, Masamichi (DC)  
SHIOI, Kosei (DC)  
YAMAZAKI, Norimasa (DC)  
KUNITOMO, Ikuo (DC)  
TAKAHASHI, Aiko (DC)  
INOUE, Yoko (MC)  
SAITOU, Kentaro (MC)  
NAKAGAWA, Toshiya (MC)  
HIDA, Kouichi (MC)  
KUBO, Yoji (RS)  
TODA, Toshiyuki (RS)  
MATSUMOTO, Tomoko (RS)  
YAMAGUCHI, Satoshi (RS)



Professor  
OHNO, Atsuyoshi  
(D Sc)



Associate Professor  
KAWAI, Yasushi  
(D Sc)



Associate Professor  
KAWA, Sugiyama, Takashi  
(D Sc)



Professor  
OHNO, Atsuyoshi  
(D Sc)



## Electronically Controlled Stereochemistry in the Reaction of Chiral $\text{NAD(P)}^+/\text{NAD(P)H}$ Analogs

Atsuyoshi Ohno, Akihiro Tsutsumi, Yasushi Kawai and Norimasa Yamazaki

The *N*-methylpyridinium salt of 6, 7-dihydro-6-methyl-5-oxopyridino[3, 2-*d*]-2-benzazepin has been synthesized. The salt has axial chirality with respect to the orientation of the carbonyl dipole. An enantiomer of the cation has been obtained as the iodide salt. Reduction of the salt results in the corresponding dihydropyridine derivative stereospecifically. The stereochemistry of the reduction is controlled entirely by the electronic effect of the carbonyl dipole.

**Keywords:**  $\text{NAD(P)}^+/\text{NAD(P)H}$  model compound/ Axial chirality/ Stereochemistry

Although pyridinium/dihydropyridine moieties in  $\text{NAD(P)}^+/\text{NAD(P)H}$ -coenzymes are achiral, *re*- and *si*-faces of the molecules are recognized by a substrate when they are set in a pocket of enzyme. Some oxidoreductases prefer the attack from the *re*-face, while the others react in the *si*-face. From the viewpoint of chemical evolution of an enzyme, the difference in stereochemistry as well as mechanistic trick is an interesting subject. There are two possibilities in stereochemical evolution of oxidoreductase to the present forms: functional and random [1].

We reported homogeneous reaction systems where the stereochemistry of chiral  $\text{NAD(P)}^+/\text{NAD(P)H}$  analogs ( $\text{Me}_3\text{PNP}^+/\text{Me}_3\text{PNPH}$  and  $\text{Me}_3\text{MQP}^+/\text{Me}_3\text{MQPH}$ ), in which the stereochemical course of the redox reaction is influenced by the orientation of a carbonyl group, is controlled by the reactivity of a substrate [2], in contrast to the conclusion presented by Brounts and Buck based on quantum mechanical calculation. As these authors have mentioned, the substrate assigned for the calculation

carries a positive charge, and the charge-dipole interaction appears to be important in these calculations when the carbonyl dipole is *syn* to the reacting hydrogen. Since the stereochemistry observed in these organic systems is exactly parallel to those of enzymatic systems classified by Nambiar *et al.* [3], we studied the mechanism for stereochemical control in this and similar systems extensively and came to a conclusion that the interaction at the ground state is quite important [4].

In order to obtain closer analog of  $\text{NAD(P)}^+/\text{NAD(P)H}$  coenzymes for testing the orientational effect of the carbonyl group more directly, we synthesized an *N*-methylpyridinium salt of 6, 7-dihydro-6-methyl-5-oxopyridino [3, 2-*d*]-2-benzazepin ( $\text{MeMPA}^+$ ) and its dihydropyridine derivative ( $\text{MeMPAH}$ ). Unfortunately, conformational stability of  $\text{MeMPA}^+\text{I}^-$  is not sufficient, and the optically active enantiomer of this salt racemizes at room temperature easily.

The  $^1\text{H}$  NMR spectrum of  $\text{MeMPAH}$  in  $\text{CD}_3\text{CN}$  shows completely separated signals arising from two methylene

### BIOORGANIC CHEMISTRY —Physical Bioorganic Chemistry—

#### Scope of research

Biochemical reactions are studied from the viewpoint of physical organic chemistry. Namely, the reaction mechanism and stereochemistry of *NAD*-dependent oxidoreductases are explored. Stereospecific redox transformations mediated by certain biocatalysts such as microbes, enzymes, cultured tissues are also studied. The results will be applied to develop new organic reactions.



Professor  
OHNO, Atsuyoshi  
(D Sc)



Associate Professor  
NAKAMURA, Kaoru  
(D Sc)



Instructor  
SUGIYAMA, Takashi



Instructor  
KAWAI, Yasushi  
(D Sc)

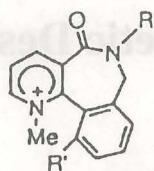
#### Technician:

HIRANO, Toshiko

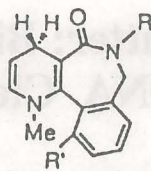
#### Students:

KAWASAKI, Masashi (RF)  
KONDO, Shin-ichi (DC)  
TSUTSUMI, Akihiro (DC)  
KINOSHITA, Masamichi (DC)  
SHIOJI, Kosei (DC)  
YAMAZAKI, Norimasa (DC)  
KUNITOMO, Jun (DC)  
TAKAHASHI, Akiko (DC)  
INOUE, Yuko (MC)  
SAITOU, Kentarou (MC)  
NAKAGAWA, Toshiya (MC)  
HIDA, Kouichi (MC)  
KUBO, Yuji (RS)  
TODA, Toshiyuki (RS)  
MATSUDA, Tomoko (RS)  
YAMAGUCHI, Satoshi (RS)





R=Me, R'=H: MeMPA<sup>+</sup>  
R=tBu, R'=H: BuMPA<sup>+</sup>  
R=Me, R'=Me: 3Me-MeMPA<sup>+</sup>



R=Me, R'=H: MeMPAH  
R=tBu, R'=H: BuMPAH  
R=Me, R'=Me: 3Me-MeMPAH

mprotons at the C<sub>4</sub>-position (*syn* and *anti* to the carbonyl oxygen). Therefore, the stereochemistry associated with the reduction of MeMPA<sup>+</sup> with a deuterated reagent can be monitored quite easily. The results are summarized in Table 1 together with those of BuMPA<sup>+</sup>. It is interesting to note that a (net) hydride originating from BNAH or its analog attacks MeMPA<sup>+</sup> from the side of the pyridinium ring where the carbonyl oxygen lies, even though this is the more sterically hindered face. Thus, the stereochemistry of the reaction cannot be explained as a steric effect, and there is no doubt that the carbonyl dipole or an electronic effect plays an important role in determining the stereochemical outcome of the reaction. The stereochemical result of the reduction with sodium dithionite in D<sub>2</sub>O affords a *syn/anti* ratio of 50/50, which is different from those with BNAH and its analogs. However, we must point out the possibility that the compound has undergone racemization during the processes of isolation and spectroscopy. Indeed, a preliminary result from the reduction of 6,7-dihydro-6-methyl-5-oxopyridino[3,2-*d*]-2-(3-methylbenz) azepin (3Me-MeMPA<sup>+</sup>), the conformation of which is stable at

**Table 1.** Reduction of Racemic Mixture of MeMPA<sup>+</sup> and BuMPA<sup>+</sup> <sup>a</sup>

NAD <sup>+</sup> -Analog	Time h	Reducing Reagent	Stereochemistry <sup>b,c</sup> <i>syn</i> : <i>anti</i>
MeMPA <sup>+</sup> (R=Me)	1.0	Na <sub>2</sub> S <sub>2</sub> O <sub>4</sub> /D <sub>2</sub> O	50 : 50
	39 <sup>d</sup>	BNAH-4, 4- <i>d</i> <sub>2</sub>	65 : 35
	1.5	( <i>R</i> )-Me <sub>2</sub> PNPH-4- <i>d</i>	58 : 42
	1.5	( <i>S</i> )-Me <sub>2</sub> PNPH-4- <i>d</i>	60 : 40
BuMPA <sup>+</sup> (R=tBu)	1.0	Na <sub>2</sub> S <sub>2</sub> O <sub>4</sub> /D <sub>2</sub> O	51 : 49
	1.5	( <i>R</i> )-Me <sub>2</sub> PNPH-4- <i>d</i>	70 : 30
	1.5	( <i>S</i> )-Me <sub>2</sub> PNPH-4- <i>d</i>	69 : 31

a: About 20% of MeMPAD or BuMPAD produced reacts with MeMPA<sup>+</sup> or BuMPA<sup>+</sup>, respectively, yielding 4,4-dihydro and 4,4-dideuterio compounds. b: Relative to the carbonyl oxygen. c: Estimated error is about ±3 for all numbers. d: Reaction at 35°C.

room temperature, in contrast to the unstability of those MeMPA<sup>+</sup> and BuMPA<sup>+</sup>, with sodium dithionite has revealed that the *syn/anti* ratio is 80/20. Further investigation is necessary before a conclusion is formed on the stereochemical difference between hot and cold reducing agents.

It has been proposed that the carbamoyl moiety in an NADH analog faces a polar side chain of the substrate or oxidizing agent at the transition state of a homogeneous reaction [5]. Magnesium ion promotes this face-to-face interaction by coordinating on itself both reducing and oxidizing agents. Not only is the stereochemistry improved by the sandwich-like interaction of magnesium ion, but the reaction rate is also increased by its catalytic effect. The present reaction, however, is retarded by the presence of magnesium ion, which is quite reasonable because one of the agents is an onium, and it is highly plausible that a cation is hardly coordinated on a cationic magnesium ion. Thus, a binary complex between the reducing and oxidizing agents is a plausible intermediate in the present reaction even in the presence of magnesium ion.

The fact that both (4*R*)- and (4*S*)-Me<sub>2</sub>PNPD afford the same *syn/anti* ratio within experimental error confirms the idea that face-to-face interaction between the carbonyl group in the onium and the one in the reducing agent is important at the transition state of the reaction as proposed previously.

To our best knowledge, MeMPA<sup>+</sup>/MeMPAH system is the first example of molecular asymmetry stemming from the orientation of the carbonyl group only and resolved to each enantiomer.

The present result strongly supports the possibility of functional model for chemical evolution of an enzyme, where it is predicted that NAD(P)<sup>+</sup>/NAD(P)H coenzymes themselves can induce chirality into an achiral substrate during a redox reaction without stereochemical assistance of a protein [6].

## References

- Benner S and Stackhouse J, In "Chemical Approaches to Understanding Enzyme Catalysis"; Green, B.S., Ashani, Y., Chipman, D., Eds.; Elsevier, New York (1982).
- Ohno A, Ohara M and Oka S, *J. Am. Chem. Soc.*, **108**, 6438–6440 (1986).
- Nambiar K P, Stauffer D M, Koloziej P A and Benner S A, *J. Am. Chem. Soc.*, **105**, 5886–5890 (1983).
- Okamura M, Mikata Y, Yamazaki N, Tsutsumi A and Ohno A, *Bull. Chem. Soc. Jpn.*, **66**, 1197–1203 (1993).
- Ohno A, Goto T, Nakai J and Oka S, *Bull. Chem. Soc. Jpn.*, **54**, 3478–3481 (1981).
- Ohno A, *Proc. 14th Int. Cong. Biochem., Prague*, **2**, 217–223 (1989).



# A Novel Zinc Finger-Based DNA Cutter: Biosynthetic Design and Highly Selective DNA Cleavage

Makoto Nagaoka, Masaki Hagihara, Jun Kuwahara, and Yukio Sugiura

In this communication, we describe the design, synthesis and testing of a novel zinc finger-based DNA cutter. Transcription factor Sp1 has three tandem repeats of a Cys<sub>2</sub>His<sub>2</sub>-type zinc finger motif and specifically binds to GC box DNA. Herein, an Sp1 derivative with an attached Ni-based DNA cleavage unit (Gly-Gly-His) has been created. In the presence of magnesium monoperoxyphthalate, the Ni(II)-coordinated zinc finger protein, designated Sp1GGH, binds to GC box and cleaves a restriction fragment at essentially a single site near the recognition sequence. This ligand which simultaneously binds in both major and minor grooves appears to bridge across the sugar-phosphate backbone. The result is of special interest because of the potential versatility of zinc finger proteins in recognizing different DNA sequences. This work is pertinent to the design of the novel artificial restriction enzyme based on the zinc finger motif applicable to chromosome mapping and sequencing.

**Keywords:** Zinc finger/ DNA cleavage/ Nuclease/ Transcription factor/ Sequence specificity

Conversion of a DNA-binding protein to a DNA-cleaving molecule by attachment of a metal-chelating ligand is one of the most versatile methods for affinity cleaving. These chimeric proteins have largely utilized helix-turn-helix or b-zip-type motifs and interacted with DNA as a dimer. Therefore, their target sites are limited to palindromic base sequences with a dyad or a pseudodyad axis. On the other hand, DNA sequences recognized by Cys<sub>2</sub>His<sub>2</sub>-type zinc finger proteins are almost asymmetric because of their monomeric binding mode. We report here the design and function of a new DNA-cleaving metalloprotein consisting of the zinc finger motif.

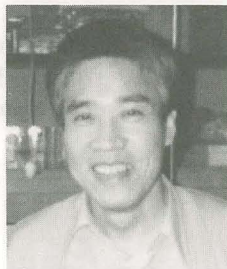
Primary sequence of the zinc finger-based DNA cutter (designated Sp1GGH) comprising two functional domains is shown in Figure 1. The DNA-binding

domain contains the C-terminal region (residues 529–696) of transcription factor Sp1 bearing three contiguous repeats of the Cys<sub>2</sub>His<sub>2</sub>-type zinc finger motif, which recognizes an asymmetric decanucleotide with consensus sequence 5'-(G/T)GGGCGG(G/A)(G/A)(C/T)-3'. Each zinc finger domain coordinates a Zn(II) in a tetrahedral complex. In an effort to give DNA-cleaving activity to zinc finger protein, the tripeptide Gly-Gly-His (GGH) was attached to the N-terminus of the DNA-binding domain because of the availability of a genetic engineering method. The GGH segment originally derived from the copper-binding domain of serum albumin is believed to bind Ni(II) in a 1:1 square-planar complex with coordination from an imidazole nitrogen, two deprotonated peptide nitrogens, and the terminal amino group, referring to the crystal structure of the Cu<sup>II</sup>-

## BIOORGANIC CHEMISTRY —Bioactive Chemistry—

### Scope of research

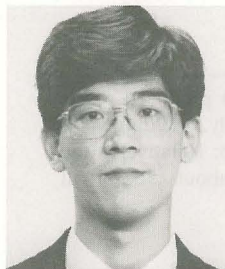
*The major goal of our laboratory is to elucidate the molecular basis of the activity of various bioactive substances by biochemical, physicochemical, and synthetic approaches. These include studies on the mechanism of sequence-specific DNA cleavage by antitumor or carcinogenic molecules, probing the DNA fine structure by various chemicals, studies on the DNA recognition of Zinc-finger proteins, construction of artificial restriction enzyme, and model study on the cooperative mechanism of DNA binding by dimeric peptides. Also studied are the design and synthesis of functional molecules that effectively regulate the intracellular signal transduction or that applicable to fluorescence detection of DNA.*



Professor  
SUGIURA, Yukio  
(D Pharm Sc)



Associate Professor  
OTSUKA, Masami  
(D Pharm Sc)



Instructor  
MORII, Takashi  
(D Eng)

### Guest Research Associate:

KLATT, Martin

### Students:

UESUGI, Motonari (DC)  
GUAN, Le Luo (DC)  
KUSHIDA, Tatsushi (DC)  
FUJITA, Mikako (DC)  
MATASUMOTO, Takuyuki (DC)  
NAGAOKA, Makito (DC)  
OKUNO, Yasushi (MC)  
KUSAKABE, Tetsuya (MC)  
SATAKE, Honoo (MC)  
HAGAHARA, Masaki (MC)  
AIZAWA, Yasunori (MC)  
INOUE, Teruhiko (MC)  
EMORI, Takashi (MC)  
KUBOTA, Naoki (UG)  
SATO, Tetsuo (UG)  
FUJITA, Kazutoshi (UG)



GGH complex. The Ni (II) complex of the peptide ligand attached to the DNA-binding protein can successfully cut DNA in the presence of peroxide. The amino terminus of the GGH segment must be a primary amine, although all bacterially expressed proteins have methionine residues on their N-termini. This problem can be overcome by incorporation of the recognition sequence IEGR of blood coagulation factor (factor Xa) preceding the GGH segment. Repeated dialysis of Sp1GGH against buffers containing different concentrations of metals enables selective binding of Zn (II) in the finger region and of Ni (II) in the GGH segment, respectively, reflecting inherent metal preference of two functional domains. It has been confirmed that the three-finger region of Sp1 binds three Zn (II) ions. Incorporation of the GGH segment onto the N-terminal region of Sp1 presumably does not affect the binding geometry of the three-finger domain, because extension of 12 amino acid residues from the N-terminus of Sp1 (167\*) has shown the exact same methylation interference pattern as that for the shorter form, Sp1 (167\*) [1].

In the presence of magnesium monoperoxyphthalate (100 mM), quite specific cleavage of DNA occurred predominantly at two cytosine bases on both strands with single-base specificity. Cutting at the cytosine on the guanine-rich strand (G-strand) was much stronger than that for the other cytosine base on the opposite cytosine-rich strand (C-strand) (Figure 2). Termini at the cleavage sites appear to be 3'-phosphate groups. The remarkably restricted range of cleavage at the single-base position suggests that a nondiffusible oxidant might be generated by the Ni-GGH complex in the minor groove. The facts show that orientation of the peptide backbone in Sp1 is antiparallel to the primarily interacting strand (G-strand). The cleavage center for the above two bases was 4 bp apart from the 3' end of GC box on the G-strand.

The 3'-staggered cutting pattern clearly demonstrates that the cleavage event occurs in the minor groove of DNA, and thus the Ni-GGH domain of Sp1GGH appears to be situated in the minor groove. In contrast, previous studies have shown that the three-finger domain of Sp1 contacts with guanine bases in the major groove. The Ni-GGH domain attached to the N-terminal arm of Hin recombinase (139–190) also shows the 3'-staggered cleavage pattern. Indeed, the homeodomains and Hin recombinase make base contacts in both grooves, with the helix-turn-helix region in the major groove of DNA and the N-terminal arm in the adjacent minor groove. Two functional domains of Sp1GGH are spanned by seven amino acid residues (GGHGD<sup>P</sup>GKKKQHIC). Given that the N-terminal linker region adopts an extended, flexible conformation in a manner similar to the conformation of the N-terminal arm of the homeo-

domains, the linker region can bridge across the sugar-phosphate backbone of DNA and permits the Ni-GGH domain to locate at the cleavage center in the minor groove. The finding that the N-terminal finger 1 of Sp1 makes loose contacts with DNA might reinforce our explanation [2].

Tandemly repeated structures of multiple finger modules and asymmetry of the recognition base sequences are notable features of the Cys<sub>2</sub>His<sub>2</sub>-type zinc finger proteins. The modular structure revealed by the crystal structure of the three-finger protein Zif268-DNA complex, in which the single finger domain strictly recognizes three base pairs, sheds light on the great versatility of the Cys<sub>2</sub>His<sub>2</sub>-type zinc finger proteins in terms of designing DNA-binding protein with novel specificities. It might be possible to recognize any desired sequence by combination of different finger motifs. Our work is pertinent to the design of the novel artificial restriction enzyme based on the zinc finger motif applicable to chromosome mapping and sequencing.

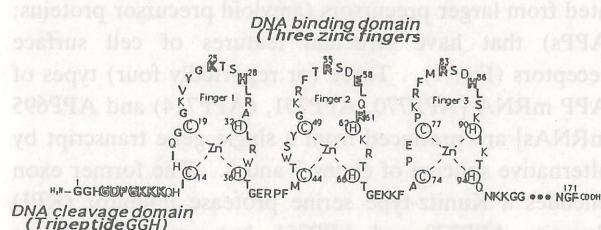


**Figure 1.** Schematic representation of Sp1GGH. Amino acid residues of Sp1GGH are indicated by one-letter abbreviations and numbered from the amino terminus. The tripeptide GGH, the linker region, and the amino acid relevant to specific base contact are represented as bold, outlined, and shadowed types, respectively.



**Figure 2.** Histograms of cleavage sites in GC box DNA sequence based on densitometric analysis of the gel autoradiograms. Top and bottom sequences show G- and C-strands, respectively. The box indicates the GC box, and the length of bars represents the extent of cleavage. Relative extent of cleavage was estimated by the intensity of autoradiograms.

## References

1. Nagaoka M, Kuwahara J and Sugiura Y, *Biochem. Biophys. Res. Commun.*, **194**, 1515–1520 (1993).
2. Kuwahara J, Yonezawa A, Futamura M and Sugiura Y, *Biochemistry*, **32**, 5994–6001 (1993).



## Molecular Etiology of Alzheimer's Disease: Aberrant Splicing of APP Gene Transcript and Linkage to Apolipoprotein $\epsilon 4$ Allele

Seigo Tanaka and Kunihiro Ueda

Aberration of alternative splicing of amyloid precursor protein (APP) gene transcript was found in AD brains, which may cause an imbalance between protease(s) and inhibitor, and possibly lead to deposition of amyloid as a result of incomplete digestion of APP. The  $\epsilon 4$  allele of apolipoprotein E (APOE) gene was found more frequently in late-onset cases of AD than in control, indicating that apolipoprotein E4 is a risk factor of AD.

**Keywords:** Amyloid precursor protein/ Alternative splicing/ Aging/ Apolipoprotein E

Alzheimer's disease (AD) is one of the most common cause of dementia, and pathologically characterized by the deposition of  $\beta A 4$  protein in senile plaque cores and cerebral vessels as amyloid. The  $\beta A 4$  protein is generated from larger precursors (amyloid precursor proteins; APPs) that have structural features of cell surface receptors (Fig. 1). Three (or reportedly four) types of APP mRNA [APP770, APP751, (APP714) and APP695 mRNAs] are produced from a single gene transcript by alternative splicing of exons 7 and 8. The former exon encodes a Kunitz-type serine protease inhibitor (KPI) domain; APP770 and APP751, but not APP695 (nor APP714), have this KPI domain in the extra-cellular region. Our previous study [1] showed that the proportion of APP770 mRNA (or APP770 mRNA + APP751 mRNA) is higher in the brain of AD than in control, particularly in the cerebral cortex and hippocampus. Additionally, AD patients showing histologically a high density of senile plaques exhibited a

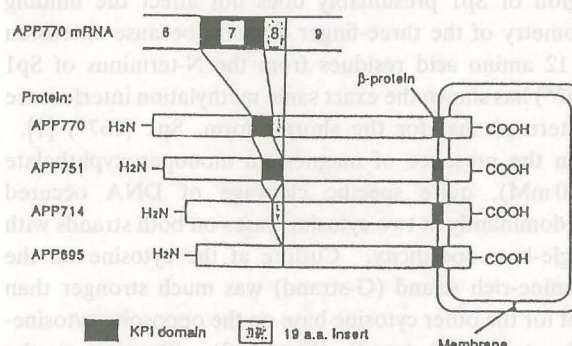


**Figure 1.** Structures of APP770 mRNA and four types of APPs that have structural features of cell surface receptors. The number of each domain corresponds to that of exon in the APP gene. Exon 7 encodes the KPI domain.

high ratio of (APP770 mRNA + APP751 mRNA) / APP695 mRNA.

In this study, we analysed, by the method of RNase protection assay, the proportion of APP mRNAs in

### BIOORGANIC CHEMISTRY —Molecular Clinical Chemistry—

#### Scope of research

This laboratory was founded in 1994, aiming at linkage between chemical/molecular sciences and basic/clinical medicine. Thus, our research effort is focused on elucidation of patho-physiological significance of various bioreactions, such as poly(ADP-ribosylation) of nuclear proteins and alternative splicing of amyloid precursor protein gene transcript, in etiology of diseases, such as malignancies and Alzheimer's disease. Gene diagnosis, particularly its laboratory technology and application to pathogenic genes, is another subject of our current research.



Professor  
UEDA, Kunihiro  
(D Med Sc)



Instructor  
TANAKA, Seigo  
(D Med Sc)

#### Instructors in Cooperation:

KIDO, Takahiro (Kyoto Univ. Col. of Med. Technol.)

ADACHI, Yoshifumi (Kyoto Univ. ICR)



various neurological disorders with special reference to aging. We found that the ratio of (APP770 mRNA + APP751 mRNA)/APP695 mRNA increased approximately 1.5-fold in the frontal cortex of AD compared with other neurodegenerative or cerebrovascular disorders [2] (Fig. 2). Furthermore, we found a positive correlation

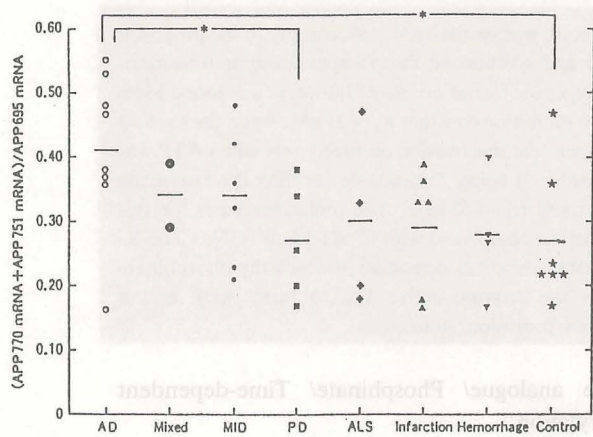


**Figure 2.** The ratio of (APP770 mRNA + APP751 mRNA)/APP695 mRNA in the frontal cortex in various neurological disorders and control. MID: multi-infarct dementia, PD: Parkinson's disease, ALS: amyotrophic lateral sclerosis.

\*  $p < 0.05$  (Student's *t*-test).

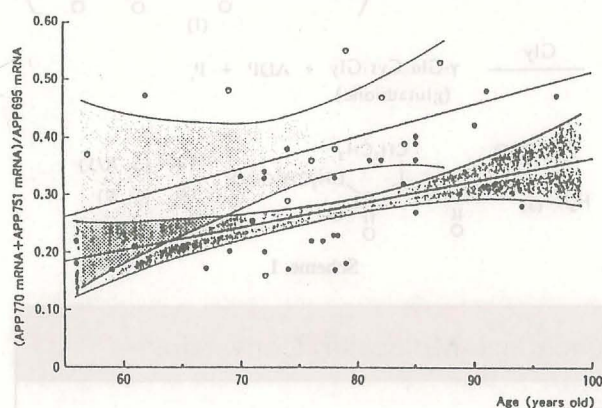


**Figure 3.** Correlation between the ratio of (APP770 mRNA + APP751 mRNA)/APP695 mRNA in the frontal cortex and age. The regression line for AD group ( $\circ$ ,  $n=10$ ) is  $y=0.005x+0.014$  ( $r=0.372$ ), and that for non-AD group ( $\bullet$ ,  $n=33$ ) is  $y=0.004x-0.037$  ( $r=0.486$ ). The  $\geq 90\%$  confidence areas are indicated with shadowing. The AD group includes AD and mixed-type dementia.

between the ratio ( $y$ ) and age ( $x$ ) both in AD and non-AD groups (Fig. 3). The relationship between the ages of AD ( $x_{AD}$ ) and non-AD ( $x_{non-AD}$ ) giving the same ratio was  $x_{AD}=0.8x_{non-AD}-10.2$ , indicating that the AD brain reached the same ratio of KPI-harboring to lacking APP mRNAs more than 20 years earlier than the non-AD brain in senescence. This age-related change of APP mRNAs proportion is prominent in the gray matter of cerebral cortex, where senile plaques abound, compared with the white matter [3]. These findings led us to the idea that an imbalance between protease(s) and inhibitor, caused by the aberrant splicing of APP gene transcript, may perturb normal degradation of APPs, thereby leading to deposition of  $\beta A4$  protein as amyloid. The proportion of APP mRNAs may serve as a molecular index of brain aging or a marker of AD.

Apolipoprotein E (apoE) is a structural component of chylomicron and lipoproteins and plays an important role in lipid metabolism. There are three major isoforms, referred to as apoE2, E3 and E4, that are encoded by  $\epsilon 2$ ,  $\epsilon 3$  and  $\epsilon 4$  alleles, respectively, of a single gene located on the long arm of chromosome 19. The  $\epsilon 4$  allele was reported to be associated with late-onset familial and sporadic ADs in the United States [4]. In this study, we analysed apoE genotypes in Japanese cases of sporadic AD by using PCR (polymerase chain reaction) coupled with RFLP (restriction fragment length polymorphism). We found a significant increase in the frequency of  $\epsilon 4$  allele in late-onset cases (0.25), but not in early-onset ones (0.04), compared with control (0.09) [5]. The  $\epsilon 4$  allele frequency was not so high among Japanese AD patients as reported for Caucasians, which could explain the relatively lower morbidity from AD in Japan. Thus, the apoE  $\epsilon 4$  allele appears to serve as a risk factor of AD.

#### References

1. Tanaka S, Shiojiri S, Takahashi Y, *et al*, *Biochem. Biophys. Res. Commun.*, **165**, 1406–1414 (1989).
2. Tanaka S, Liu L, Kimura J, *et al*, *Mol. Brain Res.*, **15**, 303–310 (1992).
3. Tanaka S, Nakamura S, Kimura J and Ueda K, *Neurosci. Lett.*, **163**, 16–21 (1993).
4. Strittmatter W J, Saunders A M, Schmechel D, *et al*, *Proc. Natl. Acad. Sci. USA*, **90**, 1977–1981 (1993).
5. Kawamata J, Tanaka S, Shimohama S and Kimura J, *J. Neurol. Neurosurg. Psychiatr.*, **57**, 1414–1416 (1994).



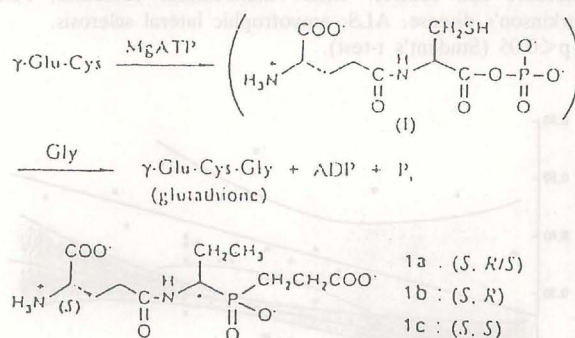
# Mechanism-Based Inactivation of Glutathione Synthetase by Phosphinic Acid Transition-State Analogue

Jun Hiratake, Hiroaki Kato, and Jun'ichi Oda

A potent and time-dependent inactivator of glutathione synthetase was synthesized. According to the proposed reaction mechanisms of glutathione synthetase, we designed and synthesized the phosphinate-type transition-state analogue **1**. The (*S*, *R*)-isomer of **1** having the same relative configurations as  $\gamma$ -Glu-L-Cys was found to be a potent and time-dependent inactivator of this enzyme with an inhibition constant  $K_i$  of 21 nM, while the (*S*, *S*)-**1** related to  $\gamma$ -Glu-D-Cys was practically inactive. The time-dependent inactivation occurred only when ATP was present, with the onset rate of inactivation ( $k_{on}=8.29 \text{ sec}^{-1} \text{ mM}^{-1}$ ) being 75-times slower than the enzymatic reaction, and the inactivated enzyme slowly regained its activity ( $t_{1/2}=53 \text{ hr}$ ). The molecular basis for this inactivation was probed by an X-ray crystallography of the enzyme complexed with (*S*, *R*)-**1** and ATP. The X-ray diffraction analysis has shown that a mechanism-based inactivation was operative in which the phosphinate oxygen ( $\text{P}-\text{O}^-$ ) of **1** was phosphorylated by ATP within the enzyme active site to form ADP and a phosphorylated **1** which is highly analogous to the proposed transition state.

**Keywords:** Glutathione synthetase/ Transition-state analogue/ Phosphinate/ Time-dependent inactivation/ Mechanism-based phosphorylation

Glutathione synthetase (GSHase, EC 6.3.2.3), catalyzing the ligation of  $\gamma$ -Glu-Cys and glycine with the aid of ATP, is a key enzyme in glutathione biosynthesis. The detailed reaction mechanisms, however, are yet to be well understood, although the X-ray crystal structure of this enzyme has recently been defined [1]. In the light of mechanistically well-studied other ligases such as glutamine synthetase [2] or D-Ala-D-Ala ligase [3], the reaction catalyzed by GSHase is thought to proceed through the initial formation of a putative acyl phosphate intermediate (I), followed by nucleophilic attack of glycine to yield glutathione, ADP and inorganic phosphate (Scheme 1).

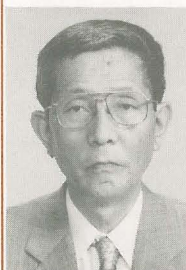


Scheme 1

## MOLECULAR BIOFUNCTION —Functional Molecular Conversion—

### Scope of research

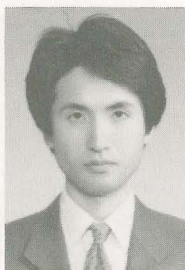
Our research aims are to analyze structure-function relationships of biocatalysts in combination with organic chemistry, structural biology and computer science, and to apply biocatalysts to stereospecific organic synthesis. Major subjects are the design and preparation of antibodies catalyzing stereoselective reactions, the reaction mechanisms of glutathione synthetase from *E. coli* with static and time-resolved X-ray crystallography, the mode of action of lipase-activating protein, crystallographic analysis of asparagine synthetase and  $\gamma$ -L-glutamyl-L-cystein synthetase, and creation of enzymatic reaction database and development of algorithms for protein sequence analysis.



Professor  
ODA,  
Jun'ichi  
(D Agr)



Assoc Prof  
NISHIOKA,  
Takaaki  
(D Agr)



Instructor  
KATO,  
Hiroaki  
(D Agr)



Instructor  
HIRATAKE,  
Jun  
(D Agr)



Instructor  
TANAKA,  
Takuji  
(D Agr)

### Students:

SUYAMA, Mikita (DC)  
HARA, Takane (DC)  
NAKATSU, Toru (DC)  
SHIBATA, Hiroyuki (DC)  
KATO, Makoto (MC)  
IMAEDA, Yasuhiro (MC)  
MATSUDA, Keiko (MC)



We therefore designed the transition-state analogue **1** in which the C-terminal carboxyl group is replaced by a tetrahedral phosphinyl group with a 2-carboxyethyl moiety mimicking the incoming glycine, and used the phosphinate **1** to probe the reaction mechanisms of this enzyme. Starting with racemic, (*R*)-, and (*S*)-1-(amino-propyl)phosphinic acid derivative [4], the diastereomeric mixture (*S*, *R/S*)-**1a** and each diastereomer (*S*, *R*)-**1b** and (*S*, *S*)-**1c** were synthesized.

The phosphinate **1a** was found to be a remarkably potent inactivator of GSHase. Treatment of GSHase with **1a** resulted in time-dependent inactivation of the enzyme as shown by the progress curves (Figure 1). Interestingly, no inactivation was observed without ATP, whereas complete inactivation resulted when both **1a** and ATP were present.

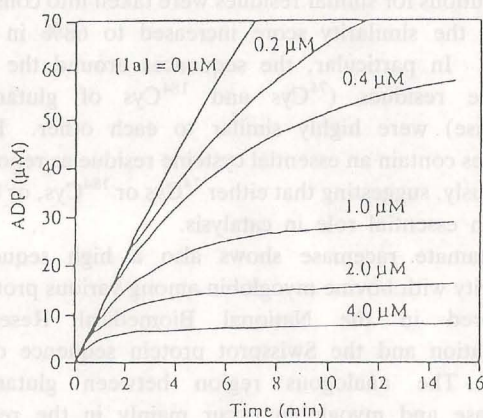
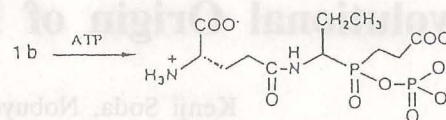


**Figure 1.** Progress curves for the inactivation of GSHase by **1a**. The reaction was initiated by adding enzyme to an assay mixture containing  $\gamma$ -Glu-Cys (0.2 mM), Gly (15 mM), ATP (5 mM) and **1a** (0.2–4  $\mu$ M) in 50 mM Tris-HCl (pH 7.5) at 37°C.

The inactivated enzyme slowly regained its activity ( $t_{1/2}$  = 53 hr) when incubated for several days, but not within a steady-state time scale, thus the inhibition being practically irreversible. The onset rate of inactivation ( $k_{on}$ ) [5] was calculated from the progress curves and was found to be  $8.29 \text{ s}^{-1} \text{ mM}^{-1}$  with **1a**. This value, compared with the kinetic constants for  $\gamma$ -Glu-Cys [ $k_0/K_m = 625 \text{ s}^{-1} \text{ mM}^{-1}$ ], means that the inactivation process is 75 times slower than the enzymatic reaction. Steady-state kinetic analysis revealed that the inhibition was competitive with  $\gamma$ -Glu-Cys, with the inhibition constant  $K_i$  being 53 nM with **1a**. As expected, the (*S*, *R*)-**1b** having the same relative configuration as  $\gamma$ -Glu-L-Cys was found to be an extremely potent and time-dependent inactivator ( $K_i$  = 21 nM), whereas the (*S*, *S*)-isomer **1c** related to D-Cys showed only 18% inhibition at 39 mM.

The molecular basis for the time- and ATP-dependent inactivation by **1** was examined. Considering that the enzyme inactivation was observed only when both ATP and phosphinate **1** were present, the inhibition pattern is



most likely to reflect a mechanism-based phosphorylation of the phosphorus oxyanion ( $\text{PO}^-$ ) of **1b** by ATP within the enzyme active site.

If this is the case, then the tightly bound phosphorylated inhibitor **1b** and ADP should be visible with an X-ray diffraction analysis of GSHase complexed with **1b** and ATP. This in fact proved to be the case: the electron density map around the active site has clearly shown that the  $\gamma$ -phosphate of ATP has been transferred to the inhibitor phosphorus oxyanion ( $\text{PO}^-$ ) to form a phosphorylated **1b** and ADP within the enzyme active site (Figure 2). Since the phosphorylated **1b** is highly analogous to the proposed transition state, the phosphinate **1** serves as an excellent probe for defining what the real transition state is like and how this enzyme stabilizes it to facilitate the reaction.

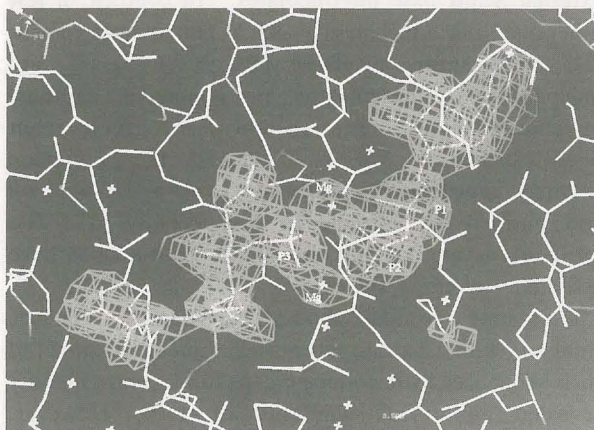


**Figure 2.** The  $F_o - F_c$  electron density surface of the phosphorylated phosphinate **1b** and MgADP, superimposed with refined structure of the active site region. The contributions of the phosphorylated **1b** and MgADP were omitted from the  $F_c$  calculation. The contour level is  $3.5\sigma$ .

## References

1. Kato H, Tanaka T, Yamaguchi H, Hara T, Nishioka T, Katsube Y and Oda J, *Biochemistry*, **33**, 4995–4999 (1994).
2. Meister A, In *The Enzymes*, Boyer P.D., Ed.; Academic Press, New York, 1974; Vol. 10, pp. 699–754.
3. Mullins L.S., Zawadzke L.E., Walsh C.T. and Raushel F.M., *J. Biol. Chem.*, **265**, 8993–8998 (1990).
4. Hiratake J, Kato H and Oda J, *J. Am. Chem. Soc.*, **116**, 12059–12060 (1994).
5. Morrison J.F. and Walsh C.T., In *Advances in Enzymology*; Meister A., Ed.; John Wiley: New York, 1988; Vol. 61, pp. 201–301.



## Evolutional Origin of Bacterial Glutamate Racemase

Kenji Soda, Nobuyoshi Esaki and Tohru Yoshimura

Glutamate racemase (EC 5.1.1.3), an enzyme of microbial origin, shows significant sequence similarity with mammalian myoglobins, in particular in the regions corresponding to the E and F helices, which constitute the heme binding pocket of myoglobins. Glutamate racemase binds tightly an equimolar amount of hemin leading to loss of racemase activity. Although this enzyme shows sequence similarity with aspartate racemase, the latter does not bind hemin. Neither racemase has cofactors, but contain essential cysteine residues.

**Keywords:** Specific inhibition by hemin/ E and F helices of myoglobin/ Essential cysteine residues

D-Glutamate is an essential component of peptidoglycans of bacterial cell walls, and is produced from L-glutamate by glutamate racemase (EC 5.1.1.3) or from  $\alpha$ -ketoglutarate by D-amino acid aminotransferase (EC 2.6.1.21) [1]. Most amino acid racemases, such as alanine racemase (EC 5.1.1.1), require pyridoxal 5'-phosphate (PLP) as a coenzyme, and the racemase reaction is facilitated by formation of internal and external Schiff base intermediates. In contrast, a few other amino acid racemases, such as glutamate racemase [2] and aspartate racemase (EC 5.1.1.13) [3], are independent of any cofactor, and contain no carbonyl moieties or metals. Their reaction mechanisms have not been elucidated. We have cloned the glutamate racemase gene from *P. pentosaceus*, expressed it in *E. coli* and purified the enzyme to homogeneity [4]. The purified enzyme contains no co-factors, but does have essential cysteine residues.

Glutamate racemase showed considerable sequence similarity with aspartate racemase. Linear alignment of their sequences by introducing gaps to maximize identity revealed an overall similarity of 14%. However,

sequence similarity in the internal region (69–192 of the glutamate racemase sequence) was much higher; 31 of 124 residues being common. If the mutationally allowed substitutions for similar residues were taken into consideration, the similarity score increased to 68% in this region. In particular, the sequences around the two cysteine residues ( $^{74}\text{Cys}$  and  $^{184}\text{Cys}$  of glutamate racemase) were highly similar to each other. Both enzymes contain an essential cysteine residue as reported previously, suggesting that either  $^{74}\text{Cys}$  or  $^{184}\text{Cys}$ , or both play an essential role in catalysis.

Glutamate racemase shows also a high sequence similarity with bovine myoglobin among various proteins registered in the National Biomedical Research Foundation and the Swissprot protein sequence data-banks. The analogous region between glutamate racemase and myoglobin occur mainly in the region between  $^{46}\text{Phe}$  and  $^{150}\text{Gly}$  of bovine myoglobin which corresponds to the region from  $^{92}\text{Val}$  to  $^{183}\text{Gly}$  of glutamate racemase. Twenty-seven of the 92 residues of glutamate racemase are common to the corresponding residues of the myoglobin. The similarity score is 52%

### BIOFUNCTIONAL MOLECULES —Molecular Microbial Science—

#### Scope of research

*Structure and function of biocatalysts, in particular, pyridoxal enzymes and NAD enzymes are studied to elucidate the dynamic aspects of the fine mechanism for their catalysis in the light of recent advances in gene technology, protein engineering and crystallography. In addition, the metabolism and biofunction of selenium and some other trace elements are also investigated. Development and application of new biomolecular functions of microorganisms are also studied to open the door to new fields of biotechnology. For example, molecular structures and functions of thermostable enzymes and their application are under investigation.*



Professor  
SODA, Kenji  
(D Agr)



Associate Professor  
ESAKI, Nobuyoshi  
(D Agr)



Instructor  
YOSHIMURA, Tohru  
(D Agr)



Instructor  
KURIHARA, Tatsuo  
(D Eng)

#### Associate Instructor:

HIRASAWA, Toshiko

#### Students:

TCHORZEWSKI, Marek (DC)  
LIU, Jiquan (DC)  
KUROKAWA, Yoichi (DC)  
JHEE, Kwang-hwan (DC)  
KISHIMOTO, Kazuhisa (DC)  
GUTTIERREZ,  
Aldo Francisco (DC)  
CHOO, Dong-Won (DC)  
PARK, Chung (DC)  
LIU, Lidong (DC)  
AOKI, Tomoko (MC)  
KITAMURA, Tae (MC)  
MIHARA, Hisaaki (MC)  
KURONO, Takeshi (MC)  
MIYAKE, Hitoki (MC)



in this region, if the similar residues of permissible mutational substitution are taken into account. The amino acid sequences of myoglobins from various sources are highly conserved. The abalone myoglobin shows high sequence similarity with human indoleamine 2,3-dioxygenase, but not with other myoglobins. We found no significant sequence similarity between the abalone myoglobin and glutamate racemase. Similarity scores between glutamate racemase and the other myoglobins were: 21–27% identity in the range of the 92 amino acid residues. Cyanobacterial myoglobin from *Nostoc commune* showed the lowest sequence similarity (21%) with glutamate racemase. Significant sequence similarities were also found between glutamate racemase and other globin family proteins such as hemoglobins in this same region. Bacterial hemoglobin from *Vitreoscilla* shows the lowest sequence similarity with glutamate racemase among the various hemoglobins examined.

Proteins analogous to bovine myoglobin in primary structure were also searched by means of the same data-banks. The sequence similarity is dependent on the kind of proteins and their sources: myoglobins from other sources, 38–85%;  $\alpha$  and  $\beta$ -chains of mammalian hemoglobins, 21–31%; *Vitreoscilla* hemoglobin, 24%; *N. commune* myoglobin, 16%; glutamate racemase, 26% (in the range between <sup>46</sup>Phe and <sup>150</sup>Gly of bovine myoglobin). Bovine myoglobin shows higher sequence similarity with glutamate racemase than prokaryotic myoglobin and hemoglobin. Aspartate racemase was also analogous to bovine myoglobin in the region from <sup>102</sup>Ile to <sup>196</sup>Gly corresponding to that from <sup>46</sup>Phe to <sup>150</sup>Gly of bovine myoglobin: 14 residues were common between the two proteins. However, this sequence similarity was much lower than that found between glutamate racemase and bovine myoglobin.

The analogous range (residue numbers, 46–150) of bovine myoglobin contains the regions corresponding to E and F helices, which constitute the heme binding pocket. E7 of the E helix of bovine myoglobin, <sup>64</sup>His, which is essential in binding molecular oxygen, is replaced by Gln in the bacterial myoglobin and the bacterial hemoglobin. An analogous Gln occurs as <sup>110</sup>Gln in glutamate racemase. Moreover, <sup>68</sup>Val of E11, which is highly conserved among globin family proteins, is also conserved as <sup>114</sup>Val. Accordingly, we examined the interaction of glutamate racemase and aspartate racemase with hemin. When the enzymes were assayed in the presence of various concentrations of hemin, only glutamate racemase was inhibited by hemin. The inhibition was concentration-dependent. A plot of reciprocal of glutamate racemase activity against hemin concentrations showed that hemin produced a mixed type inhibition. The  $K_i$  value for hemin was estimated to be about 3.7 mM from these data. When glutamate racemase was incubated with hemin at various concentrations, a stoichiometric complex was formed and isolated by gel filtration. However, no appreciable amount of hemin was bound with aspartate racemase under the same conditions. The complex of glutamate

racemase with hemin was reduced with dithionite. The ESR spectrum of the oxidized form resembled that of hemoglobin under the same conditions. Thus, glutamate racemase resembles hemoglobins in having a heme binding pocket, in which two nitrogen atoms of some amino acid residues are probably ligated to iron in the coordination complex with hemin. Hemin inhibits glutamate racemase either by binding near the active site or at some other site where the binding causes a conformational change of the active site.

Proline racemase, 4-hydroxyproline epimerase and diaminopimelate epimerase contain an essential cysteine residue, and show sequence similarity with each other in the moiety around the cysteine residues. These enzymes have been proposed to evolve from a common ancestral protein. Glutamate racemase as well as aspartate racemase also contains an essential cysteine residue, but shows no sequence similarity to these three enzymes. However, a high sequence similarity in the regions of two cysteine residues occurs between glutamate racemase and aspartate racemase. It is suggested that glutamate racemase and aspartate racemase have derived from a common evolutionary origin which is different from the common ancestor for proline racemase, 4-hydroxyproline epimerase and diaminopimelate epimerase.

The high sequence similarity between glutamate racemase and the globin family proteins, in particular myoglobins, and formation of its inactive equimolar complex with hemin, suggest that the enzyme may be derived from the evolutionary origin of globin family proteins. Aspartate racemase also may have evolved from the common ancestral protein, but its structure may have been altered more extensively than glutamate racemase by divergence. Lactic acid bacteria may have been producing glutamate racemase and aspartate racemase, namely globin family-like proteins, which diverged from an ancestral globin protein after the ability to synthesize hemin was lost. Alternatively, lactic acid bacteria inherently never produced hemin, and acquired from other organisms the gene for the globin family proteins, which then diverged to glutamate racemase and aspartate racemase. Whatever may be the case, glutamate racemase is the first proven microbial enzyme that is structurally similar to globin family proteins and to stoichiometrically bind hemin to form a catalytically inactive complex.

#### References

1. Yoshimura T, Ashiuchi M, Esaki N, Kobatake C, Choi S and Soda K, *J. Biol. Chem.*, **268**, 24242–24246 (1993).
2. Choi S, Esaki N, Yoshimura T and Soda K, *J. Biochem.*, **112**, 139–142 (1992).
3. Yamauchi T, Choi S, Okada H, Yohda M, Kumagai H, Esaki N and Soda K, *J. Biol. Chem.*, **267**, 18361–18364 (1992).
4. Choi S, Esaki N, Yoshimura T and Soda K, *Protein Expr. Purif.*, **2**, 90–93 (1991).



## Peptide Induce Membrane Fusion: Peptide Structure Required for the Fusion

Sho Takahashi, Ryo Ishiguro, and Tomoharu Matsumoto

Amphiphilic  $\alpha$ -helical peptides may induce biomembrane fusion. Measurements of fusion activity of about 80 peptides having modified amino acid sequences of influenza hemagglutinin HA-2 subunit N-terminal domain revealed that, in addition to amphiphilic properties, intermittent distribution of bulky hydrophobic residues is crucial for peptides to be active in triggering membrane fusion.

**Keywords:** Synthetic peptides/ Membrane fusion/  $\alpha$ -Helix/ Amphiphilic peptide/  $\beta$ -Structure

The subdivision of Biopolymer Structure has two activities: Physicochemical studies of synthetic peptides as a model of protein structure in the aspects of stability of secondary or super secondary structures and function, and elucidation of protein structures by X-ray crystallography. This year, we will focus on the recent results in the former activity, mainly a structure formation of small peptides in biomembranes and a peptide function to induce lipid membrane fusion.

Phospholipid bilayers consist of a basic structure in living organisms. They form not only a cell wall to segregate a living system from the environment, also intracellular vesicles called organelles such as nucleus, mitochondrion, Golgi apparatus, endosome, etc., each of which takes a specific action in a living cell. As a cell is encapsulated by cell wall, incorporation or secretion of substances (except small molecules) into or from a cell requires a specific mechanism to pass through the membrane. A Golgi system and endosome are responsible for these processes. For example, infection of enveloped viruses, a release of viral genomes in

cytoplasm, takes place either by direct fusion of a viral envelope with cell membrane or by fusion of viral membrane with endosomal one after incorporation of viral particles in an endosome (endocytosis). The influenza virus infects a living cell by an endocytic pathway. The viral envelope fuses to an endosome membrane when pH inside the organelle was lowered below 5.5 in the process of endocytosis. A specific protein, hemagglutinin, was identified to be responsible to trigger the fusion at acidic pH, while it is inactive at neutral. Hemagglutinin is a multifunctional protein embedded in a viral envelope and its subunit HA-2 has a stretch of hydrophobic amino acids as an N-terminal segment, which had been called putative fusion peptide. We found that a synthetic 20-residue peptide having the same amino acid sequence as that of influenza virus strain A/PR/8/34 (H-1) could induce lipid vesicle fusion with the similar dependency on pH [1]. Several aspects have been revealed: (1) the peptides that cause membrane fusion must interact with lipid membranes and have an amphiphilic nature by forming ordered secondary

### MOLECULAR BIOLOGY AND INFORMATION —Biopolymer Structure—

#### Scope of research

(1) Peptide secondary or supersecondary structures in aqueous or hydrophobic environments are studied to get a principle of protein architecture, employing various spectroscopic methods. (2) Protein X-ray crystallography is carrying out to reveal a tertiary structure of protein. Efforts are also paid on elucidation of structure-function relationships of enzymes.



Professor  
TAKAHASHI, Sho  
(D Sc)



Associate Professor  
HATA, Yasuo  
(D Sc)



Instructor  
HIRAGI, Yuzuru  
(D Sc)



Instructor  
FUJII, Tomomi

#### Associate Instructor:

AKUTAGAWA, Tooru

#### Students:

ISHIGURO, Ryo (Dc)

MIYATAKE, Hideyuki  
(DC)

HISANO, Tamao (DC)

MATSUMOTO, Tomoharu  
(MC)

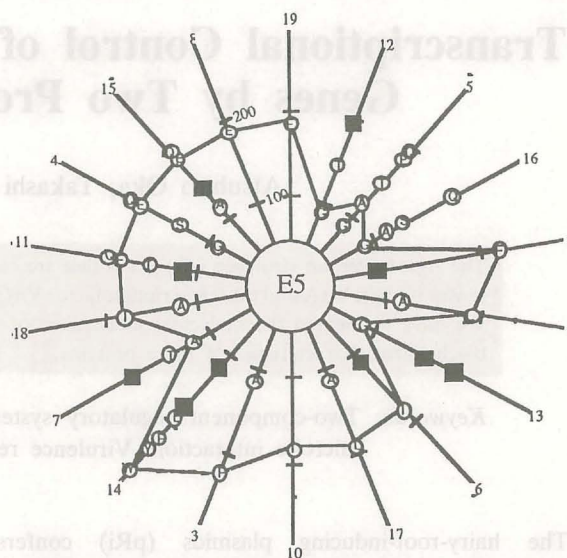


structures; (2) complementarily structured peptides, or when a peptide was structured with the aid of other substances, also could trigger the fusion; and (3) a fusion-active peptide takes  $\alpha$ -helix in lipid bilayers, with the helix axis  $30^\circ$  from the membrane plane [2].

Not all of amphiphilic peptides are active fusogen of lipid membranes. It is quite apparent that specific amino acid sequences or compositions must be required. We have tried to reveal the necessary conditions that are required for peptides to be active in inducing membrane fusion from a study of amino acid sequence-modified peptides starting from the original influenza HA-2 peptide, which is shown below. Sequence modifications

HA-Peptide GLFGAIAGFIEGGWTGMIDG

were such as a one residue was substituted by other amino acid at a time or a group by a group and about 80 peptides were obtained in this way. In every situation, amphipathic nature of the peptides was conserved since that was one of the necessary conditions for peptide to interact with lipid bilayers. Membrane fusion activities of these peptides were collected, summarized, and evaluated to yield a structure-activity relationship [3]. Point (one residue) modifications usually reserved the activity, at some specific points such as N-terminal, however, the nature of the substituted residue critically affected the activity. For example, an introduction of a charged group at N-terminus abolished the activity while substitutions with neutral amino acids, either large or small, hydrophobic or hydrophilic, did not affect the activity. At the position 14, substitutions with large hydrophobic residues reserved the activity but small or charged did not. The place necessary for activity expression is not localized because those peptides having amino acid sequences doubled for the N- or C-terminal half of the original peptide were inactive. Furthermore, interchange of the N- and C-terminal halves gave a peptide which was still active. This suggests that a combination of residues more than half of the original peptide is critical for the activity. Our present explanation what properties of amino acid residues are correlated to the activity of a peptide is following. Peptides under consideration are considered to be helical in lipid bilayers. To fuse apposed membranes some perturbation must be caused by the peptide-lipid interactions. It is reasonable to assume such interactions are due to contacts of peptide surface and surrounding lipid molecules. We considered the surface area of amino acid residue as most important in the view of peptide-lipid interactions and, therefore, plotted calculated surface area of each residue side chain ( $\text{\AA}^2$ ) as a helical wheel representation (Figure below), where the outermost numbers showed residue numbers, marked circles for residues by which substitution afforded fusion-active peptides, and filled squares for residues to reduce the activity, respectively (the kite-like polygon represents



a residue surface area profile of a peptide called E-5 taken as a reference). We could notice a remarkable feature on the picture, namely a small residue was required at some points for a peptide to be fusion active, or in other words, constrictions in a surface area profile must be present somewhere. Our inactive peptides, such as those having N- or C-terminal half-doubled or having an optimized amino acid sequence for an amphipathic  $\alpha$ -helix, show uniform or smooth (without constrictions) surface area profiles. Also we surveyed other fusion peptide sequences reported for various viruses and could recognize a similar feature as shown in above figure. As our acidic peptides become active at pH below 6, protonations of carboxylate groups are apparently related to the fusion activity. Presumably the protonation increases hydrophobicity of the peptides and makes the peptides deeper inserted inside lipid bilayers. Deeper insertion of peptides causes a larger amount of perturbation on the order of lipid bilayer structure, crossing a critical degree of disorder or perturbation will trigger fusion between closely apposed membranes.

As an application of fusion-active peptides to other field of science, Hirata's group have found the presence of a fusion-active complementary peptide pair significantly enhanced incorporation of recombinant DNA into cells by a lipofection method [4].

#### References

1. Murata M, Sugahara Y, Takahashi S and Ohnishi S, *J. Biochem.*, **102**, 957-962 (1987).
2. Takahashi S, Matsumoto T and Ishiguro R, to be submitted.
3. Ishiguro R, Kimura N and Takahashi S, *Biochemistry*, **32**, 9792-9797 (1993).
4. Kamata H, Yagisawa H, Takahashi S and Hirata H, *Nucleic Acids Res.*, **22**, 536-537 (1994).



# Transcriptional Control of the *Agrobacterium* Virulence Genes by Two Proteins VirA and VirG

Atsuhiko Oka, Takashi Aoyama and Hideki Endoh

The *Agrobacterium* virulence (*vir*) genes that are essential for pathogenicity on plants are induced through the sensor protein VirA and the transcription factor VirG by phenolic compounds released from plant wounded sites. We have delineated the molecular mechanism of this VirA-VirG signal transduction system by elucidating biochemical characteristics of these proteins.

**Keywords:** Two-component regulatory system/ DNA-binding protein/ Phosphotransfer/ Plant-microbe interaction/ Virulence regulon

The hairy-root-inducing plasmids (pRi) confers tumorigenic symptoms at wound sites on a wide variety of dicotyledonous plants upon infection by its host bacterium, *Agrobacterium rhizogenes*. Tumorigenesis by pRi is caused by the transfer of a defined DNA segment (T-DNA) from the plasmid into the plant nuclear genome and the subsequent constitutive production of plant phytohormones directed by the T-DNA. The 25-base-pair imperfect direct repeats at both extremities of T-DNA are indispensable for T-DNA transfer, but no other portions inside T-DNA are required. Plasmid genes essential for T-DNA transfer are located in the virulence (*vir*) loci outside T-DNA. The plasmid *vir* genes (about 20 genes) constitute six transcriptional units, *virA*, *virB*, *virC*, *virD*, *virE*, and *virG*. Their expression is tightly regulated as a regulon by the *virA* and *virG* gene products, being inducible by plant phenolic compounds such as acetosyringone [1]. Here we describe biochemical characteristics of the VirA (829 amino acid residues) and VirG (241 amino acid

residues) proteins, and delineate molecular mechanisms of transcriptional activation of the *vir* genes by plant factors.

For plant factors to signal *vir* expression, extracellular recognition is required. This process appears to be mediated by VirA because its N-terminal half contains the periplasmic portion (220 residues) flanked by the two membrane-spanning regions. The C-terminal domain of VirA is well conserved among the sensor components of every two-component regulatory system. However, unlike other sensor components, VirA has an additional domain at the most C-terminal end (115 residues). This portion is called VirG-like domain (VGL domain) because of its resemblance to the N-terminal half of VirG. Deletion and point mutants within the VGL domain show poorly inducible expression of the *vir* genes by acetosyringone, and generate no or reduced tumorigenic symptoms on plants.

To characterize VirA biochemically, N-truncated versions of VirA (VirA') have been overproduced in

## MOLECULAR BIOLOGY AND INFORMATION —Molecular Biology—

### Scope of research

Attempts have been made to elucidate structure-function relationships of genetic materials and various gene products. The major subjects are mechanisms involved in regulation of gene expression, initiation of DNA replication, signal transduction responsive to environmental stimuli, morphogenesis of plant leaves and flowers, and plant-microbe interaction. As of December 1994, study is being concentrated on signal transduction for plant morphogenesis, and identification of protein kinases and phosphoprotein phosphatases essential for plant signal transduction.



Professor  
OKA, Atsuhiko  
(D Sc)



Associate Professor  
AOYAMA, Takashi  
(D Sc)



Instructor  
GOTO, Koji  
(D Sc)

### Students:

ENDO, Hideki (DC)  
KATSUMATA, Atsushi (DC)  
TANAKA, Toshiaki (DC)  
IMAJUKU, Yoshiro (DC)  
KITAZAWA, Taro (DC)  
AOKI, Mikio (DC)  
ITAHANA, Koji (DC)  
ISHIDA, Norihiro (DC)  
TSUKUDA, Mayumi (MC)



*Escherichia coli*. These VirA' derivatives are capable of phosphorylating their own His-474 residue in the presence of ATP provided their deletions do not extend beyond His-474. Furthermore, VirA' molecules with larger N-truncations are generally higher autophosphorylating activities [1]. Substitution of Gln for His-474 abolishes autophosphorylation function, the ability to induce *vir* expression, and pathogenicity on plants, indicating autophosphorylation as being essential in signal transduction for transcriptional activation. Based on these facts and other several lines of circumstantial evidence, we believe that the active center of VirA kinase is usually masked by its N-terminal half, and upon recognition of plant factors, becomes unmasked for activation.

When the VirG protein that has been purified from overproducing *E. coli* cells is mixed with VirA' in the presence of ATP, VirG together with VirA' is phosphorylated. The phosphate group of phospho-VirG comes from phospho-VirA' but not ATP because VirG is similarly phosphorylated by the purified phospho-VirA', concurrently with dephosphorylation of phospho-VirA'. The Asp-52 residue of VirG has been found to be the phosphorylation target [1]. Thus, the N-terminal half of VirG is the signal receiver domain. Site-directed mutagenesis toward Asp-52 leads to an extreme reduction of pathogenicity. These facts support the view that phosphotransfer is an important process involved in signal transduction required for transcriptional activation.

The VGL domain of VirA resembles the VirG signal receiver domain as described above. In particular, three residues (Asp-9, Asp-52, and Lys-102) critical for acquiring the phosphate group are completely conserved. This VGL domain does not contribute to the enzymatic activity of autophosphorylation but considerably enhances phosphotransfer from VirA' to VirG *in vitro* [2]. Therefore, VirA-VirG interaction appears to occur through two homologous regions, namely the VGL domain of VirA and the N-terminal signal receiver domain of VirG, presumably mimicking the oligomerization process of VirG molecules [3]. Although this modest decrease in phosphotransfer activity *in vitro* does not seem to account for the drastic phenotype alteration *in vivo*, this contradiction is probably derived from the difference of VirA molecules tested *in vivo* and *in vitro*: the former VirA is the native membrane-anchored protein (VirA), while the latter VirA is the N-truncated cytoplasmic proteins (VirA').

To confirm that VirA and VirG are sufficient for inducible *vir* expression, we have constructed an *in vitro* transcription system, consisting of the *Agrobacterium* RNA polymerase, VirG, and template DNAs containing the *vir* promoter regions. In this system, RNA is synthesized entirely depending on VirG, and its start site is exactly identical to that of *in vivo* mRNA. VirG works as a positive transcription factor but not as an alternative sigma factor because the RNA polymerase

core enzyme is unable to replace the holoenzyme in this system [4].

This transcription system has been coupled with the phosphotransfer reaction from VirA' to VirG. Under neutral conditions for transcription (pH 7.3–7.7), coupling shows no effects or slight reduction of the VirG-dependent transcription activity. Under moderate acidic conditions for transcription (pH 6.5–7.0), VirG-dependent RNA synthesis is significantly enhanced by the coupling. Since phosphotransfer reactions are done in the same conditions, it is obvious that VirG has enough potential for transcriptional activation without being phosphorylated and that phospho-VirG promotes transcriptional activation more competently than nonphospho-VirG in the rather acidic conditions. This peculiar pH-dependency may relate to the fact that *vir* induction by plant factors *in vivo* occurs only under acidic conditions. Since phosphotransfer from VirA to VirG appears critical for *vir* expression *in vivo*, functional nonphospho-VirG *in vitro* seems to be interpreted as that VirG phosphorylation is essential for transcriptional activation when the concentration of VirG is low, and function of phospho-VirG can be compensated by an excess of nonphospho-VirG.

There is a point mutant of VirG (VirG I77V), containing a substitution of Val for Ile-77. Its phenotype is hypersensitive *vir* induction by plant factors. Phosphotransfer from VirA' to VirG I77V is considerably higher than to the wild-type VirG. Thus, its phenotype has been attributed to an elevated affinity of VirG I77V to VirA [5]. Another mutant (VirG N54D) carrying an amino acid substitution near the phosphorylation target, Asp-52, shows constitutive *vir* expression *in vivo*, independent of both plant factors and VirA. In comparison to the wild-type VirG, VirG N54D has a higher activity for transcriptional activation *in vitro*, but has comparable activity for phosphotransfer from VirA'. In addition, no enhancement in RNA production has occurred by phosphorylation of VirG N54D. Therefore, VirG N54D is likely to have a molecular conformation close to the phosphorylated form of the wild-type VirG [5]. All of these experimental results obtained *in vitro* correctly reflect *in vivo* phenomena of *vir* expression induced by plant factors.

#### References

1. Oka A, Aoyama T and Endoh H, *Bull. Inst. Chem. Res. Kyoto Univ.*, **71**, 355–367 (1993).
2. Endoh H and Oka A, *Plant Cell Physiol.*, **34**, 227–235 (1993).
3. Tamamoto S, Aoyama T, Takanami M and Oka A, *J. Mol. Biol.*, **215**, 537–547 (1990).
4. Endoh H, Aoyama T and Oka A, *FEBS Lett.*, **334**, 277–280 (1993).
5. Endoh H, Hooykaas PJJ and Oka A, unpublished results.



## BRITE: Biomolecular Reactions for Information Transmission and Expression

Susumu Goto, Kenji Suzuki, Yutaka Akiyama and Minoru Kanehisa

We are developing a knowledge base of "Biomolecular Reactions for Information Transmission and Expression" (BRITE). As a first step of this project, we developed a signal transduction database and a metabolic pathway knowledge base. The signal transduction database and the metabolic pathway knowledge base represent molecular interactions involved in the signaling pathways and enzyme interactions, respectively. Both are linked to the other public databases such as PIR protein sequence database, the PDB protein three-dimensional structural database, and the OMIM database on genetic diseases. We provide a graphical user interface to access them.

**Keywords:** Biomolecular reactions/ Molecular interaction/ Signaling pathways/ Metabolic pathways/ Database/ Knowledge base/ Graphical user interface

The signal transduction from extracellular signals to gene expression is one of the significant cellular events that are beginning to be unraveled in molecular details. The event starts at the cell surface receptor accepting an external signal. The signal is transmitted inside the cell to key signaling molecules such as Ras and G-protein. The activation of these molecules is often followed by a cascade of protein phosphorylation events which results in the activation of specific transcription factors in the cell nucleus. Such an overall picture is derived from numerous experiments on molecular interactions, i.e., data on one molecule affecting other molecules either directly or indirectly.

There are various kinds of molecular biology databases specialized to amino acid sequences, nucleotide sequences, protein three-dimensional structures, and so on. However, they are not the databases for overall

picture on molecular interactions, but for one molecule or a piece of data. So far, the picture is only in the biologists' image. Our long-term objective is to automatically construct such an overall picture from pieces of data stored in molecular interaction databases.

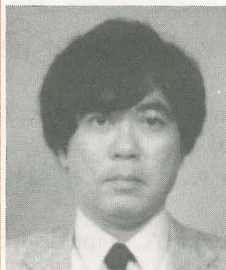
Toward that end, we have started collecting data on molecular interactions that play parts in the signal transduction pathways and experimenting various representations and manipulations of those data. Table 1 shows one possible description of molecular interactions in the Ras pathway, where the basic element is a pair of interacting molecules or molecular complexes, called a donor and an acceptor, together with the description of molecular events [1].

We have also started developing a method to automatically construct the pathways and their graphical views from pieces of data. We exploited data on

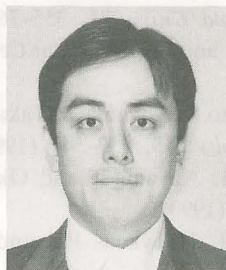
### MOLECULAR BIOLOGY AND INFORMATION —Biological Information Science—

#### Scope of research

The following five attempts have been mainly made in this laboratory. (1) Characterization of amino acid sequences by extracting signature oligopeptides from protein structure and sequence databases. (2) Characterization of nucleotide sequences around promoter, translation initiation and splice sites. (3) Construction of new databases that describe molecular interactions, such as signal transduction and metabolic pathways. (4) Modeling three-dimensional structure of RNA, DNA and protein. (5) Development of database systems and tools to support researchers in genome community. Almost all of them can be used to access the databases maintained in this laboratory and analyze data from all over the world via Internet.



Professor  
KANEHISA, Minoru  
(D Sc)



Associate Professor  
AKIYAMA, Yutaka  
(D Eng)



Instructor  
UCHIYAMA, Ikuro



Instructor  
GOTO, Susumu  
(D Eng)

#### Students:

MIZUNO, Masahiko (DC)  
OHKUBO, Zenmei (DC)  
FUJIBUCHI, Wataru (DC)  
OGATA, Hiroyuki (DC)  
SUZUKI, Kenji (MC)  
TOMII, Kentarou (MC)  
YOSHIDA, Ayahiko (MC)  
KIHARA, Daisuke (MC)  
TSUKAMOTO, Nobuo (MC)  
FUKUSHIMA, Nobuhiro  
(RF, D Sc)  
PARK, Keun-joon (RS)



metabolic pathways, which is another data on molecular interactions and is better known than the signal transduction, as an application. Using the enzyme reaction database LIGAND, we developed a knowledge base system for searching and browsing metabolic pathways [2]. Biologists can ask the information about metabolism like below with the knowledge base,

- whether there is an alternative pathway in case that the given enzyme is deficient or altered, and
- which enzyme or pathway relates to the given disease.

Because the system constructs enzyme networks only by traversing the common substrates in two reactions, improvement of this system is indispensable to construct more precise view of the interactions. For example, interface and mechanism to use various condition such as organism and site specific information and quantitative information on the substrates can improve the system.

Another and our short-term objective is to provide a browser of different types of data in an integrated environment. Thus, the molecular interaction data are linked to consensus views of the transduction pathways or metabolic pathways, as well as to other databases including Medline (bibliographic data), SWISS-PROT, PIR (amino acid sequence data), PDB (protein three-dimensional structure data), LIGAND (chemical compounds in enzyme reactions), and OMIM (genetic diseases). Using the links, users can easily retrieve the related information stored in the separated databases. We also developed the LinkDB that links databases not only directly but also indirectly or reversely. Some databases have a lot of cross reference information, but others have few. If users retrieve the database that has few cross reference, they have to repeatedly retrieve other databases until they have required information. The LinkDB provides the precomputed indirect and reverse links, thus users can retrieve necessary cross reference information directly.

There are two alternative ways to provide user interface to access the databases. One is the use of Mosaic in the World Wide Web (WWW) system. Mosaic has an easy-to-use graphical user interface and we have already developed an integrated retrieval system called WebDBget linking sixteen databases in molecular biology. We have also provided LinkDB as a part of WebDBget. The other way is to provide graphical interface by our own software. Since the Mosaic interface does not provide sufficient functions to dynamically draw pictures of pathways for now, we adopted our own interface for metabolic pathway

**Table 1.** A description of molecular interactions in the Ras pathway. The basic element is a pair of interacting molecules or molecular complexes, called a donor and an acceptor, together with the description of molecular events. The description of molecular events is not shown, but like "GF binding RTK leads to RTK dimerization & autophosphorylation" for the first line.

Donor	Acceptor	Signal	Interaction
GF	RTK	+	binding
RTK	GRB2	+	binding
GRB2	Sos	+	complex
GRB2/Sos	Ras	+	binding
Ras	Raf	+	translocation
Raf	MEK	+	phosphorylation
MEK	MAPK	+	phosphorylation
MAPK	Myc	+	phosphorylation
Myc	DNA	+	binding
MAPK	Jun	+	phosphorylation
Jun	Fos	+	dimerization
Jun/Fos	DNA	+	binding

knowledge base to draw dynamically constructed pathways. We are consulting which interface is better for the BRITE system.

Since this work is the first step to construct BRITE system, we have many works to do. One of the most important works is the automatic and intelligent construction of pathways from the pieces of data. We have an experience to construct long nucleotide sequence from the pieces of sequences under various conditions by using techniques in deductive database systems [3]. Those techniques can be also used to construct pathways and we are planning to implement them as a part of the BRITE system.

#### Acknowledgment

This work was supported by the Grant-in-Aid for Scientific Research on the Priority Area 'Genome Informatics' from the Ministry of Education, Science and Culture of Japan.

#### References

1. Suzuki K, Goto S, Akiyama Y and Kanehisa M, *Proc. Genome Informatics Workshop 1994*, 144-145 (1994).
2. Goto S and Kanehisa M, *Proc. Genome Informatics Workshop 1994*, 234-235 (1994).
3. Sakamoto N, Goto S and Takagi T, *Intl. J. Bio-Medical Computing*, **36**, 171-179 (1994).



## Improvements of the Beam Characteristics of the 7 MeV Proton Linear Accelerator

Akira Noda, Hideki Dewa, Hirokazu Fujita, Masaki Kando,  
Masanori Ikegami, Yoshihisa Iwashita, Shigeru Kakigi and Makoto Inoue

The beam intensity of the ion linear accelerator has been gradually increased although the space charge effect limits the transferable current at the Low Energy Beam Transport (LEBT). The beam emittance are measured at LEBT and at the section between RFQ and Drift Tube Linac (DTL) and after the DTL. It is found that no emittance blow up has occurred in the cavities of the linac up to the present intensity. Beam profiles are also measured at the same sections with use of fluorescent screens. As the beam intensity has been increased to the order of mA, preparation for the beam irradiation tests has been initiated.

**Keywords:** Ion Source/ Space Charge/ LEBT/ RFQ/ DTL/ Emittance/ Beam Profile

The main effort this year of our group has been made in order to increase the beam intensity of the ion linear accelerator. For this purpose, various beam diagnoses have been applied. Formerly the beam current in LEBT has been limited up to  $\sim 1$  mA because of the strong repulsion due to space charge force because beam energy is rather low (50 keV). This situation was promoted by the former beam optics which focuses the beam to the small size at several points in LEBT in order to clear the small aperture of the existing Mixing Magnet, which bended the 50 keV proton with the deflection angle of  $45^\circ$ . So as to modify this situation, the Mixing Magnet was replaced by the one with wider gap of 60 mm and beam optics was also modified to such a one which has rather smoother and wider beam envelope. Vertical edge focusing is also used at the entrance of the Mixing Magnet so as to avoid too small horizontal beam size at the exit of the magnet due to radial focusing [1,2].

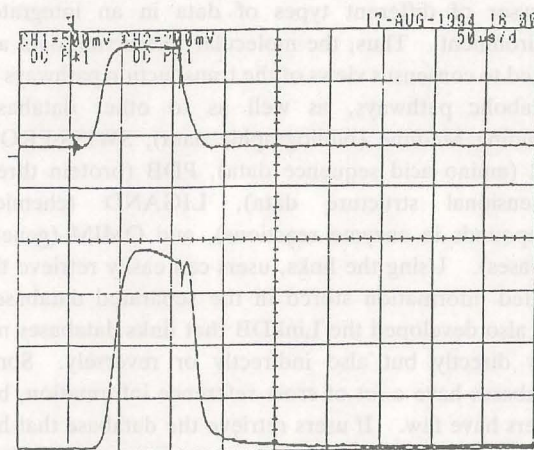


**Figure 1.** The beam signal at the entrance of the RFQ (lower trace, 2 mA/div.) shown together with the arc signal of the ion source (upper trace, 50 A/div.) Horizontal scale is 50  $\mu$ s/div.

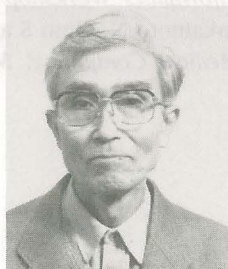
### NUCLEAR SCIENCE RESEARCH FACILITY —Particle and Photon Beams—

#### Scope of research

Particle and photon beams generated with accelerators and their use both for fundamental research and practical applications are studied. The main subjects are: beam dynamics in high intensity accelerators: beam handling at injection and extraction process of the accelerator ring: beam diagnoses in accelerators: radiation mechanism of photons from an electron storage ring: interactions in the few-nucleon systems: development of a compact accelerator dedicated for cancer therapy; and irradiation of materials with particle and photon beams.



Professor  
NODA, Akira  
(D Sc)



Associate Professor  
KAKIGI, Shigeru  
(D Sc)



Instructor  
SHIRAI, Toshiyuki

#### Lecturer (part-time):

HATTORI, Toshiyuki  
(Associate Prof. of Tokyo  
Institute of Technology)

#### Guest Scholar:

GRIESER, Manfred  
(Max-Planck Institut für  
Kernphysik, Heidelberg)

#### Students:

IKEGAMI, Masanori (DC)  
KANDO, Masaki (MC)  
SUGIMURA, Takashi (MC)



In addition to the above modification, the geometry of the extraction electrode was changed to increase the extracted current and 20 mA of beam is extracted at the straight section before the Mixing Magnet, among which 8 mA is  $H^+$  beam needed for acceleration with the linac. In Fig. 1, the beam signal guided to the entrance of the RFQ is shown together with the arc signal of the ion source. In this case, arc current is more than 90 A so as to increase the fraction of  $H^+$  by increasing the plasma density in the chamber of the ion source. So as to increase the plasma density much more, it is needed to improve the magnetic confinement of the plasma by replacing with much stronger permanent magnets, which requires further studies.

The transverse phase space matching is further to be completed with use of axially symmetric magnetic lenses made of permanent magnets [3]. As the focusing at the entrance of the RFQ is not strong enough at the moment without above lenses, the transmission through the RFQ is not high enough (less than 74%).

The beam emittance at the LEBT has been measured with combination of moving slits and view screen made of alumina ceramic doped with chromium oxide. The measured 100% unnormalized emittance is  $170 \pi \text{mm}\cdot\text{mrad}$  [4]. With the same method the beam emittance is also measured after the RFQ and measured 90% unnormalized emittance is  $30 \pi \text{mm}\cdot\text{mrad}$ .

For the purpose of monitoring the beam current continuously, a pulsed beam current monitor with a toroidal core has been fabricated and installed in front of the DTL. The beam current causes the change of the magnetic flux in the toroidal core, which results in the current in the secondary winding of the core. By detecting this current, the beam current can be measured. Application of negative impedance enabled high enough gain of the system with long enough decaying time. Its sensitivity is calibrated with the beam. It is found that the monitor can be used in a wide range of beam current from  $30 \mu\text{A}$  to 10 mA, with the frequency range of 30 Hz to 1 MHz [5]. The monitor can represent the beam signal quite well as shown in Fig. 2. The accuracy of absolute value of current measurement is better than 10%.

After the DTL, the beam emittance of 7 MeV proton is also measured with use of conventional method which utilize moving double slits and Faraday cups. However, the method is usually only applied to continuous beam. In the present measurement, high gain and rather fast amplifier is developed to enable the emittance measurement for pulsed beam with duration of  $50 \mu\text{s}$ . The measured rms emittance is  $5 \pi \text{mm}\cdot\text{mrad}$  [6].

Summarizing the above results, accelerated beam current has reached the order of mA and its diagnosis system at each stage of the accelerator system has been safely started its operation, although further studies are needed in order to realize much higher intensity of the order of few tens of mA. Based on these results, material irradiation is to be started soon and the vacuum

chamber for measurement of neutron production rate from various alloys has been fabricated and installed. In order to realize easy access to the target materials to be irradiated, the vacuum system separated from the one for the accelerator cavities by a gate valve is prepared. After the test experiment, the facility is to be ready for open use of outside users.

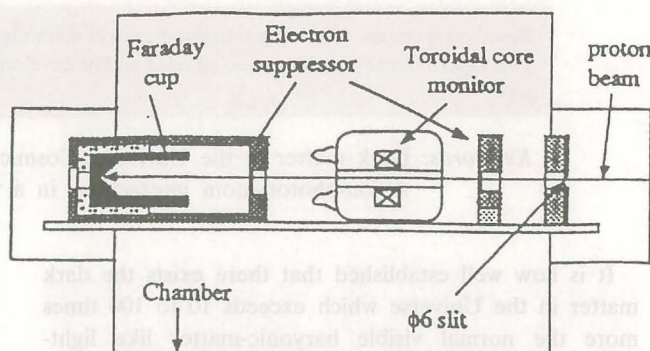


Figure 2(a). Configuration of the calibration of the toroidal core monitor.

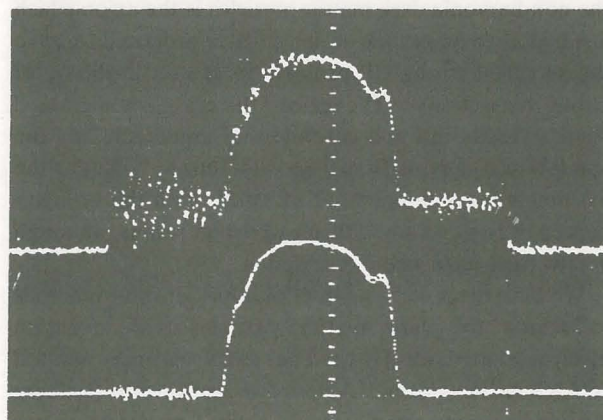


Figure 2(b). Beam signals from the core monitor (upper trace) and the Faraday cup (lower trace).

#### References

1. Noda A, Dewa H, Fujita H, Ikegami M, Iwashita Y, Kakigi S, Kando M, Shirai T and Inoue M, Proc. of the 4th European Particle Accelerator Conf. London, United Kingdom, 2423–2425 (1994).
2. Kando M, Ikegami M, Iwashita Y, Kakigi S, Shirai T, Dewa H, Fujita H, Noda A and Inoue M, Proc. of the LINAC94, Tsukuba, Japan, 122–124 (1994).
3. Iwashita Y, Proc. of 1993 Particle Accelerator Conf. Washington D.C., USA, 3154–3156 (1993).
4. Shirai T, Dewa H, Fujita H, Kando M, Ikegami M, Iwashita Y, Kakigi S, Noda A and Inoue M, Proc. of the LINAC94, Tsukuba, Japan, 908–910 (1994).
5. Dewa H, Iwashita Y, Fujita H, Ikegami M, Inoue M, Kakigi S, Kando M, Noda A, Okamoto H and Shirai T, *ibid.*, 854–856.
6. Ikegami M, Kando M, Dewa H, Fujita H, Shirai T, Iwashita Y, Kakigi S, Noda A and Inoue M, *ibid.*, 857–859.



## Search for Dark Matter Axions with Rydberg Atoms in a Resonant Cavity

Izumi Ogawa, Shin Nakamura, Takahiro Takimoto,  
Masaru Tada and Seishi Matsuki

Based on quantum electronic techniques, novel methods to search for dark matter axions have been proposed. The experimental systems are being used and/or developed to detect axions in the mass range between 5 to 12  $\mu\text{eV}$ .

**Keywords:** Dark matter in the Universe/ Cosmic axions/ Quantum electronics/ Rydberg atoms/  
Axion-photon-atom interactions in a resonant cavity

It is now well established that there exists the dark matter in the Universe which exceeds 10 to 100 times more the normal visible baryonic-matter like light-emitting stars. However no definite evidence for the constituent particles of the dark matter has yet been found so far. One of the mostly attractive candidates of the non-baryonic dark matter particles is the axion which is a hypothetical pseudo-scalar particle proposed to solve the so-called strong CP problem in the QCD theory of strong interactions. The mass of the axion is constrained from astrophysical and cosmological arguments and the window still open is from 1  $\mu\text{eV}$  to 1 meV. Due to the extremely weak interactions of axions with the ordinary matter, it is inevitably difficult to detect axions, although a few tries have been reported.

We have proposed a number of novel sensitive methods to search for dark matter particles with quantum electronic methods [1-4]: The most sensitive method (CARRACK: Cosmic Axion Research with Rydberg Atom in a resonant Cavity in Kyoto) to detect axions

among them is to firstly convert the axion into a microwave photon in a resonant cavity via the Primakoff effect in a strong magnetic field [1, 3]. The converted photons are then detected by Rydberg atoms passed through the cavity. The cavity is cooled down to 10 mK so that the background due to thermal blackbody radiations from the wall of the cavity is appreciably suppressed. Since the Rydberg atom is expected to have inherently no noise, this scheme is much more sensitive compared to conventional amplifier-heterodyne method. Schematic diagram of the experimental system with the method is shown in Fig. 1. The axions are converted to microwave photons in the conversion cavity which is in a magnetic field of 7 T. These photons thus produced are transferred to the detection cavity and absorbed by Rydberg atoms. The external magnetic field at the detection cavity is less than 0.9 kG due to the cancellation coils set between the main magnet and the cavity. The inside of the detection cavity made of Nb is kept to be free from magnetic field due to the Meissner effect in

### NUCLEAR SCIENCE RESEARCH FACILITY —Beams and Fundamental Reaction—

#### Scope of research

Particle beams, accelerators and their applications are studied. Structure and reactions of fundamental substances are investigated through the interactions between beams and materials such as nuclear scattering. Tunable lasers are also applied to investigate the structure of unstable nuclei far from stability and to search for as yet unknown cosmological dark-matter particles in the Universe.



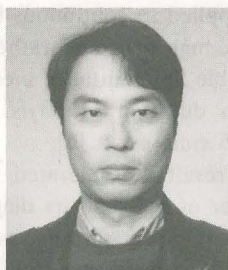
Professor  
INOUE, Makoto  
(D Sc)



Associate Professor  
MATSUKI, Seishi  
(D Sc)



Instructor  
IWASHITA, Yoshihisa  
(D Sc)



Instructor  
OKAMOTO, Hiromi  
(D Sc)

**Associate Instructor:**  
FUJITA, Hirokazu

**Students:**  
OGAWA, Izumi (DC)  
DEWA, Hideki (DC)  
NAKAMURA, Shin (DC)  
KAPIN, Valerij (DC)  
TAKIMOTO, Takahiro (MC)  
TADA, Masaru (MC)  
IKEDA, Kazumi (RF)  
FUJISAWA, Hiroshi (RF)



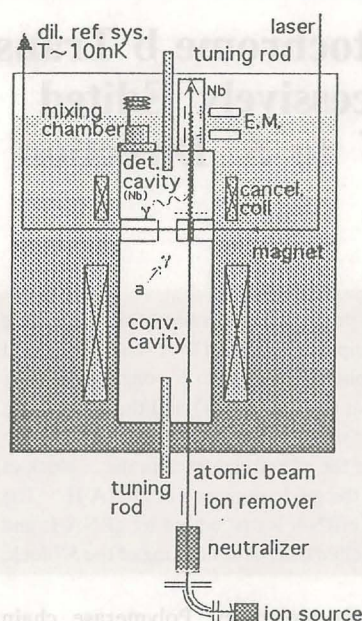


**Figure 1.** Schematic experimental diagram of CARRACK to search for dark matter axions with Rydberg atoms in a resonant cavity. The detection and the conversion cavities are cooled down to 10 mK with a dilution refrigerator.

superconducting Nb, the critical field of which is 1.2 kG.

The Rydberg atoms, prepared by three-step laser-excitation of alkaline atoms just before entering into the detection cavity, are passed through the detection cavity and analyzed with the field ionization method out of the cavity. In order to get atomic beam with higher velocity than thermal and also with narrow velocity spread, the atomic beam is produced by neutralizing ions accelerated to a suitable energy (200 eV to 5 keV). Both the cavities are cooled down to about 10 mK to suppress the background thermal photons from the cavity wall with a dilution refrigerator (Oxford, Kelvinox 300). Quantum theory of axion-photon-atom interactions in a resonant cavity was developed [5] by taking into account the dissipation effect of the cavity. The vacuum Rabi splitting due to the dressed atom-photon interactions in a resonant cavity arises also in this case. The detection efficiency of the axion-converted photons is thus evaluated precisely from the theory by numerical calculations.

The whole experimental system was divided into several parts and each part has been successfully tested separately with bench-test systems. The dilution refrigerator was installed in this summer. Cooling test was successfully performed, the lowest temperature achieved being 8 mK. A laser system for producing Rydberg atoms was constructed with three diode lasers. The wavelengths of the first and the second stage lasers are stabilized on resonance by using the Doppler-free saturation-absorption spectroscopy with a resonance cell [6]. The frequency stability of these lasers was found to be better enough to continuously excite the levels for more than 5 hours. The wavelength of the third stage

laser is varied together with the resonance frequency of the cavity to scan the mass of the axion.

To confirm the excitation of Rydberg atoms with this laser system, a prototype cavity and an atomic beam apparatus were constructed. The cavity can be cooled down to 0.5 K with a liquid  $^3\text{He}$  cryostat system. The Rydberg states with the principal quantum number ( $n$ ) of around 40 were successfully excited with the diode laser system and detected with the field ionization method out of the cavity, thus indicating satisfying performance of the laser-Rydberg system. This experimental system is now being used to search for cosmic axions by directly detecting axions with Rydberg atoms [1, 6]: Due to the axion-electron coupling, the axions are directly absorbed by Rydberg atoms, inducing the transition from the lower to the upper fine-structure states. The cavity is tuned out of the resonance to suppress the excitation of the upper state with photons. With this scheme, the upper limit of the coupling strength of the axion-electron interaction is obtained, giving more severe constraint than the previous laboratory experiments. The mass of the axions now searching for is around  $5 \mu\text{eV}$ .

After finishing the search experiment with the direct detection method mentioned above, the whole experimental parts of CARRACK system are to be assembled. The first run of search with this system is scheduled in the middle of the next year, 1995.

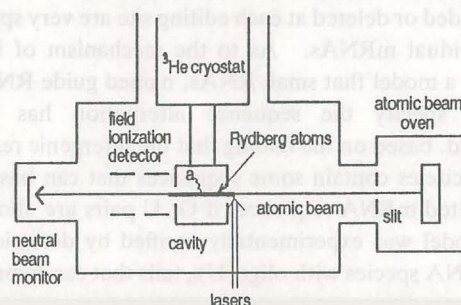


**Figure 2.** Schematic experimental diagram to search for dark matter axions by directly detecting axions with Rydberg atoms. Due to the axion-electron coupling, the axions are directly absorbed by Rydberg atoms, inducing the transition from the lower to the upper fine-structure states.

## References

1. Matsuki S and Yamamoto K, *Phys. Lett.*, **B263**, 523–528 (1991).
2. Matsuki S and Yamamoto K, *Phys. Lett.*, **B289**, 194–198 (1992).
3. Matsuki S and Yamamoto K, *Oyo-Buturi*, **62**, 919–922 (1993).
4. Matsuki S, Ogawa I and Yamamoto K, *Phys. Lett.*, **B336**, 573–580 (1994).
5. Matsuki S, Ogawa I and Yamamoto K, submitted to *Phys. Lett.*, **B**.
6. Ogawa I, Nakamura S, Takimoto T, Tada M, Yamamoto K and Matsuki S, to be submitted to *Phys. Lett.*, **B**.



## The 5' Terminal Region of the Apocytochrome b Transcript in *Crithidia fasciculata* is Successively Edited by Two Guide RNAs in the 3' to 5' Direction

Hiroyuki Sugisaki

I analysed the chimeric gRNA-mRNA molecules in *C. fasciculata* that are predicted to transiently exist in editing of the 5' terminal domain of apocytochrome b (CYb) mRNA, by PCR amplification and DNA sequencing, and obtained evidence indicating that among the fourteen editing sites numbered from 3' to 5', one guide RNA species (gRNA-I) directs the sequence from site 1 to the first U residue at site 7 (3' block) and the other guide RNA species (gRNA-II) directs the sequence from the second U residue at site 7 to site 14 (5' block), and that the direction of editing in each block is 3' to 5'. I also found that a stretch of the edited sequence in the 3' block of mRNA can form a stable duplex with a stretch immediately upstream of the guide sequence in gRNA-II. The result leads to a successive editing model that the 3' block of pre-edited mRNA is first edited by gRNA-I, and after completion of editing, the 5' portion of gRNA-II basepairs with the edited mRNA for editing of the 5' block.

**Keywords:** Kinetoplastid/ Mitochondria/ gRNA-mRNA chimera molecules/ Polymerase chain reaction/ Transesterification model

Several mitochondrial mRNA in kinetoplastid protozoans such as *Crithidia*, *Leishmania* and *Trypanosoma* are extensively edited after transcription [1]. The location of editing domains, number of editing sites within a single editing domain, and number of U residues to be added or deleted at each editing site are very specific to individual mRNAs. As to the mechanism of RNA editing, a model that small RNAs, named guide RNA or gRNA, specify the sequence alternation has been proposed, based on the finding that the intergenic regions of maxicircles contain some sequences that can basepair with edited mRNA sequences if G:U pairs are allowed. This model was experimentally verified by detection of small RNA species with oligo(U)<sub>n</sub> tails that can hybridize

to the corresponding regions of the maxicircles and minicircles, and further by identification of chimeric gRNA-mRNA molecules containing U clusters covalently linked at sites of RNA editing [2]. Nevertheless, the precise mode of action of the gRNA molecules is yet unknown. According to the computer search data, some of a single editing domain are covered by a few different gRNA species, but its molecular mechanism is also an unsettled question.

The 5' terminal region of the transcript of the apocytochrome b (CYb) cryptogene in *C. fasciculata* contains fourteen editing sites, including the one that generates the AUG initiation codon [3]. These sites are tentatively numbered in the 3' to 5' direction. By

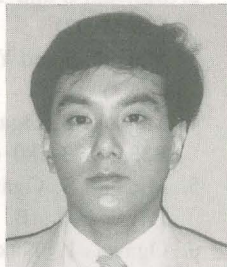
### RESEARCH FACILITY OF NUCLEIC ACIDS

#### Scope of Research

With emphasis on regulatory mechanisms of gene expression in higher organisms, the research activity has been focused on analysis of signal structures at the regulatory regions of transcriptional initiation and of molecular mechanisms involved in post-transcriptional modification by the use of eukaryotic systems appropriate for analysis. As of December 1994, studies are concentrated on the molecular mechanism of RNA editing in mitochondria of kinetoplastids and gene expression of human retroviruses.



Associate Professor  
SUGISAKI, Hiroyuki  
(D Sc)



Instructor  
ADACHI, Yoshifumi  
(D Med Sc)

#### Technician:

YASUDA, Keiko



computer analysis, two candidate gRNAs, named gRNA-I and gRNA-II, have been assigned for editing of sites 1 to 4 (3' or downstream block) and sites 5 to 14 (5' or upstream block), respectively. The existence of two gRNA species in cells has also been demonstrated. The editing pattern is well conserved between *L. tarentolae* and *C. fasciculata*, except that mRNA in *L. tarentolae* contains an additional editing site at the most 3' end and one less U residue at the most 5' editing site. The computer assignments of the editing blocks by gRNA-I and gRNA-II are very similar in both strains, but no direct evidence supporting these predictions has been presented.

To gain information on the mechanism how different gRNAs specify the RNA sequence alternation in a single editing domain, we analysed the kinetoplast RNA (kRNA) of *C. fasciculata* by PCR amplification and DNA sequencing, assuming that both putative gRNA-I and gRNA-II undergo transient covalent interaction with mRNA during editing process. As a result, we could identify the chimeric molecules of both gRNA-I and gRNA-II linked with partially edited mRNA.

Detection of both gRNA molecules that are covalently linked to partially edited mRNA through oligo(U)<sub>n</sub> strongly supports the transesterification model (3). Allowing G: U pairing, the gRNA-I sequence in the chimeric molecules can fold back on the edited mRNA sequences from editing site 1 to the first U in editing site 7 and the gRNA-II sequence on the remaining mRNA sequence. According to the transesterification model, the 3' terminal U of gRNA, that formed a duplex with preedited mRNA at the anchor site, first attacks mRNA at the first mismatched base and produces the chimeric molecule by transesterification. The U stretch in the gRNA molecule then basepairs with the guide A or G residue of the gRNA itself, and the second transesterification takes place at the next mismatched base. Oligo(U)<sub>n</sub> in the majority of clones is connected with the G residue just 3' of editing site 7, but the A residue just 5' of the oligo(U)<sub>n</sub> can basepair with the first U within editing site 7 (see Figure 1 of Reference 5). It is therefore likely that the transition site of editing from gRNA-I to gRNA-II is between the first and second U residues within editing site 7. The mRNA moieties that were connected to oligo(U)<sub>n</sub> in all the clones have completely been edited. Thus it is evident that the editing reaction progressively proceeds in the 3' to 5' direction in both the editing blocks. This is essentially consistent with the conclusion deduced from analysis of preedited-edited mRNA junctions.

When the two gRNA sequences were assigned on the mRNA sequence, we noted that the 12 bases long sequence of edited mRNA, 5'-uGuuAuuuAGAA-3', from editing sites 4 to 6 can basepair with both the guide sequence of gRNA-I and the 5' moiety of gRNA-II (see Figure 3 of Reference 5). The gRNA-II molecule does

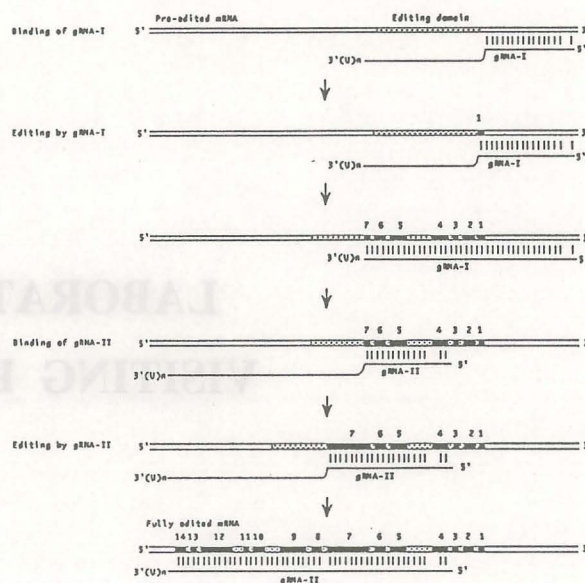


**Figure 1.** Diagram of a sequential editing model by two different gRNA molecules. mRNA is indicated by double lines, on which the entire editing domain is shown by hatched boxes and inserted U residues at individual editing sites by filled boxes. Single lines represent the gRNA molecules and basepairs between mRNA and gRNA are indicated by vertical lines.

not carry any region that can form a stable duplex with preedited mRNA. Although the 5' terminus of gRNA-I has not been determined yet, the region upstream from the guide sequence of gRNA-I can basepair with the mRNA region just downstream of the 3' block (see Figure 3 of Reference 5). Assuming that the regions of gRNA molecules which can form stable duplexes with mRNA provide the anchor sites for mRNA editing (see Figure 3 of Reference 5), an editing model emerged is schematically shown in Figure 1. The editing reaction on mRNA of the CYb cryptogene first initiates by basepairing-mediated recognition of the preedited mRNA sequence with the anchor sequence of gRNA-I. Followed by editing of the 3' block with the guide sequence of gRNA-I, the anchor sequence of gRNA-II recognizes the edited mRNA sequence and initiates editing of the 5' block. Although the mechanism involved in switching of binding from gRNA-I to gRNA-II is not known, the edited mRNA sequence can form a more stable duplex with the anchor sequence of gRNA-II than that with the guide sequence of gRNA-I.

## References

1. Benne R, *Eur. J. Biochem*, **221**, 9-23 (1994).
2. Blum B, Sturm NR, Simpson AM and Simpson L, *Cell*, **65**, 543-550 (1991).
3. Cech TR, *Cell*, **64**, 667-669 (1991).
4. Feagin JE, Shaw JM, Simpson L and Stuart K, *Proc. Natl. Acad. Sci. U.S.A.*, **85**, 539-543 (1988).
5. Sugisaki H and Takanami M, *J. Biol. Chem.* **268**, 887-891 (1993).



## LABORATORIES OF VISITING PROFESSORS

### SOLID STATE CHEMISTRY —Structure Analysis—

Professor Yasuo ENDO

Department of Physics II, Faculty of Science, Tohoku University (Aramaki-Aza-Aoba, Aoba-ku, Sendai 980)

#### Lectures at ICR

Introduction for Neutron Diffraction  
Basic Physics for Neutron Diffraction  
Structural Study by Neutron Diffraction  
Multilayered Structure  
Structural Fluctuation Observed by Neutron Techniques

Associate Professor Koji KISHIO

Department of Applied Chemistry, Faculty of Engineering, University of Tokyo (7-3-1 Hongo, Bunkyo-ku, Tokyo 113)

#### Lectures at ICR

Superconductivity and Behavior of Magnetic Flux; I, II and III  
Magnetic Properties and Applications of High T<sub>c</sub>

Magnetic Structure Studied by Neutron Diffraction  
Microscopic Magnetic Structures  
Magnetism and Transport  
Neutron Diffraction for Giant-Magnetoresistance Systems  
Spin-Dependent Scattering and Interface Structure

Cupric Oxide Superconductors: I, II and III  
Stabilization and Physical Properties of Mercury-Based Cupric Oxide Superconductors: I, II and III



Professor  
ENDO, Yasuo  
(D Sc)



Associate Professor  
KISHIO, Koji  
(Ph D)



## FUNDAMENTAL MATERIAL PROPERTIES —Composite Material Properties—

Professor Tadamoto SAKAI

Deputy Manager of Hiroshima Plant, Director, The Japan Steel Works, Co. Ltd. (1-6-1, Funakoshi-minami, Aki-ku, Hiroshima 736)

### Lectures at ICR

Injection Molding Procedures of New Ceramics  
Injection Molding for Plastic Bonded Magnet  
Injection Molding Methods for Various Plastics  
Fine Molding of Plastics

Single Screw Extrusion

Twin Screw Extrusion of Foods

Twin Screw Extrusion

Twin Screw Reactive Processing

Associate Professor Junji WATANABE, promoted to Professor on Dec. 16, 1994

Department of Polymer Chemistry, Tokyo Institute of Technology (2-12-1, O-okayama, Meguro-ku, Tokyo 152)

### Lectures at ICR

Rigid-Rod Polyesters with Flexible Side Chains  
Based on 1,4-Dialkylesters of Pyromellitic Acid -  
Synthesis and Mesophase Structure  
Layered Crystals and Mesophase of Aromatic  
Rigid-Rod Polyesters with Flexible Side Chains

Novel Block Copolymers Containing Side Chain  
Liquid Crystal Polymer Segments - Phase  
Behaviors of LC Segments in the Microphase -  
Separated System



Professor  
SAKAI, Tadamoto  
(D Eng)



Associate Professor  
WATANABE, Junji  
(D Eng)

## SYNTHETIC ORGANIC CHEMISTRY —Synthetic Theory—

Professor Hideo NAKAO

Vice President, Synthetic Organic Chemistry Research Institute, Sankyo Co. Ltd. (1-2-58, Hiromachi, Shinagawa-ku, Tokyo 140)

### Lectures at ICR

Epoch-making New Drugs and Improved Drugs

Associate Professor Masataka IHARA

Department of Pharmaceutical Science, Faculty of Pharmaceutical Science, Tohoku University (Aramaki-Aza-Aoba, Aoba-ku, Sendai 980)

### Lectures at ICR

Construction of Polycyclic System Using Tandem

Intramolecular Reactions and the Application to the  
Natural Product Synthesis



Professor  
NAKAO, Hideo  
(D Pharm Sc)



Associate Professor  
IHARA, Masataka  
(D Pharm Sc)



# PUBLICATIONS

## STATES AND STRUCTURE

### I. Atomic and Molecular Physics

Yasumi S, Maezawa H, Kishimoto S, K. Shima, Mizogawa T, Mukoyama T, Sera K, Fujioka M, Ishii K, Omori T., Inagaki Y and Izawa G: Measurement of the Mass of Electron Neutrino using Electron Capture in  $^{163}\text{Ho}$ , Photon Factory Activity Report 1992 (National Laboratory for High Energy Physics, Tsukuba, 1993), 28.

Emura S, Takahashi M, Omote K, Yoshikado S, Ito Y, Takahashi N and Mukoyama T: X-Ray Absorption Structure on Multielectron Excitation in Br, in Abst. X'93 16th Intern. Conf. on X-Ray and Inner-Shell Processes, July 12–16, 1993, Debrecen, Hungary, ed. by L. Sarkadi and D. Berenyi (ATOMKI, Debrecen, 1993), 77–78.

Nakamatsu H, Taniguchi K, Adachi H and Mukoyama T: Chemical Effect on  $L\beta/L\alpha$  X-Ray Intensity Ratios—Relativistic Electronic Structure Calculations of Fe Compounds, in Abst. X'93 16th Intern. Conf. on X-Ray and Inner-Shell Processes, July 12–16, 1993, Debrecen, Hungary, ed. by L. Sarkadi and D. Berenyi (ATOMKI, Debrecen, 1993), 205–206.

Ohmura Y, Nakamatsu H and Mukoyama T: Electronic States in the Presence of the Inner-Shell Hole Studied by the Method of DV- $X\alpha$ , in Abst. X'93 16th Intern. Conf. on X-Ray and Inner-Shell Processes, July 12–16, 1993, Debrecen, Hungary, ed. by L. Sarkadi and D. Berenyi (ATOMKI, Debrecen, 1993), 210–211.

Mukoyama T, Nakamatsu H and Adachi H: Relativistic Molecular Orbital Calculations of Photoelectron and Conversion Electron Spectra, in Abst. X'93 16th Intern. Conf. on X-Ray and Inner-Shell Processes, July 12–16, 1993, Debrecen, Hungary, ed. by L. Sarkadi and D. Berenyi (ATOMKI, Debrecen, 1993), 338–339.

Kumar A and Mukoyama T: Radiative Transition Probabilities, *Physics Education (India)*, **10**, 109–115 (1993).

Onoe J, Nakamatsu H, Sekine R, Mukoyama T, Adachi H and Takeuchi K: Quantum Chemical Study of the UV Photo-Excited States of  $\text{UF}_6$ , *Laser Kagaku Kenkyuu*, **15**, 88–91 (1993) (in Japanese).

Onoe J, Takeuchi K, Nakamatsu H, Mukoyama T, Sekine R, Kim, B-I and Adachi H: Relativistic Effects on the Electronic Structure and Chemical Bonding of  $\text{UF}_6$ , *J. Chem. Phys.*, **99**, 6810–6817 (1993).

Mukoyama T, Nakamatsu H and Adachi H: Relativistic Calculations of Photoelectron and Conversion-electron Spectra for  $\text{UF}_4$ , *J. Electron Spectrosc. Relat. Phenom.*, **63**, 409–417 (1993).

Mukoyama T and Adachi H: Electronic Structures of  $d^0$  Complexes by the DV- $X\alpha$  Method, *Chem. Phys. Lett.*, **215**, 93–96 (1993).

Yasumi S, Maezawa H, Shima K, Inagaki Y, Mukoyama T, Mizogawa T, Sera K, Kishimoto S, Fujioka M, Ishii K, Omori T, Izawa G and Kawakami O: Measurement of the Mass of the Electron Neutrino Using Electron Capture in  $^{163}\text{Ho}$ , *KEK Preprint*, 93–173 (KEK, Tsukuba) (1993).

Mukoyama T, Ito Y, Takahashi M and Emura S: Energy Dependence of Multielectron Transitions in X-Ray Absorption of Atoms, *Bull. Inst. Chem. Res., Kyoto Univ.*, **71**, 94–103 (1993).

Ito Y, Mukoyama T, Omote K, Shimizu K, Nisawa A, Shoji T, Terauchi H and Kuehner S: Characterization of Mo/Si Multilayer by X-Rays, *Bull. Inst. Chem. Res., Kyoto Univ.*, **71**, 104–110 (1993).

Tőkési K and Mukoyama T: Theoretical Investigation of the ECC Peak for Charged Particle with the CTMC Method, *ATOMKI Annual Report 1992* (Institute of Nuclear Research of the Hungarian Academy of Sciences, Debrecen, Hungary), 71–72 (1993).

Mukoyama T and Ito Y: Relativistic Calculations of Shakeup and Shakeoff Probabilities as the Result of 1s-Shell Vacancy Production, *Bull. Inst. Chem. Res., Kyoto Univ.*, **71**, 398–405 (1994).

Mukoyama T, Ito Y, Takahashi M and Emura S: Analytical Expression of Photoionization Cross Sections for Rare Gases, *Bull. Inst. Chem. Res., Kyoto Univ.*, **71**, 406–410 (1994).

Onoe J, Sekine R, Takeuchi K, Nakamatsu H, Mukoyama T and Adachi H: Atomic-number Dependence of Relativistic Effects on Chemical Bonding Using the Non-relativistic and Relativistic Discrete-variational  $X\alpha$  Methods, *Chem. Phys. Lett.*, **217**, 61–64 (1994).

Ito Y, Mukoyama T, Funatomi H, Yoshikado S and Tanaka T: The Crystal Structure of Tetragonal form  $\text{PbSnF}_4$ , *Solid State Ions. Diffus. React.*, **67**, 301–305 (1994).

Ito Y, Mukoyama T, Yoshikado S and Koto K: On Anharmonicity of  $\beta\text{-PbF}_2$ , *Solid State Ions. Diffus. React.*, **67**, 307–309 (1994).

Mukoyama T and Hock G: Analytical Expressions of Potentials and Wave Functions for Atoms and Ions, *Nucl. Instr. and Meth.*, **B86**, 155–157 (1994).

Mukoyama T and Ito Y: Multielectron Transitions in X-ray Absorption and Inner-shell Ionization Phenomena, *Nucl. Instr. and Meth.*, **B87**, 26–33 (1994).

Ohmura Y, Ikeda T, Nakamatsu H and Mukoyama T: Electronic States in the Presence of the Inner-shell Hole Studied by the Method of DV- $X\alpha$ , *Nucl. Instr. and Meth.*, **B87**, 237–240 (1994).

Nakamatsu H, Adachi H and Mukoyama T: Molecular Orbital Calculations of Continuum Wavefunctions for  $\text{H}_2^+$  with Basis Functions of Atoms, *Bull. Inst. Chem. Res., Kyoto Univ.*, **72**, 45–50 (1994).

Tőkési K and Mukoyama T: Theoretical Investigation of the ECC Peak for Charged Particles with the CTMC Method, *Bull. Inst. Chem. Res., Kyoto Univ.*, **72**, 63–68 (1994).

Tőkési K, Sarkadi L and Mukoyama T: Model Calculation for the ECC Peak at Neutral Projectile Impact, *ATOMKI Annual Report 1993* (Institute of Nuclear Research of the Hungarian Academy of Sciences, Debrecen, Hungary), 71–72 (1994).



Mukoyama T and Tórkési K: Monte Carlo Simulation of Electron Spectrum of Al near the Elastic Peak, *ATOMKI Annual Report 1993* (Institute of Nuclear Research of the Hungarian Academy of Sciences, Debrecen, Hungary), 90–91 (1994).

Tórkési K and Mukoyama T: Monte Carlo Code for the Study of Charged Particle-solid Interaction, *ATOMKI Annual Report 1993* (Institute of Nuclear Research of the Hungarian Academy of Sciences, Debrecen, Hungary), 92–93 (1994).

Yasumi S, Maezawa H, Shima K, Inagaki Y, Mukoyama T, Mizogawa T, Sera K, Kishimoto M, Fujioka S, Ishii K, Omori T, Izawa G and Kawakami O: The Mass of the Electron Neutrino from Electron Capture in  $^{163}\text{Ho}$ , *Phys. Lett.*, **B334**, 229–233 (1994).

Mukoyama T and Yamaguchi K: Solving Schrödinger Equation with Wavelets, in *Abst. of Contributed Papers, ICAP-14 Fourteenth Internat. Conf. on Atomic Physics*, July 31–August 5, 1994, Boulder, Colorado (University of Colorado, Boulder), 2N-12 (1994).

Yasumi S, Maezawa H, Shima K, Inagaki Y, Mukoyama T, Mizogawa T, Sera K, Kishimoto S, Fujioka M, Ishii K, Omori T, Izawa G and Kawakami O: Measurement of the Mass of Electron Neutrino Using Electron Capture in  $^{163}\text{Ho}$ , *Photon Factory Activity Report 1993* (National Laboratory for High Energy Physics, Tsukuba), 16 (1994).

Emura S, Takahashi M, Omote K, Yoshikado S, Ito Y, Takahashi N and Mukoyama T: X-ray Absorption Structure on Multielectron Excitation in Br, *Photon Factory Activity Report 1993* (National Laboratory for High Energy Physics, Tsukuba), 121 (1994).

Ito Y, Takahashi N, Mukoyama T, Omote K, Yoshikado S, Takahashi M and Emura S: Multielectron Excitation of Ni and Zn Metals in x-ray Absorption Spectroscopy, *Photon Factory Activity Report 1993* (National Laboratory for High Energy Physics, Tsukuba), 124 (1994).

Onoe J, Nakamatsu H, Sekine R, Mukoyama T, Adachi H and Takeuchi K: Note on the Contribution of Relativity to  $\text{Cu}_2$  Bonding, *J. Phys. Soc. Japan*, **63**, 3992–3995 (1994).

Ito Y, Mukoyama T, Kanamaru F and Yoshikado S: Crystal Structure of Beta-lead Fluoride Doped Potassium Fluoride and Ionic Conduction, *Solid State Ionics*, **73**, 283–287 (1994).

Ito S, Tosaki M, Maeda N, Katano R and Isozumi Y: Behavior of the SQS Mode Observed as Function of the Radial Distance of the Position of Primary Ionization, *Nucl. Instrum. Methods*, **A239**, 564–566 (1993).

Ito S, Tosaki M, Maeda N, Katano R and Isozumi Y: Application of a Pressurized Position-sensitive Proportional Counter to X-ray Measurement, *Nucl. Instrum. Methods*, **B75**, 112–115 (1993).

Fujii T, Hosoi N, Katano R and Isozumi Y: Operation of a Cryogenic Conversion Electron Proportional Counter under Strong Magnetic Fields, *Nucl. Instrum. Methods*, **B76**, 207–209 (1993).

Fujii T, Takano M, Katano R, Isozumi Y and Banbo Y: Spin-flip Anomalies in Epitaxial  $\alpha\text{-Fe}_2\text{O}_3$  Films by Mössbauer Spectroscopy, *J. Magn. Magn. Mat.*, **135**, 231–236 (1994).

Ito Y, Nakamatsu H, Mukoyama T, Omote K, Yoshikado S, Takahashi M and Emura S: Multielectron Excitations of Ni and Zn in X-ray Absorption, *Jpn. J. Appl. Phys.*, **32**, Suppl. 32–2, 58–60 (1993).

Takahashi M, Emura S, Omote K, Yoshikado S, Ito Y, Takahashi N and Mukoyama T: Contribution of multielectron transitions to XAFS, *Bull. Inst. Chem. Res., Kyoto Univ.*, **71**, 37–41 (1993).

Kövér L, Némethy A, Cserny I, Nisawa A and Ito Y: Local Electronic structures in phosphorus oxyanions. in *Proc. European Conference on Application of Surface and Interface Analysis (ECASIA)*, October, 1993, Catania, Italy.

Ishida A, Emura S, Takahashi M, Ito Y, Kanamaru H and Takamuku S: EXAFS Studies on the Interaction between Eu and Crown Ethers in Organic Solvents, *Photon Factory Activity Reports*, **11**, 445 (1993).

Takahashi M, Emura S, Ito Y, Mukoyama T, Yoshikado S and Omote K: The Contribution of the Shakeup and Shakeoff Effects to XAFS, in *Proc. of 8th Intern. Conf. on X-ray Absorption Fine Structure*. MoTu-15 (1994).

Emura S, Takahashi M, Ito Y, Mukoyama T, Yoshikado S and Omote K: Multiexcitations on Br in Organic Solvents in XAFS, in *Proc. of 8th Intern. Conf. on X-ray Absorption Fine Structure*. MoTu-75 (1994).

Ishida A, Emura S, Takahashi M, Kanamaru H, Takamuku S and Ito Y: EXAFS Studies on the Interaction between Eu and Crown Ethers in Organic Solvents, in *Proc. of 8th Intern. Conf. on X-ray Absorption Fine Structure*. ThFr-174 (1994).

Suga Y, Asio K, Mukai S, Kitagaki R, Yamamoto K, Yoshikado S, Ito Y, Tanaka T, Mukoyama T and Taniguchi I: F Ion Conduction and Crystal Structure in Fluorite-type  $\text{PbF}_2\text{-SnF}_2$  Solid Solution System, *The Science and Engineering Review of Doshisha Univ.*, **35**, 128–143 (1994).

Nakamatsu H, Mukoyama T and Adachi H: DV- $X\alpha$  Molecular Orbital Method for X-ray Absorption Near-Edge Structure—Application to  $\text{N}_2$  and  $\text{CrO}_4^{2-}$ , *Jpn. J. Appl. Phys.*, **32**, suppl. 32–2, 23–25 (1993).

Nakamatsu H: DV- $X\alpha$  Method, *Oyo-Butsuri*, **62**, 1138–1139 (1993) (in Japanese).

Nakamatsu H and Mukoyama T: XANES and Molecular Orbital Method, *Nippon Hoshako Gakkai-shi*, **7**, 1–14 (1994) (in Japanese).

## II. Crystal Information Analysis

Kurata H and Colliex C: Electron-energy-loss Core-edge Structures in Manganese Oxides, *Phys. Rev.*, **B48**, 2102–2108 (1993).

Kurata H, Lefevre E, Colliex C and Brydson R: Electron-energy-loss Near-edge Structures in the Oxygen K-edge Spectra of Transition-metal Oxides, *Phys. Rev.*, **B47**, 13763–13768 (1993).

Nagai K, Kurata H, Isoda S and Kobayashi T: Structural Transitions in the Graphite- $\text{AlCl}_3\text{-FeCl}_3$  System, *J. Phys. Chem. Solids*, **54**, 533–542 (1993).



- Kobayashi T, Isoda S and Kurata H: Reaction Process in Solid States Studied by High Resolution Electron Spectro-Microscopy in Reactivity in Molecular Crystals ed. by Y. Ohashi, 44-57, *Kodansha* (1993).
- Kobayashi T, Moriguchi S, Kurata H, Ogawa T and Isoda S: High Resolution Electron Spectromicroscope (HRESM), *Bull. Inst. Chem. Res., Kyoto Univ.*, **70**, 451-461 (1993).
- Moriguchi S, Hoshino A, Hashimoto S, Kubono K, Nagai K, Asaka N, Ogawa T, Kurata H, Isoda S and Kobayashi T: High Resolution Electron Spectromicroscope (HRESM), Applications, *Bull. Inst. Chem. Res., Kyoto Univ.*, **70**, 462-481 (1993).
- Kubono K, Kurata H, Isoda S and Kobayashi T: Formation of Cyclophosphazene Clathrate Compounds by Vapour-Solid Reaction: Four Crystalline Forms Depending on Guest Molecules, *J. Mater. Chem.*, **3**, 615-621 (1993).
- Kubono K, Asaka N, Isoda S and Kobayashi T: Structures of 1:1 Clathrate between Tris(2,3-naphthalenedioxy) Cyclotriphosphazene and p-Xylene, *Acta Cryst.*, **C49**, 404-406 (1993).
- Kawase N, Kurata H, Kubono K, Isoda S and Kobayashi T: Study of Structure and Polymerization Process of Epitaxially Grown SiPc(OH)<sub>2</sub> Thin Films by High-Resolution Electron Microscopy, *J. Polym. Sci., Polymer Phys.*, **31**, 1713-1723 (1993).
- Kobayashi T and Isoda S: Lattice Images and Molecular Images of Organic Materials, *J. Mater. Chem.*, **3**, 1-14 (1993).
- Kurata H, Isoda S and Kobayashi T: Electron Energy-Loss Spectroscopy for Organic Compounds, *Bull. Inst. Chem. Res., Kyoto Univ.*, **71**, 212-225 (1993).
- Isoda S, Hoshino A and Kobayashi T: Interface Structures of Phthalocyanines Double-layers by High Resolution Electron Microscopy, *Chemistry of Functional Dyes*, **2**, 252-257 (1993).
- Ogawa T, Moriguchi S, Isoda S and Kobayashi T: Application of an Imaging Plate to Electron Crystallography at Atomic Resolution, *Polymer*, **35**, 1132-1136 (1994).
- Kubono K, Asaka N, Taga T, Isoda S and Kobayashi T: Selective Clathration in a Cage-type Host Lattice of Cyclophosphazene, *J. Mater. Chem.*, **4**, 291-297 (1994).
- Kubono K, Asaka N, Isoda S, Kobayashi T and Taga T: 2, 2, 4, 4, 6, 6-Tris(2,3-naphthylenedioxy)cyclotri-phosphazene, *Acta Cryst.*, **C50**, 324-326 (1994).
- Isoda S, Hashimoto S, Ogawa T, Kurata H, Moriguchi S and Kobayashi T: Pseudomorphic Structure of Vacuum-deposited Fluorinated Vanadylphthalocyanine (VOPcFx) and Its Optical Absorption Spectra, *Mol. Cryst. Liq. Cryst.*, **247**, 191-201 (1994).
- Hoshino A, Isoda S, Kurata H and Kobayashi T: Scanning Tunneling Microscope Contrast of Perylene-3,4,9,10-tetracarboxylic-dianhydride on Graphite and its Application to the Study of Epitaxy, *J. Appl. Phys.*, **76**, 4113-4120 (1994).
- Kurata H, Isoda S and Kobayashi T: Study on Organic Crystals with Electron Spectromicroscope, *Kessho-gakkaishi*, **36**, 199-203 (1994) (in Japanese).
- Hoshino A, Isoda S, Kurata H and Kobayashi T: Initial Stage of Crystallization of Organic Materials, *Technical Report on IEICE*, **94-16**, 41-46 (1994) (in Japanese).
- Ogawa T, Moriguchi S, Isoda S and Kobayashi T: Electron Structure Analysis of  $\beta$ -PTCDA with Imaging Plate, in *Proc. of Intern. Conf. on Electron Microscopy*, **1**, 965-966 (1994).
- Hashimoto S, Ogawa T, Hoshino A, Asaka N, Isoda S and Kobayashi T: Pseudomorph of Vanadyl-Phthalocyanines and their Stable Orientation on Substrates, in *Proc. of Intern. Conf. on Electron Microscopy*, **1**, 969-970 (1994).
- Kurata H, Moriguchi S, Isoda S and Kobayashi T: Energy-Filtering in 1MeV Electron Microscope, in *Proc. of Intern. Conf. on Electron Microscopy*, **1**, 717-718 (1994).
- ### III. Polymer Condensed States Analysis
- Kohjiya S, Yamato T, Miyake Y and Shibayama M: Analysis of the Experimental Results of the Effect of Solvent Evaporation Rate by Random Phase Approximation, *J. Soc. Rubber Ind. Japan*, **66**, 483-487 (1993) (in Japanese).
- Yoon J R, Tsukahara Y and Kohjiya S: Characterization and Properties of Natural Rubber/Brominated EPDM Blends, *J. Soc. Rubber Ind. Japan*, **66**, 495-503 (1993) (in Japanese).
- Kohjiya S and Ikeda Y: Preparation of Organic/Inorganic Hybrid Materials Using the Sol-Gel Process. in *New Functional Materials, Vol.C ed. by Tsuruta T, Elsevier Pub.*, 443-448 (1993).
- Bualek S, Ikeda Y, Kohjiya S, Phaovibul O, Phinyocheep P, Suchiva K, Utani K and Yamashita S: Natural Rubber and Butadiene Rubber Blend Using Diblock Copolymer of Isoprene-Butadiene as Compatibilizer, *J. Appl. Polym. Sci.*, **49**, 807-814 (1993).
- Yamashita S, Kodama K, Ikeda Y and Kohjiya S: Chemical Modification of Butyl Rubber. I. Synthesis and Properties of Poly(ethylene oxide)-Grafted Butyl Rubber, *J. Polym. Sci.: Part A: Polym. Chem.*, **31**, 2437-2444 (1993).
- Ikeda Y, Yonezawa T, Kimura H, Kohjiya S and Okada M: Synthesis of Dextran Derivatives by Ring-opening Polymerization, *Macromol. Chem., Rapid Commun.*, **14**, 551-555 (1993).
- Kohjiya S: Preparation and Properties of Organic/inorganic Hybrid Gels via Sol-Gel Processes, *Prepr. SPGN, Tsukuba*, **20** (1993).
- Ahmad S, Abudullah I, Sulaiman C S, Kohjiya S and Yoon J R: Natural Rubber-HDPE Blends with Liquid Natural Rubber as a Compatibilizer. I. Thermal and Mechanical Properties, *J. Appl. Polym. Sci.*, **51**, 1357-1363 (1994).
- Wintermantel M, Schimidt M, Tsukahara Y, Kajiwarra K and Kohjiya S: Rodlike Combs, *Macromol. Chem. Rapid Commun.*, **15**, 279-284 (1994).
- Sando K, Yamashita S and Kohjiya S: Reinforcement of 1-chlorobutadiene-butadiene and 1-chlorobutadiene-styrene-butadiene rubbers with Glass Short Fiber, *J. Soc. Rubber Ind. Japan*, **67**, 207-218 (1994) (in Japanese).



- Hashim, A S and Kohjiya S: Curing of Epoxidized Natural Rubber with p-Phenylenediamine. *J. Polym. Sci.: Part A: Polym. Chem.*, **32**, 1149–1157 (1994).
- Tsukahara Y, Kohjiya S, Tsutsumi K, and Okamoto Y: On the Intrinsic Viscosity of Poly(macromonomer)s, *Macromolecules*, **27**, 1662–1664 (1994).
- Hashimoto T, Sakurai S, Morimoto M, Nomura S, Kohjiya S and Kodaira T: Structure and Properties of Poly(tetrahydrofuran) Viologen Inonen: Effects of Halide Counter-Anions, *Polymer*, **35**, 2672–2678 (1994).
- Tsukahara Y, Inoue J, Ohta Y, Kohjiya S and Okamoto Y: Preparation and Characterization of  $\alpha$ -Benzyl- $\omega$ -vinylbezy Polystyrene Macromonomer, *Polym. J.* **26**, 1013–1018 (1994).
- Kohjiya S: Synthesis, Structure, and Properties of Novel Thermoplastic Functionality Elastomers, *Proc. 5th SFCFP, Jinan China*, 22 (1994).
- Krakovsky I, Urakawa H, Ikeda Y, Kohjiya S and Kajiura K: Structural Characteristics of Organic/Inorganic Hybrid Gels, *Bull. Inst. Chem. Res., Kyoto Univ.*, **72**, 211–221 (1994).
- Ikeda Y, Tabuchi M, Sekiguchi Y, Miyake Y and Kohjiya S: Effect of Solvent Evaporation Rate on Microphase-separated Structure of Segmented Poly(urethane-urea) Prepared by Solution Casting, *Macromol. Chem. Phys.*, **195**, 3615–3628 (1994).
- Yamaguchi S and Tsuji M: Morphological Changes of Poly(tetrafluoroethylene) by Heat Treatment on NaCl, *J. Mater. Res.*, **8**, 2942–2947 (1993).
- Tsuji M: Direct Observation of Atoms and Molecules —Transmission Electron Microscopy—, *Sci. Univ. Tokyo Bull., No. 2*, 9–15 (1994) (in Japanese).
- Kawaguchi A, Ohara M and Tsuji M: Environment-induced Morphological Changes of Polyethylene Lamellae During Crystallization in Solution, *J. Polym. Sci.: Part B: Polym. Phys.*, **32**, 421–436 (1994).
- Hirai A, Yamamoto H, Tsuji M and Horii F: Electron Microscopic Observation of the Formation Processes of the Microfibrils and the Composite Crystals for Bacterial Cellulose. in *Proc. '94 Cellulose R & D, Tokyo*, 41 (1994).
- Hu S, Tsuji M and Horii F: Phase Structure of Poly(vinyl alcohol) Single Crystals as Revealed by High-Resolution Solid-State  $^{13}\text{C}$  n.m.r. Spectroscopy, *Polymer*, **35**, 2516–2522 (1994).
- Tsuji M: Ultra-fine Structures Observed by Microscopical Methods, *Kaigai Kobunshi Kenkyu*, **40**, 150–154 (1994) (in Japanese).
- Hirai A, Tsuji M, Horii F and Yamamoto H: Formation Process of Composite Crystals (Cellulose Ia/I $\beta$ ) for Bacterial Cellulose, in *Rep. Poval Committee* **104**, 122–131 (1994) (in Japanese).
- Hirai A, Yamamoto H, Tsuji M and Horii F: Electron Microscopic Observation of the Formation Process of the Composite Crystals for Bacterial Cellulose, in *Prepr. Kyoto Conf. Cellulosics*, 61 (1994).
- Nishikawa Y, Kawaguchi A, Murakami S and Kohjiya S: Stress Induced Helix/Helix Transition in Polyvinylcyclohexane Crystals, in *Proc. ISF '94, Yokohama*, 39 (1994).
- Murakami S, Yamakawa M, Tsuji M, Kawaguchi A and Kohjiya S: Structural Formation in the Drawing Process of PEN [Poly(ethylene naphthalene-2,6-dicarboxylate)], in *Proc. ISF '94, Yokohama*, 40 (1994).
- Katayama K and Tsuji M: Fundamental of Spinning. in *Advanced fiber spinning technology*, ed. by Nakajima T, Woodhead Pub. Ltd., Cambridge, Chapt. 1, 1–24 (1994).
- Tsuji M and Murakami S: Imaging Plate as a Recording Medium for Transmission Electron Microscopy and X-ray diffraction, *SEN-I GAKKAISHI*, **50**, P 607–P 613 (1994) (in Japanese).
- Yamakawa M, Hamada N, Tsuji M, Murakami S and Kohjiya S: Ultra-fine Structures Observed in Crystalline Polymer Solids by High-Resolution Electron Microscopy, in *Prepr. 5th SPSJ Int. Polym. Conf., Osaka*, 309 (1994).
- Yamaguchi S, Tsuji M and Kohjiya S: Morphological Changes of Poly(tetrafluoroethylene) by Heat Treatment on Alkali Halides, in *Prepr. 5th SPSJ Int. Polym. Conf., Osaka*, 311 (1994).
- Takigawa T, Urayama K and Masuda T: Time Dependent Poisson's Ratio of Polymer Gels in Solvent, *Polym. J.*, **26**, 225–227 (1994).
- Takigawa T, Urayama K and Masuda T: Theoretical Studies on the Stress Relaxation of Polymer Gels under Uniaxial Elongation, *Polym. Gels & Networks* **2**, 59–64 (1994).
- Urayama K, Takigawa T and Masuda T: Stress Relaxation and Creep of Polymer Gels in Solvent under Uniaxial and Biaxial Deformations, *Rheologica Acta*, **33**, 89–98 (1994).
- Urayama K, Morino Y, Takigawa T and Masuda T: Poisson's Ratio of Poly(vinyl alcohol) and Polyacrylamide Gels, in *Prepr. PCR'94, Kyoto*, 302 (1994).
- Urayama K, Takigawa T, Masuda T and Kohjiya S: Stress Relaxation and Creep of Polymer Gels in Solvent under Various Deformation Modes, in *Prepr, SSIPG'94, Sapporo*, 80 (1994).

## INTERFACE SCIENCE

### I. Solutions and Interfaces

- Umemura J, Takeda S, Hasegawa T and Takenaka T: Thickness and Temperature Dependence of Molecular Structure in Stearic Acid LB Films Studied by FTIR Reflection-Absorption Spectroscopy, *J. Mol. Struct.*, **297**, 57–62 (1993).
- Takenaka T and Umemura J: FT-IR Study of Structure-Pyroelectricity Relationship in Noncentrosymmetric Langmuir-Blodgett Films, *New Functionality Materials: Design, Preparation and Control* (T. Tsuruta, M. Seno and M. Doyama, Eds.), Vol. C, 565–570, Elsevier Science Pub., Amsterdam (1993).
- Hasegawa T, Umemura J and Takenaka T: Infrared External Reflection Study of Molecular Orientation in Thin Langmuir-Blodgett Films, *J. Phys. Chem.*, **97**, 9009–9012 (1993).
- Miyama T, Yonezawa Y, Sato T, Umemura J and Takenaka T: Surface-Enhanced Raman Scattering from Silver Salt of



Carboxymethyl-cellulose Photolyzed with UV-Light, *Chem. Lett.*, 1537–1540 (1993).

Okamura E, Umemura J, Iriyama K and Araki T: Microstructure of Thin Langmuir-Blodgett Films of Dipalmitoyl-phosphatidylcholine-Electron Microscopic Images Replicated with Plasma Polymerized Film by Glow Discharge, *Chem. Phys. Lipids*, **66**, 219–223 (1993).

Umemura J, Kamata T, Takenaka T, Takehara K, Isomura K and Taniguti H: Raman Spectroscopic Study of Alternate Langmuir-Blodgett Films with Pyroelectric Efficiency, *Bull. Inst. Chem. Res., Kyoto Univ.*, **71**, 120–126 (1993).

Hasegawa T, Park S R, Kim D W, Lee H and Umemura J: FT-IR Reflection-Absorption Spectra of Langmuir-Blodgett Films of Stearic Acid- $d_{35}$  on Silver, *Bull. Inst. Chem. Res., Kyoto Univ.*, **71**, 127–132 (1993).

Okamura E, Matsumura Y and Takenaka T: Effect of Wax Addition on Gel-to-Liquid-Crystalline Phase Transition of Palm-Oil as Studied by FT-IR Spectroscopy, *Bull. Inst. Chem. Res., Kyoto Univ.*, **71**, 188–192 (1993).

Park S R, Kim D W, Lee H and Umemura J: FT-IR/ATR Spectra of Octadecyl-trichlorosilane Adsorbed on Germanium Surface, *Bull. Inst. Chem. Res., Kyoto Univ.*, **71**, 193–197 (1993).

Sakai H and Umemura J: Infrared External Reflection Spectra of Langmuir Films of Stearic Acid and Cadmium Stearate, *Chem. Lett.*, 2167–2170 (1993).

Ishiguro R, Kimura N, Takahashi S: Orientation of Fusion-Active Synthetic Peptides in Phospholipid Bilayers: Determination by Fourier Transform Infrared Spectroscopy, *Biochemistry*, **32**, 9792–9797 (1993).

Wakai C and Nakahara M: Pressure Dependencies of Rotational, Translational, and Viscous Friction Coefficients in Water- $d_2$ , Acetonitrile- $d_3$ , Acetonitrile, Chloroform, and Benzene, *J. Chem. Phys.*, **100**, 8347–8358 (1994).

Kamata T, Umemura J, Takenaka T, Koizumi N, Takehara K, Isomura K and Taniguti H: Pyroelectricity of Noncentrosymmetric Langmuir-Blodgett Films of Phenylpyrazine Derivatives, *Jpn. J. Appl. Phys. I*, **33**, 1074–1078 (1994).

Umemura J, Takeda S, Hasegawa T, Kamata T and Takenaka T: Effect of Thickness and Monolayer Location on Thermostability of Metal Stearate LB Films Studied by FTIR Reflection-Absorption Spectroscopy, *Spectrochim. Acta*, **50A**, 1563–1571 (1994).

Miwa Y, Miura N, Machida K, Nakagawa T, Umemura J and Hayashi S: Simulation of Vibrational Spectra of Isotopic Benzenes by an Extended Molecular Mechanics Method, *Spectrochim. Acta*, **50A**, 1629–1646 (1994).

Kimura N, Hayashi S, Umemura J, Taga T, Machida K and Takenaka T: Polarized FT-IR Spectra of Water in Dodecyl-butylidimethylammonium Bromide Monohydrate, *J. Mol. Struct.*, **324**, 11–18 (1994).

Murata Y, Tsunashima K, Umemura J and Koizumi N: Ferroelectric Properties in Aromatic Polyamides, *CEIDP Annual Report IEEE94CH3456-1*, 779–784 (1994).

Nakahara M: New Developments of Nonaqueous Solution Chemistry. 1. A High Resolution NMR Spectroscopic Approach, *Denki Kagaku (J. Electrochem. Soc. Jpn.)*, **63**, 108–113 (1994) (in Japanese).

Nakahara M: Molecular Approaches to Nonequilibrium Processes in Solution. Dynamics of Diffusion Processes, *Gakujyutsu Geppo (Japanese Scientific Monthly)*, **47**, 383–388 (1994) (in Japanese).

Nakahara M: Roles Played by NMR in Determining Solution Structure, *Kagaku (Chemistry)*, **49**, 188–192 (1994). (in Japanese).

Takenaka T and Umemura J: Spread Monolayers and LB Films, *Membrae Experiment Series, Vol. II. Biomimetic-Functional Membranes* (Japan Membrane Society Ed.), 2–30, Kyoritsu Shuppan, Tokyo (1994) (in Japanese).

## II. Molecular Aggregates

Sato N, Sugawara T and Izuoka A: Structure and Properties of Overcrowded Condensed Polycyclic Aromatic Hydrocarbons—Tetrabenzopentacene—, *Rep. Toyota Phys. Chem. Res. Inst.*, **46**, 33–39 (1993) (in Japanese).

Mochida T, Izuoka A, Sato N and Sugawara T: Decarboxylation of Crystalline 2-Carboxy-3-hydroxydibenzo[a, c]tropone Followed by Solid-state Crystallization, *Chem. Phys. Lett.*, **210**, 389–392 (1993).

Awaga K, Yokoyama T, Fukuda T, Masuda S, Harada Y, Maruyama Y and Sato N: Photoelectron Spectroscopic Studies of an  $\alpha$ -Nitronyl Nitroxide Radical: Mechanism of Ferromagnetic Intermolecular Interaction, *Mol. Cryst. Liq. Cryst.*, **232**, 27–34 (1993).

Seki K, Sato N and Inokuchi H: Valence Electronic Structure of a Long-chain Alkane in Random-coil Forms. Gas-phase UPS of  $n$ -C<sub>36</sub>H<sub>74</sub> and MO Calculations, *Chem. Phys.*, **178**, 207–214 (1993).

Hanai T, Zhao K S, Asaka K and Asami K: Theoretical Approach and the Practice to the Evaluation of Structural Parameters Characterizing Concentration Polarization alongside Ion-exchange Membranes by Means of Dielectric Measurements, *Colloid Polym. Sci.*, **271**, 766–773 (1993).

Asami K and Hanai T: Observations and the Phenomenological Interpretation of Dielectric Relaxation due to Electrode Polarization, *Bull. Inst. Chem. Res., Kyoto Univ.*, **71**, 111–119 (1993).

Sato N: Characteristic Electronic Structures of Organic Solids Classified in Terms of Molecular Electronic Relaxation, *Synth. Metals*, **64**, 133–139 (1994).

Yoshida S, Kozawa K, Sato N and Uchida T: Photoelectric Behavior of Sublimed Films of Phenothiazine Derivatives, *Bull. Chem. Soc. Jpn.*, **67**, 2017–2023 (1994).

Asami K and Zhao K S: Dielectric Measurement of a Single Sub-millimeter Size Microcapsule, *Colloid Polym. Sci.*, **272**, 64–71 (1994).

Asami K: The Scanning Dielectric Microscope, *Meas. Sci. Technol.*, **5**, 589–592 (1994).



Asami K and Takashima S: Membrane Admittance of Cloned Muscle Cells in Culture, *Biochim. Biophys. Acta*, **1190**, 129–136 (1994).

Nagaoka Y, Iida A, Kanbara T, Lian Pin N, Fujita T, Asami K, Asaka K, Tachikawa E and Kashimoto T: Structure and Function of Channel Forming Peptides, Trichosporin-B-VIa and Aib14-trichosporin-B-VIa, in Lipid Bilayer and Biomembranes, *Peptide Chem.*, **1993**, 361–364 (1994).

Irimajiri A and Asami K: Measurement of Membrane Impedance and Capacitance, in *Method in Membrane Science*, Vol. 1, ed. Membrane Soc. Jpn., 393–399 (1994) (in Japanese).

### III. Separation Chemistry

Sohrin Y, Kokusen H, Kihara S, Matsui M, Kushi Y and Shiro M: New Mode of Ion Size Discrimination for Group 2 Metals Using Poly(pyrazolyl)borate Ligands. Control of Stability and Structure of Chelate Complexes by Intraligand Contact, *J. Am. Chem. Soc.*, **115**, 4128–4136 (1993).

Umetani S, Matsui M and Tsurubou S: Improvement of Separation in the Solvent Extraction of Alkaline Earths by the Use of 18-Crown-6 as a Masking Reagent, *J. C. S., Chem. Commun.*, 914–916 (1993).

Umetani S, Le THQ, Takahara H and Matsui M: Solvent Extraction of Metals with Strongly Acidic Extractants Derived from Heterocyclic Compounds in Solvent Extraction in the Process Industries, *Elsevier*, 643–650 (1993).

Sasaki T, Sohrin Y, Hasegawa H, Kokusen H, Kihara S and Matsui M: Separation of Methylated and Inorganic Germanium by Liquid-Liquid Extraction with Organic Ligands Containing a Negatively Charged Oxygen Donor, *Anal. Chem.*, **66**, 271–275 (1994).

Sasaki T, Umetani S, Matsui M and Tsurubou S: Quantitative Extraction-Separation of Calcium and Strontium Using Cryptand [2.2.2] as a Masking Reagent, *Chem. Letters*, 1195–1198 (1994).

Sohrin Y, Matsui M, Hata Y, Hasegawa H and Kokusen H: New Mode of Ion Size Discrimination for Group 2 Metals Using Poly(pyrazolyl)borate Ligands. 2. Control of Stability and Structure of Chelate Complexes by Intra- and Interligand Contact and Shielding Effect, *Inorg. Chem.*, **33**, 4376–4383 (1994).

Kihara S, Maeda K, Shirai O, Yoshida Y and Matsui M: Voltammetric Study on the Oscillation of Potential Difference or Current at an Aqueous/Organic (Membrane) Interface Accompanied by Ion Transfer, in *Proceedings of 2nd Bioelectroanalytical Symposium*, 331–342.

Ogura K, Kihara S, Umetani S and Matsui M: Voltammetric Study on the Transfer of Alkali and Alkaline Earth Metal Ions at the Aqueous/Organic Interface Facilitated by Phosphine Oxides, *Bull. Chem. Soc. Japan*, **66**, 1971–1978 (1993).

Ogura K, Kihara S, Suzuki M and Matsui M: Ion Transfer at the Interface between an Aqueous Solution in the Presence of Concentrated Salts and an Organic Solution Studied by Polarography at the Electrolyte Solution Dropping Electrode, *J. Electroanal. Chem.*, **352**, 131–151 (1993).

Kihara S and Maeda K: Novel Oscillations of Membrane Potential or Current Accompanied by Ion Transfer and Voltammetric Elucidation of Their Mechanisms, *Seventh Newsletter of MEBC*, 25–30 (1993).

Suzuki M, Ion Transfer from Water to Formamide or 1,2-Ethanedithiol Studied by Polarography at the Electrolyte Solution Dropping Electrode, *J. Electroanal. Chem.*, **372**, 39–48 (1994).

Kihara S and Maeda K: Membrane Oscillations and Ion Transport, *Progress in Surface Science*, **47**, 1–54 (1994).

Yoshida Z, Aoyagi H, Meguro Y, Kitatsuji Y and Kihara S: Voltammetric Study on the Transfer of U, Np and Pu Ions at the Aqueous-Organic Interface Facilitated by Phosphine Oxides, *J. Alloys and Compounds*, **213/214**, 324–327 (1994).

Yoshida Z and Kihara S: Nuclear Fuel and Electroanalytical Chemistry, *Denki Kagaku*, **62**, 8–14 (1994) (in Japanese).

Fujino O, Umetani S and Matsui M: Determination of Uranium in Apatite Minerals by Inductively Coupled Plasma Atomic Emission Spectrometry after Solvent Extraction and Separation with 3-Phenyl-4-benzoyl-5-isoxazolone into Diisobutyl Ketone, *Anal. Chim. Acta*, **296**, 63–68 (1994).

Hasegawa H, Sohrin Y, Matsui M, Hojo M and Kawashima M: Speciation of Arsenic in Natural Waters by Solvent Extraction and Hydride Generation Atomic Absorption Spectrometry, *Anal. Chem.*, **66**, 3247–3252 (1994).

Kihara S, Ishio N, Sanada M, Kuwada S, Shirai O, Yoshida Y, Suzuki M and Matsui M: Abiotic Synthesis of Substances Relative to the Origin of Life under the Oxidizing Atmosphere, *Transactions of The Research Institute of Oceanography*, **7**, 4–15 (1994) (in Japanese).

## SOLID STATE CHEMISTRY

### I. Artificial Lattice Alloys

Sato H, Aoki Y, Kobayashi Y, Yamamoto H and Shinjo T: Huge Magnetic Field-dependent Thermal Conductivity in Magnetic Multilayer Films, *J. Magn. & Magn. Mater.*, **126**, 410–412 (1993).

Nakayama N, Wu L, Dohnomae H, Shinjo T, Kim J and Falco C M: X-ray Diffraction Analysis of Lattice Strain in Metallic Superlattice Films, *J. Magn. & Magn. Mater.*, **126**, 71–75 (1993).

Nasu S, Kobayashi Y, Shibata T, Dohnomae H, Mima N and Shinjo T: <sup>197</sup>Au Mössbauer Study of Au/Ni Multilayers, *J. Magn. & Magn. Mater.*, **126**, 221–224 (1993).

Sakurai M and Shinjo T: Magnetic and Magneto-optical Properties of Pd/Au/Pd/Co and Pd/Cu/Pd/Co Multilayers, *J. Magn. & Magn. Mater.*, **128**, 237–246 (1993).

Fujii Y, Ohishi Y, Konishi H, Nakayama N and Shinjo T: High-pressure SRX-ray Diffraction Studies of Structural and Elastic aspects of Superlattices, *J. Magn. & Magn. Mater.*, **126**, 192–196 (1993).

Sakurai J, Nishimura K, Taniguchi H, Hasegawa K, Okuyama T and Shinjo T: Thermopower and Resistivity of Au/Co/Au/Ni(Fe) Multilayers, *J. Magn. & Magn. Mater.*, **126**, 510–512 (1993).



Mibu K, Hosoito N and Shinjo T: Iron Spin Directions in Fe/Rare Earth Multilayers by Mössbauer Spectroscopy, *J. Magn. & Magn. Mater.*, **126**, 343–345 (1993).

Nakamura H, Suzuki T, Shiga M, Yamamoto H and Shinjo T: NMR Study of  $^{59}\text{Co}$  in [Cu/Co/Cu/NiFe] Superlattices, *J. Magn. & Magn. Mater.*, **126**, 364–366 (1993).

Dohnomae H, Shintaku K, Nakayama N and Shinjo T: Magnetic Structure of CrSb/Sb Superlattices, *J. Magn. & Magn. Mater.*, **126**, 346–348 (1993).

Mibu K, Hosoito N and Shinjo T: Mössbauer Study of Spin Reorientation in Fe/Rare-Earth Multilayers. *Nucl. Instrum. Methods*, **B76**, 31–32 (1993).

Mekata M, Yaguchi N, Takagi T, Sugino T, Mitsuda S, Yoshizawa H, Hosoito N and Shinjo T: Successive Magnetic Ordering in  $\text{CuFeO}_2$ —A New Type of Partially Disordered Phase in a Triangular Lattice Antiferromagnet—, *J. Phys. Soc. Jpn.*, **62**, 4474–4487 (1993).

Shinjo T: Magneto-Transport Phenomena of Multilayers with Two Magnetic Components. in *Magnetism and Structure in Systems of Reduced Dimension* ed R.F.C. Farrow et al., Plenum Press, New York, 323–333 (1993).

Sakurai M and Shinjo T: Magneto-Optical Properties and Magnetic Anisotropies for Au/Cu/Au/Co and Cu/Au/Cu/Co Multilayers, *J. Appl. Phys.*, **74**, 6840–6846 (1993).

Wu L, Nakayama N, Engel BN, Shinjo T and Falco CM: X-Ray Diffraction Measurements of Lattice Strains in Co/Pd (001) Superlattice Films, *Jpn. J. Appl. Phys.*, **32**, 4726–4731 (1993).

Wu L, Shintaku K, Shinjo T and Nakayama N: Preparation and Structural Characterization of Co/Au (001) Superlattices, *J. Phys. Condens. Matter*, **5**, 6515–6524 (1993).

Wu L, Hosoito N, Nakayama N and Shinjo T: Coherent Interface Structures Observed in Co/Au (001) Epitaxial Superlattices, *J. Phys. Soc. Jpn.*, **62**, 4171–4173 (1993).

Yamamoto H, Motomura Y, Anno T and Shinjo T: Magneto-resistance of non-coupled [NiFe/Cu/Co/Cu] Multilayers, *J. Magn. & Magn. Mater.*, **126**, 437–439 (1993).

Kawawake Y, Mibu K and Shinjo T: Mössbauer Study of Co/Cu Multilayers Using  $^{119}\text{Sn}$  Probes, *J. Phys. Soc. Jpn.*, **63**, 2700–2705 (1994).

Emoto T, Mibu K, Hosoito N and Shinjo T: Magnetic Polarization of Au Layers in Co/Au Multilayers Observed by  $^{119}\text{Sn}$  Mössbauer Effect, *J. Phys. Soc. Jpn.*, **63**, 3226–3229 (1994).

Shinjo T: Recent Development of Metallic Multilayer Studies, *Gakujutsu Geppou*, **47**, 1085–1089 (1994) (in Japanese).

Ono T, Hosoito N and Shinjo T: Magnetization Process of Granular Fe-Ag GMR System Studied by Mössbauer Spectroscopy, *J. Phys. Soc. Jpn.*, **63**, 2874–2877 (1994).

Nishimura K, Sakurai J, Hasegawa K, Saito Y, Inomata K and Shinjo T: Thermoelectric Power of Co/Cu Multilayer, *J. Phys. Soc. Jpn.*, **63**, 2685–2690 (1994).

Yamamoto A, Honmyo T, Kiyama M and Shinjo T: Surface Magnetism of  $\alpha\text{-FeO}(\text{OH})$  and  $\beta\text{-FeO}(\text{OH})$  by Mössbauer Spectroscopy, *J. Phys. Soc. Jpn.*, **63**, 176–183 (1994).

Asano T, Ajiro T, Mekata M, Yamazaki H, Hosoito N, Shinjo T and Kikuchi H: Single Crystal Susceptibility of The S=1 One-Dimensional Heisenberg Antiferromagnet  $\text{AgVP}_2\text{S}_6$ , *Solid State Communications*, **90**, 125–128 (1994).

Shinjo T: in *Giant Magnetoresistance—New Branch of Physics on Metallic Multilayers*, 39–52 (1994) (in Japanese).

## II. Artificial Lattice Compounds

### III. Multicomponent Materials

Terashima T, Shimura K, Daitoh Y, Bando Y, Matsuda Y and Komiyama S: Microstructure and Superconductivity of Oxide Superconductors Ultrathin Films, in 1993 International Workshop on Superconductivity, June 28–July 1, 1993, Hakodate, Japan, International Superconductivity Technology Center (ISTEC), 9–12 (1993).

Kiyama M, Honmyo T, Nakamura T, Takano M and Takada T: The Formation of  $\alpha\text{-Fe}_2\text{O}_3$  and  $\text{BaFe}_{12}\text{O}_{19}$  in the Presence of Iron (II) Hydroxide and Nitrates with or without Ba (II), *Bull. Inst. Chem. Res., Kyoto Univ.*, **71**, 81–85 (1993).

Bando Y, Terashima T, Shimura K, Daitoh Y, Matsuda Y and Komiyama S: Microstructure and Transport Properties of One-Unit-Cell YBCO layer, *Chinese Journal of Physics*, **31**, 903–911 (1993).

Saitoh T, Bocquet A E, Mizokawa T, Namatame H, Fujimori A, Abbate M, Takeda Y and Takano M: Photoemission and X-Ray Absorption Study of  $\text{La}_{1-x}\text{Sr}_x\text{MnO}_3$ , *Jpn. J. Appl. Phys.*, **32**, 258–260 (1993).

Nakanishi M, Hashizume H, Terashima T, Bando Y, Michikami O, Maeyama S and Oshima M: Structure of the Growth Interface of Y-Ba-Cu-O Analogs on  $\text{SrTiO}_3$  (001) Substrates, *Phys. Rev. B*, **48**, 10524–10529 (1993).

Matsuda Y, Komiyama S, Onogi T, Terashima T, Shimura K and Bando Y: Thickness Dependence of the Kosterlitz-Thouless Transition in Ultrathin  $\text{YBa}_2\text{Cu}_3\text{O}_{7-\delta}$  Films, *Phys. Rev. B*, **48**, 10498–10503 (1993).

Takeda Y, Mukai Y, Imanishi N, Yamamoto O, Takano M, Azuma M, Hiroi Z and Bando Y: Synthesis of Copper Oxide Superconductors under High Oxygen Pressure—Comparison with Electrochemical Oxidation Method—, in Proceedings of 1993 Powder Metallurgy World Congress, July 12–15, 1993, Kyoto, Japan (ed. Bando Y and Kosuge K), Japan Society of Powder and Powder Metallurgy, 1291–1294 (1993).

Kusano Y, Nanba T, Takada J, Ikeda Y, Hiroi Z, Takano M and Mazaki H: Chemical and Mechanical Stability of the High- $T_c$  Phase in the Bi-Pb-Sr-Ca-Cu-O System. in Proceedings of 1993 Powder Metallurgy World Congress, July 12–15, 1993, Kyoto, Japan (ed. Bando Y and Kosuge K), Japan Society of Powder and Powder Metallurgy, 1298–1301 (1993).

Takada J, Niinae T, Endo K, Kusano Y, Nanba T, Ikeda Y, Hiroi Z, Takano M and Mazaki H: Effect of Li Addition of the Low- $T_c$  Phase in the Bi-Sr-Ca-Cu-O System. in Proceedings of 1993 Powder Metallurgy World Congress, July 12–15, 1993, Kyoto, Japan (ed. Bando Y and Kosuge K), Japan Society of Powder and Powder Metallurgy, 1302–1305 (1993).



- Kusano Y, Nanba T, Takada J, Ikeda Y and Takano M: Thermal Stability of the Bi-2223 Phase, in Proceedings of the 10th Japan-Korea Seminar on Ceramics, Oct. 27–29, 1993, Nagasaki, Japan, 427–430 (1993).
- Kusano Y, Nanba T, Takada J, Ikeda Y, Takano M and Takeda Y: Phases and their Relations in the  $\text{BiO}_{1.5}\text{-SrO}(\text{SrCO}_3)\text{-CuO}$  System at 720°C, *Funtai oyobi Funmatsu Yakin*, **40**, 1049–1052 (1993) (in Japanese).
- Kobayashi N, Fukuhara M, Doi A, Takada T, Kusano Y, Takada J, Ikeda Y and Takano M: Formation of the High- $T_c$  Phase in Bi-2223 System in Various Atmospheres—Effect of  $\text{O}_2$ -Partial Pressure—, *Funtai oyobi Funmatsu Yakin*, **40**, 1053–1056 (1993) (in Japanese).
- Kusano Y, Tanba T, Takada J, Ikeda Y, Takano M and Egi T: Chemical Stability of the Bi-2223 Phase, *Funtai oyobi Funmatsu Yakin*, **40**, 1057–1060 (1993) (in Japanese).
- Niinae T, Takada J, Ikeda Y and Bando Y: Mechanical Grinding and Reforming Process of the Bi-2201 Phase (II)—Comparing the Various Bi-2201 Solid Solutions—, *Funtai oyobi Funmatsu Yakin*, **40**, 1065–1068 (1993) (in Japanese).
- Terashima T and Bando Y: Growth of Ferroelectric Ultrathin Films, *Electronic Ceramics*, **24**, 37–41 (1993) (in Japanese).
- Takano M, Fujii T and Bando Y: Characterization of Epitaxial Iron Oxide Films by Conversion Electron Mössbauer Spectroscopy, in New Functionality Materials, Synthetic Process and Control of Functionality Materials (ed. Tsuruta T, Doyama M and Seno M), *Elsevier Science Pub. B.V., Amsterdam*, C 745–750 (1993).
- Hiroi Z, Azuma M, Takeda Y and Takano M: Curpic Oxide Superconductors in the Sr-Cu-O System. in *Advances in Superconductivity VI: Proceedings of the 6th International Symposium on Superconductivity (ISS '93)*, Oct. 26–29, 1993, Hiroshima, Japan (ed. Fujita T and Shiohara Y), *Springer-Verlag, Tokyo*, **1**, 285–290 (1994).
- Kiyama M, Honmyo T, Nakamura T, Takano M and Takada T: The Formation of  $\text{SrFe}_{12}\text{O}_{19}$  in the Presence of  $\text{Fe}(\text{OH})_2$ , *Bull. Inst. Chem. Res., Kyoto Univ.*, **71**, 393–397 (1994).
- Nishijima M, Takeda Y, Imanishi N, Yamamoto O and Takano M: Li Deintercalation in Lithium Transition Metal Nitride,  $\text{Li}_3\text{FeN}_2$ , *Ceramic Transactions*, **41**, 253–261 (1994).
- Terauchi H, Yoneda Y, Watanaba Y, Kasatani H, Sakaue K, Kamigaki K, Iijima K, Yano Y, Terashima T and Bando Y: Epitaxial  $\text{BaTiO}_3$  Crystals, *Ferroelectrics*, **151**, 21–26 (1994).
- Fujii T, Takano M, Katano R, Isozumi Y and Bando Y: Surface and Interface Properties of Epitaxial  $\text{Fe}_3\text{O}_4$  Films Studied by Mössbauer Spectroscopy, *J. Mag. Mag. Mat.*, **130**, 267–274 (1994).
- Fujii T, Takano M, Katano R, Isozumi Y and Bando Y: Spin-Flip Anomalies in Epitaxial  $\alpha\text{-Fe}_2\text{O}_3$  Films by Mössbauer Spectroscopy, *J. Mag. Mag. Mat.*, **135**, 231–236 (1994).
- Takeda Y, Imayoshi K, Imanishi N, Yamamoto O and Takano M: Preparation and Characterization of  $\text{Sr}_{2-x}\text{La}_x\text{FeO}_4$  ( $0 \leq x \leq 1$ ), *J. Mater. Chem.*, **4**, 19–22 (1994).
- Fujii T, Sakata N, Takada J, Miura Y, Daitoh Y and Takano M: Characteristics of Titanium Oxide Films Deposited by an Activated Reactive Evaporation Method, *J. Mater. Res.*, **9**, 1468–1473 (1994).
- Ishida K, Kitaoka Y, Asayama K, Azuma M, Hiroi Z and Takano M: Spin Gap Behavior in Ladder-Type of Quasi-One-Dimensional Spin ( $S=1/2$ ) System  $\text{SrCu}_2\text{O}_3$ , *J. Phys. Soc. Jpn.*, **63**, 3222–3225 (1994).
- Kanno R, Kubo H, Kawamoto Y, Kamiyama T, Izumi F, Takeda Y and Takano M: Phase Relationship and Lithium Deintercalation in Lithium Nickel Oxides, *J. Solid State Chem.*, **110**, 216–225 (1994).
- Yamamoto T, Kanno R, Takeda Y, Yamamoto O, Kawamoto K and Takano M: Crystal Structure and Metal-Semiconductor Transition of the  $\text{Bi}_{2-x}\text{Ln}_x\text{Ru}_2\text{O}_7$  Pyrochlores ( $\text{Ln}=\text{Pr-Lu}$ ), *J. Solid State Chem.*, **109**, 372–383 (1994).
- Nishijima M, Takeda Y, Imanishi N, Yamamoto O and Takano M: Li Deintercalation and Structural Change in the Lithium Transition Metal Nitride  $\text{Li}_3\text{FeN}_2$ , *J. Solid State Chem.*, **113**, 205–210 (1994).
- Takano M:  $\text{SrCuO}_2$  and Related High-Pressure Phases, *Journal of Superconductivity*, **7**, 49–54 (1994).
- Takeda Y, Nakahara K, Nishijima M, Imanishi N, Yamamoto O, Takano M and Kanno R: Sodium Deintercalation from Sodium Iron Oxide, *Mater. Res. Bull.*, **29**, 659–666 (1994).
- Hiroi Z, Kobayashi N and Takano M: Probable Hole-Doped Superconductivity without Apical Oxygens in  $(\text{Ca}, \text{Na})_2\text{CuO}_2\text{Cl}_2$ , *Nature*, **371**, 139–141 (1994).
- Nakamura M, Sekiyama A, Namatame H, Fujimori A, Yoshihara H, Ohtani T, Misu A and Takano M: Metal-Semiconductor Transition and Luttinger-Liquid Behavior in Quasi-One-Dimensional  $\text{BaVS}_3$  Studied by Photoemission Spectroscopy, *Phys. Rev. B*, **49**, 16191–16201 (1994).
- Aomine T, Nishizaki T, Ichikawa F, Fukami T, Terashima T and Bando Y: Temperature and Magnetic Field-Direction Dependence of Transport Critical Currents in Single-Crystalline Thin Films of  $\text{YBa}_2\text{Cu}_3\text{O}_{7-\delta}$ , *Physica B*, **194–196**, 1613–1614 (1994).
- Kusano Y, Nanba T, Takada J, Egi T, Ikeda Y and Takano M: Segregation and Dissolution Reactions of the 2223 Phase in the Bi, Pb-Sr-Ca-Cu-O System on Annealing in Air, *Physica C*, **219**, 366–370 (1994).
- Shimura K, Daitoh Y, Yano Y, Terashima T, Bando Y, Matsuda Y and Komiyama S: Superconductivity in the Surface of  $\text{YBa}_2\text{Cu}_3\text{O}_{7-\delta}$  Films. Role of the Charge Reservoir Block on the Occurrence of the Superconductivity in One-Unit-Cell Thick  $\text{YBa}_2\text{Cu}_3\text{O}_{7-\delta}$ , *Physica C*, **228**, 91–102 (1994).
- Yamaura K, Hiroi Z and Takano M: High-Pressure Synthesis of an Oxide Carbonate Superconductor with a  $T_c$  of 92 K in the Ca-Sr-Cu-C-O System, *Physica C*, **229**, 183–187 (1994).
- Takahashi H, Mori N, Azuma M, Hiroi Z and Takano M: Effect of Pressure on  $T_c$  of Hole- and Electron-Doped Infinite-Layer Compounds up to 8 GPa, *Physica C*, **227**, 395–398 (1994).



Shimakawa Y, Jorgensen JD, Mitchell JF, Hunter BA, Shaked H, Hinks DG, Hitterman RL, Hiroi Z and Takano M: Structural Study of  $\text{Sr}_2\text{CuO}_{3+\delta}$  by Neutron Powder Diffraction, *Physica, C*, **228**, 73–80 (1994).

Hiroi Z: High-Pressure Synthesis and HRTEM Characterization of Oxide Superconductors. in Proceedings of the NIRIM International Symposium on Advanced Materials '94, March 13–17, 1994, Tsukuba, Japan (ed. Kamo M, Kanda H, Matsui Y and Sekine T), National Institute for Research in Inorganic Materials, 46–51 (1994).

Shimura K, Terashima T and Bando Y: Microstructures and Superconductivity of Ultrathin  $\text{YBa}_2\text{Cu}_3\text{O}_7$  Films, *Funtai oyobi Funmatsu Yakin*, **41**, 365–369 (1994) (in Japanese).

Ikeda Y, Sano Y, Bando Y, Niinae T and Takada J: Consideration of  $\text{Bi}_2\text{CuO}_4$  in the  $\text{Bi}_2\text{O}_3$ -CuO System, *Funtai oyobi Funmatsu Yakin*, **41**, 384–387 (1994) (in Japanese).

Kusano Y, Nanba T, Takada J, Ikeda Y and Takano M: Effect of Heating Atmosphere on Segregation and Dissolution of the Pb-Compound in the Bi-2223 Phase, *Funtai oyobi Funmatsu Yakin*, **41**, 388–391 (1994) (in Japanese).

Niinae T, Kusano Y, Takada J, Ikeda Y and Bando Y: The Precipitation of the Pb-Compounds from Pb-Substituted Bi-2201 Phase—Comparison of Precipitation Behavior in the 2201 and the 2223 Phases—, *Funtai oyobi Funmatsu Yakin*, **41**, 392–395 (1994) (in Japanese).

Takada J, Nagae M, Kusano Y, Nanba T, Ikeda Y and Takano M: Mechanical Grinding and Reforming Process of the Pb-Substituted 2223 Phase, *Funtai oyobi Funmatsu Yakin*, **41**, 396–399 (1994) (in Japanese).

Kobayashi N, Fukuhara M, Doi A, Takada T, Takada J and Ikeda Y: Formation of the Pb-Rich 2212 Phase, *Funtai oyobi Funmatsu Yakin*, **41**, 400–403 (1994) (in Japanese).

Masada K, Kobayashi N, Doi A, Takada T, Takada J and Ikeda Y: Change of the Bi-2223 Phase by Repeat of Mechanical Grinding and Heat Treatment, *Funtai oyobi Funmatsu Yakin*, **41**, 404–407 (1994) (in Japanese).

Bando Y: Epitaxy in Oxides and their Interface, *Hyomen Kagaku*, **15**, 79–84 (1994) (in Japanese).

Ikeda Y: Phase Diagram of Superconducting Oxides, *Funtai oyobi Funmatsu Yakin*, **41**, 377–383 (1994) (in Japanese).

Takano M: Cupric Oxide Superconductors: Where are Rare Earth Elements, *Kidorui*, 29–40 (1994) (in Japanese).

Bando Y: High- $T_c$  Superconducting Ultrathin Films, *Odoroki no Materialu, Dainippon Tosho*, **19**, 101–122 (1994) (in Japanese).

Takano M, Takeda Y and Ohtaka O: in High Pressure Synthesis of Solids. Encyclopedia of Inorganic Chemistry (ed. King RB), John Wiley & Sons Ltd., England, **3**, 1372–1386 (1994).

#### IV. Amorphous Materials

Kim SH, Yoko T and Sakka S: Linear and Nonlinear Optical Properties of  $\text{TeO}_2$  Glasses, *J. Am. Ceram. Soc.*, **76**, 2486–2490 (1993).

Hayakawa S, Yoko T and Sakka S:  $^{51}\text{V}$  NMR Studies of Crystalline Divalent Metal Vanadates and Divanadates, *Bull. Chem. Soc. Jpn.*, **66**, 3393–3400 (1993).

Sakka S, Aoki K, Kozuka H and Yamaguchi J: Sol-Gel Synthesis of Silica Gel Disc as Applied to Supports of Organic Molecules with Optical Functions, *J. Mater. Sci.*, **28**, 4607–4614 (1993).

Sakka S, Kozuka H and Adachi T: Preparation of Porous Materials by the Sol-Gel Method, *Ceram. Trans.*, **31**, 27–40 (1993).

Fujihara S, Kozuka H, Yoko T and Sakka S: Superconductivity of  $\text{La}_{2-x}\text{Sr}_x\text{CuO}_4$  with High Strontium Concentration by Sulfur Doping, *J. Mater. Sci.*, **28**, 3874–3878 (1993).

Hashimoto T, Yoko T and Sakka S: Third-Order Nonlinear Optical Properties of Sol-Gel Derived  $\text{FeTiO}_3$  Thin Films, *Bull. Inst. Chem. Res., Kyoto Univ.*, **71**, 420–429 (1994).

Hashimoto T, Yoko T and Sakka S: Sol-Gel Preparation and Third-Order Nonlinear Optical Properties of  $\text{TiO}_2$  Thin Films, *Bull. Chem. Soc. Jpn.*, **67**, 653–660 (1994).

Miyaji F, Yoko T and Sakka S: Structure of Sodium Gallotitanate Glass in Relation to Glass Formation, *J. Ceram. Soc. Jpn.*, **102**, 247–251 (1994).

Miyaji F, Yoko T, Jin J, Sakka S, Fukunaga T and Misawa M: Neutron and X-Ray Diffraction Studies of  $\text{PbO-Ga}_2\text{O}_3$  and  $\text{Bi}_2\text{O}_3\text{-Ga}_2\text{O}_3$  Glasses, *J. Non-Cryst. Solids*, **175**, 211–223 (1994).

Hayakawa S, Yoko T and Sakka S: Glass Transition and Crystallization Behavior of Binary Divalent Metal Vanadate Glasses, *Bull. Inst. Chem. Res., Kyoto Univ.*, **71**, 411–419 (1994).

Hayakawa S, Yoko T and Sakka S: Structural Studies on Alkaline Earth Vanadate Glasses (Part 1)— $^{51}\text{V}$  NMR Spectroscopic Study—, *J. Ceram. Soc. Jpn.*, **102**, 530–536 (1994).

Hayakawa S, Yoko T and Sakka S: Structural Studies on Alkaline Earth Vanadate Glasses (Part 2)—IR Spectroscopic Study—, *J. Ceram. Soc. Jpn.*, **102**, 522–529 (1994).

Hayakawa S, Yoko T and Sakka S:  $^{51}\text{V}$  NMR Studies of Crystalline Monovalent and Divalent Metal Metavanadates, *J. Solid State Chem.*, **112**, 329–339 (1994).

Jin J, Yoko T, Miyaji F, Sakka S, Fukunaga T and Misawa M: Neutron Diffraction and Solid-State MAS-NMR Studies of the Structure of Y-Al-Si-O-N Oxynitride Glasses, *Phil. Mag.*, **B70**, 191–203 (1994).

Jin J, Yoko T, Miyaji F and Sakka S: Incorporation of Nitrogen in Alkaline Earth Aluminate Glasses, *Bull. Inst. Chem. Res., Kyoto Univ.*, **71**, 430–436 (1994).

Kozuka H and Sakka S: Formation of Silica Gels Composed of Micrometer-Sized Particles by the Sol-Gel Method, in *Advances in Chemistry Series*, No. 234, Colloid Chemistry of Silica ed. by H.E. Bargna, American Chemical Society, Washington D.C., 1994, 129–141.

Innocenzi P, Kozuka H and Sakka S: Preparation of Coating Films Doped with Gold Metal Particles from Methyl-



triethoxysilane-Tetraethoxysilane Solutions, *J. Sol-Gel Sci. Techn.*, **1**, 305–318 (1994).

Kozuka H, Zhao G and Sakka S: Control of Optical Properties of Gel-Derived Oxide Coating Films Containing Fine Metal Particles, *J. Sol-Gel Sci. Techn.*, **2**, 741–744 (1994).

Sakka S, Kozuka H and Zhao G: Sol-Gel Preparation of Metal Particle/Oxide Nanocomposites, *SPIE*, **2288**, 108–119 (1994).

Fujihara S, Kozuka H, Yoko T and Sakka S: Mechanism of Formation of  $\text{YBa}_2\text{Cu}_3\text{O}_8$  Superconductor in the Sol-Gel Synthesis, *J. Sol-Gel Sci. Techn.*, **1**, 133–139 (1994).

Fujihara S, Kozuka H and Yoko T: Structure, Oxygen Deficiency and Electrical Properties of  $\text{Nd}_{1-x}\text{Y}_x\text{NiO}_{3-y}$  ( $x=0, 0.1$ ) Prepared by Sol-Gel Method, *J. Ceram. Soc. Jpn.*, **102**, 1005–1009 (1994).

## FUNDAMENTAL MATERIAL PROPERTIES

### I. Molecular Rheology

Hwang E-J, Inoue T and Osaki K: Viscoelasticity and Birefringence of Amorphous Polyarylates I, *Polymer (Korea)*, **17**, 249–259 (1994) (in Korean).

Hwang E-J, Inoue T and Osaki K: Viscoelasticity of Some Engineering Plastics Analyzed with the Modified Stress-Optical Rule, *Polym. Eng. Sci.*, **34**, 135–140 (1994).

Hwang E-J, Inoue T, Osaki K and Takano A: Viscoelasticity and Birefringence of Poly(2-vinylnaphthalene), *Nihon Reoroji Gakkaishi*, **22**, 192–134 (1994) (in Japanese).

Inoue T, Takiguchi O, Osaki K, Kohara T and Natsuume T: Dynamic Birefringence of Amorphous Polyolefins I. Measurements on Poly[1-ethyl-5-methyl-octahydro-4, 7-metano-<sup>1</sup>H-indene-12, 3-diyl], *Polym. J.*, **26**, 133–139 (1994).

Osaki K, Inoue T, Hwang E-J, Okamoto H and Takiguchi O: Dynamic Birefringence of Amorphous Polymers, *J. Non-Crystalline Solids*, **172–174**, 838–849 (1994).

Osaki K: On the Damping Function of Shear Relaxation Modulus for Entangled Polymers, *Rheol. Acta*, **32**, 429–437 (1993).

Inoue T and Osaki K: Rheological Properties of Poly(vinyl alcohol)/Sodium Borate Aqueous Solutions, *Rheol. Acta*, **32**, 550–555 (1993).

Osaki K, Inoue T and Ahn K H: Shear and Normal Stresses of a Poly(vinyl alcohol)/Sodium Borate Aqueous Solution at the Start of Shear Flow, *J. Non-Newtonian Fluid Mech.*, **54**, 109–120 (1994).

Ahn K H and Osaki K: A Network Model for Predicting the Shear Thickening Behavior of a Poly(vinyl alcohol)/Sodium Borate Aqueous Solution, *J. Non-Newtonian Fluid Mech.*, **55**, 215–227 (1994).

Nemoto N, Watanabe Y, Koike A and Osaki K: Dynamic Viscoelasticity of End-Linking  $\alpha, \omega$ -Dihydroxyl Polybutadiene Solutions near the Gel Point, *Bull. Inst. Chem. Res., Kyoto Univ.*, **71**, 437–444 (1993).

Koike A, Yamamura T and Nemoto N: Dynamic Light Scattering of CTAB: NaSal Threadlike Micelles in the Semidilute Regime. II. Effect of Surfactant Concentration, *Colloid Polym. Sci.*, **272**, 955–961 (1994).

Koike A, Nemoto N, Takahashi M and Osaki K: Dynamic Viscoelasticity of End-Linking  $\alpha, \omega$ -Dimethyl Silyl Poly (Propylene Oxide) Solutions near the Gel Point, *Polymer.*, **35**, 3005–3010 (1994).

Kuwahara M, Nemoto N, Hirayama T and Osaki K: Viscoelasticity of CTAB: NaSal/W Detergent Micelles. Salt and Temperature Effects, *Nihon Reoroji Gakkaishi*, **22**, 57–62 (1994) (in Japanese).

### II. Polymer Materials Science

Imai M, Kaji K and Kanaya T: Orientational Fluctuations of Poly(ethylene terephthalate) during the Induction Period of Crystallization, *Phys. Rev. Lett.*, **71**, 4163–4165 (1993).

Kanaya T, Kawaguchi T and Kaji K: Low-energy Excitation and Fast Motion near  $T_g$  in Amorphous cis-1,4-Polybutadiene, *J. Chem. Phys.*, **98**, 8262–8270 (1993).

Kanaya T, Nishida K and Kaji K: Structure of Polyelectrolyte Solutions, *Kobunshi Kako*, **42**, 432–443 (1993) (in Japanese).

Kawakatsu T, Kawasaki K, Furusaka M, Okabayashi H and Kanaya T: Late Stage Dynamics of Phase Separation Processes of Binary Mixtures Containing Surfactants, *J. Chem. Phys.*, **99**, 8200–8217 (1993).

Kanaya T: Light Scattering from Non-Ergodic Polymer Systems, *Kobunshi*, **42**, 982–983 (1993) (in Japanese).

Kanaya T, Patkowski A, Fischer E W, Seils J, Glaeser H and Kaji K: Light Scattering Studies on Long-range Density Fluctuations in a Glass-forming Polymer, *Acta Polym.*, **45**, 137–142 (1994).

Kanaya T and Kaji K: Dynamics of Glass Transition in Polymers, *Solid State Physics (Kotai Butsuri)*, **29**, 303–313 (1994) (in Japanese).

Imai M and Kaji K: Crystallization of Polymers—When entangled one-dimensional chain molecules are incorporated into crystal lattices, *Hyomen (Surface)*, **32**, 436–445 (1994) (in Japanese).

Kanaya T: Long-range Fluctuations in Glass-forming Polymers, *Kagai Kobunshi Kenkyu*, **40**, 132–135 (1994) (in Japanese).

Kanaya T, Kawaguchi T and Kaji K: Low Energy-excitation and Fast Motion near  $T_g$  in Amorphous Polymers, *J. Non-Cryst. Solids*, **172/174**, 327–335 (1994).

Buchenau U, Schönfeld C, Richter D, Kanaya T, Kaji K and Wehrmann R: Neutron Scattering Study of the Vibration-Relaxation Crossover in Amorphous Polycarbonates, *Phys. Rev. Lett.*, **73**, 2344–2347 (1994).

Kanaya T, Ohkura T, Kaji K, Furusaka M and Misawa M: Structure of Poly(vinyl alcohol) Gels Studied by Wide- and Small-Angle Neutron Scattering, *Macromolecules*, **27**, 5609–5615 (1994).



Kawakatsu T, Kawasaki K, Furusaka M, Okabayashi H and Kanaya T: Theories and Computer Simulations of Self-assembling Surfactant Solutions, *J. Phys.: Condens. Matter*, **6**, 6385–6408 (1994).

Kojima Y, Usuki A, Kawasumi M, Okada A, Kurauchi T, Kamigaito O and Kaji K: Fine Structure of Nylon-6-Clay Hybrid, *J. Polym. Sci., Part B: Polym. Phys.*, **32**, 625–630 (1994).

Imai M, Kaji K and Kanaya T: Structural Formation of Poly(ethylene terephthalate) during the Induction Period of Crystallization. 3. Evolution of Density Fluctuations to Lamellar Crystal, *Macromolecules*, **27**, 7103–7108 (1994).

### III. Molecular Motion Analysis

Yamamoto H and Horii F: In Situ Crystallization of Bacterial Cellulose 1. Influences of Polymeric Additives, Stirring and Temperature on the Formation Celluloses  $I_\alpha$  and  $I_\beta$  as Revealed by Cross Polarization/Magic Angle Spinning (CP/MAS)  $^{13}\text{C}$  NMR Spectroscopy, *Cellulose*, **1**, 57–66 (1994).

Horii F: Collections of Practical Technologies for Analyses of Polymer Materials, *Gijutsujoho-Kyokai*, 352–371 (1994) (in Japanese).

Kai A, Xu P, Horii F and Hu S: CP/MAS  $^{13}\text{C}$  NMR Study on Microbial Cellulose-Fluorescent Brightener Complexes, *Polymer*, **35**, 75–79 (1994).

Kitamaru R, Horii F, Zhu Q, Bassett D C and Olley R H: The Phase Structure of High-Pressure-Crystallized Polyethylene, *Polymer*, **35**, 1171–1181 (1994).

Hu S, Tsuji M and Horii F: Phase Structure of Poly(vinyl alcohol) Single Crystals as Revealed by High-Resolution Solid-State  $^{13}\text{C}$  NMR Spectroscopy, *Polymer*, **35**, 2516–2522 (1994).

Horii F: Solid NMR Analyses of the Crystal Structure of Native Cellulose, *Kagaku-to-Seibutsu*, **32**, 361–366 (1994) (in Japanese).

Tsunashima Y and Kawamata Y: Dynamics of Polystyrene Subchains of a Styrene-Methyl Methacrylate Diblock Copolymer in Solution Measured by Dynamic Light Scattering. 2. Semidilute Solution Region, *Macromolecules*, **27**, 1799–1807 (1994).

Tsunashima Y: Polymer Solutions. Polymer Science One Point-3, *The Society of Polymer Science (Japan)*, Ed., Kyoritsu (1993) (in Japanese).

Nakanishi K, Yamasaki Y, Kaji H, Soga N, Inoue T and Nemoto N: Phase Separation Kinetics in Silica Sol-Gel System Containing Polyethylene Oxide. I. Initial Stage, *J. Sol-Gel Sci. Technol.*, **2**, 227–231 (1994).

Kaji H, Nakanishi K, Soga N, Inoue T and Nemoto N: In Situ Observation of Phase Separation Processes in Gelling Alkoxy-Derived Silica System by Light Scattering Method, *J. Sol-Gel Sci. Technol.*, **3**, 169–188 (1994).

Jia L, Fu H, Xu J, Hirai A and Odani H: Studies on the Sulfonation of Poly(phenylene oxide) (PPO) and Permeation Behavior of Gases and Water Vapor through Sulfonated PPO Membranes. V. Sorption Behavior of Water Vapor in PPO

and Sulfonated-PPO Membranes, *J. Appl. Polym. Sci.*, **52**, 29–37 (1994).

Hirai A and Odani H: Sorption and Transport of Water Vapor in Alginic Acid, Sodium Alginate, and Alginate-Cobalt Complex Films. *J. Polym. Sci. Part B: Polym. Phys.*, **32**, 2329–2337 (1994).

Hirai A, Yamamoto H, Tsuji M and Horii F: Electron Microscopic Observation of the Formation Processes of the Microfibrils and the Composite Crystals for Bacterial Cellulose, in *Proceedings of '94 Cellulose R & D*, pp. 41–42 (1994).

Yamamoto H, Hirai A and Horii F: In Situ Crystallization of Bacterial Cellulose, Effects of Polymer Additives on the Mass Fractions of Cellulose  $I_\alpha$  and  $I_\beta$ , in *Proceedings of '94 Cellulose R & D*, pp. 43–44 (1994).

## ORGANIC MATERIALS CHEMISTRY

### I. Polymeric Materials

Kawabata K, Fukuda T, Tsujii Y and Miyamoto T: Orientation-Dependent Interactions in Polymer Systems. 3. Segmental Orientation in Poly(2,6-dimethyl-1,4-phenylene oxide)/Polystyrene Miscible Blends, *Macromolecules*, **26**, 3980–3985 (1993).

Ma Y-D, Won Y-C, Kubo K and Fukuda T: Propagation and Termination Processes in the Free-Radical Copolymerization of Methyl Methacrylate and Vinyl Acetate, *Macromolecules*, **26**, 6766–6770 (1993).

Kokubo T, Tanahashi M, Yao T, Minoda M, Miyamoto T, Nakamura T and Yamamuro T: Apatite-Polymer Composites Prepared by Biomimetic Process: Improvement of Adhesion of Apatite to Polymer by Glow-Discharge Treatment, *Bioceramics*, **6**, 327–332 (1993).

Minoda M, Sawamoto M and Higashimura T: Sequence-Regulated Oligomers and Polymers by Living Cationic Polymerization. III. Synthesis and Reactions of Sequence-Regulated Oligomers with a Polymerizable Group, *J. Polym. Sci., Part A: Polym. Chem.*, **31**, 2789–2797 (1993).

Sato T, Minoda M and Miyamoto T: High-Performance Dielectric Polymer from Cellulose Derivatives, *Cellulosics: Chemical, Biochemical and Materials Aspects*, Kennedy J F et al. Ed., Ellis Horwood, 1993, 403–408.

Tsujii Y, Itoh T, Ito S and Miyamoto T: Langmuir-Blodgett Films from Cellulose Ester Derivatives, *Cellulosics: Chemical, Biochemical and Materials Aspects*, Kennedy J F et al. Ed., Ellis Horwood, 1993, 483–488.

Mizutani C, Onogi Y, Inagaki H and Miyamoto T: Chemical Modifications of Cotton Fibers for Improved Water Absorbency, *Cellulosics: Pulp, Fiber and Environmental Aspects*, Kennedy J F et al. Ed., Ellis Horwood, 1993, 236–241.

Miyamoto T, Sato T, Tsujii Y and Fukuda T: Reversible Gelation of Short-Chain O-(2,3-Dihydroxypropyl)cellulose Borax Solutions, *Kasen-Kouenshu*, **50**, 9–16 (1993) (in Japanese).

Donkai N, Schmidt M and Miyamoto T: Lyotropic Mesophase of Imogolite: Molecular Weight Fractionation and Polydispersity Effect, *Makromol. Chem., Rapid Commun.*, **14**, 611–617 (1993).



Miyamoto T and Minoda M: Structural Characteristics of Cellulosic Fibers and Their New Developments, *Senshoku-Kougyou*, **41**, 534–542 (1993) (in Japanese).

Fukuda T: Kinetics of Free Radical Copolymerization, *Koubunshi*, **42**, 992–995 (1993) (in Japanese).

Miyamoto T and Tsujii Y: Recent Progress of Cellulosic Materials, *Hyomen*, **31**, 818–825 (1993) (in Japanese).

Minoda M and Miyamoto T: Chemical Modification of Oligosaccharides and Their Application, *Kagaku-Kougyou*, **45**, 489–497 (1994) (in Japanese).

Tsujii Y, Miyamoto T and Sato T: Preparation and Electric Properties of Highly Dielectric Cellulose Derivatives, *Senryou-to-Yakuhin*, **39**, 193–204 (1994) (in Japanese).

Ma Y-D, Takada A, Sugiura M, Fukuda T, Miyamoto T and Watanabe J: Thermotropic Liquid Crystals Based on Oligosaccharides. *n*-Alkyl 1-O- $\beta$ -D-Cellobiosides, *Bull. Chem. Soc. Jpn.*, **67**, 346–351 (1994).

Ito H, Muraoka Y, Umehara R, Shibata Y and Miyamoto T: Shrink-Resistant Properties and Surface Characteristics of Wool Fibers Treated with Multifunctional Epoxides, *Text. Res. J.*, **64**, 440–444 (1994).

Muraoka Y, Ito H, Umehara R, Shibata Y and Miyamoto T: Physical Properties of Wool Treated with Multifunctional Epoxides, *Text. Res. J.*, **64**, 514–518 (1994).

Fukuda T: Molecular Shape and Conformation. *Shin-Koubunshi-Jikkengaku*, **1**, SPSJ Ed., Kyoritsu, 1994, 240–302.

Fukuda T, Takada A and Miyamoto T: Thermotropic Cellulose Derivatives, *Cellulosic Polymers, Blends and Composites*, Gilbert RD Ed., Hanser, Munich, 1994, 47–70.

Takada A, Fujii K, Watanabe J, Fukuda T and Miyamoto T: Chain-Length Dependence of the Mesomorphic Properties of Fully Decanoated Cellulose and Cellooligosaccharides, *Macromolecules*, **27**, 1651–1653 (1994).

Ma Y-D, Kim P-S, Kubo K and Fukuda T: Propagation and Termination Processes in Free Radical Copolymerization of Styrene and Ethyl Acrylate, *Polymer*, **35**, 1375–1381 (1994).

Miyamoto T: Recent Developments in Cellulose Chemistry and Technology, *Cell. Commun.*, **1**, 2–5 (1994) (in Japanese).

Tanahashi M, Yao T, Kokubo T, Minoda M, Miyamoto T, Nakamura T and Yamamuro T: Apatite Formation on Organic Polymers by Biomimetic Process Using Na<sub>2</sub>O-SiO<sub>2</sub> Glasses as Nucleating Agent, *J. Ceram. Soc. Jpn. Int. Ed.*, **102**, 822–829 (1994).

Miyamoto T, Fukuda T and Watanabe J: Origins of Thermotropicity of Cellulose Derivatives, *Kasen-Kouenshu*, **51**, 1–8 (1994) (in Japanese).

Tanahashi M, Yao T, Kokubo T, Minoda M, Miyamoto T, Nakamura T and Yamamuro T: Apatite Coating on Organic Polymers by a Biomimetic Process, *J. Am. Ceram. Soc.*, **77**, 2805–2808 (1994).

Sugiura M, Minoda M, Watanabe J and Miyamoto T: Thermotropic Liquid Crystals Based on Chito-Oligosaccharides.

3. Effects of the Molecular Shape of N,O-Acylated Chito-Oligosaccharides on Discotic Mesomorphism, *Polym. J.*, **26**, 1236–1243 (1994).

Hayashi T, Ito S, Yamamoto M, Tsujii Y, Matsumoto M and Miyamoto T: Thermal Relaxation Process of Stearate LB Films Sandwiched by Chromophoric Polymer LB Layers Studied by the Energy Transfer Method and Transmission Electron Microscopy, *Langmuir*, **10**, 4142–4147 (1994).

## II. High-Pressure Organic Chemistry

Kudo K, Mitsunashi K, Mori S, Komatsu K and Sugita N: Palladium (II)-Catalyzed Cyclocarbonylation of Enol Ester of Acetone. A Novel Synthesis of 1,3-Dioxolan-4-one, *Chem. Lett.*, 1615–1618 (1993).

Tsuiji R, Komatsu K, Takeuchi K, Shiro M, Cohen S and Rabinovitz M: Structural Study on 1-Phenyl- and 1-(2-Naphthyl)-8-tropylionaphthalene Hexafluoroantimonates, *J. Phys. Org. Chem.*, **6**, 435–444 (1993).

Komatsu K, Murata Y, Miyabo A, Takeuchi K and Wan TSM: Chemical Transformation of C<sub>60</sub>. Addition of Carbenes and Cycloaddition of Anthracene, *Fullerene Science and Technology*, **1**, 231–238 (1993).

Takeuchi K, Kitagawa T, Miyabo A, Hori H and Komatsu K: Precise Control of the Formation of a Covalent and an Ionic Bond in Carbocation-Carbanion Combination Reactions, *J. Org. Chem.*, **58**, 5802–5810 (1993).

Nishinaga T, Komatsu K, Sugita N, Lindner HJ and Richter J: First X-Ray Structure of a Cyclooctatetraene Cation Radical: Hexachloroantimonate of the Tetrakis(bicyclo[2.2.2]octeno)-cyclooctatetraene Cation Radical, *J. Am. Chem. Soc.*, **115**, 11642–11643 (1993).

Komatsu K, Kagayama A, Murata Y, Sugita N, Kobayashi K, Nagase S and Wan TSM: Reaction of C<sub>60</sub> with Chlorophenyldiazirine. Spectral and Electronic Properties of the C<sub>60</sub>-Chlorophenylcarbene 1:1 Adduct, *Chem. Lett.*, 2163–2166 (1993).

Komatsu K, Murata Y, Sugita N, Takeuchi K and Wan TSM: Use of Naphthalene as a Solvent for Selective Formation of the 1:1 Diels-Alder Adduct of C<sub>60</sub> with Anthracene, *Tetrahedron Lett.*, **34**, 8473–8476 (1993).

Kitagawa K, Okazaki T, Komatsu K and Takeuchi K: Solvolysis of [3-<sup>13</sup>C]-4-Homoadamantyl Tosylate. Limited Degeneracy of 4-Homoadamantyl Cation via Multiple Wagner-Meerwein Rearrangement and Vicinal Hydride Shifts under Solvolytic Conditions, *J. Org. Chem.*, **58**, 7891–7898 (1993).

Komatsu K, Murata Y, Sugita N, Wan TSM: Ene Reaction as a New Method for Functionalization of Fullerene C<sub>60</sub>, *Chem. Lett.*, 635–636 (1994).

Komatsu K, Murata Y, Takimoto N, Mori S, Sugita N and Wan TSM: Synthesis and Properties of the First Acetylene Derivatives of C<sub>60</sub>, *J. Org. Chem.*, **59**, 6101–6102 (1994).

Kagayama A, Komatsu K, Nishinaga T, Takeuchi K and Kabuto C: A Novel Carbocation Composed of Two Tris(bicyclo[2.2.2]octeno) tropylium Units Connected by a Triple Bond: Synthesis, Structure, and Properties, *J. Org. Chem.*, **59**, 4999–5004 (1994).



Komatsu K, Nishinaga T, Maekawa N, Kagayama A and Takeuchi K: Syntheses, Properties, and Redox Behaviors of 7-Phenyl-1,2:3,4:5,6-tris(bicyclo[2.2.2]octeno)propylium Ion and the Dications Composed of Two 1,2:3,4:5,6-Tris(bicyclo[2.2.2]octeno)propylium Units Connected by para- and meta-Phenylene Spacer, *J. Org. Chem.*, **59**, 7316–7321 (1994).

Komatsu K, Nishinaga T, Takeuchi K, Lindner H J and Richter J: A Polycyclic Pentamer of Bicyclo[2.2.2]octene. A Hydrocarbon Molecule with a Long C-C Single Bond Connecting Two Cofacially Disposed Cyclopentadiene Rings, *J. Org. Chem.*, **59**, 7322–7328 (1994).

Nishinaga T, Komatsu K and Sugita N: Tetrakis(bicyclo [2.2.2]-octeno)cyclooctatetraene Dication: A Stable COT Dication with a Tub Structure, *J. Chem. Soc., Chem. Commun.*, 2319–2320 (1994).

Komatsu K: Organochemical Application of Fullerenes, *Nikkei Science*, **24**, 6–9 (1994) (in Japanese).

## SYNTHETIC ORGANIC CHEMISTRY

### I. Synthetic Design

Toshimitsu A, Abe H, Hirosawa C and Tamao K: Conversion of Chiral Oxiranes to Chiral Aziridines with Retention of Configuration by Way of "Chiral Episulfonium Ions" and Reactions of the Aziridines with Grignard Reagents, *J. Chem. Soc., Perkin Trans. 1*, 3465 (1994).

Tamao K, Yamaguchi S and Shiro M: Oligosiloles: First Synthesis Based on a Novel Endo-Endo Mode Intramolecular Reductive Cyclization of Diethynylsilanes, *J. Am. Chem. Soc.*, **116**, 11715 (1994).

Toshimitsu A, Hirosawa C and Tamao K: Retention of Configuration in the Ritter-type Substitution Reaction of Chiral  $\beta$ -Arylthio Alcohols through the Anchimeric Assistance of the Arylthio Group, *Tetrahedron*, **50**, 8997 (1994).

Tamao K, Nagata K, Ito Y, Maeda K and Shiro M: (Dichloromethyl) dimethylsilyl Group as a Hydroxymethylidene Diradical Equivalent: Radical Annulation of Dienols and Its Application to the Stereoselective Synthesis of cis- and trans-Hydrindan Ring Systems, *Synlett*, 257 (1994).

Tamao K, Kawachi A, Nakagawa Y and Ito Y: Electronic Spectra of (Amino) (phenyl) disilanes, *J. Organomet. Chem.*, **473**, 29 (1994).

Tamao K, Yamaguchi S and Ito Y: Synthesis and Properties of Thiophene-Cyclopentadiene Cooligomers, *J. Chem. Soc., Chem. Commun.*, 229 (1994).

Tamao K, Nakagawa Y and Ito Y: Deuterium-Labeling Studies on the Regio- and Stereoselective Intramolecular Hydrosilation of Allyl Alcohols and Allyl amines Catalyzed by Platinum and Rhodium Complexes, *Organometallics*, **12**, 2297 (1993).

Tamao K, Taro Y, Nakagawa Y, Nagata K and Ito Y: Synthesis, Structure and Reactivity of Trisilanes Containing the 8-Dimethylamino-1-naphthyl Group at the Central Silicon Atom. A Novel Nickel- or Palladium-Catalyzed Degradation of Trisilane to Disilane and Silylene Species, *Organometallics*, **12**, 1113 (1993).

### II. Fine Organic Synthesis

Kawabata T, Kiryu Y, Sugiura Y and Fuji K: An Enantiodivergent Synthesis of threo  $\beta$ -Amino Alcohols: Preparation of Key Intermediates for Bestatin and the Related Peptides, *Tetrahedron Lett.*, **34**, 5127–5130 (1993).

Mátyus P, Fuji K and Tanaka K: The Diels-Alder Reaction of Pyridazinones as Dienophiles, *Heterocycles*, **36**, 1975–1978 (1993).

Fuji K, Tanaka K and Miyamoto H: Chiral Piperazines as Catalysts for the Enantioselective Addition of Diethylzinc to Aldehydes, *Chem. Pharm. Bull.*, **41**, 1557–1561 (1993).

Li B, Tanaka K, Fuji K, Sun H and Taga T: Three New Diterpenoids from *Tuxus Chinensis*, *Chem. Pharm. Bull.*, **41**, 1672–1673 (1993).

Fuji K: Asymmetric Creation of Quaternary Carbon Centers, *Chem. Rev.*, **93**, 2037–2066 (1993).

Fuji K, Tanaka K, Li B, Shingu T, Sun H and Taga T: Novel Diterpenoids from *Taxus Chinensis*, *J. Nat. Products*, **56**, 1520–1531 (1993).

Miyajima K, Komatsu H, Sun H, Aoki H, Handa H, Xu H, Fuji K and Okada S: Effects of Cholesterol on the Miscibility of Synthetic Glucosamine Diesters in Lipid Bilayers and the Entrapment of Superoxide Dismutase into the Positively Charged Liposomes, *Chem. Pharm. Bull.*, **41**, 1889–1894 (1993).

Kawabata T and Fuji K: Recent Studies on the Asymmetric Synthesis. 4. Asymmetric Formation of Carbon-Carbon Bonds, *Chem. and Biol.*, **31**, 817–825 (1993) (in Japanese).

Mátyus P, Fuji K and Tanaka K: Efficient and Facile Syntheses of [4,5]-Annelated Pyridazines from 4-Pyridazinecarboxaldehydes, *Heterocycles*, **37**, 171–174 (1994).

Fuji K: Chiral Construction of Quaternary Carbons through Addition-Elimination Process: in Application to the Natural Product Syntheses. Atta-ur-Rahman, Ed., in studies in Natural Product Chemistry; Elsevier: Amsterdam, 631–644 (1994).

Mátyus P, Fuji K and Tanaka K: Density Functional Calculations on Heterocyclic Compounds. Part I. Studies of Protonations of 5- and 6-membered Nitrogen Heterocycles, *Tetrahedron*, **50**, 2405–2414 (1994).

Fuji K, Tanaka K, Ahn M and Mizuchi M: Diastereoselectivity in Addition of Methylmagnesium Halide to Benzoylformate of Chiral 1,1'-Binaphthalene-2,2'-diol Chem, *Pharm. Bull.*, **42**, 957–959 (1994).

Fuji K, Kawabata T, Naniwa Y, Ohmori T and Node M: Enhanced Reactivity of Zinc Enolates Over Lithium Enolates in Asymmetric Nitroolefination Chem, *Pharm. Bull.*, **42**, 999–1001 (1994).

Fuji K, Tanaka K, Abe H, Matsumoto K, Harayama T, Ikeda A, Taga T, Miwa Y and Node M: Diastereoselective Diels-Alder Cycloadditions with Chiral 1-(Alkylsulfanyl)2-nitroalkenes, *J. Org. Chem.*, **59**, 2211–2218 (1994).

Tanaka K, Fuji K, Yokoi T, Shingu T, Li B and Sun H: On the Structures of Six New Diterpenoids, Taxchinins E, H, I, J, K, and Taxchin B, *Chem. Pharm. Bull.*, **42**, 1539–1541 (1994).



Kawabata T and Fuji K: Memory of Chirality Japn, *J. Synth. Org. Chem.*, **52**, 589–595 (1994) (in Japanese).

Mátyus P, Fuji K, Tanaka K, Rohonczy J, Hargitai R and Sohár P: Density Functional Calculations on Heterocyclic Compounds. Part 2. On the Protonation of 4,5-Dichloro-2-methyl-3(2H)-pyridazinone, *Heterocycles*, **38**, 1957–1960 (1994).

Kawabata T, Wirth T, Yahiro K, Suzuki H and Fuji K: Direct Asymmetric  $\alpha$ -Alkylation of Phenylalanine Derivatives Using No External Chiral Sources, *J. Am. Chem. Soc.*, **116**, 10809–10810 (1994).

## BIOORGANIC CHEMISTRY

### I. Bioorganic Reaction Theory

Ohno A, Tsutsumi A, Kawai Y, Yamazaki N, Mikata Y and Okamura M: NAD(P)<sup>+</sup>/NAD(P)H Models. 83. Molecular Asymmetry with a Carbonyl Group: Electronically Controlled Stereochemistry in the Reaction of NAD(P)<sup>+</sup>/NAD(P)H Analogs, *J. Am. Chem. Soc.*, **116**, 8133–8137 (1994).

Ohno A and Kawai Y: Reaction Intermediate of Enzymatic Reaction, *Kagaku*, **49**, 298–299 (1994) (in Japanese).

Kawai Y, Takanobe K, Tsujimoto M and Ohno A: Stereoselective Synthesis of Ethyl (2S, 3S)-Anti-2-Methyl-3-Hydroxybutanoate Mediated by an Oxidoreductase from *Geotrichum candidum*, *Tetrahedron Lett.*, **35**, 147–148 (1994).

Kawai Y, Tsujimoto M, Kondo S, Takanobe K, Nakamura K and Ohno A: Asymmetric Reduction of  $\beta$ -Keto Esters with an Enzyme from Bakers' Yeast, *Bull. Chem. Soc. Jpn.*, **67**, 524–528 (1994).

Kawai Y, Kondo S, Tsujimoto M, Nakamura K and Ohno A: Stereochemical Control in Microbial Reduction. XXIII. Thermal Treatment of Bakers' Yeast for Controlling the Stereoselectivity of Reductions, *Bull. Chem. Soc. Jpn.*, **67**, 2244–2247 (1994).

Ogawa S, Ohara S, Kawai Y and Sato R: Synthesis and Molecular Structure of 3,4,13,14-Tetraselenatricyclo [14.4.0.06,11] Icosa-1 (16),6,8,10,17,19-Hexaene, *Heterocycles*, **38**, 491 (1994).

Yasui S, Shioji K and Ohno A: Reaction of a Cation Radical Generated From Trivalent Phosphorus Compound Through Single-Electron Transfer to Arenediazonium Salt, *Tetrahedron Lett.*, **35**, 2695–2698 (1994).

Yasui S, Shioji K, Ohno A and Yoshihara M: The Catalytic Role of Iodide Ion/Iodine Couple in the Photo-Reduction of 10-Methylacridinium Ion with Diphenylphosphine Oxide, *Chem Lett*, 1393–1396 (1993).

Yasui S, Shioji K, Yoshihara M, Maeshima T and Ohno A: The Arbuzov Reaction of Alkyl Diphenylphosphinites with 10-Methylacridinium Ion. Kinetic Study on the Formation and the Decomposition of Phosphonium Intermediates, *Bull. Chem. Soc. Jpn.*, **66**, 2077–2083 (1993).

Yasui S, Shioji K and Ohno A: Reactivity of a Phosphoranyl Radical Generated by Photoreaction of Phenyl Diphenylphosphinite with 10-Methylacridinium Iodide.  $\alpha$ -Scission VS. Single Electron Transfer, *Heteroatom Chem.*, **5**, 85–90 (1994).

Yasui S, Fujii M, Kawano C, Nishimura Y, Shioji K and Ohno A: Mechanism of Dediazonation of Arenediazonium Salts with Triphenylphosphine and Trialkyl Phosphites. Generation of Cation Radicals from Trivalent Phosphorus Compounds and Their Reactions, *J. Chem. Soc. Perkin Trans.*, **2**, 177–183 (1994).

Kimura T, Maruyama T, Okamura M, Sugiyama T, Ando T and Ohno A: Structural Effect on Chelation Selectivity of Alkaline Earth Metal Ions with Aminopolycarboxylate-Type Chelators, *Bull. Chem. Soc. Jpn.*, **67**, 1615–1621 (1994).

Nakamura K, Takano S and Ohno A: Diastereoselective Reduction of Ethyl  $\alpha$ -Methyl- $\beta$ -Oxobutanoate by Immobilized *Geotrichum candidum* in an Organic Solvent, *Tetrahedron Lett.*, **34**, 6087–6090 (1993).

Uemura M, Nishimura H, Yamada S, Nakamura K and Hayashi Y: Kinetic Resolution of Hydroxymethyl Substituted (Diene) Fe(CO)<sub>3</sub> Complexes by Lipase, *Tetrahedron Lett.*, **34**, 6581–6582 (1993).

Nakamura K, Kondo S, Kawai Y and Ohno A: Stereochemical Control in Microbial Reduction. XXI. Effect of Organic Solvents on Reduction of  $\alpha$ -Keto Esters Mediated by Bakers' Yeast, *Bull. Chem. Soc. Jpn.*, **66**, 2738–2743 (1993).

Nakamura K, Inoue Y and Ohno A: Enantioselective Microbial Oxidation of 1-Arylethanol in an Organic Solvent, *Tetrahedron Lett.*, **35**, 4375–4376 (1994).

Uenishi J, Nishiwaki K, Hata S and Nakamura K: An Optical Resolution of Pyridyl and Bipyridylethanol and A Facile Preparation of Optically Pure Oligopyridines, *Tetrahedron Lett.*, **35**, 7973–7976 (1994).

Hamada H, Nakajima N, Shisa Y, Funahashi M and Nakamura K: Enantioselective Reduction of Ethyl 3-Methyl-2-Oxobutanoate by an Enzymatic System from Callus of *Catharanthus roseus*, *Bioorg. Med. Chem. Lett.*, **4**, 907–910 (1994).

Uemura M, Nishimura H, Yamada S, Hayashi Y, Nakamura K, Ishihara K and Ohno A: Kinetic Resolution of Hydroxymethyl-Substituted (Arene) Cr(CO)<sub>3</sub> and (Diene)Fe(CO)<sub>3</sub> by Lipase, *Tetrahedron: Asymmetry*, **5**, 1673–1682 (1994).

Nakamura K, Kinoshita M and Ohno A: Effect of Solvent on Lipase-Catalyzed Transesterification in Organic Media, *Tetrahedron*, **50**, 4681–4690 (1994).

Nakamura K, Kondo S, Kawai Y, Nakajima N and Ohno A: Purification and Characterization of  $\alpha$ -Keto Ester Reductases from Bakers' Yeast, *Biosci. Biotech. Biochem.*, **58**(12), 2236–2240 (1994).

Nakamura K, Kondo S and Ohno A: Effect of Cyclodextrin on Improvement of Enantioselectivity in the Reduction of Ketopantolactone with Bakers' Yeast, *Bioorg. Med. Chem.*, **2**, 433–437 (1994).

Nakamura K, Kawasaki M and Ohno A: Effect of Substrate Structure on Lipase-Catalyzed Transesterification of  $\omega$ -Substituted 1-Alkanols in Organic Solvents, *Bull. Chem. Soc. Jpn.*, **67**, 3053–3056 (1994).

Nakajima N, Ishihara K, Tsuboi S, Utaka M, and Nakamura K: Differences in Protein Structure and Similarities in Catalytic Function of Two L-Selective Carbonyl Reductases from Bakers' Yeast, *Biosci. Biotech. Biochem.*, **58**(11), 2080–2081 (1994).



## II. Bioactive Chemistry

Nagaoka M, Kuwahara J and Sugiura Y: Alteration of DNA Binding Specificity by Nickel (II) Substitution in Three Zinc (II) Fingers of Transcription Factor Sp1, *Biochem. Biophys. Res. Commun.*, **194**, 1515–1520 (1993).

Tokuyama H, Yamago S, Nakamura E, Shiraki T and Sugiura Y: Photoinduced Biochemical Activity of Fullerene Carboxylic Acid, *J. Am. Chem. Soc.*, **115**, 7918–7919 (1993).

Kawabata T, Kiryu Y, Sugiura Y and Fuji K: An Enantio-divergent Synthesis of three  $\beta$ -Amino Alcohols. Preparation of Key Intermediates for Bestatin and the Related Peptides, *Tetrahedron Lett.*, **34**, 5127–5130 (1993).

Matsumoto T, Okuno Y and Sugiura Y: Specific Interaction between a Novel Enediyne Chromophore and Apoprotein in Macromolecular Antitumor Antibiotic C-1027, *Biochem. Biophys. Res. Commun.*, **195**, 659–666 (1993).

Uesugi M, Kusakabe T and Sugiura Y: Induced-fit Association between DNA and Esperamicin. Importance of Structural Flexibility in Host DNA Duplex, *Nucleic Acids Res. (Sym. Ser.)*, **29**, 89–90 (1993).

Kusakabe T, Maekawa K, Ichikawa A, Uesugi M and Sugiura Y: Conformation-Selective DNA Strand Breaks by Dynemicin. A Molecular Wedge into Flexible Regions of DNA, *Biochemistry*, **32**, 11669–11675 (1993).

Takahashi T, Tanaka H, Hirai Y, Doi T, Yamada H, Shiraki T and Sugiura Y: Syntheses and DNA Cleavage of New Neocarzinostatin-Chromophore Analogues, *Angew. Chem.*, **105**, 1719–1722 (1993).

Yonezawa A and Sugiura Y: Tachyplesin I-induced Inhibition of Sequence-Specific Protein Binding to DNA, *Bull. Inst. Chem. Res. Kyoto Univ.*, **71**, 245–251 (1993).

Otsuka M, Satake H, Sugiura Y, Murakami S, Shibasaki M and Kobayashi S: Restructuring of the Bleomycin Metal Core. Novel Oxygen-Activating Ligands with Symmetrized Structure, *Tetrahedron Lett.*, **34**, 8497–8500 (1993).

Sugiyama T, Ohno M, Shibasaki M, Otsuka M, Sugiura Y, Kobayashi S and Maeda K: Transition Metal Binding Site of Bleomycin. Significance of the  $\beta$ -Aminoalaninamide Appendage in Regulating Oxygen Activation, *Heterocycles*, **37**, 275–282 (1994).

Kushida T, Uesugi M, Sugiura Y, Kigoshi H, Tanaka H, Hirokawa J, Ojika M and Yamada K: DNA Damage by Ptaquiloside, a Potent Bracken Carcinogen. Detection of Selective Strand Breaks and Identification of DNA Cleavage Products, *J. Am. Chem. Soc.*, **116**, 479–486 (1994).

Sugiyama T, Ohno M, Shibasaki M, Otsuka M, Sugiura Y, Kobayashi S and Maeda K: On the Mechanism of Enzymatic Inactivation of Bleomycin. The  $\beta$ -Aminoalaninamide Moiety as an Enzyme-Dependent Molecular Switch, *Bioorg. Med. Chem. Lett.*, **4**, 705–710 (1994).

Nagaoka M, Hagihara M, Kuwahara J and Sugiura Y: A Novel Zinc Finger-Based DNA Cutter: Biosynthetic Design and Highly Selective DNA Cleavage, *J. Am. Chem. Soc.*, **116**, 4085–4086 (1994).

Okuno Y, Otsuka M and Sugiura Y: Computer Modeling Analysis for Enediyne Chromophore-Apoprotein Complex of Macromolecular Antitumor Antibiotic C-1027, *J. Med. Chem.*, **37**, 2266–2273 (1994).

## III. Molecular Clinical Chemistry

Miyahara T, Ueda K, Akaboshi M, Shimada Y, Imamura M and Utsumi H: Hyperthermic Enhancement of Cytotoxicity and Increased Uptake of cis-Diaminedichloro-platinum (II) in Cultured Human Esophageal Cancer Cells, *Jap. J. Cancer Res.*, **84**, 336–340 (1993).

Ikemoto M, Ishida A, Tsunekawa S, Ozawa K, Kasai Y, Totani, M and Ueda, K: Enzyme Immunoassay of Liver-type Arginase and Its Potential Clinical Applications, *Clin. Chem.*, **39**, 794–799 (1993).

Tanaka S, Nakamura S, Kimura J and Ueda K: Age-related Change in the Proportion of Amyloid Precursor Protein mRNAs in the Gray Matter of Cerebral Cortex, *Neurosci. Lett.*, **163**, 16–21 (1993).

Urakami K, Takahashi K, Okada A, Oshima T, Adachi Y, Nakamura S, Kitaguchi N, Tokushima Y, Yamamoto S and Tanaka S: Clinical Course and CSF Amyloid  $\beta$ -Protein Precursor Having the Site of Application of the Protease Inhibitor (APPI) Levels in Patients with Dementia of the Alzheimer Type, *Dementia*, **4**, 59–60 (1993).

Ueda K and Kido T: Ligand Western Blotting for Specific Detection of Active Forms of Protease, *Clin. Biochem. Revs.*, **14**, S30 (1993).

Ikemoto M, Totani M, Mori T and Ueda K: Arginase as a New Marker of Hepatic Lesions, *Clin. Biochem. Revs.*, **14**, S38 (1993).

Ueda K, Yamaoka Y and Ikemoto M: Biochemical Monitoring of Partial Liver Transplantation from Living Donors, *Clin. Biochem. Revs.*, **14**, 200 (1993).

Totani M, Ikemoto M, Mori T and Ueda K: Autoantibody against Human Liver-type Arginase and Its Clinical Significance, *Clin. Biochem. Revs.*, **14**, 240 (1993).

Masliah E, Ueda K and Mucke L: Pathophysiological Basis of Alzheimer's Disease, in *Volumetto Estratto da 17th World Congress of Anatomic and Clinical Pathology* (G.S. Santoscioy, ed.), Monduzzi Editore, Bologna 315–320 (1994).

Kawamata J, Hasegawa H, Shimohama S, Kimura J, Tanaka S, and Ueda K: Leu<sup>106</sup>→Val (CTC→GTC) Mutation of Superoxide Dismutase-1 Gene in Patient with Familial Amyotrophic Lateral Sclerosis in Japan, *Lancet*, **343**, 1501 (1994).

Kawamata J, Tanaka S, Shimohama S, Ueda K and Kimura J: Apolipoprotein E Polymorphism in Japanese Patients with Alzheimer's Disease or Vascular Dementia, *J. Neurol. Neurosurg. Psychiatr.*, **57**, 1414–1416 (1994).

Banasik M and Ueda K: Inhibitors and Activators of ADP-Ribosylation Reactions, *Mol. Cell. Biochem.*, **138**, 185–197 (1994).

Ueda K: PCR in Laboratory Tests (1), *Igakukensa*, **42**, 892–895 (1993) (in Japanese).



Ueda K: PCR in Laboratory Tests (2), *Igakukensa*, **42**, 1008–1010 (1993) (in Japanese).

Ueda K: Glossary of Genomic Biology, *Clinical Endocrinology*, **41** (Supplement), 177–203 (1993) (in Japanese).

Ueda K: Methods of Gene Analysis, *Popular Medicine*, **173**, 72–75 (in Japanese).

Tanaka S and Ueda K: Dementia and Inheritance, in *Basic Research of Dementia—How Far the Dementia Has Been Resolved?* (M. Matsushita, ed.), Chuo-Hohki-Shuppan, Tokyo (1993), 201–217 (in Japanese).

Ueda K: DNA Diagnosis of Genes. in *Manual of Laboratory Tests of Children* (M. Ohkuni and K. Kawano, eds.), Bunkoudou, Tokyo (1993), 269–273 (in Japanese).

Miyahara T, Akaboshi M, Kawai K, Utsumi H and Ueda K: Mechanism of Thermal Potentiation of Cytocidal Effect of Cisplatin on Cultured Oesophageal Cancer Cells, *Rad. Biol. Res. Commun.*, **29**, 338–341 (1994) (in Japanese).

Ueda K: Certified Clinical Pathologists and the Program of Postgraduate Training in Clinical Chemistry, *Clin. Pathol.*, **42**, 504–507 (1994) (in Japanese).

Ueda K: Principle of DNA Diagnosis. Nippon Rinsho, Special Issue ("Clinical Molecular Biology"), 496–501 (1994) (in Japanese).

## MOLECULAR BIOFUNCTION

### I. Functional Molecular Conversion

Hibi T, Kato H, Nishioka T, Oda J, Yamaguchi H, Katsube Y, Tanizawa K and Fukui H: Use of Adenosine(5')polyphospho(5')pyridoxals to Study the Substrate-Binding Region of Glutathione Synthetase from *Escherichia coli* B, *Biochemistry*, **32**, 1548–1554 (1993).

Inagaki M, Hiratake J, Nishioka T and Oda J: One-Pot Conversion of Aldehydes to (S)-2-Acetoxy Nitriles via Reversible Cyanohydrin Formation, *Preparative Biotransformations*, **2nd Supplement** (1993).

Nakatani T, Hiratake J, Shinzaki A, Umeshita R, Suzuki T, Nishioka T, Nakajima H and Oda J: A Mode of Product Inhibition of an Esterolytic Antibody, *Tetrahedron Letters*, **34**, 4945–4948 (1993).

Oshima-Hirayama N, Yoshikawa K, Nishioka T and Oda J: Lipase from *Pseudomonas aeruginosa*—Production in *Escherichia coli* and Activation in vitro with a protein from the Downstream Gene, *Eur. J. Biochem.*, **215**, 239–246 (1993).

Suyama M, Nishioka T and Oda J: Extraction of the Ligand-Related Motifs in Enzymes, Takagi, T., Imai, H., ed. Miyano, S., Mitaku, S. and Kanehisa, M. *Proceedings of Genome Informatics Workshop IV*, Universal Academy Press, Tokyo, 245–254 (1993).

Suyama M, Ogiwara A, Nishioka T and Oda J: Searching for Amino Acid Sequence Motifs among Enzymes: the Enzyme-Reaction Database, *Comput. Applic. Biosci.*, **9**, 9–15 (1993).

Tanaka T, Sakai T, Chihara-Shiomi M, Takeshima K, Kato H, Misawa T, Hashimoto T, Nishioka T and Oda J: Construction,

Expression, and Characterization of Glutathione Synthetase Chimeras: Substitution of a Loop with a Homologous Peptide Region of Dihydrofolate Reductase, *Bull. Inst. Chem. Res., Kyoto Univ.*, **71**, 274–287 (1993).

Tanaka T, Yamaguchi H, Kato H, Nishioka T, Katsube Y and Oda J: Flexibility Impaired by Mutations Revealed the Multifunctional Roles of the Loop in Glutathione Synthetase, *Biochemistry*, **32**, 12398–12404 (1993).

Yamaguchi H, Kato H, Hata Y, Nishioka T, Kimura A, Oda J and Katsube Y: Three-dimensional Structure of the Glutathione Synthetase from *Escherichia coli* B at 2.0 Å Resolution, *J. Mol. Biol.*, **229**, 1083–1100 (1993).

Oda J, Nakatani T and Hiratake J: Catalytic Antibodies and Multiple Turnovers—a "Substrate Tuning" for Relieving Catalytic Antibodies of Product Inhibition, *New Functionality Materials, Vol. C, Synthetic Process and Control of Functionality Materials* (T. Tsuruta, M. Doyama, M. Seno), 561–564, Elsevier, Amsterdam, (1993).

Kato H, Tanaka T, Yamaguchi H, Hara T, Nishioka T, Katsube Y and Oda J: Flexible Loop That is Novel Catalytic Machinery in a Ligase. Atomic Structure and Function of the Loopless Glutathione Synthetase, *Biochemistry*, **33**, 4995–4999 (1994).

Suyama M, Nishioka T and Oda J, Detecting Common Amino Acid Sequence Patterns with a Gap, *Proceedings Genome Informatics Workshop*, 1994, S. Miyano, T. Akutsu, H. Imai, O. Goto, T. Takagi, 180–181, Universal Academy Press, Tokyo (1994).

Yamaguchi H, Kato H, Nishioka T, Oda J and Katsube Y: Data Collection of Glutathione Synthetase—Substrates Complex Crystal Obtained from PEG Solution, *Photon Activity Report 1993*, **11**, 111 (1994).

Hara H, Kato H, Nishioka T, Yamaguchi H, Katsube Y and Oda J: Structure Analysis of Binary Complex of Glutathione Synthetase from *Escherichia coli* B with ATP, *Photon Activity Report 1993*, **11**, 115 (1994).

Nakatani T, Umeshita R, Hiratake J, Shinzaki A, Suzuki T, Nakajima H and Oda J: Characterization of a Catalytic Residue and Mode of Product Inhibition, *Bioorg. Med. Chem.*, **2**, 457–468 (1994).

### II. Molecular Microbial Science

Yoshimura T, Nishimura K, Ito J, Esaki N, Kagamiyama H, Manning J M and Soda K: Unique Stereospecificity of D-Amino Acid Aminotransferase and Branched-Chain L-Amino Acid Aminotransferase for C-4' Hydrogen Transfer of the Coenzyme, *J. Am. Chem. Soc.*, **115**, 3897–3900 (1993).

Ohshima T and Soda K: Valine Dehydrogenase from a Non-spore-forming Bacterium, *Alcaligenes faecalis*: Purification and Characterization, *Biochim. Biophys. Acta*, **1162**, 221–226 (1993).

Lim Y, Yokoigawa K, Esaki N and Soda K: A New Amino Acid Racemase with Threonine  $\alpha$ -Epimerase Activity from *Pseudomonas putida*: Purification and Characterization, *J. Bacteriol.*, **175**, 4213–4217 (1993).

Bhatia M B, Pozo A M, Ringe D, Yoshimura T, Soda K and Manning J M: Role Reversal for Substrates and Inhibitors Slow



- Inactivation of D-Amino Acid Transaminase by Its Normal Substrates and Protection by Inhibitors, *J. Biol. Chem.*, **268**, 17687–17694 (1993).
- Ashiuchi M, Yoshimura T, Esaki N, Ueno H and Soda K: Inactivation of Glutamate Racemase of *Pediococcus pentosaceus* with L-Serine O-Sulfate, *Biosci. Biotech. Biochem.*, **57**, 1978–1979 (1993).
- Yoshimura T, Ashiuchi M, Esaki N, Kobatake C, Choi S and Soda K: Expression of *glr(murI, dga)* Gene Encoding Glutamate Racemase in *Escherichia coli*, *J. Biol. Chem.*, **268**, 24242–24246 (1993).
- Yoshimura T, Jhee K, Esaki N and Soda K: Stereochemistry and Evolution of Aminotransferases, *Bull. Inst. Chem. Res., Kyoto Univ.*, **71**, 368–375 (1993).
- Bhatia MB, Futaki S, Ueno H, Manning JM, Ringe D, Yoshimura T and Soda K: Kinetic and Stereochemical Comparison of Wild-type and Active-Site K145Q Mutant Enzyme of Bacterial D-Amino Acid Transaminase, *J. Biol. Chem.*, **268**, 6932–6938 (1993).
- Soda K, Kurihara T, Tchorzewski M, Esaki N and Ohishi N: Nitroalkane-Oxidizing Flavoenzymes (K. Yagi), *Flavins and Flavoproteins 1993*, Berlin New York, Walter de Gruyter & Co., 185–193 (1994).
- Kurihara T, Esaki N, Soda K and Ohishi N: A 340-nm Chromophore of Nitroalkane Oxidase from *Fusarium oxysporum* (K. Yagi), *Flavins and Flavoproteins 1993*, Berlin New York, Walter de Gruyter & Co., 195–198 (1994).
- Tchorzewski M, Kurihara T, Esaki N and Soda K: Genomic DNA Structure of a Unique Flavoprotein, 2-Nitropropane Dioxygenase from *Hansenula mrakii* (K. Yagi), *Flavins and Flavoproteins 1993*, Berlin New York, Walter de Gruyter & Co., 267–270 (1994).
- Kim D W, Yoshimura T, Esaki N, Satoh E and Soda K: Studies of the Active-Site Lysyl Residue of Thermostable Aspartate Aminotransferase: Combination of Site-Directed Mutagenesis and Chemical Modification, *J. Biochem.*, **115**, 93–97 (1994).
- Matsushima Y, Kim DW, Yoshimura T, Kuramitsu S, Kagamiyama H, Esaki N and Soda K: Replacement of Active-Site Lysine-239 of Thermostable Aspartate Aminotransferase by S-(2-Aminoethyl)Cysteine: Properties of the Mutant Enzyme, *J. Biochem.*, **115**, 108–112 (1994).
- Esaki N, Itoh S, Blank W and Soda K: Biotransformation of Oleic Acid by *Alcaligenes* sp. 5–18, a Bacterium Tolerant to High Concentrations of Oleic Acid, *J. Ferment. Bioeng.*, **77**, 148–151 (1994).
- Yoshimura T, Wakayama M, Kim DW, Esaki N and Soda K: Effects of Pyridoxal 5'-Phosphate on the Refolding of Aspartate Aminotransferase, *Biosci. Biotech. Biochem.*, **58**, 363–365 (1994).
- Esaki N, Ito S, Blank W and Soda K: Biotransformation of Oleic Acid by *Micrococcus luteus* Cells, *Biosci. Biotech. Biochem.*, **58**, 319–321 (1994).
- Esaki N, Watanabe M, Kurihara T and Soda K: Fungal Thermostable  $\alpha$ -Dialkylamino Acid Aminotransferase: Occurrence, Purification and Characterization, *Arch. Microbiol.*, **161**, 110–115 (1994).
- Jones WM, Ringe D, Soda K and Manning JM: Determination of Free D-Amino Acids with a Bacterial Transaminase; Their Depletion Leads to Inhibition of Bacterial Growth, *Anal. Biochem.*, **218**, 204–209 (1994).
- Sawada S, Tanaka Y, Hayashi S, Ryu M, Hasegawa T, Yamamoto Y, Esaki N, Soda K and Takahashi S: Kinetics of Thermostable Alanine Racemase of *Bacillus stearothermophilus*, *Biosci. Biotech. Biochem.*, **58**, 807–811 (1994).
- Soda K and Esaki N: Pyridoxal Enzymes Acting on D-Amino Acids, *Pure & Appl. Chem.*, **66**, 709–714 (1994).
- Itoh S, Esaki N, Masaki K, Blank W and Soda K: Production of New Tricarboxylic Acid Anhydrides from Stearic Acid by *Pseudomonas cepacia* A-1419, *J. Ferment. Bioeng.*, **77**, 513–516 (1994).
- Liu J Q, Kurihara T, Hasan A K M Q, Nardi-Dei V, Koshikawa H, Esaki N and Soda K: Purification and Characterization of Thermostable and Nonthermostable 2-Haloacid Dehalogenases with Different Stereospecificities from *Pseudomonas* sp, Strain YL, *Appl. Environ. Microbiol.*, **60**, 2389–2393 (1994).
- Liu J-Q, Kurihara T, Esaki N and Soda K: Reconsideration of the Essential Role of a Histidine Residue of L-2-Halo Acid Dehalogenase, *J. Biochem.*, **116**, 248–249 (1994).
- Nardi-dei V, Kurihara T, Okamura T, Liu J, Koshikawa H, Ozaki H, Terashima Y, Esaki N and Soda K: Comparative Studies of Genes Encoding Thermostable L-2-Halo Acid Dehalogenase from *Pseudomonas* sp. Strain YL, Other Dehalogenases, and Two Related Hypothetical Proteins from *Escherichia coli*, *Appl. Environ. Microbiol.*, **60**, 3375–3380 (1994).
- Ohshima T, Nishida N, Bakthavatsalam S, Kataoka K, Takada H, Yoshimura T, Esaki N and Soda K: The purification, characterization, cloning and sequencing of the gene for a halostable and thermostable leucine dehydrogenase from *Thermoactinomyces intermedius*, *Eur. J. Biochem.*, **222**, 305–312 (1994).
- Hasan A K M Q, Takada H, Koshikawa H, Liu J Q, Kurihara T, Esaki N and Soda K: Two Kinds of 2-Halo Acid Dehalogenases from *Pseudomonas* sp. YL Induced by 2-Chloroacrylate and 2-Chloropropionate, *Biosci. Biotech. Biochem.*, **58**, 1599–1602 (1994).
- Sakamoto Y, Kondo H and Soda K: Spectrophotometric Assay of Aminopeptidase with Thermostable Alanine Dehydrogenase from *Bacillus stearothermophilus*, *Biosci. Biotech. Biochem.*, **58**, 1675–1678 (1994).
- Sakamoto Y, Nakajima H, Nagata K, Esaki N and Soda K: Large-Scale Production of Thermostable Alanine Dehydrogenase from Recombinant Cells, *J. Ferment. Bioeng.*, **78**, 84–87 (1994).
- Kataoka K, Takada H, Tanizawa K, Yoshimura T, Esaki N, Ohshima T and Soda K: Construction and Characterization of Chimeric Enzyme Consisting of an Amino-Terminal Domain of Phenylalanine Dehydrogenase and a Carboxy-Terminal Domain of Leucine Dehydrogenase, *J. Biochem.*, **116**, 931–936 (1994).



Nishimura K, Ito J, Yoshimura T, Esaki N and Soda K: A Simple Method for Determination of Stereospecificity of Aminotransferases for C-4' Hydrogen Transfer of the Coenzyme, *Bioorganic & Medicinal Chemistry*, **2**, 605–607 (1994).

Furuyoshi S, Soda K: Important Role of Phospholipids in Visible Cycle, *Kagaku*, **49**, 222–223 (1994) (in Japanese)

Esaki N, Soda, K: Gene and Trace Elements, *Clinical Neuroscience*, **12** (1994) (in Japanese)

Esaki N, Soda, K: Trace Element and Genes, *Geka to Taisha Eiyo*, **28**, 251–258 (1994) (in Japanese)

## MOLECULAR BIOLOGY AND INFORMATION

### I. Biopolymer Structure

Ishiguro R, Kimura N and Takahashi S: Orientation of Fusion-active Synthetic Peptides in Phospholipid Bilayers: Determination by Fourier Transform Infrared Spectroscopy, *Biochemistry*, **32**, 9792–9797 (1993).

Murata M, Shirai Y, Ishiguro R, Kagiwada S, Tahara Y, Ohnishi S and Takahashi S: Fusion of Dioleoylphosphatidylcholine Vesicles Induced by an Amphiphilic Cationic Peptide and Oligophosphates at Neutral pH, *Biochim. Biophys. Acta*, **1152**, 99–108 (1993).

Kamata H, Yagisawa H, Takahashi S and Hirata H: Amphiphilic Peptides Enhance the Efficiency of Liposome-mediated DNA Transfection, *Nucleic Acids Res.*, **22**, 536–537 (1994).

Sawada S, Tanaka Y, Hayashi S, Ryu M, Hasegawa T, Yamamoto Y, Esaki N, Soda K and Takahashi S: Kinetics of Thermostable Alanine Racemase of *Bacillus stearothermophilus*, *Biosci. Biotech. Biochem.*, **58**, 807–811 (1994).

Kizaki K, Hata Y, Watanabe K, Katsube Y and Suzuki Y: Polypeptide Folding of *Bacillus cereus* ATCC7064 Oligo-1, 6-glucosidase Revealed by 3 Å Resolution X-ray Analysis, *J. Biochem.*, **113**, 646–649 (1993).

Fujii T, Oozeki M, Moriyama H, Tanaka N, Wakagi T and Oshima T: Crystallographic Studies on *Sulfolobus acidocaldarius* Ferredoxin, *Acta Cryst.*, **A49**, Suppl. 73–74 (1993).

Hata Y, Kizaki K, Watanabe K, Suzuki Y and Katsube Y: Structure of Oligo-1, 6-glucosidase Refined at 2.0 Å, *Acta Cryst.*, **A49**, Suppl. 101 (1993).

Hamada K, Hiramatsu H, Fujiwara T, Katsuya Y, Hata Y, Matsuura Y and Katsube Y: Structural Analysis of *Serratia* Protease, *Acta Cryst.*, **A49**, Suppl. 102 (1993).

Hamada K, Hiramatsu H, Fujiwara T, Katsuya Y, Hata Y and Katsube Y: X-ray Crystallographic Study of *Serratia* Protease, *Photon Factory Activity Report*, **#11**, 86 (1993).

Watanabe K, Hata Y, Kizaki H, Katsube Y and Suzuki Y: X-ray Crystal Structure Analysis of Oligo-1, 6-glucosidase, *Photon Factory Activity Report*, **#11**, 87 (1993).

Miyatake H, Hata Y, Fujii T, Morihara K and Katsube Y: Crystal Structure Determination of Alkaline Protease from

*Pseudomonas aeruginosa* Strain PAO1, *Photon Factory Activity Report*, **#11**, 108 (1993).

Hata Y, Natori K, Ooi T, Arai M, Okada H and Katsube Y: Crystallization and Preliminary X-ray Diffraction Studies of an Endoglucanase from *Aspergillus aculeatus*, *J. Mol. Biol.*, **241**, 278–280 (1994).

Sato T, Ozaki H, Hata Y, Kitagawa Y, Katsube Y and Shimonishi Y: Structural Characteristics for Biological Activity of Heat-Stable Enterotoxin Produced by Enterotoxigenic *Escherichia coli*: X-ray Crystallography of Weakly Toxic and Nontoxic Analogs, *Biochemistry*, **33**, 8641–8650 (1994).

Sohrin Y, Matsui M, Hata Y, Hasegawa H and Kokusen H: New Mode of Ion Size Discrimination for Group 2 Metals Using Poly(pyrazolyl)borate Ligands. 2. Control of Stability and Structure of Chelate Complexes by Intra- and Interligand Contact and Shielding Effect, *Inorg. Chem.*, **33**, 4376–4383 (1994).

### II. Molecular Biology

Oka A, Aoyama T and Endoh H: Transcriptional Control of the *Agrobacterium* Virulence Genes by Two Proteins VirA and VirG, *Bull. Institute Chemical Research Kyoto University*, **71**, 355–367 (1993).

Aoyama T, Endoh H, Takanami M and Oka A: DNA Signal Architecture for Transcriptional Activation by the Regulatory Protein VirG, *Bull. Institute Chemical Research Kyoto University*, **71**, 288–294 (1993).

Aoki M and Oka A: Phosphoprotein Phosphatase Genes of *Arabidopsis thaliana*, *Bull. Institute Chemical Research Kyoto University*, **71**, 295–307 (1993).

Tanaka N and Oka A: Identification of *rol* Genes on pRi1724 in *Agrobacterium rhizogenes* Strain MAFF03-01724 Isolated in Japan, *Ann. Phytopath. Soc. Japan*, **60**, 45–52 (1994).

Endoh H, Aoyama T and Oka A: Transcription in Vitro Promoted by the *Agrobacterium* VirG Protein, *FEBS Let.*, **334**, 277–280 (1993).

Tanaka N and Oka A: Restriction Endonuclease Map of the Root-inducing Plasmid (pRi1724) of *Agrobacterium rhizogenes* strain MAFF03-01724, *Biosci. Biotech. Biochem.*, **58**, 297–299 (1994).

Tanaka N, Ikeda T and Oka A: Nucleotide Sequence of the *rol* Region of the Mikimopine-Type Root-inducing Plasmid pRi1724, *Biosci. Biotech. Biochem.*, **58**, 548–551 (1994).

Goto K and Meyerowitz EM: Function and Regulation of the *Arabidopsis* Floral Homeotic Gene *PISTILLATA*, *Genes Dev.*, **8**, 1548–1560 (1994).

Hirai M Y, Fujiwara T, Goto K, Komeda Y, Chino M and Naito S: Differential Regulation of Soybean Seed Storage Protein Gene Promoter-GUS Fusions by Exogenously Applied Methionine in Transgenic *Arabidopsis thaliana*, *Plant Cell Physiol.*, **35**, 927–934 (1994).

Takahashi Y, Hanaoka K, Goto K and Kondoh H: Lens-specific Activity of the Chicken  $\delta$ 1-crystallin Enhancer in the Mouse, *Inter. J. Dev. Biol.*, **38**, 365–368 (1994).



Goto K: Genetic Interactions Among Homeotic Genes in *Arabidopsis* Flower Development, *Shokubutu-Saibou-Kougaku*, **6**, 199–208 (1994) (In Japanese).

### III. Biological Information Science

Waizumi K, Masuda H, Einaga H and Fukushima N: Intrinsic Structures of  $[\text{CuCl}_4]^{2-}$  and  $[\text{CuBr}_4]^{2-}$  Anions by Ab Initio Density Functional Calculations, *Chem. Lett.*, 1145–1148 (1993).

Waizumi K, Masuda H and Fukushima N: Structural Rigidity of First Hydration Spheres of  $\text{Na}^+$  and  $\text{Ca}^{2+}$  in Cluster Models. Full Geometry Optimizations of  $[\text{M}(\text{H}_2\text{O})_6]^{n+}$ ,  $[\text{M}(\text{H}_2\text{O})_6 \cdots \text{H}_2\text{O}]^{n+}$  and  $[\text{M}(\text{H}_2\text{O})_6 \cdots \text{Cl}]^{(n-1)+}$  ( $\text{M}=\text{Na}$  and  $\text{Ca}$ ,  $n=1$  for  $\text{Na}$  and 2 for  $\text{Ca}$ ) by Density Functional Calculations, *Inorg. Chim. Acta*, **209**, 207–211 (1993).

Goto S, Sakamoto N, Takagi T and Ushijima K: A Deductive Language in Object-Oriented Database for Genome Analysis, in *Proc. the Int. Symp. on Next Generation Database Systems and Their Applications*, 123–129, (1993).

Fujibuchi W and Kanehisa M: A Method to Extract Functional Motifs for Transcriptional Regulation in Eukaryotic Sequences, *Bull. Inst. Chem. Res., Kyoto Univ.*, **71**, 3, 317–326 (1993).

Ohkubo Z and Kanehisa M: Characterization of Spatially Close Peptide Segments in Proteins, *Bull. Inst. Chem. Res., Kyoto Univ.*, **71**, 3, 327–337 (1993).

Masuda H, Fukushima N and Einaga H: Ab Initio Density Functional Calculations on Copper(I)- $\text{CO}_2$  Coordinations, *Bull. Chem. Soc. Jpn.*, **66**, 3643–3647 (1993).

Waizumi K, Masuda H, Einaga H and Fukushima N: Application of Density Functional Calculations to the Structures and Formation Energies of  $[\text{MCl}_4]^{2-}$  Complexes ( $\text{M}=\text{Cr}$ ,  $\text{Mn}$ ,  $\text{Fe}$ ,  $\text{Co}$ ,  $\text{Ni}$ ,  $\text{Zn}$ ), *Bull. Chem. Soc. Jpn.*, **66**, 3648–3651 (1993).

Araki S, Goshima M, Mori S, Nakashima H, Tomita S, Akiyama Y and Kanehisa M: Application of Parallelized DP and A\* Algorithm to Multiple Sequence Alignment, in *Proc. Genome Informatics Workshop IV*, 94–102 (1993).

Ohkubo Z and Kanehisa M: A Method for Extracting Spatially Close Peptide Segments in Proteins, in *Proc. Genome Informatics Workshop IV*, 167–174 (1993).

Uchiyama I, Ogiwara A, Ohkubo Z and Kanehisa M: Automatic Procedure to Extract Signature Pentapeptides from the Protein Sequence Database, in *Proc. Genome Informatics Workshop IV*, 255–263 (1993).

Ogata H, Akiyama Y and Kanehisa M: A Computer Modeling Method for the Three-dimensional Structure of RNA, in *Proc. Genome Informatics Workshop IV*, 270–274 (1993).

Fujibuchi W, Kanehisa M: Construction of a Functional Word Dictionary for Primate Promoter Sequences, in *Proc. Genome Informatics Workshop IV*, 275–282 (1993).

Goto S, Sakamoto N and Takagi T: Integration of Genome Databases Using a Deductive Object-Oriented Database, in *Proc. Genome Informatics Workshop IV*, 352–261 (1993).

Suzuki T, Nakashima S, Takagi T, Kuhara S and Kanehisa M: Enhancement of the Integrated Database "HyperGenome" for

Genome Maps and Sequence Information, in *Proc. Genome Informatics Workshop IV*, 362–369 (1993).

Niiyama T, Tokimori T, Ogiwara A, Uchiyama I and Nakai K: GNOME: A Sequence Data Management Tool to Access Homology, Motif, and Other Data Analysis Servers, in *Proc. Genome Informatics Workshop IV*, 385–393 (1993).

Akiyama Y, Mori H, Kuhara S, Ogasawara N, Miyajima N, Furukawa T, Satou K and Murakami Y: Genomata: An Integrated Data Management and Analysis Tool for Genome Sequencing Projects, in *Proc. Genome Informatics Workshop IV*, 394–401 (1993).

Ogiwara A, Uchiyama I and Kanehisa M: Sequence Motif Analysis and Retrieval Tool, in *Proc. Genome Informatics Workshop IV*, 402–410 (1993).

Suzuki T, Takagi T, Kuhara S and Kanehisa M: Development of an Integrated Database for Genome Mapping and Nucleotide Sequences, in *Proc. 27th Hawaii Int. Conf. on System Sciences*, **5**, 68–76 (1994).

Goto S, Sakamoto N and Takagi T: A Deductive Object-Oriented Language for Integrated Genome Databases (Extended Abstract), in *Proc. 27th Hawaii Int. Conf. on System Sciences*, **5**, 108–109 (1994).

Uchiyama I, Ogiwara A and Kanehisa M: A Library of Signature Pentapeptides for the Protein Data Bank. In *Protein Structure by Distance Analysis* (Bohr H and Brunak S, eds.), 237–246, IOS Press (1994).

Sakamoto N, Goto S and Takagi T: A Deductive Database System for Analyzing Human Nucleotide Sequence Data, *Int. J. Bio-Medical Computing*, **36**, 171–179 (1994).

Nakai K, Tokimori T, Ogiwara A, Uchiyama I and Niiyama T: Gnome—an Internet-based Sequence Analysis Tool, *Comput. Appl. in Biosci.*, **10**, 5, 547–550 (1994).

Mizuno M and Kanehisa M: Distribution Profiles of GC Content around the Translation Initiation Site in Different Species, *FEBS Lett.*, **352**, 7–10 (1994).

Kanehisa M: Information processing for analysis of genes and genomes, *Jouhoushori*, **35**, 983–990 (1994) (In Japanese).

Mizuno M and Kanehisa M: Distribution of Base Composition around the Splice Sites in Different Species, in *Proc. Genome Informatics Workshop 1994*, 130–137 (1994).

Itoh T, Yano M, Takemoto K, Akiyama Y and Mori H: Construction and Analysis of Escherichia coli Genome Database, in *Proc. Genome Informatics Workshop 1994*, 138–139 (1994).

Suzuki K, Goto S, Akiyama Y and Kanehisa M: A Signal Transduction Database, in *Proc. Genome Informatics Workshop 1994*, 144–145 (1994).

Niiyama T, Takeuchi A, Kotani K, Uchiyama I, Ogiwara A and Nakai K: Gnome: Recent Development, in *Proc. Genome Informatics Workshop 1994*, 200–201 (1994).

Akiyama Y, Yakoh T, Mori H and Ogasawara N: A Server-Client Version of "Genomata" for Genome Maps and



Sequence Information, in *Proc. Genome Informatics Workshop 1994*, 202–203 (1994).

Goto S, Kuhara S, Takagi T and Kanehisa M: Extension of the Integrated Database "HyperGenome" for Genome Maps and Sequence Information, in *Proc. Genome Informatics Workshop 1994*, 204–205 (1994).

Ogiwara A, Uchiyama I, Takagi T and Kanehisa M: Further Improvements on SMART: Sequence Motif Analysis and Retrieval Tool, in *Proc. Genome Informatics Workshop 1994*, 206–207 (1994).

Oda A, Yano J and Kanehisa M: A DNA/Protein Sequence Retrieval System: an Xtpanel Application, in *Proc. Genome Informatics Workshop 1994*, 220–221 (1994).

Goto S and Kanehisa M: A Knowledge Base for Searching and Browsing Metabolic Pathways, in *Proc. Genome Informatics Workshop 1994*, 234–235 (1994).

## NUCLEAR SCIENCE RESEARCH FACILITY

### Particle and Photon Beams Beams and Fundamental Reaction

Cheng W-H, Gluckstern R L and Okamoto H: Synchrotron Resonance Effects in Alternating Phase Focusing, in *Proc. 1993 Particle Accelerator Conf.*, 221–223 (1993).

Gluckstern R L, Krinsky S and Okamoto H: Saturation of a High Gain FEL, in *Proc. 1993 Particle Accelerator Conf.*, 1545–1547 (1993).

Jiang S, Okamoto H and Gluckstern R L: Transverse Impedance of an Iris in a Beam Pipe, in *Proc. 1993 Particle Accelerator Conf.*, 3390–3392 (1993).

Okamoto H: One-dimensional Beam Stability Analysis Based on the Waterbag Model, *Nucl. Instr. Meth.*, **A332**, 1–22 (1993).

Gluckstern R L, Krinsky S and Okamoto H: Analysis of the Saturation of a High Gain FEL, *Phys. Rev.*, **E47**, 4412–4429 (1993).

Cheng W-H, Gluckstern R L and Okamoto H: Synchrotron-Coupling Effects in Alternating-Phase-Focusing Linacs, *Phys. Rev.*, **E48**, 4689–4698 (1993).

Okamoto H, Jiang S and Gluckstern R L: Longitudinal and Transverse Impedance of an Iris in a Beam Pipe, *Phys. Rev.*, **E50**, 1501–1515 (1994).

Okamoto H, Sessler A M and Möhl D: Three Dimensional Laser Cooling of Stored and Circulating Ion Beams by Means of a Coupling Cavity, *Phys. Rev. Lett.*, **72**, 3977–3980 (1994).

Okamoto H: Beam Breakup in Bunch Trains, *CERN Report*, SL/94–75.

Okamoto H: Transverse Laser Cooling induced through Dispersion at an rf Cavity, *Phys. Rev.*, **E50**, 4982–4995 (1994).

Warner R E, Fetter J M, Swartz R A, Okihana A, Konishi T, Yoshimura T, Kuntz P D, Fujiwara M, Fukunaga K, Kakigi S, Hayashi T, Kasagi J and Koori N:  $^4\text{He}(^4\text{He}, ^3\text{He})^5\text{He}$  (g.s.)

Reaction at 118 MeV, and its Distorted Wave Born Approximation Interpretation, *Phys. Rev.*, **C49**, 1534–1539 (1994).

Kakigi S, Yoshimura T and Okihana A: Energy Dependences of Cross Sections for (p, 2p) Quasifree Scattering on  $^2\text{H}$ ,  $^3\text{He}$  and  $^4\text{He}$ , *Bull. Inst. Chem. Res., Kyoto Univ.*, **72**, 27–35 (1994).

Yoshimura T, Okihana A, Kakigi S, Warner R E, Fujiwara M, Matsuoka N, Fukunaga K, Hayashi T, Kasagi J, Tosaki M and Greenfield M B: Quasi-free Process in the  $^6\text{Li}(\alpha, ^3\text{He}, ^5\text{He})^2\text{H}$  Reaction at  $E_\alpha=119$  MeV, *Bull. Inst. Chem. Res., Kyoto Univ.*, **72**, 51–61 (1994).

Yamagata T, Utsunomiya H, Nakayama S, Koori H, Tanaka M, Tamii A, Fujita Y, Katori K, Inoue M, Fujiwara M, Ogata H and Hirabayashi Y: Successful Description of Elastic Scattering of  $^3\text{He}$  Particles at 150 MeV/nucleon with the Single Folding Potential Model, *Phys. Rev.*, **C50**, 2606–2607 (1994).

Inoue M, Dewa H, Fujisawa H, Fujita H, Ikegami M, Iwashita Y, Kakigi S, Noda A, Okamoto H and Shirai T: Beam Acceleration of the Compact Proton Linac and the Light Ion Linac at ICR Kyoto University, in *Proc. of the fifth Japan-China Joint Symp. on Accelerators for Nuclear Science and Their Applications*, 192–194 (1993).

Fujisawa H: A CW 4-Rod RFQ Linac, *Nucl. Instr. Meth.*, **A345**, 23–42 (1994).

Iwashita Y: Disk-and Washer Structure with Biperiodic Support, *Nucl. Instr. Meth.*, **A348**, 15–33 (1994).

Fujisawa H, Tamada M, Matsumoto M, Iwashita Y, Noda A, Inoue M: Beam Tests of a CW 4-Rod RFQ, in *Proc. of the 9th Symp. on Accelerator Science and Technology*, 146–148 (1993).

Inoue M, Dewa H, Fujita H, Ikegami M, Iwashita Y, Kakigi S, Noda A, Okamoto H and Shirai T: Present Status of the 7 MeV Proton Linac at ICR Kyoto University, in *Proc. of the 9th Symp. on Accelerator Science and Technology*, 196–198 (1993).

Shirai T, Dewa H, Fujita H, Ikegami M, Iwashita Y, Kakigi S, Okamoto H, Noda A and Inoue M: Performance of the ICR 433 MHz RFQ Linac, in *Proc. of the 9th Symp. on Accelerator Science and Technology*, 223–225 (1993).

Iwashita Y: Compact Strong Permanent Magnet Symmetric Lens, in *Proc. of the 9th Symp. on Accelerator Science and Technology*, 267–269 (1993).

Hiramoto K, Tadokoro M, Hirota J, Nishi M, Noda A and Inoue M: A Compact Proton Synchrotron based on a Low Emittance Beam Extraction Scheme using Transverse RF Noise, in *Proc. of the 9th Symp. on Accelerator Science and Technology*, 309–311 (1993).

Noda A, Iwashita Y, Shirai T, Ikegami M, Dewa H and Inoue M: Possibility of High Brightness Micro-Beam by a Combination of a Linac and an Ion Stretcher and Cooler Ring, in *Proc. of the 9th Symp. on Accelerator Science and Technology*, 330–332 (1993).

Ikeda K, Kan T, Yoshizawa K, Hirota J, Iwashita Y, Noda A and Inoue M: Cold Model Test of Slot Coupling between RFQ and DTL Cavities, *Bull. Inst. Chem. Res., Kyoto Univ.*, **72**, 1–11 (1994).



Noda A, Ikegami M, Iwashita Y, Kakigi S, Kando M, Shirai T, Dewa H, Fujita H and Inoue M: Space Charge dominated Beam Transport and Matching Section between Ion Source and Linac, *Bull. Inst. Chem. Res., Kyoto Univ.*, **72**, 12–19 (1994).

Fijita H, Ikegami M, Inoue M, Iwashita Y, Shirai T and Noda A: Vacuum System of Beam Irradiation and Monitoring Apparatus, *Bull. Inst. Chem. Res., Kyoto Univ.*, **72**, 20–26 (1994).

Fujisawa H, Matsumoto T and Tamada M: 34 MHz  $\lambda/4$  Spiral Resonator, *Bull. Inst. Chem. Res., Kyoto Univ.*, **72**, 36–44 (1994).

Inoue M, Noda A, Iwashita Y and Shirai T: Conceptual Design of the 800 MeV Multi-purpose Proton Accelerator, *Bull. Inst. Chem. Res., Kyoto Univ.*, **72**, 69–75 (1994).

Dewa H, Iwashita Y, Fujita H, Ikegami M, Inoue M, Kakigi S, Kando M, Noda A, Okamoto H and Shirai T: Beam Current Monitor with a Troidal Coil for a Pulsed Proton Beam, *Bull. Inst. Chem. Res., Kyoto Univ.*, **72**, 76–86 (1994).

Shirai T, Dewa H, Fujita H, Kando M, Ikegami M, Iwashita Y, Kakigi S, Noda A and Inoue M: RF System of ICR Proton Linac, *Bull. Inst. Chem. Res., Kyoto Univ.*, **72**, 87–94 (1994).

Noda A, Dewa H, Fujita H, Ikegami M, Iwashita Y, Kakigi S, Kando M, Shirai T and Inoue M: Design of an Electron Storage Ring for Synchrotron Radiation, in *Proc. of the 4th European Particle Accelerator Conference*, London, U.K. 645–647 (1994).

Noda K, Kanazawa M, Takada E, Itano A, Sudou M, Torikoshi M, Araki N, Kumada M, Sato K, Ogawa H, Kitagawa A, Kohno T, Sato Y, Murakami T, Yamada S, Yoshizawa J, Hirao Y, Itoh H, Noda A, Tomizawa M and Yoshizawa M: Beam Test of Ring Property in HIMAC Synchrotron, in *Proc. of the 4th European Particle Accelerator Conference*, London, U.K. 982–984 (1994).

Okamoto H, Sessler A and Möhl D: Three-Dimensional Laser Cooling, in *Proc. of the 4th European Particle Accelerator Conference*, London, U.K. 1205–1207 (1994).

Noda A, Dewa H, Fujita H, Ikegami M, Iwashita Y, Kakigi S, Kando M, Shirai T and Inoue M: Low Energy Beam Transport and Matching Section under Space Charge Effect, in *Proc. of the 4th European Particle Accelerator Conference*, London, U.K. 2423–2425 (1994).

Matsuki S and Yamamoto K: Search for Dark Matter Particles in the Universe, *Oyo-Buturi*, **62**, 919–922 (1993) (in Japanese).

Hisamochi K, Iwamoto O, Kisanuki A, Budihardjo S, Widodo S, Nohtomi A, Uozumi Y, Sakae T, Matoba M, Nakano M, Maki T, Matsuki S and Koori N: Hole Strengths and Spreading Widths Observed in  $^{92}\text{Mo}(p, d)^{91}\text{Mo}$  Reaction at 65 MeV, *Nucl. Phys.*, **A564**, 227–251 (1993).

Matsuki S: Present Status of Laser Spectroscopy in Nuclear Physics: Review, *Genshikaku-Kenkyu*, **39**, 3–12 (1994) (in Japanese).

Matsuki S, Ogawa I and Yamamoto K: Coherent Interactions of Axions with Microwave Photons in a Resonant Cavity to Search for Cosmic Axions, *Phys. Lett.*, **B336**, 573–580 (1994).

## NUCLEIC ACID RESEARCH FACILITY

Sugisaki H: Nucleotide Sequence of the Gene of HgaI Restriction Endonuclease, *Bull. Inst. Chem. Res., Kyoto Univ.*, **71**, 338–342 (1993).

Adachi Y, Palakis GN and Copeland TD: Identification and Characterization of SET, a Nuclear Phosphoprotein Encoded by the Translocation Break Point in Acute Undifferentiated Leukemia, *J. Biol. Chem.*, **269**, 2258–2262 (1994).

Adachi Y, Palakis GN and Copeland TD: Identification of in Vivo Phosphorylation Sites of SET, a Nuclear Phosphoprotein Encoded by the Translocation Break Point in Acute Undifferentiated Leukemia, *FEBS Letters*, **340**, 231–235 (1994).

Gluckstein R L, Krinsky S and Okamoto H: Analysis of the Structure of a High Gain FEL, *Phys. Rev. E*, **44**, 12–1429 (1993).

Cheng W-H, Gluckstein R L and Okamoto H: Synchrotron-Coupling Effects in Alternating-Phase-Focusing Linacs, *Phys. Rev. E*, **48**, 1480–1488 (1993).

Okamoto H, Jiang S and Gluckstein R L: Longitudinal and Transverse Impedance of an Iris in a Beam Pipe, *Phys. Rev. E*, **50**, 1501–1515 (1994).

Okamoto H, Sessler A M and Möhl D: Three Dimensional Laser Cooling of Stored and Circulating Ion Beams by Means of a Coupling Cavity, *Phys. Rev. Lett.*, **73**, 3977–3980 (1994).

Okamoto H: Beam Breakup in Bunch Trains, CERN Report, SL-94-75.

Okamoto H: Transverse Laser Cooling Induced through Dispersion in an RF Cavity, *Phys. Rev. E*, **50**, 4983–4995 (1994).

Warner R E, Fetter J M, Swartz R A, Okamura A, Konishi T, Yoshimura T, Kuma P D, Fujiwara M, Fukunaga K, Kakigi S, Hayashi T, Kasagi I and Koon N:  $^3\text{He}^+\text{He}^+$  (g.s.)



# SEMINARS

Professor Christian Colliex

CNRS, Orsay, France

"Recent Progress in EELS Techniques and Applications to a Selection of Materials Science Problems"

Monday 7 March 1994

Dr. Yoshikazu Miyahara

Japan Atomic Energy Research Institute, Tokai, Ibaraki, Japan

"Free Electron Laser with a Storage Ring"

Thursday 10 March 1994

Dr. Robert A. Jameson

Los Alamos National Laboratory, Los Alamos, USA

"The Physics of Beam Halos"

Thursday 17 March 1994

Professor Toshiyuki Hattori

Tokyo Institute of Technology, Tokyo, Japan

"RFQ Linear Accelerator as a Heavy-Ion Irradiation Facility at Tokyo Institute of Technology"

Thursday 24 March 1994

Professor Maat Leendert

Department of Chemistry, Delft Institute of Technology, Delft, Netherlands

"Enzymatic Oxidation of Carbohydrates"

Tuesday 12 April 1994

Professor Howard Slater

University of Wales, Wales, UK

"Expression of Cryptic Genes-Dehalogenases and Chloroamidases"

Friday 15 April 1994

Dr. David J. Hardman

University of Kent, Kent, UK

"Application of Dehalogenases in a Clean-Technology Manufacturing Process"

Friday 15 April 1994

Professor Manfred Schmidt

Makromolekulare Chemie II, Universität Bayreuth, Bayreuth, Germany

"Intermolecular Structure in Dilute Polymer Solutions; A New Route to New Materials?"

Monday 18 April 1994

Professor Kazuyuki Akasaka

Faculty of Science, Kobe University, Kobe, Japan

"NMR Study of Protein Structure"

Monday 18 April 1994

Dr. Peter Dubowski

Moscow Institute of Fine Chemical Technology, Moscow, Russia

"Investigation of Peptide Structure in Biomembranes by NMR"

Monday 18 April 1994

Professor Dao Dao Zhang

Fudan University, Shanghai, China

"Biotechnology of Cyclodextrins"

Friday 22 April 1994

Dr. Anna Potznanskaja

All Union Vitamin Institute, Moscow, Russia

"Inclusion Complex of  $\beta$ -Carotene with  $\beta$ -Cyclodextrin"

Friday 22 April 1994

Professor Daniel L. Reger

Department of Chemistry and Biochemistry, The University of South Carolina, Columbia, USA

"Post Transition Metals Chemistry Using the Poly(pyrazolyl) borate Ligands"

Monday 9 May 1994

Dr. Yoshinori Fujiiyoshi

Protein Engineering Institute, Suita, Japan

"Structure of Membrane Proteins Revealed by Electron Micrography of Two-dimensional Crystals"

Monday 9 May 1994

Associate Professor Fumiaki Yamao

National Institute of Genetics, Mishima, Japan

"Recent Progress in Ubiquitin Research"

Friday 27 May 1994

Professor Nobuhiro Go

Department of Chemistry, Faculty of Science, Kyoto University, Kyoto, Japan

"Dynamics in Steric Structure of Proteins"

Friday 3 June 1994

Jean Marie Friedt

Air Liquid Laboratories, Tsukuba, Japan

"Research in Industries and Universities"

"Approches to Technological Innovation for survival in the 21st Century"

Friday 10 June 1994

Professor Adrian Carpov

"P. PONI" Institute of Macromolecular Chemistry, Iasi, Rumania

"Chemical Modification of Polysaccharides"

Tuesday 14 June 1994

Professor Steve Granick

Department of Materials Science and Engineering, University of Illinois, Urbana, Illinois, USA

"Surface Rheology"

Tuesday 14 June 1994

Sat P. Taneja

Maharshi Dayanand University, Rohtak 124001, India

"Mössbauer Study of Compounds Including Rare-Earth Ions"

Thursday 30 June 1994

Dr. Kai L. Ngai

Naval Research Laboratories, Washington D.C., USA

"Relaxation in Glassy Materials"

Tuesday 5 July 1994

Professor Guy Lucazeau

Institut Polytechnique de Grenoble, Grenoble, France

"Raman Spectroscopy in Solid State Physics and Material Science: theory, techniques and applications"

Thursday 14 July 1994

Robert L. White

Stanford University, Stanford, California, USA



"Multilayer Study in Stanford"  
Friday 15 July 1994

Professor Hideto Sotobayashi  
Fritz-Haber Institut der Max-Planck Gesellschaft, Berlin,  
Germany  
"LIGA Process - Micromachine Technique"  
Monday 18 July 1994

Dr. Robert James Cava  
AT & T Bell Laboratories, Murray Hill, New Jersey, USA  
"Status of New Materials Research in Copper Oxide  
Superconductivity and Related Fields"  
Monday 22 August 1994

Professor Waldemar Priebe  
Department of Medicinal Chemistry, University of Texas,  
Houston, Texas, USA  
"Design and Tumor Targeting of Anthracyclines Able to Over-  
come Multidrug Resistance: A Double-advantage Approach"  
Saturday 27 August 1994

Dr. Manfred Grieser  
Max-Planck-Institut für Kernphysik, Heidelberg, Germany  
"Upgrading of the Heidelberg Accelerator Facility with a New  
High Current Injector"  
Wednesday 31 August 1994

Dr. Manfred Grieser  
Max-Planck-Institut für Kernphysik, Heidelberg, Germany  
"The Heidelberg Heavy Ion Cooler Storage Ring TSR"  
Friday 2 September 1994

Dr. Michael Hess  
Gerhard-Mercator-University of Duisburg, Duisburg, Germany  
"Characterization of Soluble Polymers with Size-Exclusion  
Chromatography Coupled with Multi-Angle Light Scattering"  
Monday 12 September 1994

Professor Hans Bock  
Johann-Wolfgang-von Goethe University, Frankfurt am Main,  
Germany  
"Distorted Molecules: design, preparation and structures"  
Saturday 17 September 1994

Professor Julia A. Kornfield  
Chemical Engineering Department, California Institute of  
Technology, Pasadena, California, USA  
"Interplay of Molecular Weight and Mesophase Order in the  
Dynamics of Side-Group Liquid-Crystalline Polymers."  
Tuesday 20 September 1994

Dr. Miguel Abbate  
Laboratorio Nacional de Luz Sincrotron, CNPq, Caixa Postal  
6192, Campinas 13081-970 SP, Brazil  
"Changes in the Electronic Structure of  $Ti_4O_7$  across the  
Semiconductor-Metal Transitions"  
Tuesday 20 September 1994

Professor Bernard T. Golding  
Department of Chemistry, University of Newcastle upon Tyne,  
Newcastle, UK  
"Mechanism of Action of Vitamin B<sub>12</sub>"  
Tuesday 27 September 1994

Professor Timothy P. Lodge  
Department of Chemistry, University of Minnesota, Minne-

apolis, Minnesota, USA  
"Dynamic Light Scattering from Block Copolymer Liquids"  
Wednesday 5 October 1994

Jiang En-Ying  
Tianjin University, Tianjin 300072, China  
"Multilayer Studies in Tianjin University"  
Tuesday 11 October 1994

Professor Heinrich Wamhoff  
University of Bonn, Bonn, Germany  
"Iminophosphoranes, Versatile Tools in Heterocyclic Synthesis"  
Monday 17 October 1994

Professor Dieter Richter  
Institut für Festkörperforschung, Forschungszentrum Jülich  
GmbH, Jülich, Germany  
"Low Frequency Vibrations and Fast Relaxations near the Glass  
Transition in Polymers"  
Wednesday 19 October 1994

Professor Rolf Gleiter  
University of Heidelberg, Heidelberg, Germany  
"Synthesis and Reactions of Homo- and Heterocyclic Diynes"  
Friday 21 October 1994

Dr. Yoshiaki Kimura  
Protein Engineering Research Institute, Osaka, Japan  
"Structure Analysis of Bacteriorhodopsin"  
Thursday 27 October 1994

Dr. Nikolai Denkov  
Laboratory of Thermodynamics and Physico-Chemical Hydro-  
dynamics, Faculty of Chemistry, University of Sofia, Bulgaria  
"Formation Mechanism of Two-Dimensional Colloid Crystals in  
Liquid Films"  
Thursday 27 October 1994

Professor Robert J.P. Corriu  
University of Montpellier, Montpellier, France  
"The Chemistry of Cationic Hypercoordinated Silicon Species"  
Tuesday 1 November 1994

Professor R. Malcolm Brown, Jr.  
The University of Texas at Austin, Texas, USA  
"Recent Breakthroughs in Understanding Cellulose Assembly"  
Wednesday 2 November 1994

Dr. Henri Chanzy  
Centre de Recherches sur les Macromolécules Végétales,  
CNRS, Grenoble, France  
"Aspects of Polysaccharide Crystals"  
Wednesday 2 November 1994

Professor Candace H. Haigler  
Department of Biological Sciences, Texas Tech University,  
Lubbock, Texas, USA  
"Control of Cellulose Biogenesis in Secondary Cell Walls"  
Wednesday 2 November 1994

Professor Mukerrem Cakmak  
Institute of Polymer Engineering, College of Polymer Science  
and Polymer Engineering, The University of Akron, Akron,  
USA  
"Phase Behavior and Structure Development in Blends of Melt  
Spun PEEK/PEI Fibers"  
Friday 4 November 1994



Professor Derek G. Gray  
Pulp & Paper Research Institute of Canada;  
Department of Chemistry, McGill University, Montreal, Canada  
"Chiral Properties of Cellulose, Wood Fibers and Paper"  
Friday 4 November 1994

Professor Kraus Drauz  
Degussa Central Research Institute  
"Proline: Chemistry of an Unusual Amino Acid"  
Thursday 10 November 1994

Professor Paul A. Grieco  
Department of Chemistry, Indiana University, Indianapolis, USA  
"Organic Chemistry in High Polar Media"  
Saturday 12 November 1994.

Professor Frank Seela  
Institut für Chemie, Universität Osnabrück, Germany  
"Oligonucleotides with Unnatural Bases or a Configurationally Altered Backbone"  
Monday 14 November 1994

Professor Walter Bulchard  
Institute for Macromolecular Chemistry, University of Freiburg, Germany  
"Structure Formation Induced by Intermolecular Interaction"  
Tuesday 22 November 1994

Dr. Bernard Lotz  
Institut Charles Sadron, Strasbourg, France  
"Crystal Structures and Crystal Transformation of Polyolefins: Recent Advances"  
Thursday 24 November 1994

Professor Heinrich Hühnerfuss  
Institute of Organic Chemistry, University of Hamburg, Germany  
"Characterization of the Molecular Order of Monolayers at the Air/Water Interface"  
Thursday 24 November 1994

Professor Shigetoshi Oiki  
National Institute for Physiological Science

"From Pore to Gate: Structure and Function of Ion-Channels"  
Friday 25 November 1994

Professor Hidematsu Suzuki  
Department of Bioengineering, Nagaoka University of Technology, Nagaoka, Japan  
"Structure and Properties of Cellulosic Composite Materials"  
Monday 28 November 1994

Professor Gerhard Wegner  
Max-Planck-Institut für Polymerforschung, Mainz, Germany  
"Recent Progress in the Design and Analysis of Supramolecular Architectures of Shape-Persistent Macromolecules"  
Friday 2 December 1994

Professor Yuliang Yang  
Department of Macromolecular Science, Fudan University, China  
"Rotor Synchronized C-13 NMR: Correlation between Structure, Order and Dynamics in Rotating Polymer Solids"  
Tuesday 6 December 1994

Professor. Clément Sanchez  
Laboratoire de Chimie de la Matière Condensée, Université Pierre et Marie Curie, Paris, France  
"Molecular Design of Hybrid Organic Inorganic Materials Synthesized via Sol-Gel"  
Wednesday 7 December 1994

Professor Katsuhiko Nakamae  
Department of Applied Chemistry, Faculty of Engineering, Kobe University, Kobe, Japan  
"Molecular Structure and Properties of High Performance Polymer Materials"  
Friday 16 December 1994

Professor Alexander P. Potylitsin  
Tomsk Polytechnic University, Tomsk, Russia  
"Interaction of High Energy Electron Beam with Crystals"  
Friday 16 December 1994

Professor Yuzuru Suzuki  
Kyoto Prefectural University, Kyoto, Japan  
"Proline Theory—A Strategy to Make Proteins Thermostable"  
Tuesday 20 December 1994



# MEETINGS AND SYMPOSIUMS

## ICR ANNUAL MEETING 1994

December 9, 1994

### I. Oral Presentations

(Wood Composites Hall, Wood Research Institute, Kyoto University, Uji, Kyoto-fu)

1. Amyloid-Related Genes in Alzheimer's Disease  
Tanaka S and Ueda K
2. Time-Resolved X-Ray Crystallography of Glutathione Synthase Catalyzing Reactions in Crystalline State  
Nishioka S, Hara T, Kato H and Oda J
3. Solid NMR Analysis of the Molecular Motion of Organic Materials  
Horii F
4. Electron Crystal Structure Analysis with Imaging Plate  
Ogawa T, Moriguchi S, Isoda and Kobayashi T
5. Advanced Electrochemistry Useful for the Elucidation of Membrane Reactions  
Kihara S and Matsui M
6. Third-Order Nonlinear Optical Properties of Sol-Gel Derived Transition Metal Oxide Thin Films  
Hashimoto T and Yoko T
7. Development of New Accelerator Tube Structures for Linear Accelerators  
Iwashita Y

### II. Posters

(5th Floor Large Meeting Room, Institute for Chemical Research, Kyoto University, Uji, Kyoto-fu)

1. The Epitaxial Growth of VOPc and VOPcFx on Alkali Halides  
Hashimoto S
2. Swelling and Mechanical Behavior of Polymer Gels in Solvent Under Uniaxial and Biaxial Constraints  
Urayama K, Takigawa T, Masuda T and Kohjiya S
3. Structural Change in the Drawing Process of PEN [Poly(ethylene naphthalate)] at High Temperatures II  
Murakami S, Yamakawa M, Tsuji M and Kohjiya S
4. Polarized FT-IR Spectra of Water in the Gel Phase of Nonionic Surfactant Triton X100-Water System  
Kimura N
5. Analysis of Microcapsule Structure by Dielectric Measurements  
Sekine K
6. Magnetism of Europium/Transition Metal Interfaces  
Mibu K and Shinjo T
7. Preparation and Properties of SrRuO<sub>3</sub> Thin Films  
Izumi M and Bando Y
8. Phase Separation of Pb-Substituted Bi-Based Superconductors  
Niinae T, Ikeda Y and Bando Y
9. Magnetism of SrCu<sub>2</sub>O<sub>3</sub> and Sr<sub>2</sub>Cu<sub>3</sub>O<sub>5</sub> Comprising Spin 1/2 Ladders  
Azuma M, Hiroi Z and Takano M

10. Magnetic and Electrical Properties of SrFe<sub>1-x</sub>Co<sub>x</sub>O<sub>3</sub> Synthesized under High Pressure  
Kawasaki S and Takano M
11. High Pressure Synthesis and Characterization of a New High-Tc Cuprate Superconductor Without Apical Oxygens-  
(Ca<sub>1-x</sub>Na<sub>x</sub>)<sub>2</sub> CuO<sub>2</sub>Cl<sub>2</sub>  
Kobayashi N, Hiroi Z and Takano M
12. Growth of Pb-Substituted Bi-2201 Single Crystal by Floatation Zone Method  
Chong I, Niinae T, Ikeda Y, Takano M and Bando Y
13. Sol-Gel Preparation of Oxide Thin Films Dispersed with Metal Nanoparticles: Control of the Size, Shape and Orientation of Metal Particles  
Kozuka H, Okuno M and Yoko T
14. Dielectric Relaxation of Dipole-Inverted Type-A Chains  
Watanabe H
15. Dynamic Birefringence of Polyisoprene and Polyisobutylene  
Okamoto H, Inoue T and Osaki K
16. Structure of Polyelectrolyte Solutions-Charge Density Dependence of Interchain Correlation Length  
Nishida K, Kanaya T and Kaji K
17. Fast Relaxation Process in Amorphous Polystyrene  
Kawaguchi T, Kanaya T and Kaji K
18. 1D and 2D Solid State <sup>13</sup>C NMR Analysis of the Molecular Motion in the Crystalline State of Polymers  
Kaji H and Horii F
19. Gelation and Lyotropic Liquid Crystal of Fully Acylated Cellobiose in n-Alkane Solution  
Ide N, Fukuda T and Miyamoto T
20. Effects of Molecular Orientation on the Miscibility Threshold of Polystyrene/Poly(vinyl methyl ether) Blends  
Fujimoto K, Murakami M, Tsujii Y, Fukuda T and Miyamoto T
21. Synthesis and Mesophase Properties of Discotic Liquid Crystalline Polymers Having Fully Acylated Cellobiose Pendants  
Takaragi A, Minoda M, Watanabe J and Miyamoto T
22. Amphiphilic Block Polymers with Pendant Glucose Residues: Synthesis and Morphological Observation  
Yamada K, Minoda M and Miyamoto T
23. Palladium (II)-Catalyzed Carbonylation of Enol Esters  
Kudo K, Oida Y, Mitsuhashi K, Mori S, Komatsu K and Sugita N
24. Carbon-Carbon Bond Formation via the Chiral Episelemonium Ion Bearing Bulky Arylseleno Group as Protective Auxiliary  
Toshimitsu A, Nakano K, Mukai T and Tamao K
25. Structure and Reactivity of Novel Pentacoordinated Organosilicon Compounds  
Asahara M, Kawachi A, Yamaguchi S and Tamao K
26. Novel Atropisomers Through Two Bonds  
Fuji K, Kawabata T and Oka T
27. Molecular Design of Inhibitors of the Transcription Factors Which Bind to a  $\kappa$ B Site of DNA  
Fujita M, Otsuka M and Sugiura Y



28. A Mechanism-Based Inactivation of Glutathione Synthetase by Phosphinic Acid Transition-State Analogue  
Kato H, Hiratake J and Oda J
29. Chaperone-Like Activity of C-Terminal Domain of Alanine Racemase  
Yoshimura T, Kitamura T, Kurokawa Y, Esaki N and Soda K
30. Mechanism of the Thick Filament Formation by Assemble of Muscle Protein Myosin  
Akutagawa T
31. Study of Membrane Fusion-Active Peptides  
Ishiguro R, Matsumoto T and Takahashi S
32. Structure Features of a Zinc-metalloprotease Family Revealed by the X-ray Diffraction Study of *Pseudomonas aeruginosa* Alkaline Protease  
Miyatake H, Fujii T and Hata Y
33. Regulatory Network of Transcription in Higher Plants by Homeodomain Proteins  
Tsukuda M, Aoyama T and Oka A
34. Signal Transduction Pathways in Higher Plants Through Protein Phosphorylation-Dephosphorylation Reactions  
Aoki M, Aoyama T and Oka A
35. A Knowledge Base for Searching and Browsing Metabolic Pathways  
Goto S and Kanehisa M
36. Development of the Injector Linac for the Electron Storage Ring  
Shirai T, Iwashita Y, Kando M, Ikegami M, Dewa H, Okamoto H, Kakigi S, Fujita H, Noda A, Inoue M and Mashiko K
37. Pulsed Beam Current Monitor Using a Toroidal Coil  
Dewa H, Iwashita Y, Kando M, Ikegami M, Shirai T, Okamoto H, Kakigi S, Fujita H, Noda A and Inoue M
38. Abnormality of Calpatin-Calpastatin System after HTLV-1 Infection  
Adachi Y and Ueda K

## ICR SYMPOSIUM 1994

November 11, 1994

(Kyoto Research Park, Kyoto)

1. Hydrocarbon Molecules with Novel Structure: New Development in Fullerene Chemistry  
Komatsu K
2. Organosilicon Chemistry: Past, Present and Future  
Tamao K
3. Reasonable Reactions and Reactions beyond Common Knowledge Examples from Enantioselective Reactions  
Fuji K
4. Enantioselective Reaction Using Biocatalyst: New Method for Preparation of L- and D-Enantiomers  
Ohno A
5. Solid State Chemistry of New High-Tc Superconductors  
Kishio K
6. Creation of New Functional Materials by Artificial Superlattices  
Bando Y

## SYMPOSIUMS ORGANIZED BY RESEARCH FACILITY OF NUCLEIC ACIDS

### SYMPOSIUM ON "Molecular Mechanism of Transcription and RNA Functions" Wednesday 1 December 1993

"Regulation of Transcription by the TATA Box Binding Factor TFIID"

Associate Professor Masami Horikoshi

Institute of Molecular and Cellular Biology, University of Tokyo, Tokyo, Japan

"Plant bZIP Proteins Gather at ACGT Elements"

Dr Tsuyoshi Izawa

Plantech Research Institute, Yokohama, Japan

"Regulation of Transcription by the *myb* Oncogene Product"

Dr Shunsuke Ishii

Tsukuba Life Science Center, Institute of Physical and Chemical Research (RIKEN), Ibaraki, Japan

"Binding of the *Drosophila* Sex-lethal Gene Product to the Alternative Splice Sites of Transformer Primary Transcript"

Associate Professor, Hiroshi Sakamoto

Department of Biology, Faculty of Science, Kobe University, Kobe, Japan

"A Model for the Mechanism of Initial Generation of Retroposons"

Professor Norihiro Okada

Faculty of Bioscience and Biotechnology, Tokyo Institute of Technology, Yokohama, Japan

## TECHNICAL SYMPOSIUM

Thursday 2 December 1993

"Purification of Transcription Regulatory Factors with Affinity Chromatographies"

Associate Professor Masami Horikoshi

Institute of Molecular and Cellular Biology, University of Tokyo, Tokyo, Japan

Dr Tsuyoshi Izawa

Plantech Research Institute, Yokohama, Japan

Dr Shunsuke Ishii

Tsukuba Life Science Center, Institute of Physical and Chemical Research (RIKEN), Ibaraki, Japan

"Preparation of Extracts Having Transcription and Splicing Activities from Hela Cells"

Associate Professor Hiroshi Sakamoto

Department of Biology Faculty of Science, Kobe University, Kobe, Japan

Professor Norihiro Okada

Faculty of Bioscience and Biotechnology, Tokyo Institute of Technology, Yokohama, Japan



## THESES

SHIMAKAWA, Yuichi

D Sc, Kyoto University

"Chemical and Structural Study of High-Tc Superconductor  $Tl_2Ba_2CuO_6$ "

Supervisor: Professor Bando Y

23 January 1993

IMAI, Masayuki

D Eng, Kyoto University

"Studies on Structure Formation Crystallization of Poly(ethylene terephthalate)"

Supervisor: Professor K. Kaji

23 March 1993

NANIWA, Yoshimitsu

D Pharm Sc, Kyoto University

"Studies on the Direct Asymmetric Synthesis Utilizing Optically Active Pyrrolidines"

Supervisor: Professor Fuji K

23 March 1993

MIKATA, Yuji

D Sc, Kyoto University

"Mechanism and Stereochemistry of the Hydride Transfer Reaction from NAD(P)H Models"

Supervisor: Professor Ohno A

23 March 1993

SHIRAKI, Takashi

D Pharm Sc, Kyoto University

"Studies on DNA Cleavage Reactions by a Hybrid Antitumor Antibiotic Dynemicin A"

Supervisor: Professor Sugiura Y

23 March 1993

ISHIHARA, Yuji

D Pharm Sc, Kyoto University

"Studies on Design and Synthesis of Non-Peptide Inhibitor for Angiotension II Receptor"

Supervisor: Professor Sugiura Y

23 March 1993

ITOH, Takahiro

D Eng, Kyoto University

"Structural Studies on Langmuir-Blodgett Films of Amphiphilic Cellulose Derivatives"

Supervisor: Professor Miyamoto T

24 March 1993

IWASAKI, Tatsuo

D Eng, Kyoto University

"Studies on Graft Copolymerization of Vinyl Monomers onto Nylon 6 Fibers"

Supervisor: Professor Miyamoto T

23 May 1993

OGURA, Kaoru

D Sc, Kyoto University

"Studies on Ion Transfer at the Aqueous/organic Interface in the Presence of Concentrated Salts and Neutral Ligands by Polarography at the Electrolyte Solution Dropping Electrode"

Supervisor: Professor Matsui M

24 May 1993

NAGAI, Kazuhiro

D Sc, Kyoto University

"Structural Changes and Formation Process of Three-Components Graphite-Intercalation-Compounds"

Supervisor: Professor Kobayashi T

23 July 1993

KATSURA, Yosuke

D Pharm Sc, Kyoto University

"Synthetic Studies of Heterocyclic Compounds with Anti-ulcer Activity"

Supervisor: Professor Fuji K

24 September 1992

HOSOI, Shinzou

D Pharm Sc, Kyoto University

"Chiral Syntheses of Aromatic Erythrina Alkaloids"

Supervisor: Professor Fuji K

24 November 1992

NISHIKAWA, Yasuhiko

D Sc, Kyoto University

"Studies on Separation and Retention Behavior of Pesticides by Supercritical Fluid Chromatography"

Supervisor: Professor Matsui M

24 November 1993

LIM, Young Hee

D Agr, Kyoto University

"Enzymological and Stereochemical Studies of Amino Acid Racemase"

Supervisor: Professor Soda K

24 November 1993

ADACHI, Tatsuhiko

D Eng, Kyoto University

"Studies on the Sol-Gel Preparation and Properties of Silica Gel and Glass"

Supervisor: Professor Sakka S

23 January 1994

JIN, Jisun

D Eng, Kyoto University

"Study on the Structure, Formation and Properties of Oxynitride Glasses"

Supervisor: Professor Sakka S

23 January 1994

MASUDA, Yoshio

D Eng, Kyoto University

"Study on the Preparation of High-Tc Oxide Superconductors by the Sol-Gel Method"

Supervisor: Professor Sakka S

23 January 1994

ABE, Hitoshi

D Pharm Sc, Kyoto University

"Studies on the Asymmetric Diels-Alder Reactions Using Optically Active Sulfinyl Compounds"

Supervisor: Professor Fuji K

24 January 1994

KUBO, Keiji

D Pharm Sc, Kyoto University



"Studies on Design and Synthesis of Competitive Drugs for Non-Peptide Typed Angiotension II Receptor"

Supervisor: Professor Sugiura Y

24 January 1994

KOHRI, Masashiro

D Pharm Sc, Kyoto University

"Studies on Design and Synthesis of Condensed 7-Membered Compounds with Inhibitory Action for Angiotension-Converting Enzyme"

Supervisor: Professor Sugiura Y

23 March 1994

YONEZAWA, Atsuo

D Pharm Sc, Kyoto University

"Studies on Interaction between DNA and Biologically Active Peptides or Proteins by Footprinting Methods"

Supervisor: Professor Sugiura Y

23 March 1994

XU, Hai-jian

D Pharm Sc, Kyoto University

"Design and Synthesis of Untitumor Compounds"

Supervisor: Professor Fuji K

23 March 1994

HIGAKI, Masato

D Sc, Kyoto University

"Stereochemistry of Sulfur-Stabilized Carbanion"

Supervisor: Professor Ohno A

23 March 1994

HIROSAWA, Chitaru

D Eng, Kyoto University

"The Synthesis of Chiral Compounds by Use of Anchimeric Assistance of Sulfur"

Supervisor: Professor Tamao K

23 March 1994

YAMAZAKI Hiroki

D Sc, Kyoto University

"Magnetic Interaction between Fe Layers in Fe/Noble Metal Multilayers"

Supervisor: Professor Shinjo T

23 March 1994

WU Lianjun

D Sc, Kyoto University

"Structure and Magnetic Properties of Co/Au(001) Multilayers"

Supervisor: Professor Shinjo T

23 March 1994

HAYAKAWA, Satoshi

D Eng, Kyoto University

"Spectroscopic Studies on Structure of Vanadium-Containing Oxide Crystals and Glasses"

Supervisor: Professor Sakka S

23 March 1994

KIM, Sae-Hoon

D Eng, Kyoto University

"Studies on the Nonlinear Optical Properties of TeO<sub>2</sub> and Tellurite Glasses"

Supervisor: Professor Sakka S

23 March 1994

TOKI, Motoyuki

D Eng, Kyoto University

"Preparation of Silica Glasses and Organically Modified Silica Gels via Sol-Gel Method"

Supervisor: Professor Sakka S

23 March 1994

DONKAI, Nobuo

D Eng, Kyoto University

"Structure and Property of Inorganic Rod-Like Polymer, Imogolite"

Supervisor: Professor Miyamoto T

23 March 1994

TANAKA, Toshiaki

D Sc, Kyoto University

"Characterization of Genes Specifically Expressed in Mammalian Ovaries in Estrous Cycle and Establishment of Functional Granulosa Cell Lines"

Supervisor: Professor Takahashi S

23 March 1994

ENDO, Hideki

D Sc, Kyoto University

"Transcriptional Induction of the *Agrobacterium* Virulence Genes by Plant Factors"

Supervisor: Professor Oka A

23 March 1994

KUBONO Koji

D Sc, Kyoto University

"Crystal Structure Analysis and Molecular Recognition of Cyclophosphazene Inclusion Compounds"

Supervisor: Professor Kobayashi T

23 March 1994

NAKATANI, Takuji

D Agr, Kyoto University

"Generation and Characterization of Catalytic Antibodies for Stereoselective Ester Hydrolysis"

Supervisor: Professor Oda J

23 May 1994

NAKATANI, Keiichi

D Agr, Kyoto University

"Studies on The Synthesis of DBU Analogues and Their Catalytic Activities"

Supervisor: Professor Oda J

23 May 1994

FUJISAWA, Hiroshi

D Sc, Kyoto University

"A CW 4-Rod RFQ Linac"

Supervisor: Professor Inoue M

23 May 1994

KIM, Dong Woon

D Agr, Kyoto University

"Thermotable Aspartate Aminotransferase from *Bacillus* sp. YM-2"

Supervisor: Professor Soda K

23 May 1994

ONUKI, Toshihiko

D Sc, Kyoto University

"Migration Characteristics of Long-Lived Radionuclides of <sup>137</sup>Cs, <sup>90</sup>Sr and <sup>60</sup>Co in Soil"

Supervisor: Professor Matsui M

23 May 1994



MIYAMOTO, Hisashi  
D Pharm Sc, Kyoto University  
"Direct Asymmetric Syntheses Using Optically Active Piperazines"  
Supervisor: Professor Fuji K  
23 July 1994

IWASHITA, Yoshihisa  
D Sc, Kyoto University  
"Disk-and Washer Structure with Biperiodic Support"  
Supervisor: Professor Inoue M  
24 September 1994

CHIHARA-SIOMI, Mikiko  
D Agr, Kyoto University  
"Characterization of the fragile X Syndrome Gene Products"  
Supervisor: Professor Oda J  
24 November 1994

TACHINO, Hitoshi  
D Eng, Kyoto University  
"Structure and Properties of Ethylene Ionomers, Metal Salts of Poly(ethylene-co-methacrylic acid) and Poly(ethylene-co-acrylic acid)"  
Supervisor: Professor Miyamoto T  
24 November 1994

HAYASHI, Nobuyuki  
D Eng, Kyoto University  
"Syntheses, Properties and Applications of Naphthalocyanines"  
Supervisor: Professor Tamao K  
24 November 1994

IKEDA, Hisafumi  
D Pharm Sc, Kyoto University  
"Design of Functional Antisense Molecules with DNA-Cleaving Activity"  
Supervisor: Professor Fuji K  
24 November 1994

YAHIRO, Kiyoshi  
D Pharm Sc, Kyoto University  
"Studies on the Memory of Chirality"  
Supervisor: Professor Fuji K  
24 November 1994

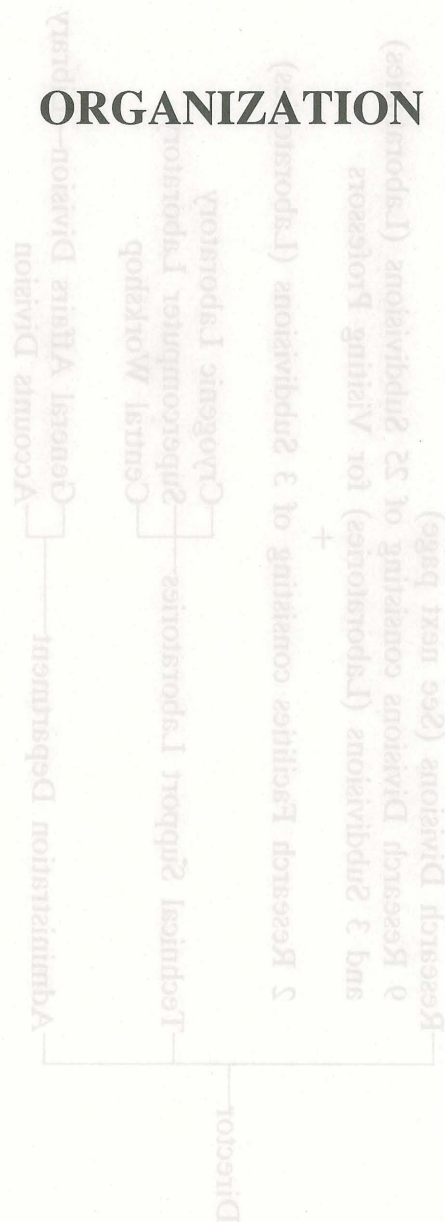
GOTOH, Michimasa  
D Pharm Sc, Kyoto University  
"Studies on Conformational Analysis and Nucleophilic Additional Reaction of 6-Membered Compounds with Electron Attracting Groups"  
Supervisor: Professor Sugiura Y  
24 November 1994

ISHIDA, Masaaki  
D Agr, Kyoto University  
"Threonine Production by Transformed Cells of Brevibacterium Bacteria"  
Supervisor: Professor Soda K  
24 November 1994

SAKAMOTO, Yonekazu  
D Agr, Kyoto University  
"Properties, Structure and Industrial Production of Thermally Stable Alanine Dehydrogenase"  
Supervisor: Professor Soda K  
24 November 1994



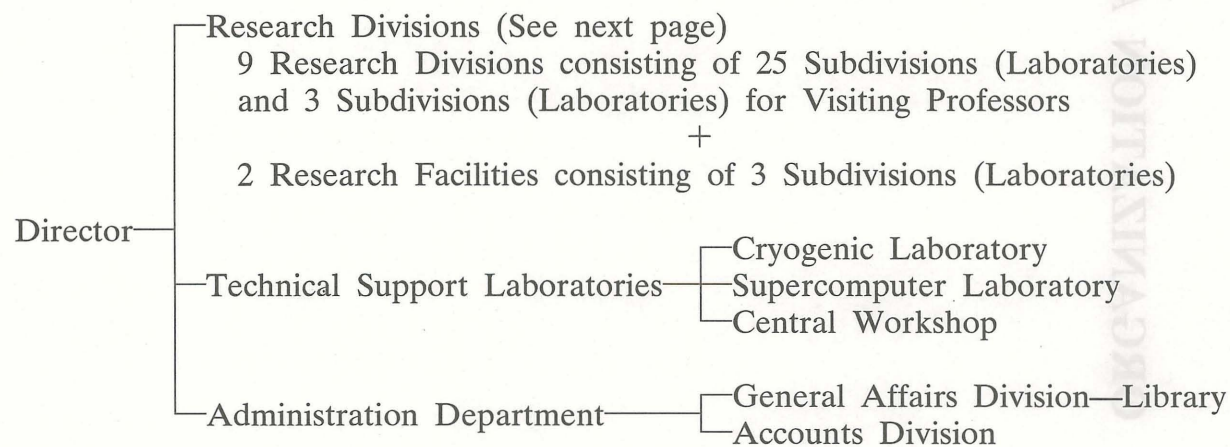
# ORGANIZATION AND STAFF



KYOTO UNIVERSITY  
INSTITUTE FOR CHEMICAL RESEARCH



INSTITUTE FOR CHEMICAL RESEARCH  
KYOTO UNIVERSITY





Research Division	Subdivision (Laboratory)	Related Graduate School Graduate School of / Division of	Professor	Associate Professor	Instructor
States and Structure	I. Atomic and Molecular Physics	Science / Physics I	MUKOYAMA, Takeshi	ISOZUMI, Yasuhito	ITO, Yoshiaki NAKAMATSU, Hirohide
	II. Crystal Information Analysis	Science / Chemistry	KOBAYASHI, Takashi	ISODA, Seiji	KURATA, Hiroki OGAWA, Tetsuya
	III. Polymer Condensed States Analysis	Engineering / Polymer Chemistry	KOHJIYA, Shinzo	TSUJI, Masaki	URAYAMA, Kenji
	I. Solutions and Interfaces	Science / Chemistry	NAKAHARA, Masaru	UMEMURA, Junzo	MATSUMOTO, Mutsuo
Interface Science	II. Molecular Aggregates	Science / Chemistry	SATO, Naoki	ASAMI, Koji	KITA, Yasuo SEKINE, Katsuhisa
	III. Separation Chemistry	Science / Chemistry	MATSUI, Masakazu	UMETANI, Shigeo	SASAKI, Yoshihiro SHOHRIN, Yoshiaki
	I. Artificial Lattice Alloys	Science / Chemistry	SHINJO, Teruya	HOSOITO, Nobuyoshi	MIBU, Ko IKEDA, Yasunori
Solid State Chemistry	II. Artificial Lattice Compounds	Science / Chemistry	BANDO, Yoshichika		TERASHIMA, Takahito
	III. Multicomponent Materials	Science / Chemistry	TAKANO, Mikio	HIROI, Zenji	
	IV. Amorphous Materials	Engineering / Molecular Engineering	YOKO, Toshinobu	KOZUKA, Hiromitsu	HASHIMOTO, Tadanori
	G. Structure Analysis		ENDO, Yasuo	KISHIO, Kohji	
Fundamental Material Properties	I. Molecular Rheology	Engineering / Molecular Engineering	OSAKI, Kunihiro	WATANABE, Hiroshi	INOUE, Tadashi
	II. Polymer Materials Science	Engineering / Polymer Chemistry	KAJI, Keisuke	KANAYA, Toshiji	NISHIDA, Koji
	III. Molecular Motion Analysis	Engineering / Molecular Engineering	HORII, Fumitaka	TSUNASHIMA, Yoshisuke	KAJI, Hironori
	G. Composite Material Properties		SAKAI, Tadamoto	WATANABE, Junji (Professor)	
Organic Materials Chemistry	I. Polymeric Materials	Engineering / Polymer Chemistry	MIYAMOTO, Takeaki	FUKUDA, Takeshi	TSUJII, Yoshinobu MINODA, Masahiko
	II. High-Pressure Organic Chemistry	Engineering / Energy & HC Chemistry	SUGITA, Nobuyuki	KOMATSU, Koichi	MORI, Sadayuki KUDO, Kiyoshi
Synthetic Organic Chemistry	I. Synthetic Design	Engineering / Energy & HC Chemistry	TAMAO, Kohei	TOSHIMITSU, Akio	KAWACHI, Atsushi YAMAGUCHI, Shigehiro
	II. Fine Organic Synthesis	Pharmaceutical Sci. / Pharmac. Chem.	FUJI, Kaoru	TANAKA, Kiyoshi	KAWABATA, Takeo
	G. Synthetic Theory		NAKAO, Hideo	IHARA, Masataka	
Bioorganic Chemistry	I. Bioorganic Reaction Theory	Science / Chemistry	OHNO, Atsuyoshi	NAKAMURA, Kaoru	SUGIYAMA, Takashi KAWAI, Yasushi
	II. Bioactive Chemistry	Pharmaceutical Sci. / Drug System	SUGIURA, Yukio	OTSUKA, Masami	MORII, Takashi
	III. Molecular Clinical Chemistry	Medicine / Internal Medicine	UEDA, Kunihiro		HAMAKUBO, Takao KATO, Hiroaki
Molecular Biofunction	I. Functional Molecular Conversion	Agriculture / Agricul. Chem.	ODA, Jun'ichi	NISHIOKA, Takaaki	HIRATAKE, Jun TANAKA, Takuji
	II. Molecular Microbial Science	Agriculture / Agricul. Chem.	SODA, Kenji	ESAKI, Nobuyoshi	YOSHIMURA, Tohru KURIHARA, Tatsuo
Molecular Biology and Information	I. Biopolymer Structure	Science / Biophysics	TAKAHASHI, Sho	HATA, Yasuo	HIRAGI, Yuzuru FUJII, Tomomi
	II. Molecular Biology	Science / Biophysics	OKA, Atsuhiko	AOYAMA, Takashi	GOTO, Koji
	III. Biological Information Science	Science / Biophysics	KANEHISA, Minoru	AKIYAMA, Yutaka	UCHIYAMA, Ikuo GOTO, Susumu
Nuclear Science Research Facility	I. Particle and Photon Beams	Science / Physics II	NODA, Akira	KAKIGI, Shigeru	SHIRAI, Toshiyuki
	II. Beams and Fundamental Reaction	Science / Physics II	INOUE, Makoto	MATSUKI, Seishi	IWASHITA, Yoshihisa OKAMOTO, Hiromi
Nucleic Acid Research Facility		Science / Biophysics		SUGISAKI, Hiroyuki	ADACHI, Yoshifumi

Director  
MIYAMOTO, Takeaki







## NAME INDEX

[A]  
ADACHI, Yoshifumi 42  
ADACHI, Yoshifumi 58  
AKITA, Katsushi 4  
AKIYAMA, Yutaka 52  
AKUTAGAWA, Tohru 48  
ANN, Miza 36  
AOKI, Mikio 50  
AOKI, Tomoko 46  
AOYAMA, Takashi 50  
ASAHARA, Masahiro 34  
ASAMI, Koji 12  
ASHUTOSH, V Bedekar 36  
AZUMA, Masaki 20

[B]  
BABA, Takeichiro 26  
BANDO, Yoshichika 18  
BEDEKAR, Beena A. 30  
BEPPU, Takayuki 28

[C]  
CHONG, Iksu 20  
CHOO, Dong-Won 46

[D]  
DEWA, Hideki 54, 56  
DOI, Noriyuki 34  
DONKAI, Nobuo 30

[E]  
EMOTO, Takeshi 16  
ENDO, Yasuo 60  
ENDO, Hideki 50  
ESAKI, Nobuyoshi 46

[F]  
FUJI, Kaoru 36  
FUJIBUCHI, Wataru 52  
FUJIHARA, Shinobu 22  
FUJII, Tomomi 48  
FUJIMOTO, Kouji 30  
FUJISAWA, Hiroshi 56  
FUJITA, Hirokazu 54, 56  
FUKUDA, Takeshi 30  
FUKUSHIMA, Nobuhiro 52

[G]  
GLATZ, Frank P. 30  
GOTO, Koji 50  
GOTO, Susumu 52  
GRIESER, Manfred 54  
GUTTIERREZ, Aldo Francisco 46

[H]  
HAGIHARA, Makota 40  
HAMADA, Noritaka 8  
HAMADA, Sunao 16  
HARA, Takane 44  
HASEGAWA, Masahiro 12  
HASHIMOTO, Syugo 6  
HASHIMOTO, Tadanori 22  
HATA, Yasuo 48  
HATTORI, Takeshi 22  
HATTORI, Toshiyuki 54  
HE, Zhen-Dan 36

HIDA, Kouichi 38  
HIRAGI, Yuzuru 48  
HIRAI, Asako 28  
HIRANO, Koichi 16  
HIRANO, Toshiko 38  
HIRASAWA, Toshiko 46  
HIRATA, Yoshitaka 8  
HIRATAKE, Jun 44  
HIROI, Zenji 20  
HORII, Fumitaka 28  
HOSHINO, Akitaka 6  
HOSOITO, Nobuyoshi 16  
HU, Shaohua 28

[I]  
ICHINOSE, Ataru 18  
IDE, Nobuhiro 30  
IHARA, Masataka 61  
IKEDA, Atsutoshi 36  
IKEDA, Hisafumi 36  
IKEDA, Kazumi 56  
IKEDA, Yasunori 18  
IKEGAMI, Masanori 54  
IKOMA, Futoshi 32  
IMAI, Masayuki 26  
IMAJUKU, Yoshiro 50  
INNOCENZI, Plinio 22  
INOUE, Makoto 54, 56  
INOUE, Tadashi 24  
INOUE, Yoshihiko 34  
INOUE, Yuko 38  
IRE, Satoshi 6  
ISHIBASHI, Keiji 22  
ISHIDA, Hiroyuki 28  
ISHIDA, Masato 28  
ISHIDA, Norihiro 50  
ISHIGURO, Ryo 48  
ISODA, Seiji 6  
ISOZUMI, Yasuhito 4  
ITAHANA, Koji 50  
ITO, Hidehiro 30  
ITO, Yoshiaki 4  
ITO, Toshihiko 6  
IWASHITA, Yoshihisa 54, 56  
IZAKI, Yoshihito 20  
IZUMI, Makoto 18  
IZUMI, Yoshio 32

[J]  
JHEE, Kwang-hwan 46  
JIN, Jisun 22

[K]  
KAGAYAMA, Akifumi 32  
KAJI, Hironori 28  
KAJI, Keisuke 26  
KAKIGI, Shigeru 54  
KANAYA, Toshiiji 26  
KANDO, Masaki 54  
KANEHISA, Minoru 52  
KAPIN, Valerij 56  
KARITA, Tetsuya 32  
KATANO, Rintarou 4  
KATO, Hiroaki 44  
KATO, Makoto 44

KATSUMATA, Atsushi 50  
KAWABATA, Kenji 30  
KAWABATA, Takeo 36  
KAWACHI, Atsushi 34  
KAWAGUCHI, Tatsuya 26  
KAWAI, Yasushi 38  
KAWAMOTO, Ikuko 12  
KAWAMURA, Tetsu 32  
KAWANISHI, Hiroyuki 28  
KAWASAKI, Masashi 38  
KAWASAKI, Shuji 20  
KAWASE, Noboru 6  
KAWAWAKE, Yasuhiro 16  
KIDO, Takahiro 42  
KIHARA, Daisuke 52  
KIHARA, Sorin 14  
KIM, Sae-Hoon 22  
KIMURA, Noriyuki 10  
KINOSHITA, Masamichi 38  
KISHIMOTO, Kazuhisa 46  
KISHIO, Koji 60  
KITA, Yasuo 12  
KITAMURA, Tae 46  
KITAOKA, Kenji 22  
KITAZAWA, Taro 50  
KOBAYASHI, Naoya 20  
KOBAYASHI, Takashi 6  
KOHJIYA, Shinzo 8  
KOIDE, Norihiro 12  
KOIKE, Akihiro 24  
KOITO, Seita 36  
KOKUSEN, Hisato 14  
KOMAI, Eiji 18  
KOMATSU, Koichi 32  
KONDO, Shin-ichi 38  
KOSHINO, Masanori 6  
KOZAWA, Masami 34  
KOZUKA, Hiromitsu 22  
KUBO, Yuji 38  
KUDO, Kiyoshi 32  
KUNITOMO, Jun 38  
KURATA, Hiroki 6  
KURIHARA, Tatsuo 46  
KURODA, Akio 36  
KUROKAWA, Yoichi 46  
KURONO, Takeshi 46  
KUSUDA, Toshiyuki 16  
KUWABARA, Kazuhiro 28  
KUWAHARA, Jun 40  
KUWAHARA, Shigenao 30  
KUWAMOTO, Kiyoshi 6

[L]  
LANG, Ming-fang 30  
LI, Bo 36  
LIESER, Günter 6  
LIU, Jiquan 46  
LIU, Lidong 46

[M]  
MAEDA, Hideyuki 10  
MAEDA, Yasuhiro 44  
MATSUBARA, Akira 12  
MATSUBAYASI, Nobuyuki 10



[T]	
TADA, Masaru	56
TAKAESU, Noboru	28
TAKAHASHI, Akiko	38
TAKAHASHI, Sho	48
TAKAHASHI, Thoru	36
TAKANO, Mikio	20
TAKARAGI, Akira	30
TAKASU, Kiyosei	36
TAKAYA, Tatsuya	22

[Z]  
ZHAO, Gaoling 22



## KEYWORD INDEX

- [A]
- $\alpha$ -diketone 36
  - $\alpha$ -helix 48
  - aberrant splicing 42
  - acetylenic C<sub>60</sub> 32
  - ACuO<sub>2</sub> 20
  - aging 42
  - agrobacterium virulence genes 50
  - alternative splicing 42
  - Alzheimer's disease 42
  - amorphous polymers 24
  - amphiphilic peptide 48
  - amyloid precursor protein 42
  - anchimeric assistance 34
  - apocytochrome b transcript 58
  - apolipoprotein E 42
  - APP gene transcript and linkage 42
  - arythio group 34
  - asymmetric synthesis 36
  - Au/Co multilayers 16
  - axial chirality 38
  - axion-photon-atom interactions in a resonant cavity 56
- [B]
- $\beta$ -structure 48
  - bacterial glutamate racemase 46
  - BaTiO<sub>3</sub> 18
  - beam profile 54
  - benzene clathrate hydrate formation 10
  - binaphthol 36
  - binary aqueous solution 10
  - biomolecular reactions for information transmission and expression 52
  - biomolecular reactions 52
  - birefringence 8
  - BRITE 52
- [C]
- capacitance 13
  - carbene addition 32
  - carbon cluster 32
  - chelate complexes 14
  - chemical shift anisotropy 28
  - chiral amide 34
  - chiral oxazoline 34
  - colloidal particle 13
  - conductance 13
  - cosmic axions 56
  - Coster-Kronig transition 4
  - crithidia fasciculata 58
  - crystal nucleation 26
  - Cu/Co multilayers 16
  - CV 32
- [D]
- dark matter in the universe 56
  - database 52
  - delocalization 12
  - density 8
  - depolarized light scattering 26
  - dielectric image 13
- [E]
- dielectric relaxation 13
  - diethynylsilanes 35
  - difunctionalized silole 35
  - DNA-binding protein 50
  - DNA cleavage 40
  - DTL 54
  - dynamic birefringence 24
- [F]
- ferroelectricity 18
  - fullerene C<sub>60</sub> 32
- [G]
- giant magnetoresistance 16
  - glass-to-rubber transition 24
  - glass structure 22
  - glasses 22
  - glassy polymers 28
  - glutathione synthetase 44
  - graphical user interface 52
  - gRNA-mRNA chimera molecules 58
- [H]
- high-resolution solid-state <sup>13</sup>C NMR 28
  - high-T<sub>c</sub> superconductor 20
  - high pressure synthesis 20
  - Horner-Wadsworth reaction 36
  - hydration cage 10
  - hydrophobic hydration 10
- [I]
- imaging plate 6
  - imaging plate 8
  - induced orientation 30
  - induction period 26
  - infinite-layer structure 20
  - inorganic photonic materials 22
  - intra- and inter-ligand contact 14
  - intramolecular reductive cyclization 35
  - ion source 54
- [J]
- kinetoplastid 58
  - knowledge base 52
- [K]
- L-series lines of tungsten 4
- [L]
- lattice model 30
  - lattice strain 18
  - LEBT 54
  - ligand design 14
  - liquid-liquid extraction 14
  - local motion 28
- [M]
- magnetic hyperfine fields 16
  - mechanism-based phosphorylation 44
  - membrane 13
  - membrane fusion 48
  - metabolic pathways 52
  - metal ion recognition 14
  - metallic multilayers 16
  - mitochondria 58
  - molecular electronic relaxation 12
  - molecular etiology 42
  - molecular interaction 52
  - molecular mechanics 14
  - molecular motion 28
  - molecular solid 12
- [N]
- NAD(P)H model compound 38
  - NAD(P)<sup>+</sup> 38
  - new mode of ion size discrimination for group 2 metals 14
  - NMR 10
  - novel endo-endo mode 35
  - nuclease 40
- [O]
- oligosiloles 35
  - organic solids 12
  - oriented crystallization 8
  - oxidative coupling reaction 35
- [P]
- peptide structure 48
  - phosphinate 44
  - phosphotransfer 50
  - photo diode array 4
  - plant-microbe interaction 50
  - polarization energy 12
  - poly(ethylene-2, 6-naphthalate) 8
  - poly(pyrazolyl) borate ligands 14
  - polycarbonates 28
  - polymer crystallization 26
  - polymer glasses 26
  - polymer melts 30
  - polymer rheology 24
  - polymerase chain reaction 58
  - potential map 6
  - proton linear accelerator 54
- [Q]
- quantum electronics 56
- [R]
- R<sub>2</sub>CuO<sub>4</sub> 20
  - reactive evaporation 18











1995 MARCH